ITS UCDAVIS
INSTITUTE OF TRANSPORTATION STUDIES

Research Report – UCD-ITS-RR-11-44

Warm-Mix Asphalt Study: Test Track Construction and First-Level Analysis of Phase 3b HVS and Laboratory Testing (Rubberized Asphalt, Mix Design #2)

June 2011

David Jones
Rongzong Wu
Bor-Wen Tsai
John T. Harvey

Institute of Transportation Studies ◦ University of California, Davis
1605 Tilia Street ◦ Davis, California 95616
PHONE (530) 752-6548 ◦ FAX (530) 752-6572
www.its.ucdavis.edu

June 2011
Research Report: UCPRC-RR-2011-03

Warm-Mix Asphalt Study: Test Track Construction and First-Level Analysis of Phase 3b HVS and Laboratory Testing (Rubberized Asphalt, Mix Design #2)

Authors:
D. Jones, R. Wu, B.-W. Tsai, and J.T. Harvey

Partnered Pavement Research Center (PPRC) Contract Strategic Plan Element 4.18:
Warm-Mix Asphalt

PREPARED FOR:

California Department of Transportation
Division of Research and Innovation
Office of Roadway Research

PREPARED BY:

University of California
Pavement Research Center
UC Davis, UC Berkeley

DOCUMENT RETRIEVAL PAGE			**Research Report: UCPRC-RR-2011-03**
Title: Warm-Mix Asphalt Study: Test Track Construction and First-Level Analysis of Phase 3b HVS and Laboratory Testing. (Rubberized Asphalt, Mix Design #2)			
Authors: David Jones, Rongzong Wu, Bor-Wen Tsai, and John T. Harvey			
Caltrans Technical Lead: Cathrina Barros			
Prepared for: Caltrans	**FHWA No:** CA132221B	**Work submitted:** 05/22/2013	**Date** June 2011
Strategic Plan Element No: 4.18	**Status:** Final		**Version No.:** 1

Abstract:

This is one of two first-level reports describing the third phase of a warm-mix asphalt study that compares the performance of two rubberized asphalt control mixes with that of seven mixes produced with warm-mix technologies. The control mixes were produced and compacted at conventional hot-mix asphalt temperatures (>300 F [150°C]), while the warm-mixes were produced and compacted at temperatures between 36°F (20°C) and 60°F (35°C) lower than the controls. This report discusses the mixes produced at the George Reed Marysville Plant and covers the *Advera WMA®*, *Astec Double Barrel Green®*, *Rediset® WMX, and Sasobit®* warm-mix technologies. The test track layout and design, mix design and production, and test track construction are discussed, as well as the results of Heavy Vehicle Simulator (HVS) and laboratory testing. Key findings from the study include:

- Adequate compaction can be achieved on rubberized warm-mixes at lower temperatures. Roller operators should, however, be aware of differences in roller response between warm-mix and conventional hot-mixes, and that rolling operations and patterns may need to be adjusted to ensure that optimal compaction is always achieved.
- Optimal compaction temperatures will differ among the different warm-mix technologies. However, a temperature reduction of at least 60°F (35°C) is possible for some technologies.
- Equal and potentially better rutting performance compared to hot-mix can be achieved from warm-mix asphalt provided that standard specified construction and performance limits for hot-mix asphalt are met.
- Laboratory test results indicate that use of the warm-mix technologies assessed in this study did not significantly influence performance when compared to control specimens. However, the mixes produced with chemical surfactant technologies did appear to be influenced in part by the lower mix production and construction temperatures, which would have resulted in less oxidation of the binder and consequent lower stiffness of the mix. Rutting performance under accelerated load testing did not appear to be affected, however, nor did fatigue performance or moisture sensitivity. The warm-mixes produced using water-foaming technologies appeared to have lower moisture resistance compared to the other warm-mixes in all the laboratory moisture sensitivity tests.
- Smoke and odors are significantly reduced on warm-mixes compared to hot-mixes, while workability is considerably better on warm-mixes compared to hot-mixes.

The HVS and laboratory testing completed in this phase have provided no results to suggest that warm-mix technologies should not be used in rubberized asphalt in California.

Keywords:
Warm-mix asphalt, WMA, rubberized asphalt, accelerated pavement testing, Heavy Vehicle Simulator

Proposals for implementation:
Continue with statewide implementation.

Related documents:
UCPRC Workplan, WP-2007-01, Research Reports, RR-2008-11, RR-2009-02, RR-2011-2.

Signatures:

D. Jones **1st Author**	J.T. Harvey **Technical Review**	D. Spinner **Editor**	J.T. Harvey **Principal Investigator**	C. Barros **Caltrans Technical Lead**	T.J. Holland **Caltrans Contract Manager**

DISCLAIMER STATEMENT

This document is disseminated in the interest of information exchange. The contents of this report reflect the views of the authors who are responsible for the facts and accuracy of the data presented herein. The contents do not necessarily reflect the official views or policies of the State of California or the Federal Highway Administration. This publication does not constitute a standard, specification or regulation. This report does not constitute an endorsement by the Department of any product described herein.

For individuals with sensory disabilities, this document is available in Braille, large print, audiocassette, or compact disk. To obtain a copy of this document in one of these alternate formats, please contact: the Division of Research and Innovation, MS-83, California Department of Transportation, P.O. Box 942873, Sacramento, CA 94273-0001.

PROJECT OBJECTIVES

The objective of this warm-mix asphalt study is to determine whether the use of additives to reduce the production and construction temperatures of hot-mix asphalt will influence the performance of the mix. This will be achieved through the following tasks:

1. Preparation of a workplan to guide the research;
2. Monitoring the construction of Heavy Vehicle Simulator (HVS) and in-service test sections;
3. Sampling of mix and mix components during asphalt concrete production and construction;
4. Trafficking of demarcated sections with the HVS in a series of tests to assess performance;
5. Conducting laboratory tests to identify comparable laboratory performance measures;
6. Monitoring the performance of in-service pilot test sections; and
7. Preparation of first- and second-level analysis reports and a summary report detailing the experiment and the findings.

This report covers Tasks 2, 3, 4, 5, and 7.

ACKNOWLEDGEMENTS

The University of California Pavement Research Center acknowledges the following individuals and organizations who contributed to the project:

- Ms. Cathrina Barros, Mr. Joseph Peterson, Ms. Terrie Bressette (retired), and Dr. T. Joseph Holland, Caltrans
- Mr. Nate Gauff, California Department of Resources Recycling and Recovery (CalRecycle)
- Mr. Tony Limas and the staff of the Bradshaw asphalt plant, Granite Construction
- Mr. Jack van Kirk and the staff of the Marysville asphalt plant, George Reed Construction
- Mr. Chris Barkley, Mr. Bill Clarkson and the paving crew, Teichert Construction
- Mr. Norm Smith, Astec Industries
- Ms. Annette Smith, PQ Corporation
- Dr. Eric Jorda, Arkema, Inc.
- Dr. Everett Crews, MWV Asphalt Innovations
- Mr. Dennis Hunt, Gencor
- Dr. Sundaram Logaraj, Akzo Nobel Surface Chemistry, LLC and Mr. Prem Naidoo consultant to Akzo Nobel Surface Chemistry, LLC
- Mr. John Shaw and Mr. Larry Michael, Sasol Wax Americas
- The UCPRC Heavy Vehicle Simulator crew and UCPRC laboratory staff

EXECUTIVE SUMMARY

The third phase of a comprehensive study into the use of warm-mix asphalt has been completed for the California Department of Transportation (Caltrans) by the University of California Pavement Research Center (UCPRC). This phase of the study, which investigated gap-graded rubberized asphalt concrete, was based on a workplan approved by Caltrans and included the design and construction of a test track, accelerated load testing using a Heavy Vehicle Simulator (HVS) to assess rutting behavior, and a series of laboratory tests on specimens sampled from the test track to assess rutting and fatigue cracking performance and moisture sensitivity. The objective of the study is to determine whether the use of technologies that reduce the production and construction temperatures of asphalt concrete influences performance of the mix. The study compared the performance of two rubberized asphalt control mixes, which were produced and constructed at conventional hot-mix asphalt temperatures (320°F [160°C]), with seven warm-mixes, produced and compacted at between 36°F (20°C) and 60°F (35°C) lower than the control. The mixes were produced at two different asphalt plants. The first part of the study, covered in a companion report (UCPRC-RR-2011-02), included mixes produced at Granite Construction's Bradshaw Plant using *Cecabase RT®*, *Evotherm DAT™*, and *Gencor Ultrafoam GX™* warm-mix technologies. The second part of the study, discussed in this report, included mixes produced at the George Reed Marysville Plant using *Advera WMA®*, *Astec Double Barrel Green®*, *Rediset™*, and *Sasobit®* technologies.

The test track is located at the University of California Pavement Research Center in Davis, California. The design and construction of the test track was a cooperative effort between Caltrans, the UCPRC, Granite Construction, George Reed Construction, Teichert Construction, and the seven warm-mix technology suppliers. The test track is 360 ft. by 50 ft. (110 m by 15 m) divided into nine test sections (two controls and seven warm-mixes). The pavement structure consists of the ripped and recompacted subgrade, 1.5 ft. (450 mm) of imported aggregate base, one 0.2 ft. (60 mm) lift of dense-graded hot-mix asphalt, and one 0.2 ft. (60 mm) lift of gap-graded rubberized hot-mix (RHMA-G) or warm-mix (RWMA-G) asphalt concrete. Each asphalt plant prepared a mix design. No adjustments were made to these mix designs to accommodate the warm-mix technologies. Target production temperatures were not set; instead the warm-mix technology suppliers set their own temperatures based on experience, ambient temperatures, and haul distance.

The production temperature for the George Reed Marysville RHMA-G control mix was 335°F (166°C) and 295°F (145°C), 295°F (145°C), 285°F (140°C), and 300°F (149°C) for the Advera, Astec, Rediset and Sasobit warm-mixes, respectively.

The rubberized asphalt sections were placed in April 2010. Specimens were removed from the test track for laboratory testing approximately six weeks after construction.

Heavy Vehicle Simulator (HVS) testing commenced in September 2010 and was completed in January 2011. Additional testing on three of the sections was conducted in August and September 2011. Testing compared early rutting performance at elevated temperatures (pavement temperature of 122°F at 2.0 in. [50°C at 50 mm]), starting with a 9,000 lb (40 kN) load on a standard dual wheel configuration and a unidirectional trafficking mode. Laboratory testing also commenced in June 2010 and was completed in December 2011. The test program included shear testing, wet and dry fatigue testing, Hamburg Wheel-Track testing, and determination of the wet-to-dry tensile strength ratio.

Key findings from the study include:

- A consistent subgrade was prepared and consistent base-course and underlying dense-graded hot-mix asphalt concrete layers were constructed on the test track using materials sourced from a nearby quarry and asphalt plant. Thickness and compaction of the base and bottom layer of asphalt were consistent across the test track.
- Asphalt plant modifications were required to accommodate the three powder/pellet based warm-mix technologies. The delivery systems were approved under the Caltrans Material Plant Quality Program. The water injection equipment was integral to the asphalt plant and was also approved under the Caltrans Material Plant Quality Program.
- A number of problems related to blocked nozzles occurred during the production of the water injection technology mix (Astec), which resulted in this and the Rediset mix construction being delayed for seven days, while the equipment was being replaced and additional binder sourced. This also resulted in the need to produce a second Control mix and to construct a second Control section. Target mix production temperatures (335°F, 300°F, 295°F, 295°F, and 285°F [166°C, 149°C, 149°C, 145°C, and 140°C] for the Control, Sasobit, Advera, Astec, and Rediset mixes respectively), set by the warm-mix technology providers, were all achieved. There was some variation in binder content among the six mixes, with the Rediset mix having a significantly higher binder content compared to the other mixes, and to the design.
- Compaction temperatures ranged between 258°F (126°C) and 219°F (104°C) for the Control and Rediset mixes, respectively, and were consistent with production temperatures. The mixes produced at lower temperatures lost heat during transport and placement at a slower rate than the mixes produced at the higher temperatures, as expected. Compaction was generally poor on all sections, especially on the Day #1 Control and Advera sections.
- Smoke and odors were significantly more severe on the Control section compared to the warm-mix sections.
- Workability of the mix, determined through observation of and interviews with the paving crew, was considerably better on the warm-mix sections compared to the Control.
- Average thicknesses of the top (rubberized) and bottom asphalt layers across the four sections were 0.22 ft. (66 mm) and 0.24 ft. (75 mm), respectively. The average thickness of the combined two layers was 0.45 ft in. (137 mm), 0.5 ft. (17 mm) thicker than the design thickness of 0.4 ft.

(120 mm). General consistency of thickness across the track was considered satisfactory and representative of typical construction projects.

- Nuclear gauge–determined density measurements were inconsistent with core-determined air-void contents. The core-determined air-void contents indicated that slightly higher density was achieved on the warm-mix sections compared to the Control sections (88 percent of the RICE specific gravity) compared to the warm-mix sections (92, 89, 91, and 92 percent for the Sasobit, Advera, Astec, and Rediset sections, respectively). Compaction across the test track appeared to be consistent, confirming that adequate compaction can be achieved on rubberized warm-mixes at lower temperatures. Based on observations from the test track construction and interviews with roller operators, optimal compaction temperatures and rolling patterns will differ between the different warm-mix technologies, but it was shown that adequate compaction can be achieved on warm-mixes at the lower temperatures. Roller operators will, however, need to consider that there might be differences in roller response between warm-mix and conventional hot mixes, and that rolling operations and patterns may need to be adjusted to ensure that optimal compaction is always achieved.
- HVS trafficking on four of the five sections indicated generally consistent performance among the mixes. Unexpected poor performance was measured on the Advera section (Section 626HA) so additional tests on this section as well as on the Control and Sasobit sections were undertaken to determine the cause and to eliminate possible seasonal and machine-related testing variables. The cause of this poor performance was attributed to a combination of high subgrade moisture content and thinner combined asphalt layers, which were identified during the forensic investigation. The duration of the tests to terminal rut (12.5 mm [0.5 in.]) on the five sections varied from 73,500 load repetitions (Section 629HB, Advera Test #2) to 365,000 load repetitions (Section 625HA, Sasobit Test #1).
- The duration of the embedment phases on all sections except the Advera section were similar. Apart from the Advera section, the depth of the ruts at the end of the embedment phases differed only slightly between sections, with the Astec section (7.5 mm [0.3 in.]) having a slightly deeper embedment than the Control, Sasobit, and Rediset sections, which had similar embedment (6.5 to 6.7 mm [0.26 in.]). This is opposite to the early rutting performance in the Phase 1 study and is being investigated in a separate project.
- Rut rate (rutting per load repetition) after the embedment phase on the Control and Sasobit sections was almost identical. The rut rate was slightly higher on the Astec and Rediset sections, and was attributed to some moisture in the asphalt layer and subgrade in the Astec section (determined during the forensic investigation), and to the higher binder content on the Rediset section. Although lower production and paving temperatures typically result in less oxidation of the binder, which can influence early rutting performance, differences in production and placement temperatures did not appear to influence performance in this set of tests.
- The laboratory test results indicate that use of the warm-mix technologies assessed in this study, produced and compacted at lower temperatures, did not significantly influence the performance of the asphalt concrete when compared to control specimens produced and compacted at conventional hot-mix asphalt temperatures. Specific observations include:
  + Laboratory performance in all tests appeared to be mostly dependent on air-void content and binder content, as expected, and less dependent on mix production temperature.

+ The water-based warm-mix technology mixes (Advera and Astec) appeared to have lower moisture resistance compared to the other three mixes in all the moisture sensitivity tests.
+ Test results were influenced by mix production temperatures, actual binder content, specimen air-void content, actual stress and strain levels, and actual test temperature. Variation in these parameters needs to be taken into consideration when comparing performance between the different mixes.

The HVS and laboratory testing completed in this phase have provided no results to suggest that warm-mix technologies should not be used in gap-graded rubberized mixes in California, provided that standard specified construction and performance limits for hot-mix asphalt are met. Significant reductions in smoke and odors and improved workability of the warm-mixes also support wider use of these technologies. Consideration should be given to further study into the effects of warm-mix asphalt technologies and production and placement of warm-mixes at lower temperatures on binder oxidation/aging rates. The effects that these may have on performance over the life of the asphalt surfacing should also be investigated. Research in this study has shown differences in early rutting performance between conventional and rubber mixes, between mixes tested after different curing periods, and between pavements subjected to mostly shade and mostly sun, respectively.

TABLE OF CONTENTS

LIST OF TABLES

LIST OF FIGURES

LIST OF ABBREVIATIONS

AASHTO	American Association of State Highway and Transportation Officials
ASTM	American Society for Testing and Materials
Caltrans	California Department of Transportation
DCP	Dynamic cone penetrometer
DGAC	Dense-graded asphalt concrete
ESAL	Equivalent standard axle load
FHWA	Federal Highway Administration
FWD	Falling weight deflectometer
HMA	Hot-mix asphalt
HVS	Heavy Vehicle Simulator
HWTT	Hamburg Wheel-Track Test
MDD	Multi-depth deflectometer
MPD	Mean profile depth
PPRC	Partnered Pavement Research Center
RHMA-G	Gap-graded rubberized hot-mix asphalt
RWMA-G	Gap-graded rubberized warm-mix asphalt
SPE	Strategic Plan Element
TSR	Tensile strength retained
UCPRC	University of California Pavement Research Center
WMA	Warm-mix asphalt

CONVERSION FACTORS

SI* (MODERN METRIC) CONVERSION FACTORS

APPROXIMATE CONVERSIONS TO SI UNITS

Symbol	When You Know	Multiply By	To Find	Symbol
		LENGTH		
in	inches	25.4	Millimeters	mm
ft	feet	0.305	Meters	m
yd	yards	0.914	Meters	m
mi	miles	1.61	Kilometers	Km
		AREA		
in^2	square inches	645.2	Square millimeters	mm^2
ft^2	square feet	0.093	Square meters	m^2
yd^2	square yard	0.836	Square meters	m^2
ac	acres	0.405	Hectares	ha
mi^2	square miles	2.59	Square kilometers	km^2
		VOLUME		
fl oz	fluid ounces	29.57	Milliliters	mL
gal	gallons	3.785	Liters	L
ft^3	cubic feet	0.028	cubic meters	m^3
yd^3	cubic yards	0.765	cubic meters	m^3
	NOTE: volumes greater than 1000 L shall be shown in m^3			
		MASS		
oz	ounces	28.35	Grams	g
lb	pounds	0.454	Kilograms	kg
T	short tons (2000 lb)	0.907	megagrams (or "metric ton")	Mg (or "t")
		TEMPERATURE (exact degrees)		
°F	Fahrenheit	5 (F-32)/9 or (F-32)/1.8	Celsius	°C
		ILLUMINATION		
fc	foot-candles	10.76	Lux	lx
fl	foot-Lamberts	3.426	candela/m^2	cd/m^2
		FORCE and PRESSURE or STRESS		
lbf	poundforce	4.45	Newtons	N
lbf/in^2	poundforce per square inch	6.89	Kilopascals	kPa

APPROXIMATE CONVERSIONS FROM SI UNITS

Symbol	When You Know	Multiply By	To Find	Symbol
		LENGTH		
mm	millimeters	0.039	Inches	in
m	meters	3.28	Feet	ft
m	meters	1.09	Yards	yd
km	kilometers	0.621	Miles	mi
		AREA		
mm^2	square millimeters	0.0016	square inches	in^2
m^2	square meters	10.764	square feet	ft^2
m^2	square meters	1.195	square yards	yd^2
ha	Hectares	2.47	Acres	ac
km^2	square kilometers	0.386	square miles	mi^2
		VOLUME		
mL	Milliliters	0.034	fluid ounces	fl oz
L	liters	0.264	Gallons	gal
m^3	cubic meters	35.314	cubic feet	ft^3
m^3	cubic meters	1.307	cubic yards	yd^3
		MASS		
g	grams	0.035	Ounces	oz
kg	kilograms	2.202	Pounds	lb
Mg (or "t")	megagrams (or "metric ton")	1.103	short tons (2000 lb)	T
		TEMPERATURE (exact degrees)		
°C	Celsius	1.8C+32	Fahrenheit	°F
		ILLUMINATION		
lx	lux	0.0929	foot-candles	fc
cd/m^2	candela/m^2	0.2919	foot-Lamberts	fl
		FORCE and PRESSURE or STRESS		
N	newtons	0.225	Poundforce	lbf
kPa	kilopascals	0.145	poundforce per square inch	lbf/in^2

*SI is the symbol for the International System of Units. Appropriate rounding should be made to comply with Section 4 of ASTM E380 (Revised March 2003)

1. INTRODUCTION

1.1 Background

Warm-mix asphalt is a relatively new technology. It has been developed in response to needs for reduced energy consumption and stack emissions during the production of asphalt concrete, long hauls, lower placement temperatures, improved workability, and better working conditions for plant and paving crews. Studies in the United States and Europe indicate that significant reductions in production and placement temperatures are possible.

Research initiatives on warm-mix asphalt are currently being conducted in a number of states, as well as by the Federal Highway Administration and the National Center for Asphalt Technology (NCAT). Accelerated pavement testing experiments are being carried out at NCAT.

The California Department of Transportation (Caltrans) has expressed interest in warm-mix asphalt with a view to reducing stack emissions at plants, to allow longer haul distances between asphalt plants and construction projects, to improve construction quality (especially during nighttime closures), and to extend the annual period for paving. However, the use of warm-mix asphalt technologies requires incorporating an additive into the mix, and/or changes in production and construction procedures, specifically related to temperature, which could influence the short- and long-term performance of the pavement. Consequently, the need for research was identified by Caltrans to address a range of concerns related to these changes before statewide implementation of the technology is approved.

1.2 Project Objectives

The research presented in this report is part of Partnered Pavement Research Center Strategic Plan Element 4.18 (PPRC SPE 4.18), titled "Warm-Mix Asphalt Study," undertaken for Caltrans by the University of California Pavement Research Center (UCPRC). The objective of this multi-phase project is to determine whether the use of additives intended to reduce the production and construction temperatures of asphalt concrete influence mix production processes, construction procedures, and the short-, medium-, and/or long-term performance of hot-mix asphalt. The potential benefits of using the additives will also be quantified. This is to be achieved through the following tasks:

- Develop a detailed workplan *(1)* for Heavy Vehicle Simulator (HVS) and laboratory testing *(Completed in September 2007).*
- Construct test tracks (subgrade preparation, aggregate base-course, tack coat, and asphalt wearing course) at the Graniterock A.R. Wilson quarry near Aromas, California *(completed in September*

2007 for the Phase 1 and Phase 2 studies), and at the UCPRC facility in Davis, California *(completed in April 2010 for the Phase 3 study)*.

- Undertake HVS testing in separate phases, with later phases dependent on the outcome of earlier phases and laboratory tests *(Phase 1 [rutting on HMA/WMA] was completed in April 2008, Phase 2 [moisture sensitivity on HMA/WMA] was completed in July 2009, and Phase 3 [rutting on RHMA-G/RWMA-G] was completed in July 2011).*
- Carry out a series of laboratory tests to assess rutting and fatigue behavior *(Phase 1 [plant-mixed, field-compacted] completed in August 2008, Phase 2a [plant-mixed, laboratory-compacted] completed in August 2009, Phase 2b [laboratory-mixed, laboratory-compacted] was completed in June 2010, and Phase 3 [plant-mixed, field-compacted] was completed in June 2011).*
- Prepare a series of reports describing the research.
- Prepare recommendations for implementation.

Selected pilot studies with warm-mix technologies on in-service pavements will also be monitored as part of the study.

1.3 Overall Project Organization

This UCPRC project has been planned as a comprehensive study to be carried out in a series of phases, with later phases dependent on the results of the initial phase. The planned testing phases include *(1)*:

- Phase 1 compared early rutting potential at elevated temperatures (pavement temperature of 122°F at 2.0 in. [50°C at 50 mm]). HVS trafficking began approximately 45 days after construction. Cores and beams sawn from the sections immediately after construction were subjected to rutting, fatigue, cracking, and moisture sensitivity testing in the laboratory. The workplan dictated that moisture sensitivity, additional rutting, and fatigue testing with the HVS would be considered if the warm-mix asphalt concrete mixes performed differently than the conventional mixes. The results from this phase are discussed in a report entitled *Warm-Mix Asphalt Study: Test Track Construction and First-Level Analysis of Phase 1 HVS and Laboratory Testing (2).*
- Depending on the outcome of laboratory testing for moisture sensitivity, a testing phase, if deemed necessary, would assess general performance under dry and wet conditions with special emphasis on moisture sensitivity. Phase 1 laboratory testing indicated a potential for moisture damage, prompting initiation of a second phase. Phase 2 compared rutting potential at elevated temperatures (pavement temperature of 122°F at 2.0 in. [50°C at 50 mm] pavement depth) and under wet conditions. HVS trafficking started approximately 90 days after completion of the Phase 1 HVS testing (12 months after construction). The results from Phase 2 are discussed in two reports entitled *Warm-Mix Asphalt Study: First-Level Analysis of Phase 2 HVS and Laboratory Testing, and Phase 1 and Phase 2 Forensic Assessments (3)* and *Warm-Mix Asphalt Study: First-Level Analysis of Phase 2b Laboratory Testing on Laboratory Prepared Specimens (4).*
- Depending on the outcome of laboratory testing for rutting, a testing phase, if deemed necessary, would assess rutting performance on artificially aged test sections at elevated temperatures (122°F at 2.0 in. [50°C at 50 mm]). The actual process used to artificially age the sections was not finalized, but it would probably follow a protocol developed by the Florida Department of

Transport Accelerated Pavement Testing program, which uses a combination of infrared and ultraviolet radiation. Phase 1 laboratory testing results and Phase 2 HVS testing results provided no indication of increased rutting on aged sections and consequently this phase was not undertaken.

- Depending on the outcome of the laboratory study for fatigue, a testing phase, if deemed necessary, would assess fatigue performance at low temperatures (59°F at 2.0 in. [15°C at 50 mm]). Phase 1 laboratory testing did not indicate that the warm-mix asphalt technologies tested would influence fatigue performance and consequently this phase was not undertaken.
- Depending on the outcome of the above testing phases and if agreed upon by the stakeholders (Caltrans, warm-mix technology suppliers), the sequence listed above or a subset of the sequence would be repeated for gap-graded rubberized asphalt concrete (RHMA-G), and again for open-graded mixes. The testing of gap-graded rubberized mixes was undertaken in two subphases and is discussed in this report and in a companion report entitled *Warm-Mix Asphalt Study: Test Track Construction and First-Level Analysis of Phase 3b HVS and Laboratory Testing (Rubberized Asphalt, Mix Design #2) (5).*
- Periodic assessment of the performance of gap-graded mixes in full-scale field experiments. This work is discussed in a separate report on that study entitled *Warm-Mix Asphalt Study: Field Test Performance Evaluation (6).*

This test plan is designed to evaluate short-, medium-, and long-term performance of the mixes.

- Short-term performance is defined as failure by rutting of the asphalt-bound materials.
- Medium-term performance is defined as failure caused by moisture and/or construction-related issues.
- Long-term performance is defined as failure from fatigue cracking, reflective cracking, and/or rutting of the asphalt-bound and/or unbound pavement layers.

The following questions, raised by Caltrans staff in a pre-study meeting, will be answered during the various phases of the study *(1)*:

- What is the approximate comparative energy usage between HMA and WMA during mix preparation? This will be determined from asphalt plant records/observations in pilot studies where sufficient tonnages of HMA and WMA are produced to undertake an assessment.
- Can satisfactory compaction be achieved at lower temperatures? This will be established from construction monitoring and subsequent laboratory tests.
- What is the optimal temperature range for achieving compaction requirements? This will be established from construction monitoring and subsequent laboratory tests.
- What are the cost implications? These will be determined with basic cost analyses from pilot studies where sufficient tonnages of HMA and WMA are produced to undertake an assessment.
- Does the use of warm-mix asphalt technologies influence the rutting performance of the mix? This will be determined from all HVS and laboratory tests.
- Is the treated mix more susceptible to moisture sensitivity given that the aggregate is heated to lower temperatures? This will be determined from Phase 1 laboratory tests and Phase 2 HVS testing.

- Does the use of warm-mix asphalt technologies influence fatigue performance? This will be determined from Phase 1 and Phase 2 laboratory tests and potential additional laboratory and HVS testing.
- Does the use of warm-mix asphalt technologies influence the performance of the mix in any other way? This will be determined from HVS and laboratory tests, and from field observations (all phases).
- If the experiment is extended to rubberized gap-graded and standard, rubberized, and polymer-modified open-graded mixes, are the impacts of using the warm-mix technologies in these mixes the same as for conventional dense-graded mixes?

1.3.1 Project Deliverables

Deliverables from the study will include:

- A detailed workplan for the entire study *(1)*;
- A report detailing construction, first-level data analysis of the Phase 1 HVS testing, first-level data analysis of the Phase 1 laboratory testing, and preliminary recommendations *(2)*;
- A report detailing first-level data analysis of the Phase 2 HVS testing, first-level data analysis of the Phase 2a laboratory testing, Phase 1 and Phase 2 forensic investigations, and preliminary recommendations *(3)*;
- A report detailing first-level analysis of the Phase 2b laboratory testing on laboratory-mixed, laboratory-compacted specimens *(4);*
- A report detailing first-level data analysis of the Phase 3a (mixes produced at Granite Construction's Bradshaw plant) HVS testing, first-level data analysis of the Phase 3a laboratory testing, Phase 3a forensic investigation, and preliminary recommendations *(5)*;
- A report detailing first-level data analysis of the Phase 3b (mixes produced at George Reed's Marysville plant) HVS testing, first-level data analysis of the Phase 3b laboratory testing, Phase 3b forensic investigation, and preliminary recommendations (this report)*;*
- A report summarizing periodic observations from test sections on in-service pavements *(6)*; and
- A summary report for the entire study.

A series of conference and journal papers documenting various components of the study will also be prepared.

1.4 Structure and Content of this Report

1.4.1 Warm-Mix Technologies Tested

In the Phase 1 and Phase 2 studies, the three most prominent warm mix technologies (*Advera WMA*®, *Evotherm DAT*™, and *Sasobit*®) were assessed. During that testing phase numerous other technologies were developed and consequently additional technologies, specifically those based on water injection (or mechanical foam), were considered for the Phase 3 study. The technologies assessed were selected based on participation of warm-mix technology providers in the Caltrans Warm-mix Asphalt Technical Working Group. Given that two different water injection technologies would be tested and that these technologies are asphalt plant-specific (i.e., they are integral components of the asphalt plant), the Phase 3 study tested

mixes from two different asphalt plants. Since two different aggregate sources and consequently two different mix designs were used, testing and reporting has been undertaken in two subphases to limit inappropriate performance comparisons, as follows:

- Phase 3a: Mix Design #1 using mixes produced at the Granite Construction Bradshaw Plant (companion report *[5]*)
  - Hot-mix control
  - *Gencor Ultrafoam GX™*, water injection technology, referred to as Gencor in this report
  - *Evotherm DAT™*, chemical surfactant technology, referred to as Evotherm in this report
  - *Cecabase RT®*, chemical surfactant technology, referred to as Cecabase in this report
- Phase 3b: Mix Design #2 using mixes produced at the George Reed Construction Marysville Plant (this report)
  - Hot-mix control
  - *Astec Double Barrel Green®*, water injection technology, referred to as Astec in this report
  - *Sasobit®*, organic wax technology, referred to as Sasobit in this report
  - *Advera WMA®*, chemical water foaming technology, referred to as Advera in this report
  - *Rediset™*, chemical surfactant technology, referred to as Rediset in this report.

1.4.2 Report Layout

This report presents an overview of the work carried out in Phase 3b to continue meeting the objectives of the study, and is organized as follows:

- Chapter 2 summarizes the HVS test track location, design, and construction.
- Chapter 3 details the HVS test section layout and HVS test criteria.
- Chapter 4 provides a summary of the Phase 3b HVS test data collected from each test.
- Chapter 5 details the forensic investigations undertaken on each HVS test section after testing.
- Chapter 6 discusses the Phase 3b laboratory testing on specimens sampled from the test track.
- Chapter 7 provides conclusions and preliminary recommendations.

1.5 Measurement Units

Although Caltrans has recently returned to the use of U.S. standard measurement units, metric units have always been used by the UCPRC in the design and layout of HVS test tracks, and for laboratory and field measurements and data storage. In this report, both English and metric units (provided in parentheses after the English units) are provided in general discussion. In keeping with convention, only metric units are used in HVS and laboratory data analyses and reporting. A conversion table is provided on page xx at the beginning of this report.

1.6 Terminology

The term “asphalt concrete” is used in this report as a general descriptor for the surfacing on the test track. The terms “hot-mix asphalt (HMA)” and “warm-mix asphalt (WMA)” are used as descriptors to differentiate between the control and warm-mixes discussed in this study.

2. TEST TRACK LOCATION, DESIGN, AND CONSTRUCTION

2.1 Experiment Location

The Phase 3 warm-mix asphalt experiment is located on the North Test Track at the University of California Pavement Research Center facility in Davis, California. An aerial view of the site is shown in Figure 2.1. This was the first test undertaken on this test track.

Figure 2.1: Aerial view of the UCPRC research facility.

2.2 Test Track Layout

The North Test Track is 361 ft. (110 m) long and 49.2 ft (15 m) wide. It has a two percent crossfall in a north-south direction. For the study, the track was divided into nine equal cells, 120.4 ft. (36.7 m) long and 16.4 ft. (5.0 m) wide for the study. Its layout is shown in Figure 2.2, with Cells 1 through 4 used in the Phase 3a study (Control, Gencor, Evotherm, and Cecabase, respectively) *(5)* and Cells 5 though 9 (Sasobit, Advera, Control, Astec, and Rediset, respectively) used in the Phase 3b study. All test track measurements and locations discussed in this report are based on this layout.

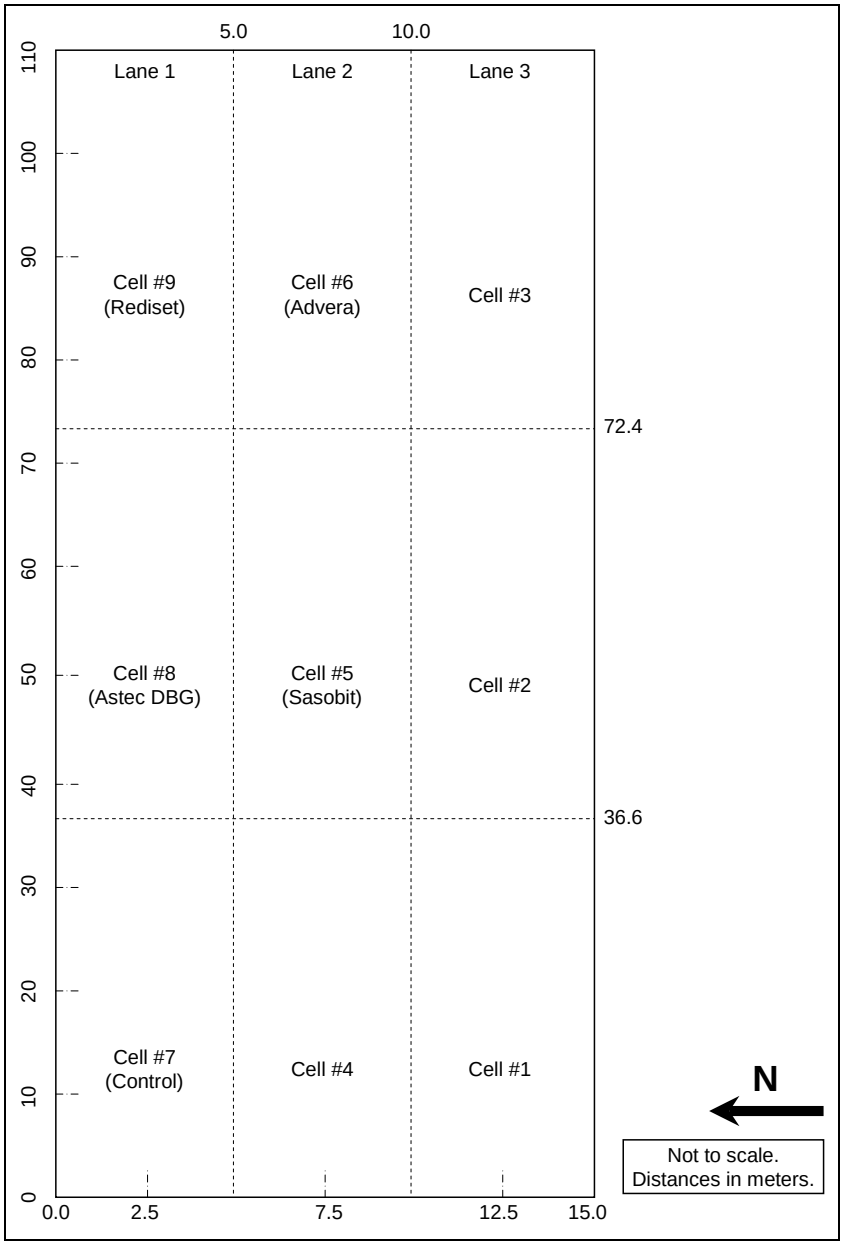

Figure 2.2: Test track layout.

2.3 Pavement Design

Dynamic cone penetrometer (DCP) tests were performed along the center lines of each lane over the length and width of the test track (Figure 2.3) prior to any construction to obtain an indication of the in situ subgrade strength. Results are summarized in Table 2.1. Penetration rates varied between 11 mm per blow and 30 mm per blow, with the weakest areas in the middle of the track spanning Cells 5 and 6. Variation was attributed to the degree of soil mixing, temporary stockpiling of lime-treated soils (lime treatment was used to dry the soil in some areas of the site), and to compaction from equipment during construction of the facility, and to varying subgrade moisture contents.

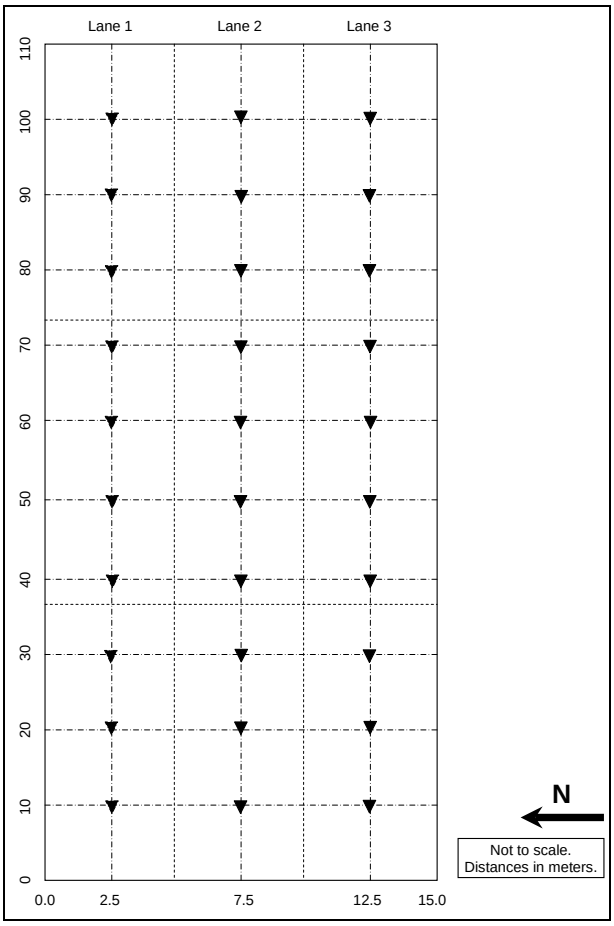

Figure 2.3: DCP test locations.

Table 2.1: Summary of DCP Survey on Subgrade Material

Test Location[1] (m)	Penetration Rate (mm/blow)			Estimated California Bearing Ratio[2]			Estimated Stiffness (MPa)[2]		
	Lane #1	Lane #2	Lane #3	Lane #1	Lane #2	Lane #3	Lane #1	Lane #2	Lane #3
10	17	21	19	11	9	9	56	41	44
20	16	18	15	12	10	13	60	46	63
30	14	16	13	14	12	15	66	60	71
40	13	22	16	15	8	12	71	40	60
50	13	26	15	15	6	13	71	36	63
60	12	25	16	17	6	12	77	37	60
70	15	30	15	13	5	13	63	30	63
80	14	28	15	14	5	13	66	34	63
90	12	26	14	17	6	14	77	36	66
100	11	20	15	19	9	13	85	42	63

[1] Measured from southwest corner of the track. [2] Estimated from DCP software tool.

A sensitivity analysis of potential pavement designs using layer elastic theory models was carried out using the DCP results obtained during the site investigation and estimates, based on previous experience, of the moduli of a representative aggregate base-course and asphalt concrete surfacing. Components of the sensitivity analysis included the following 24 cells:

- Three asphalt concrete thicknesses (100 mm, 125 mm, and 150 mm)
- Three asphalt concrete moduli (600 MPa, 1,000 MPa, and 3,000 MPa)
- Two base-course thicknesses (300 mm and 450 mm)
- Two base-course moduli (150 MPa and 300 MPa)
- One subgrade (existing soil with modulus of 60 MPa).

A test pavement design was selected to maximize the information that would be collected about the performance of warm-mix asphalt, taking into consideration that a very strong pavement would lengthen the testing time before results (and an understanding of the behavior) could be obtained, while a very weak pavement could fail before any useful data was collected. The pavement design shown in Figure 2.4 was considered appropriate for the study.

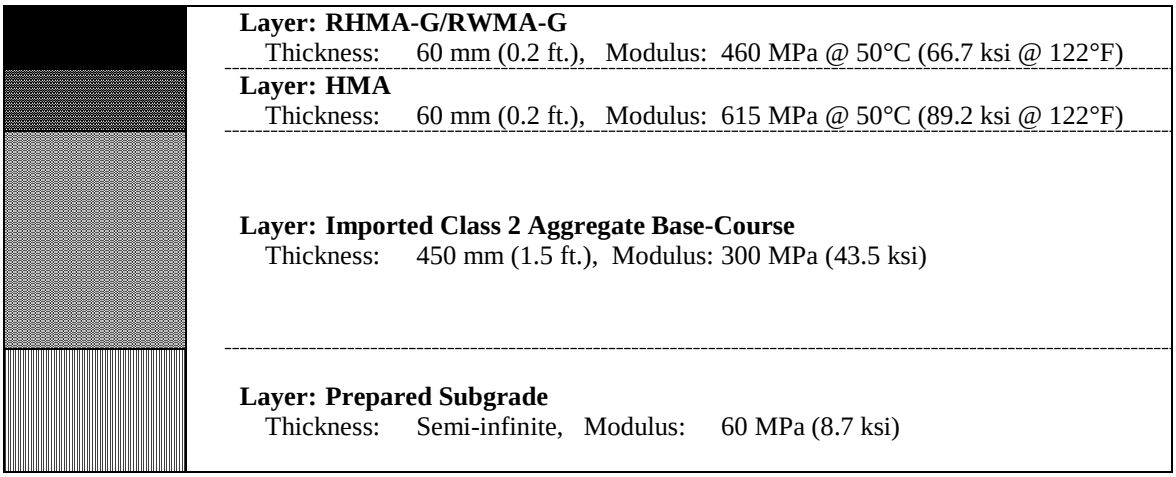

Figure 2.4: Pavement structure for rubberized warm-mix asphalt test sections.

2.4 Subgrade Preparation

2.4.1 Equipment

The following equipment was used for preparation of the subgrade:

- Water tanker (4,000 gal. [15,000°L])
- Caterpillar 163H grader
- Caterpillar 623F scraper
- Caterpillar 815F padfoot roller
- Ingersoll Rand SD-115-D vibrating steel drum roller

2.4.2 Preparation

The subgrade was prepared on September 22, 2009. Preparation included vegetation removal, preliminary leveling, ripping, watering and mixing, compaction, and final leveling to include a two percent north–south crossfall as follows:

- Removing vegetation with a grader, windrowing the deleterious material toward the center of the track, collecting this material with a scraper and dumping it in a temporary stockpile for removal (Figure 2.5).
- Preliminary leveling with a grader followed by watering (Figure 2.6).
- Ripping to a depth of 12 in. (300 mm) (Figure 2.7).
- Watering and mixing using both the scraper and grader (Figure 2.8). Pockets of high clay content soils were observed during this process, which required additional working with the grader and scraper to break up the clods (Figure 2.9).
- Initial compaction with a padfoot roller (Figure 2.10). Despite extensive mixing, some clay pockets were still observed after completion of the initial compaction, with padfoot impressions clearly visible (Figure 2.11). Clay pockets appeared to predominate on the eastern half of the track.
- Final compaction with a vibrating smooth drum roller (Figure 2.12).
- Final leveling with a grader.
- Density checks on the finished surface (Figure 2.13) with a nuclear density gauge.

Figure 2.5: Vegetation removal.

Figure 2.6: Preliminary leveling.

Figure 2.7: Ripping.

Figure 2.8: Watering and mixing.

Figure 2.9: Breaking up of clay clods.

Figure 2.10: Initial compaction.

Figure 2.11: Padfoot impressions in clay pockets.

Figure 2.12: Final compaction.

Figure 2.13: Final subgrade surface.

2.4.3 Quality Control

Quality control of the subgrade preparation was limited to density checks with a nuclear gauge following Caltrans Test Method CT 231 and comparison of the results against a laboratory maximum density of 134.2 lb/ft^3 (2,150 kg/m^3) determined according to Caltrans Test Method CT 216. Nuclear gauge measurements were taken at 10 different locations selected according to a nonbiased plan shown in Figure 2.14. Samples for laboratory density determination were taken at locations 1, 2 and 3. Results are summarized in Table 2.2 and indicate that the subgrade density was generally consistent across the test track. Relative compaction varied between 99.2 percent and 98.8 percent with an average of 97.0 percent, two percent above the Caltrans-specified minimum density of 95 percent for subgrade compaction *(7)*. No location had a relative compaction lower than this minimum.

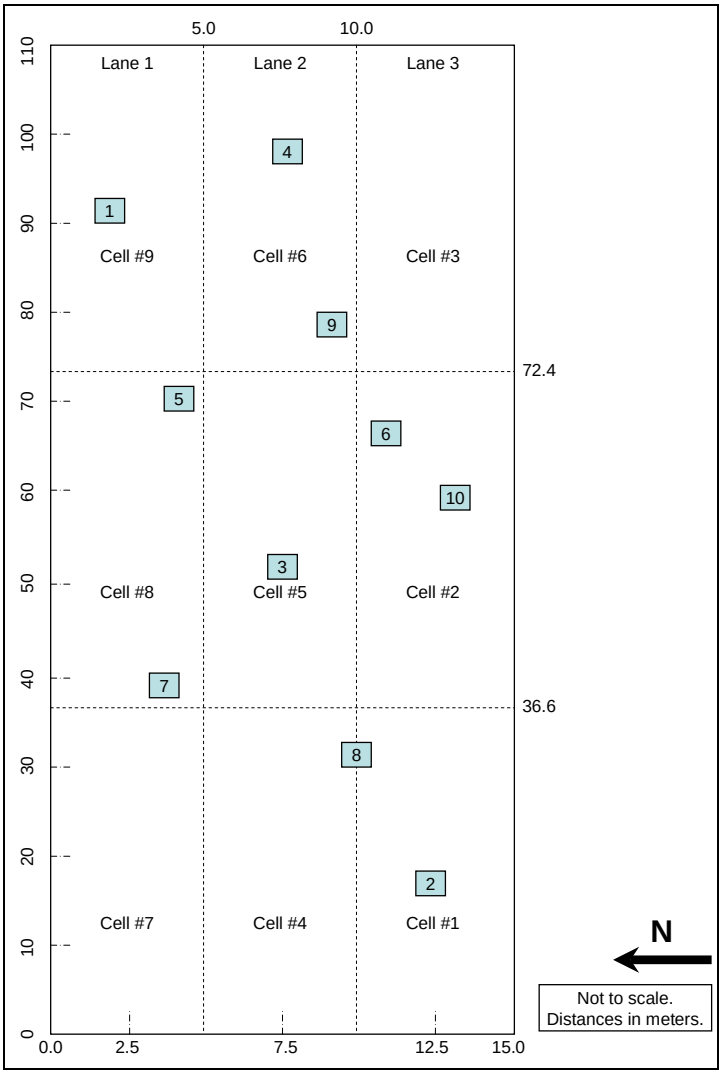

Figure 2.14: Location of subgrade density measurements.

Table 2.2: Summary of Subgrade Density Measurements

Location	Wet Density		Moisture Content	Dry Density		Relative Compaction
	(lb/ft^3)	(kg/m^3)	(%)	(lb/ft^3)	(kg/m^3)	(%)
1	130.5	2,091	15.6	112.6	1,804	97.3
2	132.6	2,124	17.3	113.1	1,811	98.8
3	131.3	2,103	16.8	112.4	1,801	97.8
4	130.2	2,086	16.2	112.1	1,796	97.0
5	133.2	2,133	15.2	115.6	1,852	99.2
6	128.9	2,065	17.8	109.5	1,754	96.0
7	132.2	2,117	17.9	112.1	1,795	98.5
8	128.1	2,052	18.7	107.9	1,728	95.4
9	132.3	2,120	16.5	113.6	1,820	98.6
10	128.7	2,062	15.0	111.9	1,793	95.9
Average	130.8	2,095	17.0	112.1	1,795	97.0
Std. Dev.	1.8	29	1.2	2.1	34	1.3

2.5 Base-Course Construction

2.5.1 Material Properties

Base-course aggregates were sourced from Teichert's Cache Creek quarry. Key material properties are summarized in Table 2.3. The material met Caltrans specifications, except for the percent passing the #200 sieve, which exceeded the specification operating range by 3.0 percent, and just met the contract compliance limits.

Table 2.3: Base-course Material Properties

Property			Result	Operating Range	Contract Compliance
Grading:	1"	(25 mm)	100	100	100
	3/4"	(19 mm)	99.1	90 – 100	87 – 100
	1/2"	(12.5 mm)	90.1	–	–
	3/8"	(9.5 mm)	83.5	–	–
	#4	(4.75 mm)	63.3	35 – 60	30 – 65
	#8	(2.36 mm)	48.8	–	–
	#16	(1.18 mm)	39.2	–	–
	#30	(600 µm)	30.8	10 – 30	5 – 35
	#50	(300 µm)	21.6	–	–
	#100	(150 µm)	15.6	–	–
	#200	(75 µm)	12.3	2 – 9	0 – 12
Liquid Limit			Non-plastic	–	–
Plastic Limit				–	–
Plasticity Index				–	–
Maximum Dry Density (lbs/ft^3/kg/m^3)			140.6 (2,252)	–	–
Optimum Moisture Content			6.0	–	–
R-Value			79	–	>78
Sand equivalent			30	25	>22
Durability index – course			78	–	>35
Durability index – fine			52	–	>35

2.5.2 Equipment

The following equipment was used during the construction of the base-course:

- Water tanker (4,000 gal. [15,000 L])

- Caterpillar 163H grader
- Caterpillar 623F scraper
- Ingersoll Rand SD-115-D vibrating steel drum roller

2.5.3 Construction

The test track base-course was constructed on September 24, 2009, two days after the subgrade preparation. The construction process included aggregate spreading, watering, compaction, and final leveling to include a two percent north-south crossfall as follows:

- Transporting crushed base-course material (alluvial) that complied with Caltrans Class 2 aggregate base-course specifications from Teichert's Cache Creek aggregate source to the test track with a fleet of bottom-dump trucks and trailers.
- Dumping the aggregate in windrows (Figure 2.15).
- Spreading the aggregate with a grader (Figure 2.16) to a thickness of approximately 4.0 in. (100 mm).
- Adding water to bring the aggregate to the optimum moisture content and re-mixing with the grader to ensure even distribution of the moisture throughout the material (Figure 2.17).
- Initial compaction of the spread material with a vibrating steel wheel roller (Figure 2.18).
- Repeating the process until the design thickness of 1.5 ft. (450 mm) was achieved.
- Applying a generous application of water (Figure 2.19) followed by compaction to pump fines to the surface to provide good aggregate interlock (slushing).
- Final leveling with a grader (Figure 2.20). Final levels were checked with a total station to ensure that a consistent base-course thickness had been achieved.
- Removal of excess material with a scraper followed by final compaction (Figure 2.21).
- Density checks on the finished surface with a nuclear density gauge.

Figure 2.15: Dumping material in windrows.

Figure 2.16: Material spreading.

Figure 2.17: Watering.

Figure 2.18: Initial compaction.

Figure 2.19: Heavy watering prior to pre-final compaction.

Figure 2.20: Final leveling with a grader.

Figure 2.21: Removing excess material and final compaction.

2.5.4 Quality Control

Quality control of the base-course construction was limited to density checks with a nuclear gauge following Caltrans Test Method CT 231 and comparison of the results against a laboratory maximum wet density of 150.5 lb/ft^3 (2,410 kg/m^3) determined according to Caltrans Test Method CT 216. Nuclear gauge measurements were taken at 10 different locations selected according to a nonbiased plan shown in Figure 2.22. A sample for laboratory density determination was taken at Location #1. Results are summarized in Table 2.4 and indicate that the base-course density properties were generally consistent across the test track, but that the material was relatively wet compared to the laboratory-determined optimum moisture content. Relative compaction varied between 96.7 percent and 99.4 percent with an average of 98.0 percent, three percent above the Caltrans-specified minimum density of 95 percent for base compaction *(7)*. No location had a relative compaction lower than this minimum.

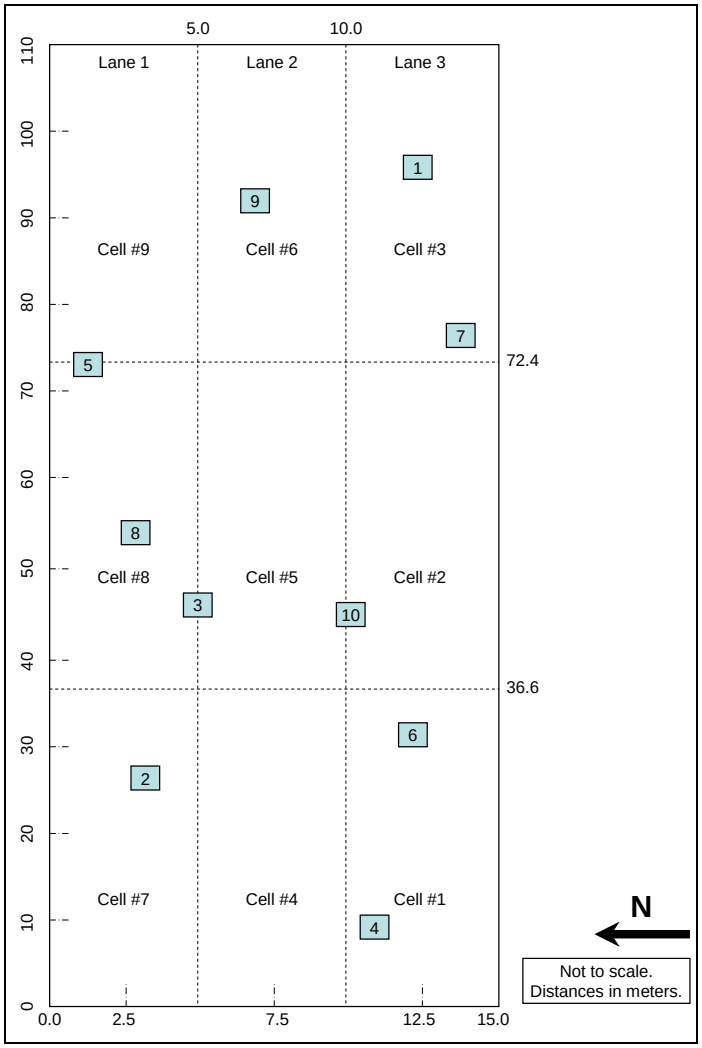

Figure 2.22: Location of base density measurements.

Table 2.4: Summary of Nuclear Gauge Base-Course Density Measurements

Location	Wet Density		Moisture Content	Dry Density		Relative Compaction
	(lb/ft^3)	(kg/m^3)	(%)	(lb/ft^3)	(kg/m^3)	(%)
1	146.5	2,346	6.6	137.4	2,201	97.3
2	148.5	2,379	7.0	138.8	2,223	98.7
3	148.0	2,371	8.0	137.0	2,195	98.4
4	147.1	2,356	7.8	136.5	2,186	97.8
5	148.7	2,382	6.3	139.9	2,241	98.8
6	145.5	2,330	6.8	136.2	2,182	96.7
7	149.0	2,387	8.2	137.7	2,206	99.0
8	145.6	2,332	7.7	135.2	2,165	96.8
9	149.5	2,395	6.9	139.8	2,240	99.4
10	145.7	2,334	7.8	135.2	2,165	96.8
Average	147.4	2,361	7.3	137.3	2,200	98.0
Std. Dev.	1.5	25	0.7	1.7	27.6	1.0

2.5.5 Follow-Up Testing Prior to Paving

Paving of the first lift of asphalt concrete was scheduled for October 7, 2009. However, contractor scheduling and then rainfall on four days (October 13, 14, 15, and 19) delayed priming of the surface until October 23, 2009, and paving until October 30, 2009. Rainfall measured over the four days totaled 3.1 in. (78 mm). Some ponding of water in Cells #1 and #2 on the western end of the test track was observed during these rainfall events (Figure 2.23).

Figure 2.23: Ponding of water on base.

Dynamic cone penetrometer (DCP) measurements were undertaken on the base at the same locations as the original subgrade DCP survey (Figure 2.3) to assess whether the rainfall had weakened the base on any parts of the track. The results are summarized in Table 2.5 and indicate that although average penetration rates (mm/blow) were consistent across the track, there was considerable difference in the average calculated stiffness of the base from the redefined layers based on actual penetration. Consequently, the contractor was requested to recompact the track with a static steel drum roller prior to priming to consolidate the base layer and accelerate movement of infiltrated water to the surface.

A significant improvement in subgrade stiffness attributed to the subgrade preparation and confinement by the base was also noted.

Table 2.5: Summary of DCP Survey on Base and Subgrade Material

Test Location (m)[1]	Penetration Rate (mm/blow)						Estimated Stiffness (MPa [ksi])[2]					
	Base			Subgrade			Base			Subgrade		
	Lane			Lane			Lane			Lane		
	#1	#2	#3	#1	#2	#3	#1	#2	#3	#1	#2	#3
10	3	-	-	9	-	-	430 (62)	-	-	111 (16)	-	-
20	-	3	-	-	8	-	-	395 (57)	-	-	119 (17)	-
30	-	-	3	-	-	7	-	-	320 (46)	-	-	139 (20)
40	4	-	-	9	-	-	332 (48)	-	-	114 (17)	-	-
50	-	4	-	-	9	-	-	299 (43)	-	-	107 (16)	-
60	-	-	4	-	-	9	-	-	279 (41)	-	-	137 (20)
70	4	-	-	10	-	-	255 (37)	-	-	99 (14)	-	-
80	-	4	-	-	10	-	-	260 (38)	-	-	105 (15)	-
90	-	-	4	-	-	7	-	-	273 (40)	-	-	148 (22)
100	4	-	-	11	-	-	259 (38)	-	-	116 (17)	-	-

[1] Measured from southwest corner of the track. [2] Estimated from DCP software tool.

2.6 Bottom Lift Asphalt Concrete Construction

2.6.1 Material Properties

Dense-graded asphalt concrete for the bottom lift was sourced from Teichert's Woodland Asphalt Plant. Key material properties are summarized in Table 2.6. The material met Caltrans specifications.

Table 2.6: Key Bottom Lift HMA Mix Design Parameters

Parameter			Wearing Course			
			Actual	Target	Specification	Compliance
Grading:	1"	(25 mm)	100	100	100	100
	3/4"	(19 mm)	98	100	100	100
	1/2"	(12.5 mm)	84	98	90 – 100	90 – 100
	3/8"	(9.5 mm)	75	83	77 – 89	76 – 90
	#4	(4.75 mm)	52	40	33 – 47	30 – 44
	#8	(2.36 mm)	34	23	18 – 28	6 – 26
	#16	(1.18 mm)	22	–	–	–
	#30	(600 µm)	15	12	–	–
	#50	(300 µm)	9	–	–	–
	#100	(150 µm)	6	–	–	–
	#200	(75 µm)	4	5	3 – 7	0 – 8
Asphalt binder grade			PG 64-16	-	–	-
Asphalt binder content (% by aggregate mass)			5.0	–	–	–
Hveem stability at optimum bitumen content			41.0	-	>37	-
Air-void content (%)			4.0	-	2 – 6	-
Dust proportion			0.9	-	0.6 – 1.3	-
Voids in mineral aggregate (LP-2) (%)			13.0	-	>13	-
Voids filled with asphalt (LP-3) (%)			69.0	-	65 – 75	-
Crushed particles (1 face) (%)			92	-	>90	-
Sand equivalent (%)			71.0	-	>47	-
Fine aggregate angularity (%)			54.0	-	>47	-
Los Angeles Abrasion at 100 repetitions (%)			5.0	-	<12	-
Los Angeles Abrasion at 500 repetitions (%)			21.3	-	<45	-

2.6.2 Equipment

The following equipment was used during the construction of the bottom lift of asphalt concrete:

- Terex Cedar Rapids CR552 paver and material transfer device
- Caterpillar CB-534D vibrating steel twin-drum roller (two)
- Ingersoll Rand PT-240R pneumatic tire roller

2.6.3 Prime Coat Application

On the day before the prime coat application (October 22, 2009), the test track was compacted with a twin-drum steel roller to consolidate the base layer and accelerate movement of infiltrated water to the surface. An SS-1 asphalt emulsion prime coat was applied to the surface at a rate of 0.25 gal./yd^2 (1.0 L/m^2). The time of application was 1:00 p.m., ambient temperature was 88°F (35°C) and relative humidity was 28 percent. A consistent application was achieved (Figure 2.24); however, differential penetration was observed, which was attributed to patches of near-surface moisture (Figure 2.25).

Figure 2.24: Prime coat application.

Figure 2.25: Differential penetration of prime coat.

2.6.4 Asphalt Placement

The bottom lift of asphalt concrete was placed on October 30, 2009. Construction started at approximately 8:30 a.m. Ambient air temperature was 50°F (10°C) and the relative humidity was 45 percent. Construction was completed at approximately 11:00 a.m. when ambient temperature was 61°F (16°C) and the relative humidity was 40 percent.

Mix was transported using bottom-dump trucks and placed in a windrow on the surface. Paving started in Lane #1, followed by Lanes #2 and #3, and was carried out in a west–east direction. A pickup machine connected to the paver collected the material and fed it into the paver hopper. Paving followed conventional procedures. The breakdown roller closely followed the paver applying about four passes. A

single pass was made with the intermediate rubber-tired roller, followed by another four passes with the finish roller. The construction process is summarized in Figure 2.26.

Placing asphalt in windrow

Paving and breakdown rolling

Intermediate rolling

Final rolling

Figure 2.26: Construction of bottom lift asphalt concrete layer.

2.6.5 Construction Quality Control

Compaction was measured by the UCPRC using a nuclear gauge on the day after construction using the mix design specific gravity values. Measurements were taken at 33 ft. (10 m) intervals along the centerline of each lane, with a focus on checking densities in the areas that would be used for HVS testing. A summary of the results is provided in Table 2.7. The results indicate that there was very little variability in the measurements and that satisfactory compaction had been achieved.

Table 2.7: Summary of Bottom Layer Asphalt Concrete Density Measurements

Position	Lane #1			Lane #2			Lane #3		
	Gauge		Relative	Gauge		Relative	Gauge		Relative
	lb/ft^3	kg/m^3	(%)	lb/ft^3	kg/m^3	(%)	lb/ft^3	kg/m^3	(%)
1	146.0	2,339	93	148.3	2,376	95	146.0	2,338	93
2	145.3	2,328	93	148.3	2,375	95	145.5	2,330	93
3	147.8	2,367	95	148.6	2,380	95	145.3	2,327	93
4	149.2	2,390	95	147.1	2,357	94	146.5	2,346	94
5	146.1	2,341	93	145.6	2,333	93	147.8	2,367	95
6	146.5	2,346	94	148.7	2,382	95	146.1	2,341	93
7	145.2	2,326	93	145.8	2,336	93	147.7	2,366	94
8	147.7	2,366	94	146.2	2,342	94	148.3	2,376	95
9	147.0	2,355	94	144.9	2,321	93	147.1	2,357	94
10	145.9	2,337	93	146.8	2,351	94	144.9	2,321	93
Average	146.7	2,350	94	146.5	2,347	94	146.5	2,347	94
Std. Dev.	1.3	0.020	0.8	1.4	0.019	0.8	1.2	0.019	0.8
RICE	2.504								

2.7 Rubberized Gap-Graded Asphalt Concrete Construction

2.7.1 Plant Modifications

Minor plant modifications were required to incorporate the Advera, Sasobit, and Rediset technologies. Customized equipment provided by the Advera and Sasobit suppliers was used. The Rediset technology was added using the Sasobit equipment. The *Astec Double Barrel Green* system was integral to the asphalt plant. All delivery systems were approved under the Caltrans Material Plant Quality Program.

2.7.2 Material Properties

A Caltrans-approved mix design, prepared by George Reed Construction Company's Marysville Plant to meet Caltrans specifications for 1/2 in. (12.5 mm) gap-graded rubberized hot-mix asphalt (RHMA-G), was used for the experiment. Key parameters for the mix design are summarized in Table 2.8. The mix design was not adjusted for accommodation of the warm-mix technologies.

2.7.3 Warm-Mix Technology Application Rates

The warm-mix additive application rates were determined by the additive suppliers and were as follows:

- Advera: 4.5 percent by mass of binder
- Astec (water): 1.5 percent by mass of binder
- Rediset: 2.0 percent by mass of binder
- Sasobit: 1.5 percent by mass of binder

2.7.4 Mix Production Temperatures

Mix production and paving temperatures were not set for the project. Instead, each technology provider was requested to select their own production temperatures based on ambient temperatures, haul distance, and discussions with the plant manager. Production temperatures were set as follows:

- Control: 335°F (166°C)
- Advera: 295°F (145°C)
- Astec: 295°F (145°C)
- Rediset: 285°F (140°C)
- Sasobit: 300°F (149°C)

Table 2.8: Key RHMA-G Mix Design Parameters

Parameter			Wearing Course		
			Target	Specification	Compliance
Grading:	3/4"	(19 mm)	100	100	100
	1/2"	(12.5 mm)	98	90 – 100	90 – 100
	3/8"	(9.5 mm)	83	77 – 89	76 – 90
	#4	(4.75 mm)	40	33 – 47	30 – 44
	#8	(2.36 mm)	23	18 – 28	6 – 26
	#16	(1.18 mm)	–	–	–
	#30	(600 µm)	12	–	–
	#50	(300 µm)	–	–	–
	#100	(150 µm)	–	–	–
	#200	(75 µm)	5	3 – 7	0 – 8
Asphalt binder grade			PG 64-16	–	-
Asphalt binder source			Paramount	–	–
Asphalt binder content (% by mass of aggregate)			7.0	–	–
Rubber content (% by mass of binder)			19.0	18 – 22	-
Scrap tire rubber (%)			75.0	–	-
High natural rubber (%)			25.0	–	-
Extender oil (Raffex 120/Tricor, % by mass of binder)			2.0	–	-
Hveem stability at recommended bitumen content			45.0	23	-
Air-void content (%)			4.5	4 ± 2	-
Voids in mineral aggregate (LP-2) (%)			19.0	>18	-
Voids filled with asphalt (LP-3) (%)			70.0	65 – 75	-
Crushed particles (1 face) (%)			100.0	>90	-
Sand equivalent (%)			70.0	>47	-
Fine aggregate angularity (%)			46.0	>45	-
Los Angeles Abrasion at 100 repetitions (%)			3.0	<10	-
Los Angeles Abrasion at 500 repetitions (%)			15.0	<45	-

2.7.5 Mix Production

Mix production was overseen by technical representatives from each of the additive suppliers. Production started on April 8, 2010, at approximately 8:00 a.m., with the Control mix. No problems were experienced. Production of the Astec mix followed, but was halted after numerous attempts due to blockage of the binder nozzles on the foaming unit. Production of this mix was postponed until the system could be repaired. Production continued with the Sasobit, followed by the Advera mix. On completion of the Advera mix production, insufficient binder remained to produce the Rediset and Astec mixes, due to wastage in the earlier attempts to produce the Astec mix. Consequently production and placement of these mixes was planned for the following day; however, rain and contractor availability ultimately postponed production until April 15, 2010, and prompted the need to construct a second Control section.

Approximately 150 tonnes of each mix were produced. Mix was stored in insulated silos for a limited time before load out and transport. The first approximately 20 tonnes of each mix was "wasted" to ensure that a consistent mix was used on the test track. The drum plant was also run for a short period with no warm-mix technology at the end of each production run to prevent any contamination of the next mix. This material was also wasted.

Plant emissions were not monitored due to the small volume of each mix produced.

2.7.6 Mix Production Quality Control

Asphalt Binder

Certificates of compliance for the modified binder were provided by the binder supplier (International Surfacing Systems in Modesto) with the delivery to the Marysville plant on both production days. Base binder was sourced from the same tank and batch for both days' production.

Asphalt Mix

Quality control of the mixes produced for the test track was undertaken by George Reed Construction on mix sampled from the trucks at the silos. The results are summarized in Table 2.9. The following observations were made:

- The aggregate gradations met the targets and were within the required ranges for all mixes, although there were notable differences among the mixes.
- Binder contents were inconsistent across the mixes with only two mixes (Astec [8.4 percent] and Sasobit [8.0 percent]) falling within the compliance range (target of 8.3 percent). The Rediset mix (10.0 percent) was significantly above the target, while the Controls (7.7 and 7.6 percent) and Advera (7.6 percent) mixes were blow the target. These differences were taken into consideration in performance discussions in Chapter 4 and Chapter 6.
- Hveem stabilities varied among the mixes, but were all well above the minimum specified requirement of 23. Stabilities were dependent on binder content, as expected, with lower stabilities recorded on mixes with higher binder contents.
- Specific gravities also varied according to binder content, but were within an acceptable range.

2.7.7 Paving Equipment

The following equipment was used during placement of the rubberized asphalt layer:

- Terex Cedar Rapids CR552 paver and material transfer device
- Caterpillar CB-534D vibrating steel twindrum roller (two)

Table 2.9: Quality Control of Mix After Production

Parameter	Specification/ Target	Control #1	Sasobit	Advera	Control #2	Astec	Rediset
Grading[1]							
3/4" (19 mm)	100	100	100	100	100	100	100
1/2" (12.5 mm)	90 – 100	98	99	99	99	99	99
3/8" (9.5 mm)	78 – 88	87	85	87	87	87	82
#4 (4.75 mm)	32 – 42	39	38	41	39	39	33
#8 (2.36 mm)	17 – 25	20	22	23	21	24	17
#16 (1.18 mm)	-	12	14	15	13	16	11
#30 (0.6 mm)	7 – 15	8	10	11	9	10	8
#50 (0.3 mm)	-	6	7	7	6	7	5
#100 (0.15 mm)	-	4	5	5	5	5	4
#200 (0.075 mm)	2 – 7	3	4	4	4	4	3
Sand equivalent[2]	>47	73	74	74	73	73	80
AC binder content (%)[3]	8.3	7.7	8.0	7.6	7.6	8.4	10.0
Hveem stability	>23	43	37	40	40	35	34
RICE specific gravity[4]	-	2.505	2.502	2.497	2.485	2.485	2.467
Unit weight	-	2.388	2.395	2.379	2.369	2.377	2.387
Moisture (before plant) (%)	-	2.3	3.3	2.4	3.0	3.2	2.5
Moisture[6] (after silo) (%)	1.0	Not tested	Not tested	Not tested	Not tested	Not tested	Not tested

[1] CT 202 [2] CT 217 [3] CT 382 [4] CT 308 [5] CT 366 [6] CT 370

2.7.8 Tack Coat Application

The test track was broomed to remove dust and organic matter from the surface prior to any work. Tack coat was applied to Cells #5 and #6 in Lane #2 and to Cell #7 in Lane #3 in single passes just prior to the start of paving on the first day of construction, and to the remaining cells and second Control section just prior to the start of paving on the second day of construction (Figure 2.27). A diluted SS-1 emulsion (70:30) was applied with a distributor at an application rate of approximately 0.08 gal./yd^2 (0.36 L/m^2). Some steam was observed during application. Weather conditions at the time of tack coat application were as follows:

- Day #1 Construction
  - Air temperature: 45°F (7°C)
  - Surface temperature: 54°F (12°C)
  - Relative humidity: 85 percent
- Day #2 Construction
  - Air temperature: 46°F (8°C)
  - Surface temperature: 54°F (12°C)
  - Relative humidity: 75 percent

Lane #2, Cells #5 and #6 **Lane #3**

Figure 2.27: Tack coat application.

2.7.9 Asphalt Placement

Control Section #1

Placement of the asphalt concrete on the first Control section started at 10:10 a.m. with the positioning of the paver at the start of the section. Three loads were used. Some chunks were noted in the trucks, paver hopper, and behind the paver (Figure 2.28) and were attributed to cooling during transport. Chunks were removed and replaced with new mix. The paver reached the end of the section about 12 minutes after starting. Considerable smoke was observed from the trucks during tipping and from the paver (Figure 2.29). A pungent odor, typical of rubberized asphalt construction projects, was also noted. The paving crew wore respirators to limit the effects of these odors (Figure 2.30). Breakdown rolling started as soon as the paver was moved off of the section. Density and temperature measurements were taken

throughout (see Section 2.7.6). Seven passes were made with the breakdown roller with vibration over a period of approximately 15 minutes (Figure 2.31). Some cooling was allowed before final rolling, which consisted of five passes with no vibration (Figure 2.32). No significant tenderness was observed and the roller operator considered the exercise typical of normal rubberized asphalt projects. Paver spillage was removed from the end of the section to ensure a clean and regular surface and join for the Astec section.

Figure 2.28: Control #1: Chunks in mix.

Figure 2.29: Control #1: Smoke from truck and paver.

Figure 2.30: Control #1: Paver operator wearing respirator.

Figure 2.31: Control #1: Breakdown rolling.

Figure 2.32: Control #1: Final rolling.

Sasobit Section

The same process described above was followed for the placement of the Sasobit mix, which started at 11:30 a.m. No smoke was observed or odors noted (Figure 2.33). Breakdown rolling was achieved with eight passes, followed by a further five passes after a short period of cooling (Figure 2.34). Final rolling was completed in ten passes. No problems were observed during any of the compaction phases and a tightly bound surface was achieved. When interviewed, the roller operator noted that the mat was a little stiffer and responded a little differently than typical rubberized asphalt projects in that the response of the roller did not relate to the density measurements taken with the nuclear gauge. The operator had considered compaction to be complete; however, the density gauge indicated that compaction levels were not the same as those measured on the previous day's Control section and consequently the additional roller passes were applied. The paving crew noted that workability of this mix in terms of raking and shoveling was much better than the Control, which was stiff and had adhered to tools. Workability was considered to be comparable to, if not better than, non-rubberized mixes. Given the absence of smoke and odors, the crew also removed their respirators during paving of this and the remaining warm-mix sections.

Figure 2.33: Sasobit: Absence of smoke from truck and paver.

Figure 2.34: Sasobit: Breakdown rolling.

Advera Section

The same process followed for the previous two sections was also followed for the Advera mix. Construction started at 12:25 p.m. No smoke or odors were observed/noted (Figure 2.35); however some chunks were observed in the hopper and behind the screed. Paving was temporarily halted while these were removed (Figure 2.36). Eight passes were made with the breakdown roller, followed by a further four passes after a period of cooling (Figure 2.37). Ten passes were applied during final rolling. Some tenderness was observed during breakdown rolling and the roller operator noted similar "discrepancies" between roller response and the density gauge readings as discussed above, when compared to typical

rubberized asphalt projects. The paving crew noted that the workability of the mix was again better than the Control, especially with regard to raking and shoveling.

Figure 2.35: Advera: No smoke from truck or paver.

Figure 2.36: Advera: Removing chunks from paver.

Figure 2.37: Advera: Breakdown rolling.

Control Section #2

This second Control section was not anticipated in the test track design. However, an appropriate section of the same structure was demarcated in the area between the North and West Test Tracks for this section. Heavy Vehicle Simulator testing would only be carried out if significant differences were noted in the Control mixes from the two production days.

The same process followed during the earlier construction was also followed on this section. Construction started at 9:00 a.m. Severe smoke and odors were noted (Figure 2.38) requiring the paving crew to wear respirators. Some chunks were observed (Figure 2.39) and workability of the mix was similar to the previous day's Control section. Breakdown rolling started as soon as the paver was moved off the section. Seven passes were made with the breakdown roller with vibration (Figure 2.40) followed by phased finish

rolling until satisfactory density and smoothness were achieved. No differences were noted between this and the other Control section construction.

Figure 2.38: Control #2: Smoke from truck and paver.

Figure 2.39: Control #2: Chunks removed from section.

Figure 2.40: Control #2: Breakdown rolling.

Astec Section

The same process followed for the previous four sections was also followed for the Astec mix. Construction started at 9:40 a.m. Some smoke was observed and odors noted, but the intensity was considerably less than that observed/noted on the Control section (Figure 2.41). Some chunks were observed in the paver hopper, but were removed before paving started. Breakdown rolling was achieved with eight passes, followed by a further four passes after a short period of cooling (Figure 2.42). Final rolling was completed in ten passes.

Figure 2.41: Astec: Some smoke from truck and paver.

Figure 2.42: Astec: Breakdown rolling.

Rediset

The same process followed for the other sections was also followed for the Rediset mix. Construction started at 10:25 a.m., but an immediate problem with the paver (broken feed chain) delayed the start until 12:15 p.m. Mix in the paver was removed with a loader, returned to the truck, and covered while the paver was repaired. Temperatures were monitored throughout this delay. No smoke was observed and no odors noted (Figure 2.43). Some chunks were noted and attributed to cooling of the mix on the sides of the truck during the delay. These were removed from the truck and paver hopper and did not influence actual paving. Breakdown rolling was achieved with eight passes, followed by a further four passes after a short period of cooling (Figure 2.44). Final rolling was completed in ten passes. The paving crew reported similar good workability to that noted on the other warm-mixes, despite the lower than planned placement and compaction temperatures.

Figure 2.43: Rediset: No smoke from truck or paver.

Figure 2.44: Rediset: Breakdown rolling.

General

The surface of the completed cells appeared to have uniform appearance, but the color of some appeared darker than others. This was attributed to differences in binder content, with the Rediset section (10.0 percent binder content) being the darkest.

2.7.10 Construction Quality Control

Quality control, both during and after construction, was undertaken jointly by Teichert Construction, the UCPRC, and an appointed contractor. This included:

- Placement and compaction temperatures
- Thickness
- Compaction density
- Deflection

Placement and Compaction Temperatures

Temperatures were systematically measured throughout the placement of the asphalt concrete using infrared temperature guns, thermocouples, and an infrared camera. Measurements included:

- Surface prior to start of paving
- Mix as it was tipped into the paver
- Mix behind the paver
- Mat before and during compaction

A summary of the measurements is provided in Table 2.10 and in Figure 2.45 and Figure 2.46.

Table 2.10: Summary of Temperature Measurements

Measuring Point	Day #1 Temperature[1]					
	Control #1		Sasobit		Advera	
	(°F)	(°C)	(°F)	(°C)	(°F)	(°C)
Production	331	166	300	149	293	145
Ambient at start of paving	55	13	59	15	61	16
Surface before paving[2]	57	14	66	19	77	25
Paver[2]	284	140	284	140	279	137
Mid-depth at start of compaction[3]	255	124	253	123	241	116
Mid-depth at end of compaction[3]	142	61	144	62	163	73
Ambient at end of compaction	57	14	61	16	63	17
Measuring Point	**Day #2 Temperature[1]**					
	Control #2		**Astec**		**Rediset**	
	(°F)	**(°C)**	**(°F)**	**(°C)**	**(°F)**	**(°C)**
Production	333	167	293	145	284	140
Ambient at start of paving	55	13	54	12	61	16
Surface before paving[2]	57	14	57	14	82	28
Paver[2]	286	141	277	136	259	126
Mid-depth at start of compaction[3]	258	126	234	112	219	104
Mid-depth at end of compaction[3]	145	63	144	62	149	65
Ambient at end of compaction	57	14	55	13	63	17

[1] Average of three sets of measurements [2] Measured with a temperature gun [3] Measured with a thermocouple

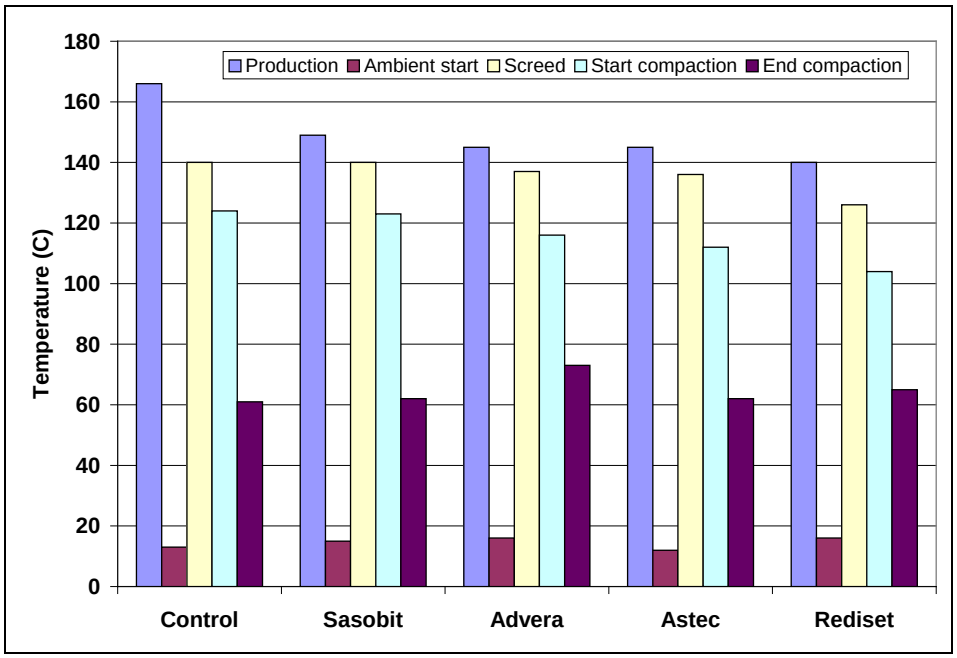

Figure 2.45: Summary of temperature measurements.
(Note that only the Day #1 Control Section is included.)

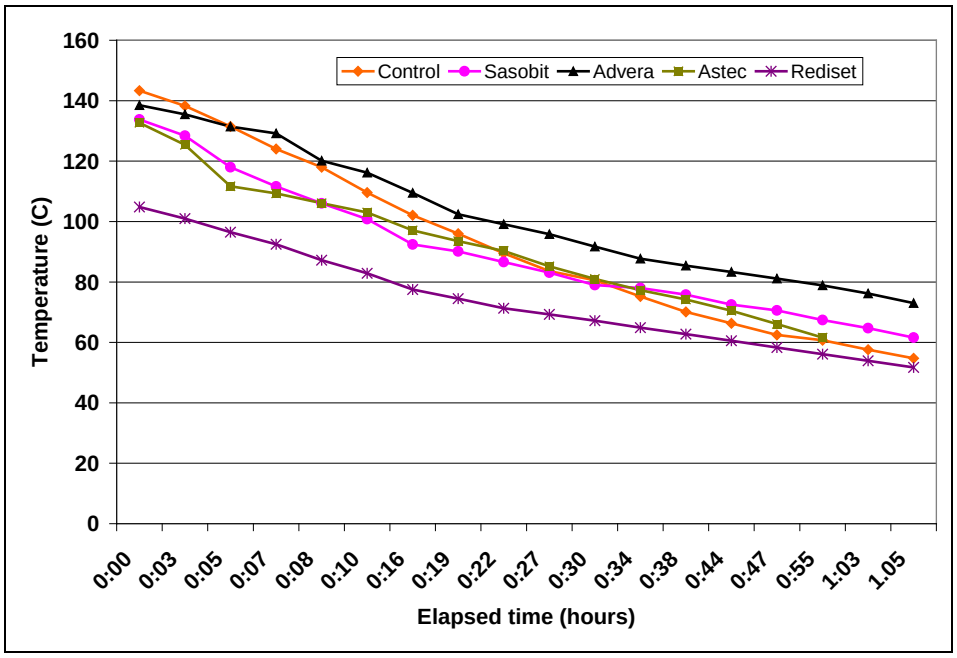

Figure 2.46: Summary of mid-depth temperatures over time.
(Note that only the Day #1 Control Section is included in the figure.)

The following observations were made:

- Ambient and paving temperatures were considered representative of early- or late-season paving.
- Paving and compaction temperatures were consistent with production temperatures, as expected.

- There was a considerable drop in temperature during the approximate 120 minute haul in covered trucks.
- Ambient temperatures at the start of paving increased slightly for each section, as expected.
- There was very little temperature difference between the material being tipped into the paver and the mat behind the paver before compaction.
- Mid-depth temperatures on the warm-mix sections decreased at a slower rate than the Control section and were consistent with the differences in production temperatures.

Thermal camera images (*FLIR Systems ThermaCAM PM290*, recorded by T.J. Holland of Caltrans) of the mat behind the paver are shown in Figure 2.47. The images clearly show consistent temperature across the mat on all sections. (Note that temperature scales on the right side of the photographs differ between images and are dependent on the time that the image was taken and distance of the camera from the paver.)

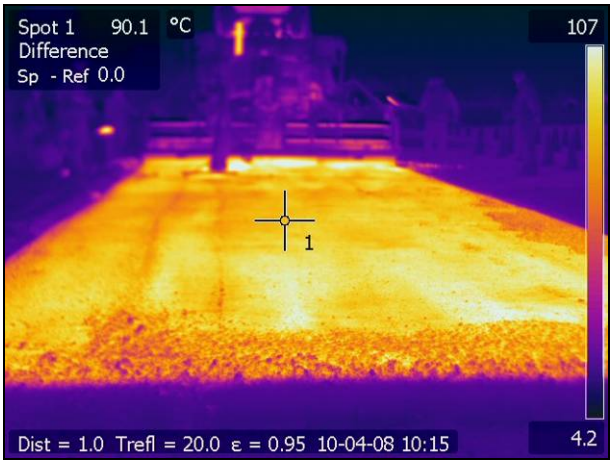

Control #1

Sasobit

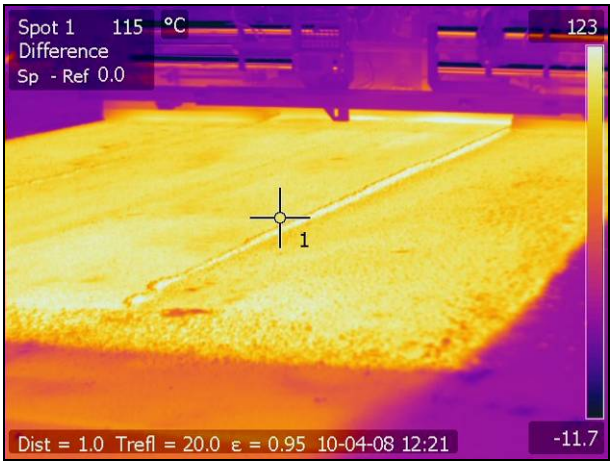

Advera

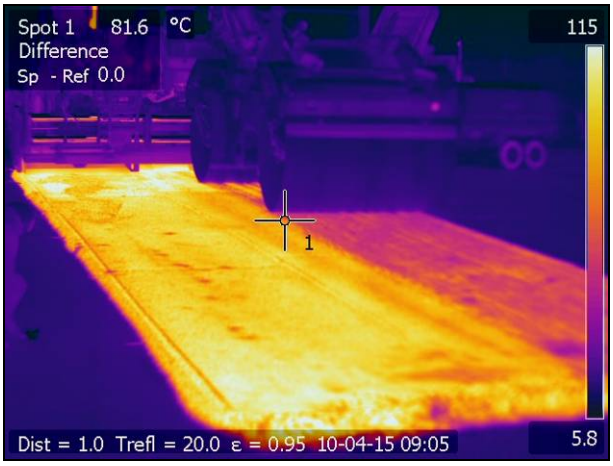

Control #2 (with first roller pass)

Figure 2.47: Thermal images of test track during construction.

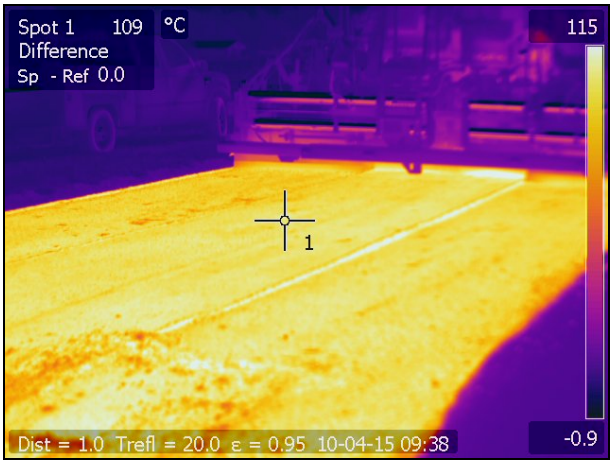

Astec **Rediset**

Figure 2.47: Thermal images of test track during construction *(continued)*.

Thickness

Thickness was monitored with probes by the paving crew throughout the construction process. The thickness of the slabs and cores removed for laboratory testing after construction (see Section 2.8) was measured for quality control purposes. The results of these measurements are summarized in Table 2.11. Layer thicknesses of actual Heavy Vehicle Simulator test sections were determined during forensic investigations after testing and are discussed in Section 5.7.

Table 2.11: Summary of Asphalt Layer Thickness

Measurement	**Day #1 Asphalt Layer Thickness**					
	Control #1		**Sasobit**		**Advera**	
	(ft.)	**(mm)**	**(ft.)**	**(mm)**	**(ft.)**	**(mm)**
Surface layer	0.22	66	0.22	67	0.21	63
Bottom layer	0.25	77	0.23	72	0.23	71
Total	0.47	143	0.45	138	0.44	134
Measurement	**Day #2 Asphalt Layer Thickness**					
	Control #2		**Astec**		**Rediset**	
	(ft.)	**(mm)**	**(ft.)**	**(mm)**	**(ft.)**	**(mm)**
Surface layer	0.22	66	0.22	67	0.22	66
Bottom layer	-	-	0.26	78	0.25	77
Total	-	-	0.48	135	0.47	143

The average thickness of the combined two layers was 0.45 ft. (137 mm), 0.05 ft. (17 mm) thicker than the design thickness of 0.4 ft. (120 mm). General consistency of thickness across the track was considered satisfactory and representative of typical construction projects.

Compaction Density

Compaction was monitored using nuclear gauges throughout the construction process using the mix design specific gravity values. Given the very small quantities of mix produced for each technology, actual mix specific gravities were not available before completion of construction of each section. The

results were used to manage the number of roller passes and roller settings and were monitored but not recorded.

Final density measurements were taken on June 18, 2010, by an independent consultant using a calibrated nuclear gauge. Measurements were taken on each section according to the plan shown in Figure 2.48, which focused primarily on checking densities in the areas selected for HVS testing, but also to assess variability across each section. A summary of the results is provided in Table 2.12. The results indicate that there was very little variability across the sections and that slightly better densities were achieved on the Sasobit and Rediset sections compared to the other sections, but that relatively poor compaction was achieved overall. A series of cores were taken from positions 7 through 10 (Figure 2.48) to check these densities in the laboratory using the CoreLok method. The results are summarized in Table 2.13 and indicate that higher densities were actually achieved. Air-void contents were also determined on each specimen sampled from the test track for laboratory testing. The results for these tests, which are similar to the results shown in Table 2.13, are discussed in Chapter 6. It is not clear why there was a difference between the gauge and core-determined densities. Core-determined densities were used for all analyses in this study.

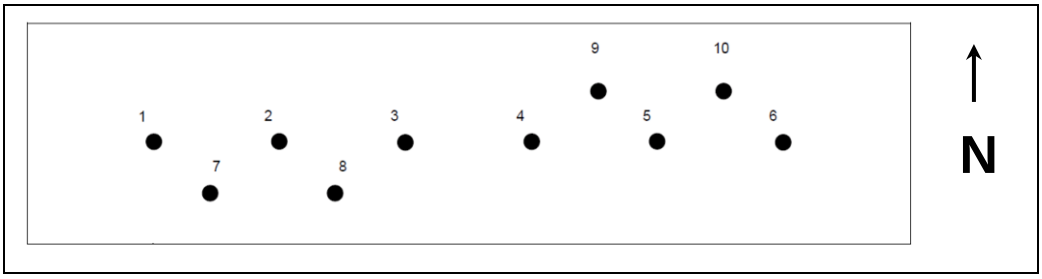

Figure 2.48: Asphalt concrete density measurement plan.

Table 2.12: Summary of Rubberized Asphalt Concrete Density Measurements

Position	Day #1 Density Measurements					
	Control #1		Sasobit		Advera	
	Gauge (kg/m^3)	% Relative	Gauge (kg/m^3)	% Relative	Gauge (kg/m^3)	% Relative
1	2,157	86	2,135	85	2,151	86
2	2,150	86	2,238	89	2,149	86
3	2,100	84	2,120	85	2,114	85
4	2,152	86	2,193	88	2,134	85
5	2,169	87	2,115	85	2,162	87
6	2,184	87	2,191	88	2,160	87
7	2,235	89	2,231	89	2,133	85
8	2,144	86	2,169	87	2,120	85
9	2,075	83	2,136	85	2,087	84
10	2,138	85	2,209	88	2,173	87
Average	2,150	86	2,174	87	2,138	86
RICE	2.505		2.502		2.497	

Table 2.12: Summary of Rubberized Asphalt Concrete Density Measurements *(continued)*

Position	Day #2 Density Measurements					
	Control #2		Astec		Rediset	
	Gauge (kg/m^3)	% Relative	Gauge (kg/m^3)	% Relative	Gauge (kg/m^3)	% Relative
1	2,030	82	2,097	84	2,151	87
2	2,091	84	2,179	88	2,179	88
3	2,173	87	2,170	87	2,170	88
4	2,175	88	2,137	86	2,137	87
5	2,081	84	2,122	85	2,122	86
6	2,200	89	2,116	85	2,116	86
7	2,101	85	2,148	86	2,148	87
8	2,173	87	2,163	87	2,163	88
9	2,020	81	2,074	83	2,074	84
10	2,212	89	2,163	87	2,163	88
Average	2,126	86	2,137	86	2,142	87
RICE	2.485		2.485		2.467	

Table 2.13: Summary of Asphalt Concrete Density Measurements from Cores

Position	Day #1 Density Measurements from Cores					
	Control #1		Sasobit		Advera	
	Air-Void (%)	Relative (%)	Air-Void (%)	Relative (%)	Air-Void (%)	Relative (%)
7	11.6	88	8.4	92	10.8	89
8	11.4	89	8.5	92	10.5	90
9	11.6	88	8.5	92	10.6	89
10	11.7	88	8.5	92	10.8	89
Average	11.6	88	8.5	92	10.7	89
Position	**Day #2 Density Measurements from Cores**					
	Control #2		Astec		Rediset	
	Air-Void (%)	Relative (%)	Air-Void (%)	Relative (%)	Air-Void (%)	Relative (%)
7	11.5	89	9.0	91	8.4	92
8	11.5	89	9.0	91	8.2	92
9	11.6	88	9.3	91	8.5	92
10	11.6	88	9.2	91	8.3	92
Average	11.6	88	9.1	91	8.4	92
RC – Relative compaction						

Deflection

Falling weight deflectometer (FWD) measurements were taken on May 27 and May 28, 2010, at 1.0 m intervals along the centerline of each lane to assess general variability across the test track. Deflection measurements were not taken on the second Control section. Average results of the second 40 kN load drop are summarized in Table 2.14 and in Figure 2.49. The D1 sensor data were used to obtain an indication of overall pavement deflection. The D2 sensor data were used to obtain an indication of deflection in the asphalt layers. The D3 and D5 sensor data were used to obtain an indication of deflection in the top and bottom of the base respectively, and the D6 sensor data were used to obtain an indication of deflection in the subgrade. All deflection measurements were normalized to 40 kN by proportioning at

20°C pavement temperature at 40 mm depth (i.e., one-third of the total asphalt concrete thickness) using the Bells Temperature calculated from actual air and surface temperatures.

There was no significant difference in the deflections measured on the warm-mix sections, all of which were lower than those measured on the primary (Day #1) Control section, indicating slightly higher stiffnesses on the warm-mix sections. Deflections were generally consistent along the length of each section.

Table 2.14: Summary of Average FWD Deflection Measurements

Section	Deflection (micron)									
	Control		Sasobit		Advera		Astec		Rediset	
	Mean	SD	Mean	SD	Mean	SD	Mean	SD	Mean	SD
Sensor D1[1]	625	76	518	8	534	33	543	17	547	40
Sensor D2[2]	401	6	338	2	347	2	353	2	353	1
Sensor D3[3]	288	48	250	5	256	16	258	10	253	21
Sensor D5[4]	115	32	113	5	108	9	112	6	99	12
Sensor D6[5]	70	11	72	3	62	3	73	2	60	4
Section	**Average Temperatures Measured**									
Air	19.7	1.1	19.8	0.4	20.0	0.6	21.1	0.6	22.9	1.4
Surface	14.9	0.4	14.8	0.4	15.4	0.3	15.7	0.2	16.4	0.3

[1] Geophone D1, 0 mm offset [2] Geophone D2, 150 mm offset [3] Geophone D3, 315 mm offset
[4] Geophone D5, 630 mm offset [5] Geophone D6, 925 mm offset SD – Standard deviation

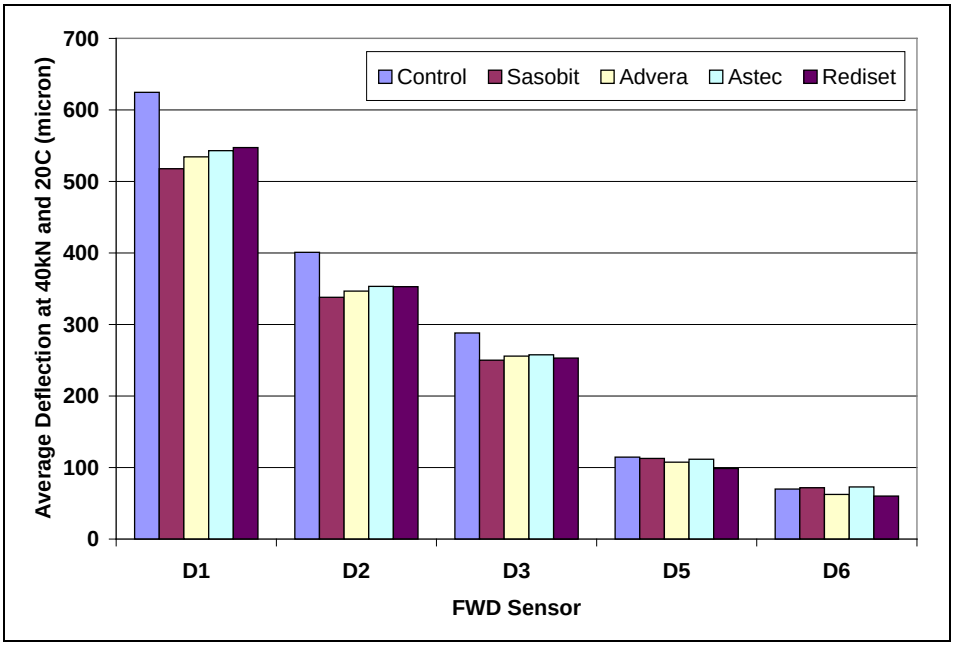

Figure 2.49: Summary of average deflection by section (40 kN load at 20°C).
(Note that only the Day #1 Control Section is included in the figure.)

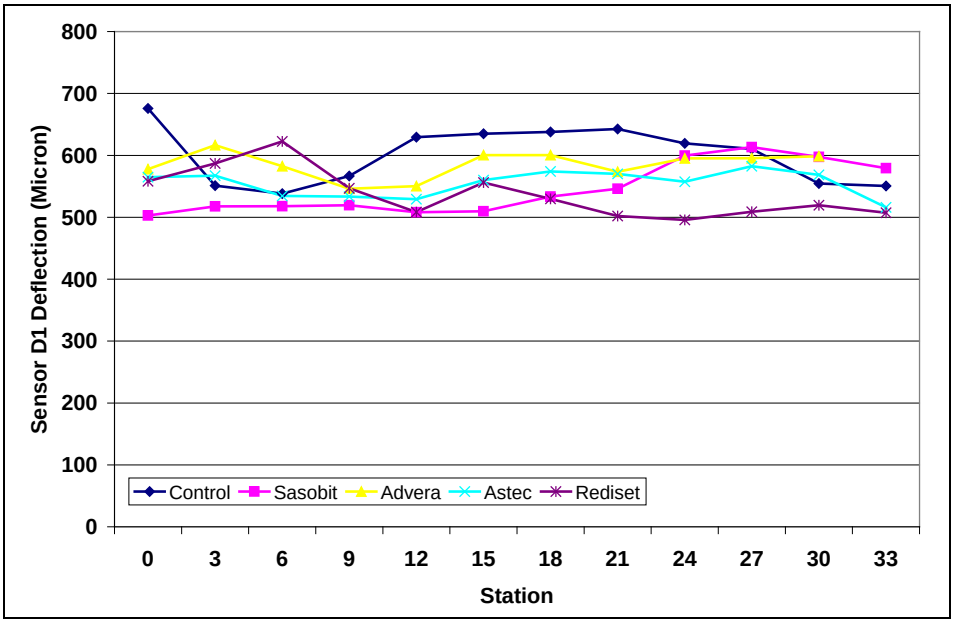

Figure 2.50: Summary of Sensor-1 deflection measurements.
(Note that only the Day #1 Control Section is included in the figure.)

2.8 Sampling

Specimens in the form of 6.0 in. (152 mm) diameter cores and slabs 20 in. by 10 in. (500 mm by 250 mm) were sawn from the middle of each section adjacent to the planned HVS test sections for laboratory testing, as shown in Figure 2.51. Slabs were sawn to the bottom of the combined asphalt concrete layers, extracted, stored on pallets, and then transported to the UCPRC Richmond Field Station laboratory. Inspection of the slabs indicated that the asphalt concrete was well bonded to the top of the base-course material, and that the two asphalt layers were well bonded to each other.

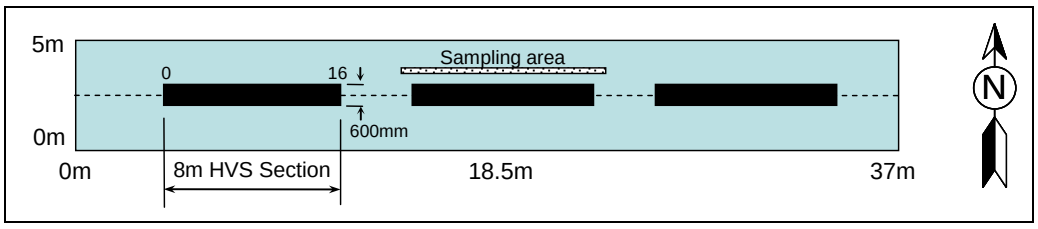

Figure 2.51: Sampling location for laboratory specimens.

2.9 Construction Summary

Key observations from the test track construction process include:

- Preparation of the subgrade resulted in a generally consistent platform on which to construct the base. Density measurements taken after final compaction indicated an average relative compaction of 97 percent of the laboratory-determined value, with very little variation across the track.
- Construction of the base-course followed conventional procedures. Measurements after final compaction indicated that the average dry density was 98 percent of the laboratory-determined maximum dry density with very little variation across the track. The final surface was tightly bound and free of loose material. Heavy rainfall after construction resulted in some loosening of the surface and the layer was consequently recompacted prior to paving the bottom lift of asphalt concrete.
- Placement of the bottom lift of hot-mix asphalt followed conventional procedures. Thickness and compaction appeared to be consistent across the test track.
- Some asphalt plant modifications were required to accommodate the warm-mix additives. These complied with the Caltrans Material Plant Quality Program requirements.
- No problems were recorded with producing three of the four warm asphalt mixes at the lower temperatures. Continued nozzle blockages on the Astec foaming system made its replacement necessary, causing a delay in production and placing the Astec and Rediset mixes because of a shortage of binder resulting from the repeated attempts to produce the original Astec mix. A second control mix was also produced on the second day for comparative purposes. Target mix production temperatures (335°F, 300°F, 295°F, 295°F, and 285°F [166°C, 149°C, 145°C, 145°C, and 140°C] for the two Controls, Sasobit, Advera, Astec, and Rediset mixes, respectively), set by the warm-mix technology providers, were all achieved.
- The rubberized binder, with 19 percent rubber content, complied with the specification requirements.
- All mixes met the project mix design grading requirements, with little variability among five of the six mixes. The Rediset mix, although still within specification, was somewhat coarser than the other mixes.
- Only two of the six mixes (Sasobit [8.0 percent] and Astec [8.4 percent]) had binder contents within an acceptable range of the target of 8.3 percent. Binder contents on the other mixes were 7.7, 7.6, 7.6, and 10.3 percent for the Controls, Advera, and Rediset mixes, respectively.
- Hveem stabilities exceeded the minimum requirement by a considerable margin.
- Compaction temperatures differed considerably among the mixes and were consistent with production temperatures. The warm-mixes lost heat during transport and placement at a slower rate that the Control mixes, produced at the higher temperatures. Apart from some crusting of the asphalt on the Astec and Advera mixes during transport, the lower temperatures in the four warm-mixes did not appear to influence the paving or compaction operations, and interviews with the paving crew after construction revealed that no problems were experienced at the lower temperatures. Improved working conditions were identified as an advantage. Chunks in the Control mixes, attributed to their cooling during transport, caused some problems with the paving process.
- Smoke and odors were more severe on the Control sections compared to the warm-mix sections. Some smoke and odors were noted during construction of the Astec section. No smoke or odors were noted during construction of the Advera, Rediset, or Sasobit sections.
- Workability of the mix, determined through observations of and interviews with the paving crew, was considerably better on the warm-mix sections compared to the Control.

- Average thicknesses of the top (rubberized) and bottom asphalt layers across the four sections were 0.22 ft. (66 mm) and 0.24 ft. (75 mm), respectively. The average thickness of the combined two layers was 0.45 ft. (137 mm), 0.5 ft. (17 mm) thicker than the design thickness of 0.4 ft. (120 mm). General consistency of thickness across the track was considered satisfactory and representative of typical construction projects.
- Nuclear gauge–determined density measurements were inconsistent with core-determined air-void contents. The core-determined air-void contents indicated that slightly higher density was achieved on the warm-mix sections (92, 89, 91, and 92 percent of the RICE specific gravity for the Sasobit, Advera, Astec, and Rediset sections respectively) compared to the Control sections (88 percent). Compaction across the test track appeared to be consistent, demonstrating that adequate compaction can be achieved on rubberized warm-mixes at lower temperatures. Based on observations from the test track construction and interviews with roller operators, optimal compaction temperatures will differ among the different warm-mix technologies. Therefore on projects where warm-mix technologies are used, roller operators will need to consider potential differences in roller response between warm-mix and conventional hot mixes, and may need to adjust rolling procedures to ensure that optimal compaction is always achieved.
- Deflection measurements showed that relatively consistent construction was achieved on the test track.

The test track was considered satisfactorily uniform for the purposes of accelerated pavement testing and sampling for laboratory testing.

3. TEST TRACK LAYOUT AND HVS TEST CRITERIA

3.1 Protocols

Heavy Vehicle Simulator (HVS) test section layout, test setup, trafficking, and measurements followed standard University of California Pavement Research Center (UCPRC) protocols *(8)*.

3.2 Test Track Layout

The Phase 3 Warm-Mix Asphalt Study test track layout is shown in Figure 3.1. Five HVS test sections were demarcated for the first phase of HVS testing for early-age rutting at high temperatures. The testing sequence did not follow the construction sequence because testing on the Phase 3a sections was already in progress and the two HVSs could not test side-by-side and (see Table 3.1). HVS testing on the Day #2 Control mix section was not considered necessary based on the findings of laboratory testing, which indicated no significant differences between the two Control mixes. Early failure on the Advera section prompted another two tests to determine whether this was a mix problem or a pavement structural problem, or whether it was related to equipment or weather variables. Second tests were also carried out on the Control and Sasobit sections for comparative purposes. The section numbers allocated were as follows (HA and HB refer to the specific HVS equipment used for testing):

- Section 624HB: Control (Test #1)
- Section 625HA: Sasobit (Test #1)
- Section 626HA: Advera (Test #1)
- Section 627HB: Astec
- Section 628HB: Rediset
- Section 629HB: Advera (Test #2)
- Section 630HB: Advera (Test #3)
- Section 631HB: Sasobit (Test #2)
- Section 632HA: Control (Test #2)

3.3 HVS Test Section Layout

The general test section layout for each of the rutting sections is shown in Figure 3.2. Station numbers (0 to 16) refer to fixed points on the test section and are used for measurements and as a reference for discussing performance.

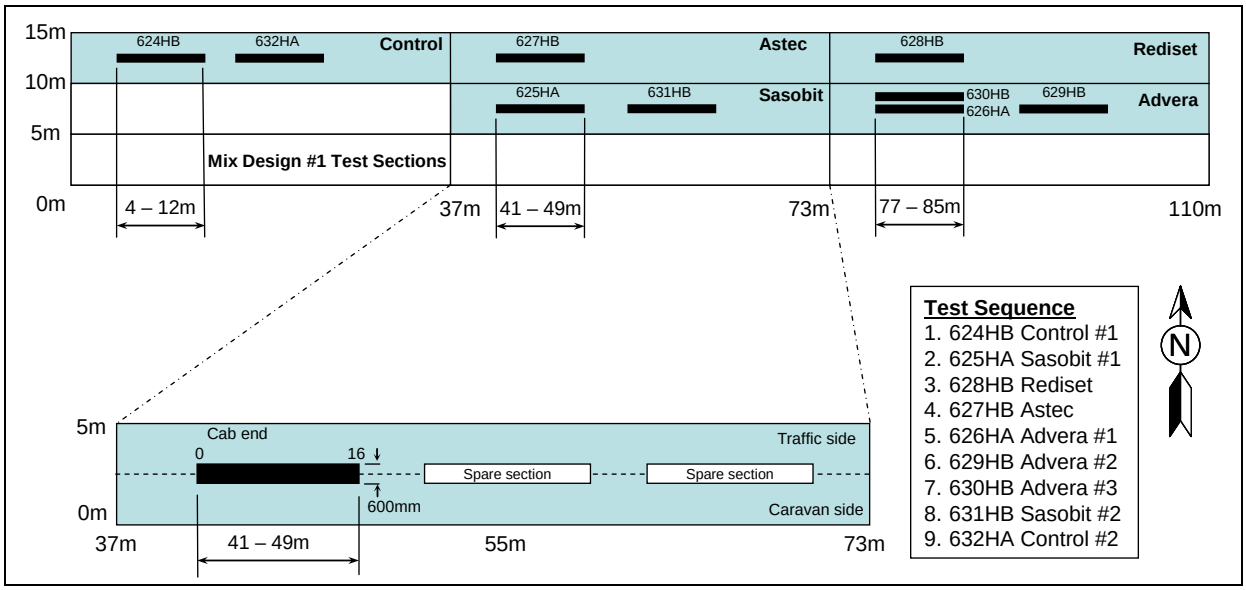

Figure 3.1: Layout of Phase 3 test track and Phase 3b HVS test sections.

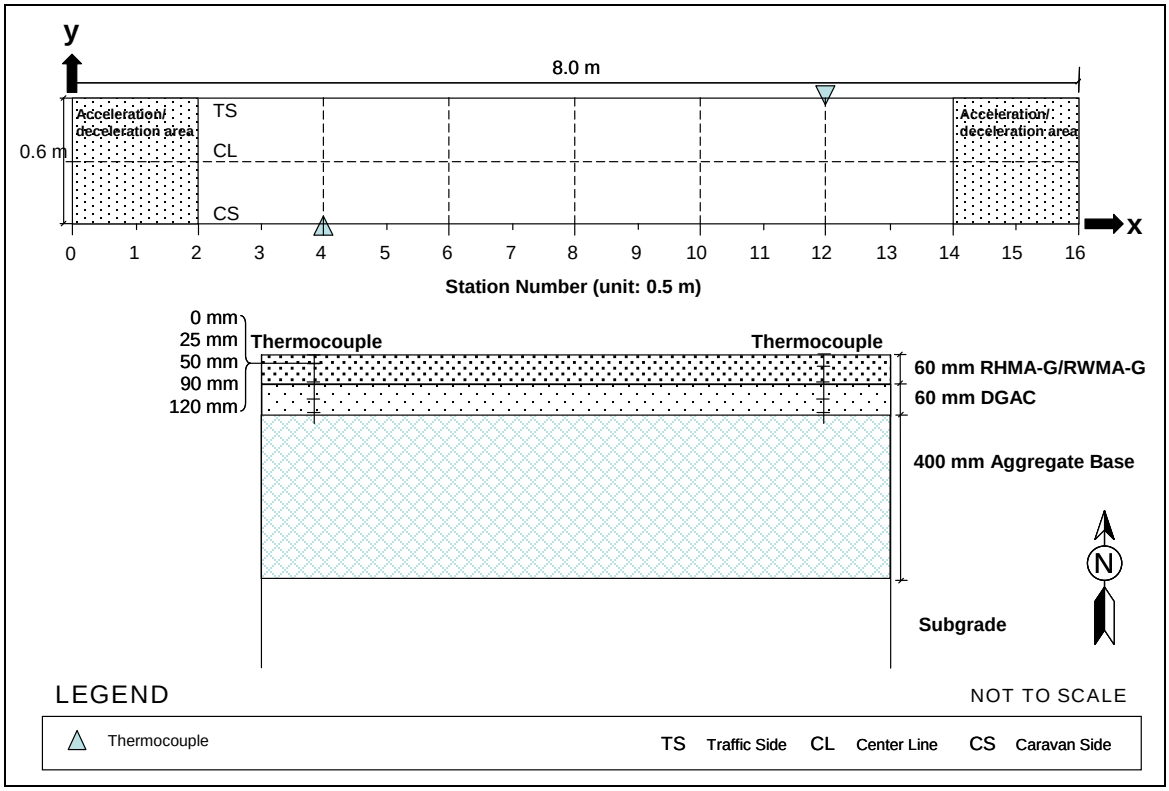

Figure 3.2: Location of thermocouples.

3.4 Pavement Instrumentation and Monitoring Methods

Measurements were taken with the instruments listed below. Instrument positions are shown in Figure 3.2. Detailed descriptions of the instrumentation and measuring equipment are included in Reference 8.

Intervals between measurements, in terms of load repetitions, were selected to enable adequate characterization of the pavement as damage developed.

- A laser profilometer was used to measure surface profile; measurements were taken at each station.
- Thermocouples measured pavement temperature (at Stations 4 and 12) and ambient temperature at one-hour intervals during HVS operation.

Air temperatures were recorded by a weather station next to the test section at the same intervals as the thermocouples. Subgrade and base moisture contents were measured with two moisture sensors positioned in the middle of the test track.

Surface and in-depth deflections were not measured. Surface deflection cannot be measured with the road surface deflectometer (RSD) on rutted pavements. In-depth deflection measured with multi-depth deflectometers (MDD) was not possible due to difficulties with installing and anchoring the instruments in the soft clay subgrade.

3.5 HVS Test Criteria

3.5.1 Test Section Failure Criteria

An average maximum rut depth of 12.5 mm (0.5 in.) over the full monitored section (Station 3 to Station 13) was set as the failure criterion for the experiment. However; in most instances, HVS trafficking was continued past this point to fully understand the rutting behavior of each mix.

3.5.2 Environmental Conditions

The pavement temperature at 50 mm (2.0 in.) was maintained at 50°C±4°C (122°F±7°F) to assess rutting potential under typical pavement conditions. Infrared heaters inside a temperature control chamber were used to maintain the pavement temperature. The test sections received no direct rainfall as they were protected by the temperature control chamber. The sections were tested predominantly during the wet season (August through February) and rainfall was recorded during each of the first round of tests. Later, additional testing on the Control, Advera, and Sasobit sections was conducted in the summer months (July through September) when no rainfall was recorded.

3.5.3 Test Duration

HVS trafficking on each section was initiated and completed as shown in Table 3.1. The sequence of testing was adjusted to accommodate positioning of the two HVS machines on the Phase 3a and Phase 3b sections (i.e., the machines could not test side-by-side on the test track configuration).

Table 3.1: Test Duration for Phase 3b HVS Rutting Tests

Section	Overlay	Test Sequence	Start Date	Finish Date	Repetitions
624HB	Control (Test #1)	1	08/10/2010	09/29/2010	320,000
625HA	Sasobit (Test #1)	2	09/09/2010	10/18/2010	365,000
626HA	Advera (Test #1)	5	12/14/2010	01/16/2011	50,000
627HB	Astec	4	11/11/2010	12/16/2010	242,000
628HB	Rediset	3	10/01/2010	11/08/2010	309,000
629HB	Advera (Test #2)	6	01/24/2011	02/07/2011	73,500
630HB	Advera (Test #3)	7	07/26/2011	08/08/2011	5,000
631HB	Sasobit (Test #2)	8	08/16/2011	09/09/2011	85,000
632HA	Control (Test #2)	9	09/15/2011	09/28/2011	80,000

3.5.4 Loading Program

The HVS loading program for each section is summarized in Table 3.2. Equivalent Standard Axle Loads (ESALs) were determined using the following Caltrans conversion (Equation 3.1):

$$ESALs = (\text{axle load}/18{,}000)^{4.2} \quad \textbf{(3.1)}$$

All trafficking was carried out with a dual-wheel configuration, using radial truck tires (Goodyear G159 - 11R22.5- steel belt radial) inflated to a pressure of 720 kPa (104 psi), in a channelized, unidirectional loading mode. Load was checked with a portable weigh-in-motion pad at the beginning of each test, after each load change, and at the end of each test.

Table 3.2: Summary of Phase 3b HVS Loading Program

Section	Overlay	Wheel Load[1] (kN)	Repetitions	ESALs[2]	Test to Failure
624HB	Control (Test #1)	40 60 80	160,000 100,000 60,000	160,000 549,000 1,102,750	Yes
625HA	Sasobit (Test #1)	40 60 80	160,000 100,000 105,000	160,000 549,014 1,929,813	Yes
626HA	Advera (Test #1)	40	50,000	50,000	No
627HB	Astec	40 60	160,000 82,000	160,000 450,191	Yes
628HB	Rediset	40 60 80	160,000 100,000 49,000	160,000 549,000 900,580	Yes
629HB	Advera (Test #2)	40	73,500	73,500	Yes
630HB	Advera (Test #3)	40	5,000	5,000	Yes
631HB	Sasobit (Test #2)	40	85,000	85,000	No
632HA	Control (Test #2)	40	80,000	80,000	No
		Total	**1,529,500**	**6,963,848**	

[1] 40 kN = 9,000 lb.; 60 kN = 13,500 lb

[2] ESAL: Equivalent Standard Axle Load

4. PHASE 3b HVS TEST DATA SUMMARY

4.1 Introduction

This chapter provides a summary of the data collected from the nine HVS tests (Sections 624HB through 632HA) and a brief discussion of the first-level analysis. Data collected includes rainfall, air temperatures outside and inside the temperature control chamber, pavement temperatures, and surface permanent deformation (rutting).

Pavement temperatures were controlled using the temperature control chamber. Both air (inside and outside the temperature box) and pavement temperatures were monitored and recorded hourly during the entire loading period. In assessing rutting performance, the temperature at the bottom of the asphalt concrete and the temperature gradient are two important controlling temperature parameters influencing the stiffness of the asphalt concrete and are used to compute plastic strain. Permanent deformation at the pavement surface (rutting) was monitored with a laser profilometer. In-depth permanent deformation at various depths within the pavement was not monitored due to the soft subgrade clay and associated difficulties with the installation and anchoring of multi-depth deflectometers. The following rut parameters were determined from these measurements, as illustrated in Figure 4.1:

- Average maximum rut depth,
- Average deformation,
- Location and magnitude of the maximum rut depth, and
- Rate of rut development.

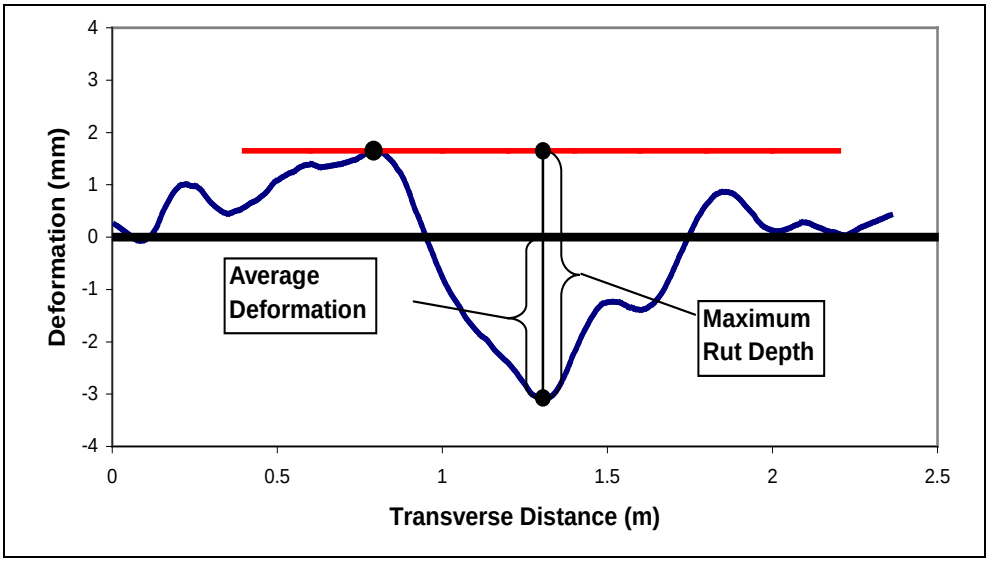

Figure 4.1: Illustration of maximum rut depth and average deformation of a leveled profile.

The laser profilometer provides sufficient information to evaluate the evolution of permanent surface deformation of the entire test section at various loading stages. The rut depth figures in this report show the average values over the entire section (Stations 3 through 13) as well as values for half sections between Stations 3 and 8 and Stations 9 and 13. These two additional data series were plotted to illustrate any differences along the length of the section. The precise nature of the permanent deformation was determined after the forensic investigation (test pits and cores) on each section and is discussed in Chapter 5.

The data from each HVS test is presented separately, with the presentation of each test following the same format. Data plots are presented on the same scale, where possible, to facilitate comparisons of performance.

4.2 Rainfall

Figure 4.2 shows the monthly rainfall data from July 2010 through October 2011 as measured at the weather station next to the test track. Rainfall was measured during the first six HVS tests (five sections plus first repeat on the Advera section). No rainfall was measured during the second round of tests on the Control, Advera, and Sasobit sections. There were a number of relatively high 24 hour rainfall events (i.e., more than 20 mm (0.75 in.) in the latter stages of the first round of testing.

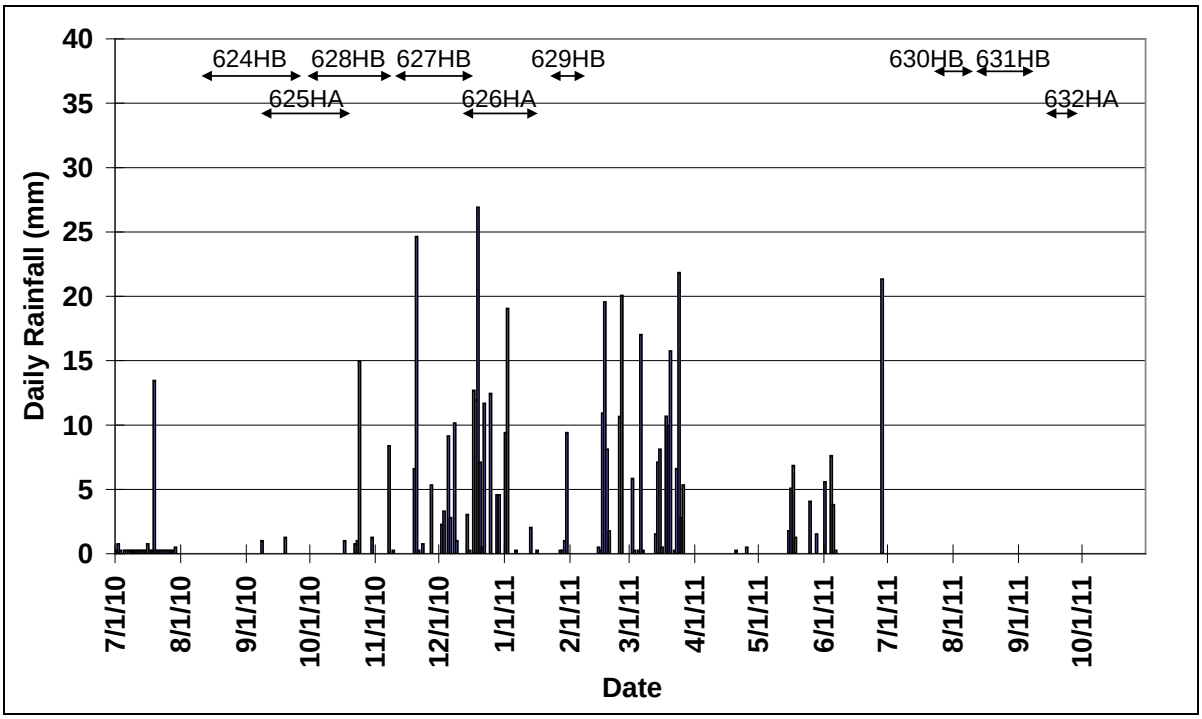

Figure 4.2: Measured rainfall during Phase 3b HVS testing.

4.3 Section 624HB: Control (Test #1)

4.3.1 Test Summary

Loading commenced on August 10, 2010, and ended on September 29, 2010. A total of 320,000 load repetitions were applied and 49 datasets were collected. Load was increased to 60 kN (13,500 lb) and 80 kN (18,000 lb) after 160,000 and 260,000 load repetitions, respectively. No breakdowns occurred during testing on this section. The HVS loading history for Section 624HB is shown in Figure 4.3.

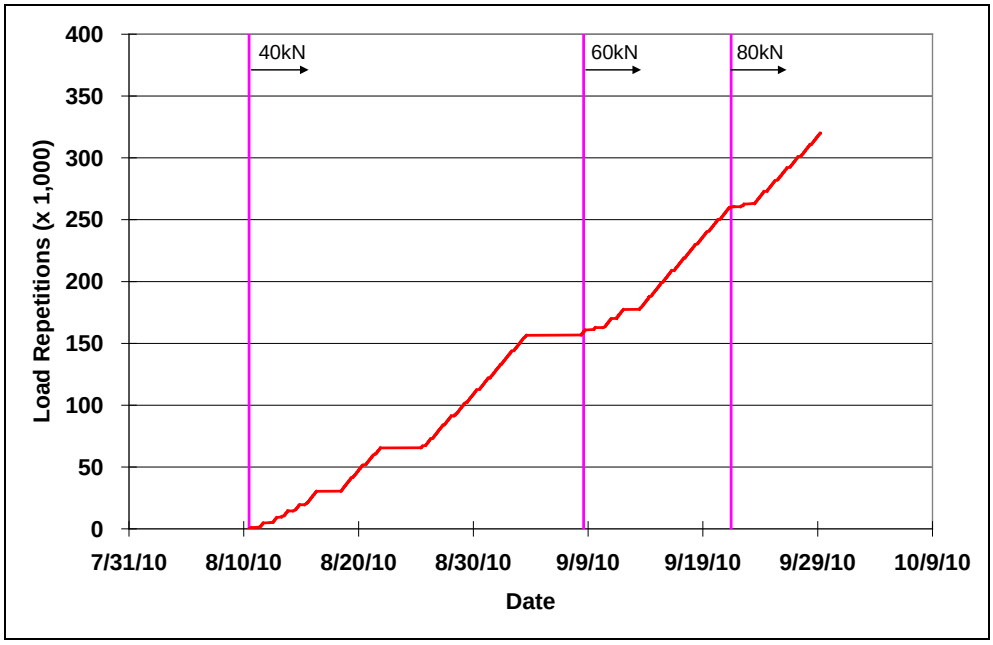

Figure 4.3: 624HB: Load history.

4.3.2 Outside Air Temperatures

Daily average outside air temperatures are summarized in Figure 4.4. Vertical error bars on each point on the graph show the daily temperature range. Temperatures ranged from 8°C to 46°C (42°F to 108°F) during the course of HVS testing, with a daily average of 24°C (75°F), an average minimum of 15°C (59°F), and an average maximum of 31°C (88°F).

4.3.3 Air Temperatures in the Temperature Control Unit

During the test, air temperatures inside the temperature control chamber ranged from 22°C to 60°C (72°F to 140°F) with an average of 45°C (113°F) and a standard deviation of 2.3°C (4.1°F). Air temperature was adjusted to maintain a pavement temperature of 50°C±4°C (122°F±7°F), which is expected to promote rutting damage. The recorded pavement temperatures discussed in Section 4.3.4 indicate that the inside air temperatures were adjusted appropriately to maintain the required pavement temperature. The daily

average air temperatures recorded in the temperature control unit, calculated from the hourly temperatures recorded during HVS operation, are shown in Figure 4.5. Vertical error bars on each point on the graph show daily temperature range.

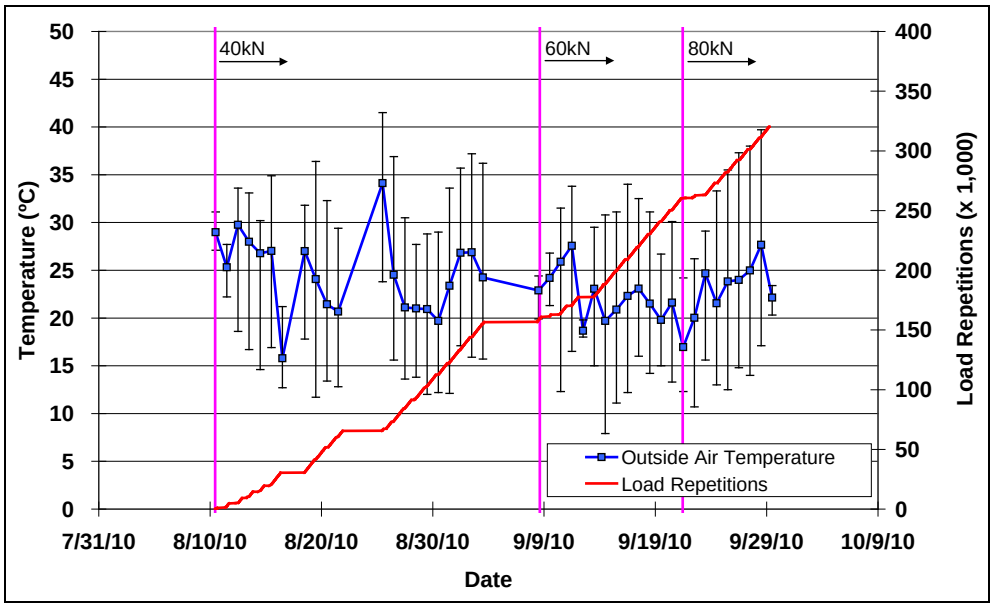

Figure 4.4: 624HB: Daily average outside air temperatures.

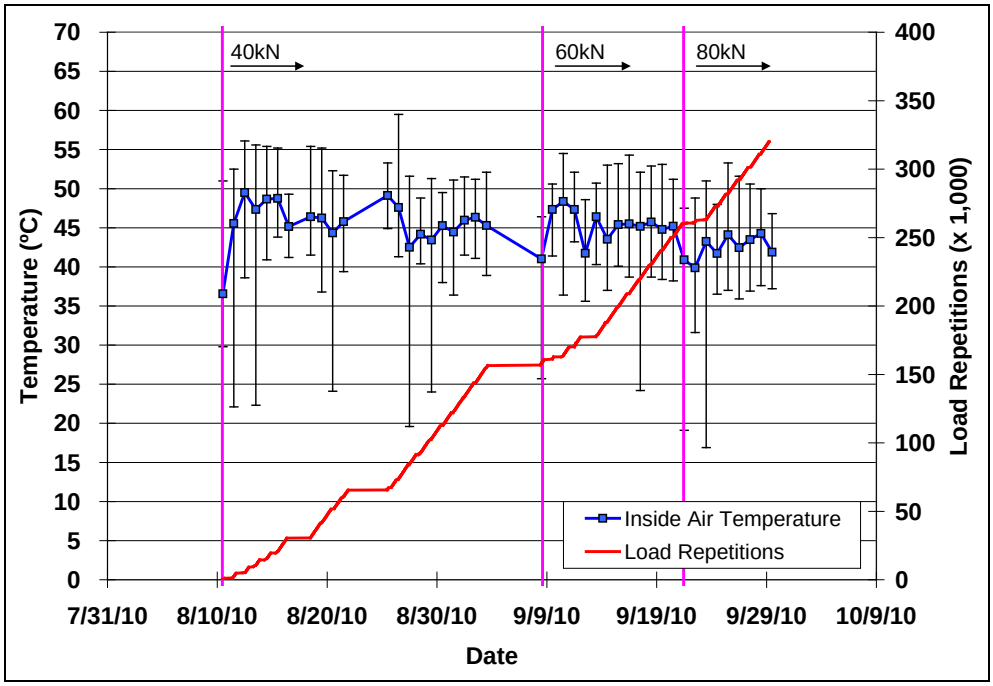

Figure 4.5: 624HB: Daily average inside air temperatures.

4.3.4 Temperatures in the Asphalt Concrete Layers

Daily averages of the surface and in-depth temperatures of the asphalt concrete layers are listed in Table 4.1 and shown in Figure 4.6. Pavement temperatures decreased slightly with increasing depth in the pavement, which was expected as there is usually a thermal gradient between the top and bottom of the asphalt concrete pavement layers.

Table 4.1: 624HB: Temperature Summary for Air and Pavement

Temperature	Average (°C)	Std. Dev. (°C)	Average (°F)	Std. Dev. (°F)
Outside air	24	3.6	75	6.5
Inside air	45	2.3	113	4.1
Pavement surface	51	1.3	124	2.3
- 25 mm below surface	51	1.1	123	2.0
- 50 mm below surface	50	1.0	122	1.8
- 90 mm below surface	49	1.0	121	1.8
- 120 mm below surface	49	1.0	120	1.8

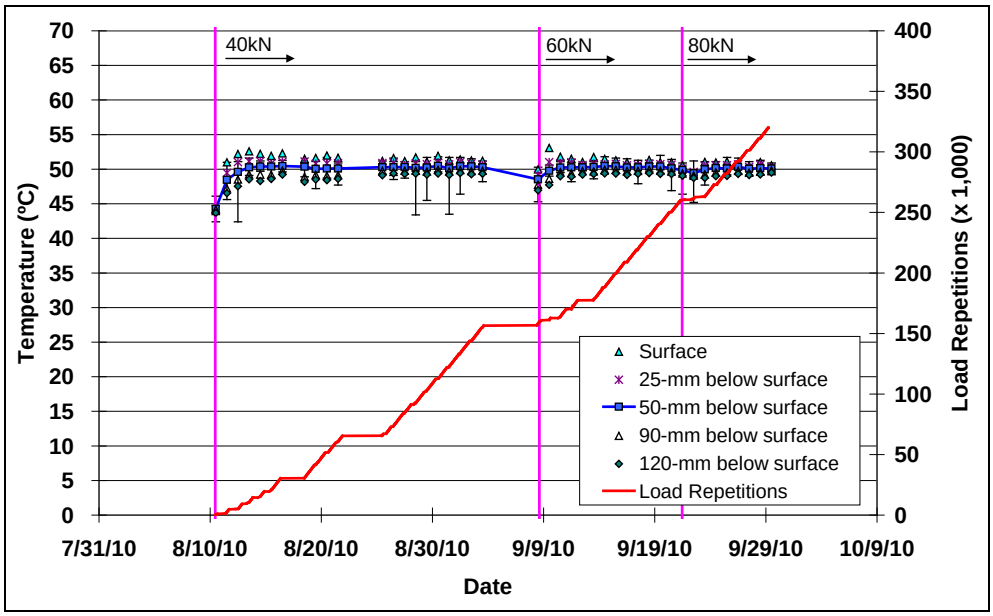

Figure 4.6: 624HB: Daily average temperatures at pavement surface and various depths.

4.3.5 Permanent Surface Deformation (Rutting)

Figure 4.7 shows the average transverse cross section measured with the laser profilometer at various stages of the test. This plot clearly shows the increase in rutting and deformation over the duration of the test.

Figure 4.8 and Figure 4.9 show the development of permanent deformation (average maximum rut and average deformation, respectively) with load repetitions as measured with the laser profilometer for the test section.

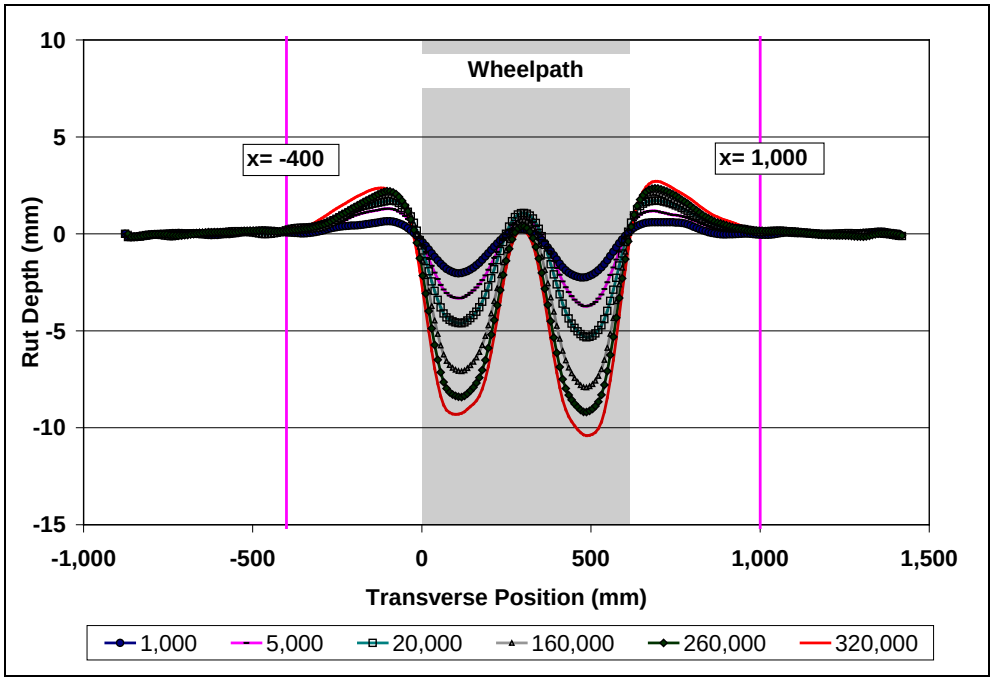

Figure 4.7: 624HB: Profilometer cross section at various load repetitions.

During HVS testing, rutting usually occurs at a high rate initially, and then it typically diminishes as trafficking progresses until reaching a steady state. This initial phase is referred to as the "embedment" phase. The embedment phase, although relatively short in terms of the number of load repetitions (i.e., ± 5,000), ended with a fairly significant rut of about 6.0 mm (0.25 in.) that was attributed to the relatively high air-void content and other problems during construction, as discussed in Section 2.7.9. The rate of rut depth increase after the embedment phase was relatively slow despite the poor compaction. Increases in the applied load (to 60 kN and then 80 kN) had very little effect on the rate of rut depth increase. Error bars on the average reading indicate that there was very little variation along the length of the section; however, rut depths were slightly deeper on the second half of the section compared to the first half.

Figure 4.10 shows contour plots of the pavement surface at the start and end of the test (320,000 repetitions), also indicating minimal variation along the section. A slightly deeper rut recorded in one of the wheel tracks was attributed to the positioning of the HVS on the crossfall on the section. Terminal rut (12.5 mm [0.5 in.]) was reached after 290,000 repetitions. Testing was continued for an additional 30,000 repetitions to further assess rutting trends.

After completion of trafficking, the average maximum rut depth and the average deformation were 13.3 mm (0.52 in.) and 7.8 mm (0.31 in.), respectively. The maximum rut depth measured on the section was 15.1 mm (0.61 in.), recorded at Station 13.

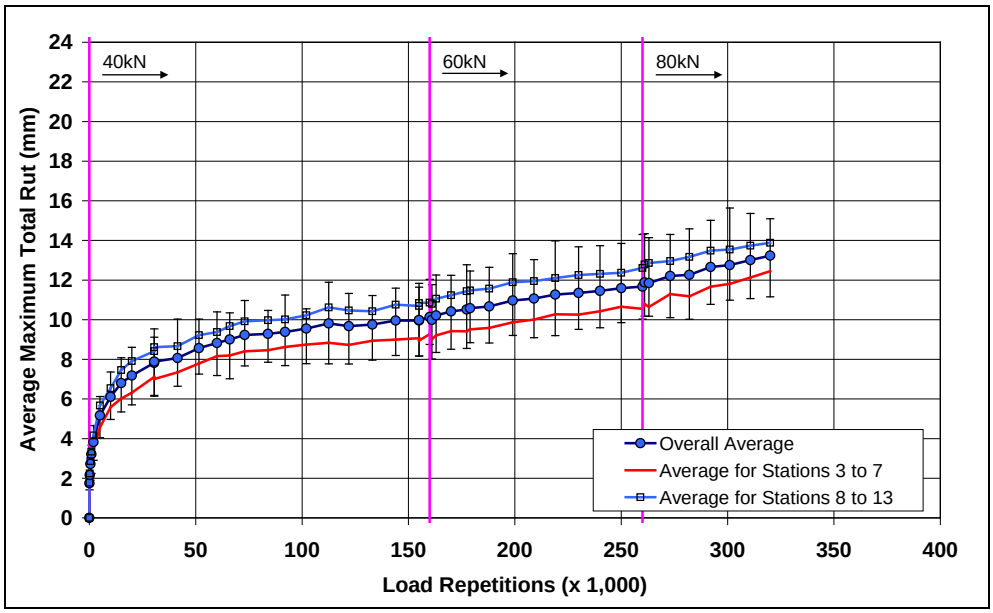

Figure 4.8: 624HB: Average maximum rut.

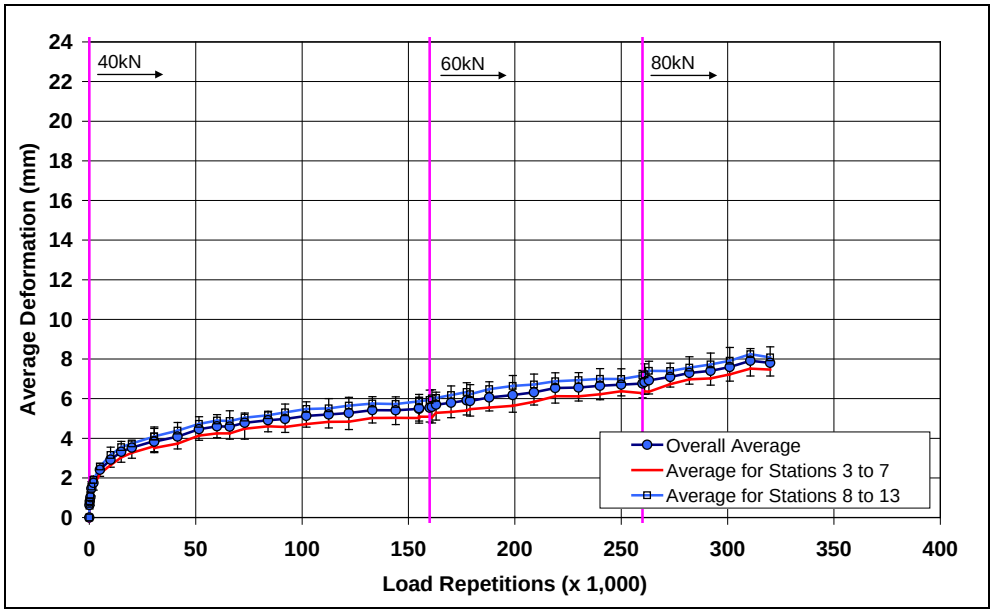

Figure 4.9: 624HB: Average deformation.

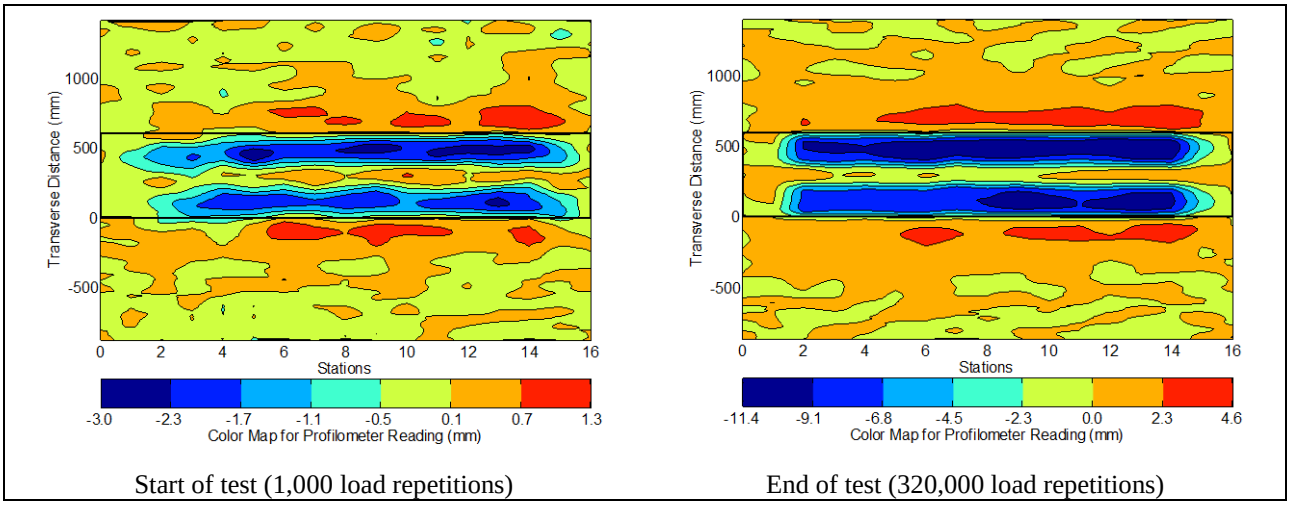

Start of test (1,000 load repetitions) End of test (320,000 load repetitions)

Figure 4.10: 624HB: Contour plots of permanent surface deformation.
(Note that key scales are different.)

4.3.6 Visual Inspection

Apart from rutting, no other distress was recorded on the section. Figure 4.11 is a photograph taken of the surface at the end of the test.

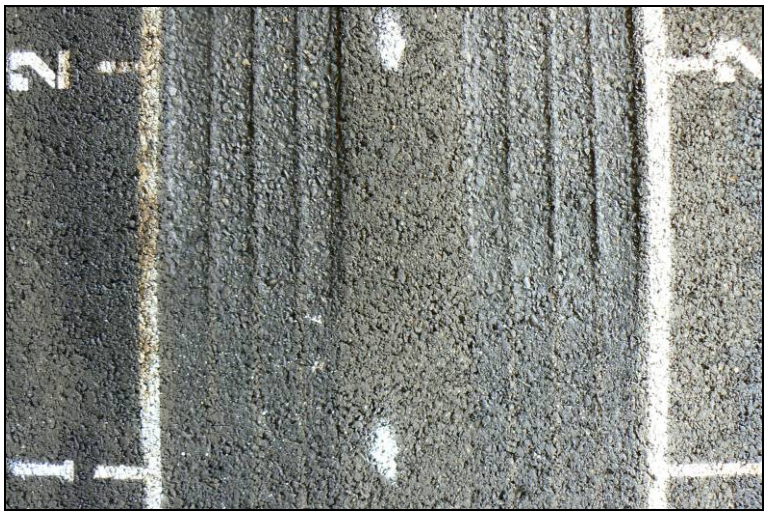

Figure 4.11: 624HB: Section photograph at test completion.

4.4 Section 625HA: Sasobit (Test #1)

4.4.1 Test Summary

Loading commenced on September 9, 2010, and ended on October 18, 2010. A total of 365,000 load repetitions were applied and 46 datasets were collected. Load was increased to 60 kN and 80 kN after 160,000 and 260,000 load repetitions, respectively. The HVS loading history for Section 625HA is shown in Figure 4.12. No shutdowns or breakdowns occurred during this test.

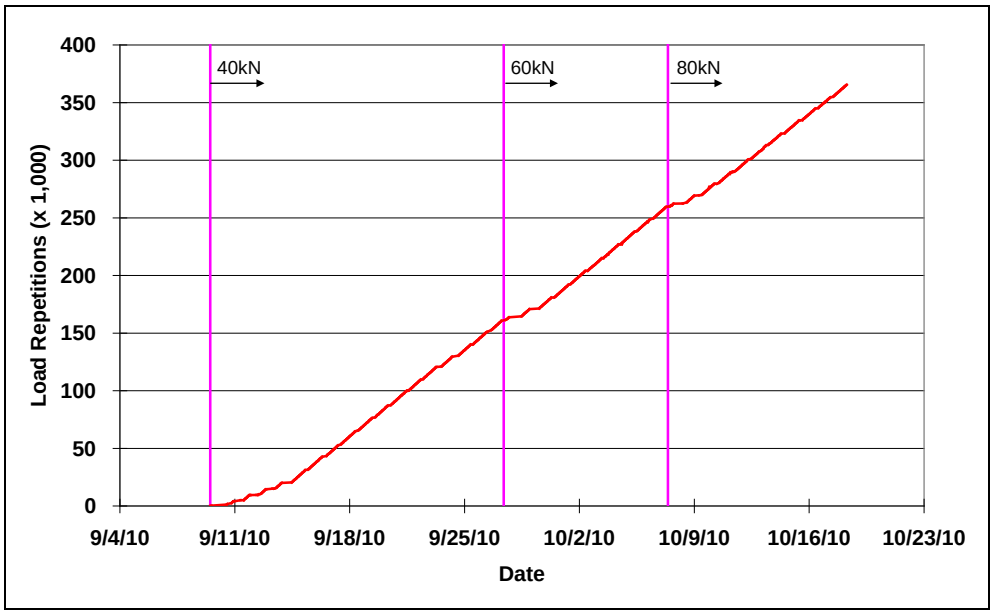

Figure 4.12: 625HA: Load history.

4.4.2 Outside Air Temperatures

Daily average outside air temperatures are summarized in Figure 4.13. Vertical error bars on each point on the graph show the daily temperature range. Temperatures ranged from 10°C to 38°C (50°F to 100°F) during the course of HVS testing, with a daily average of 22°C (72°F), an average minimum of 15°C (59°F), and an average maximum of 30°C (86°F). Temperatures decreased notably towards the end of the test. Outside air temperatures were in a similar range to those recorded during testing of the Control.

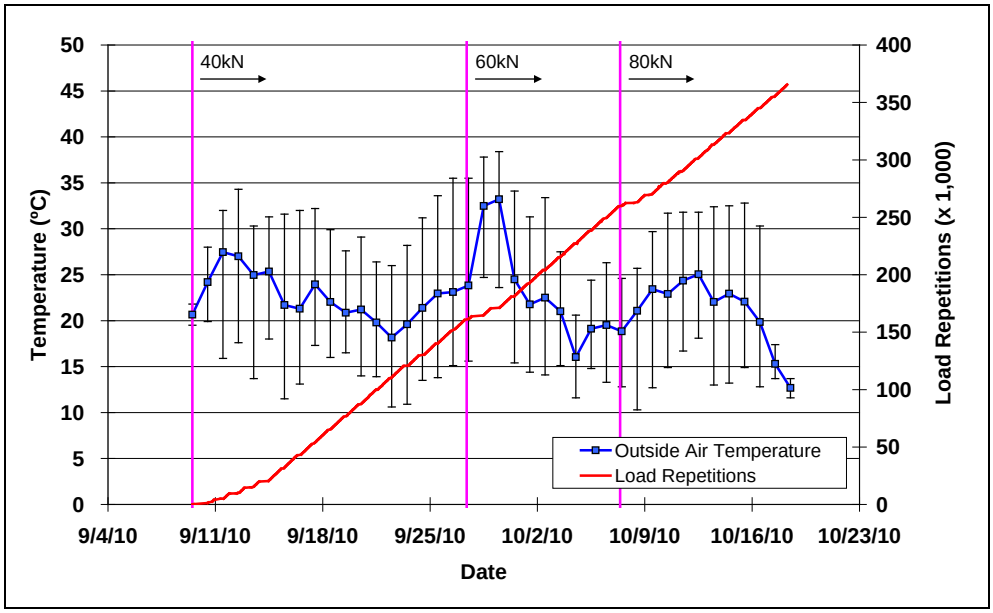

Figure 4.13: 625HA: Daily average outside air temperatures.

4.4.3 Air Temperatures in the Temperature Control Unit

During the test, the measured air temperatures inside the temperature control chamber ranged from 35°C to 54°C (95°F to 129°F) with an average of 43°C (109°F) and a standard deviation of 3.3°C (6.0°F). The air temperature was adjusted to maintain a pavement temperature of 50°C±4°C (122°F±7°F). The daily average air temperatures recorded in the temperature control unit, calculated from the hourly temperatures recorded during HVS operation, are shown in Figure 4.14. Vertical error bars on each point on the graph show daily temperature range.

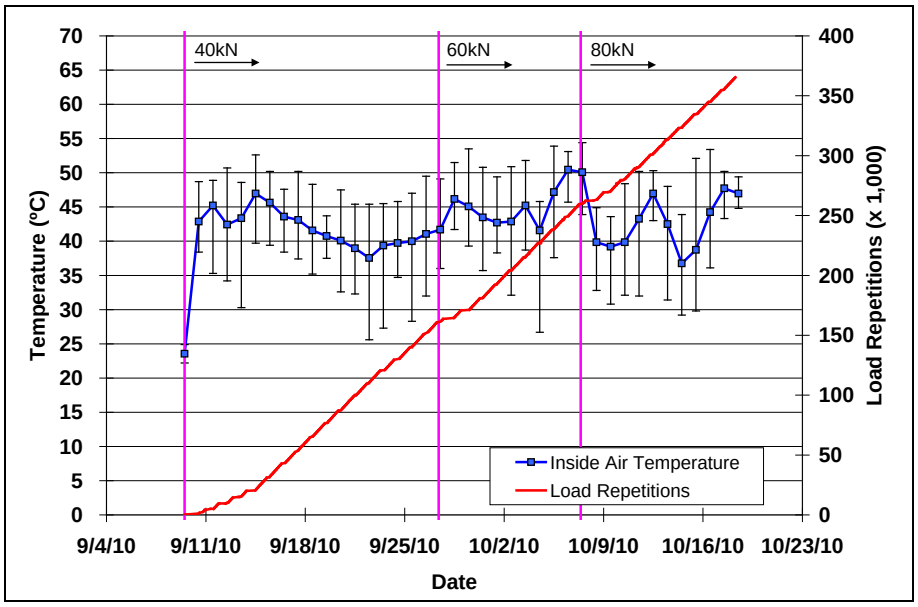

Figure 4.14: 625HA: Daily average inside air temperatures.

4.4.4 Temperatures in the Asphalt Concrete Layers

Daily averages of the surface and in-depth temperatures of the asphalt concrete layers are listed in Table 4.2, and shown in Figure 4.15. Data for the Control section are included for comparison. Temperatures were very similar to those recorded on the Control section. Pavement temperatures decreased slightly with increasing depth in the pavement, as expected. Average pavement temperatures at all depths of Section 625HA were similar to those recorded on the Control.

Table 4.2: 625HA: Temperature Summary for Air and Pavement

Temperature	625HA				624HB
	Average (°C)	Std. Dev. (°C)	Average (°F)	Std. Dev. (°F)	Average (°C)
Outside air	22	-	72	-	24
Inside air	43	3.3	109	6.0	45
Pavement surface	50	0.9	122	1.6	51
- 25 mm below surface	51	0.6	124	1.1	51
- 50 mm below surface	50	0.7	122	1.3	50
- 90 mm below surface	50	0.7	122	1.3	49
- 120 mm below surface	50	0.8	122	1.4	49

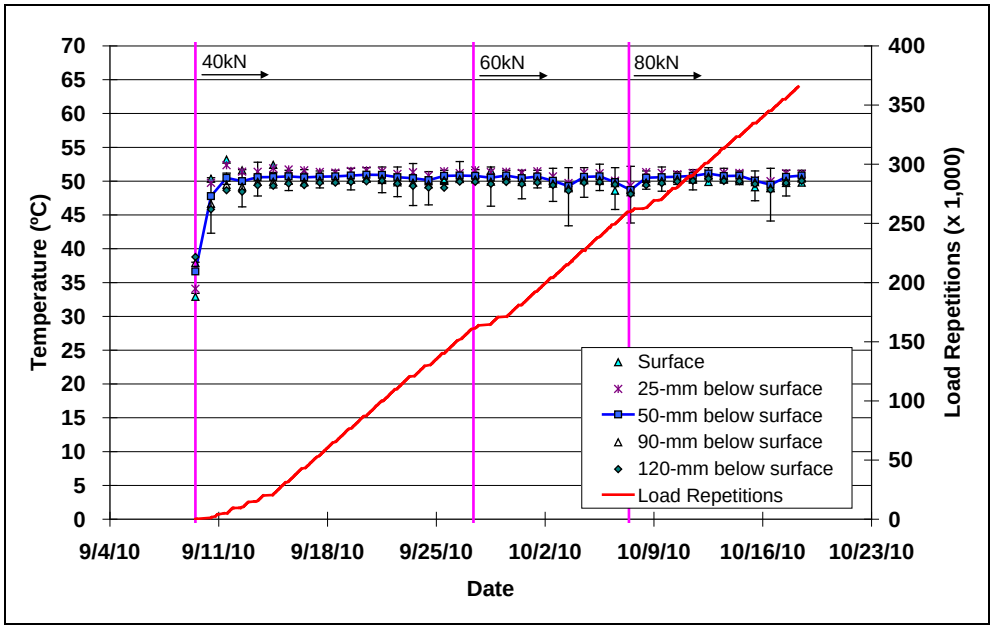

Figure 4.15: 625HA: Daily average temperatures at pavement surface and various depths.

4.4.5 Permanent Surface Deformation (Rutting)

Figure 4.16 shows the average transverse cross section measured with the laser profilometer at various stages of the test and shows the increase in rutting and deformation over time.

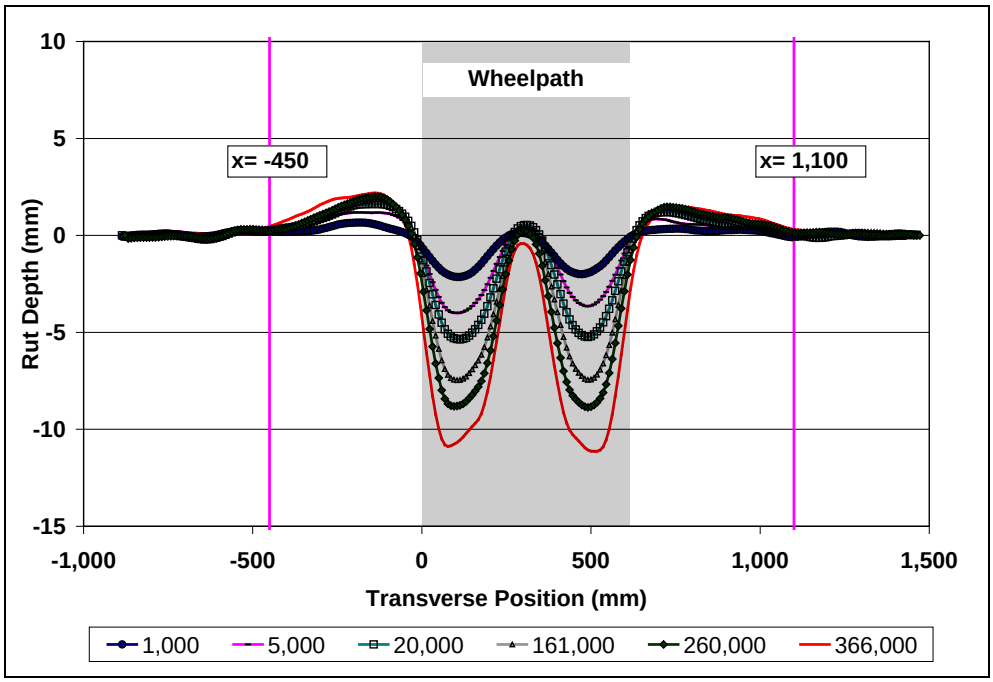

Figure 4.16: 625HA: Profilometer cross section at various load repetitions.

Figure 4.17 and Figure 4.18 show the development of permanent deformation (average maximum rut and average deformation, respectively) with load repetitions as measured with the laser profilometer for the test section. Results for the Control section (Section 624HB) are also shown for comparative purposes. Rutting performance was very similar on both sections for both the embedment and longer-term loading phases. This behavior differs from earlier testing on dense-graded mixes with conventional binders, which have typically shown warm-mixes to have deeper rutting than the Control at the end of the embedment phase. This difference in behavior could be attributed to the better compaction (lower air-void content) on the Sasobit section, and/or to the additional "curing" time between construction and the start of HVS testing. These parameters are being investigated in another phase of the Caltrans warm-mix asphalt study and will be discussed in a separate report. The terminal rut depth of 12.5 mm (0.5 in.) was reached after 313,000 repetitions compared to 290,000 repetitions on the control. Average deformation (down rut) on the Sasobit section was also very similar to that recorded on the Control at the same number of repetitions (8.3 mm [0.33 in.] compared to 7.9 mm [0.31 in.] on the Control). Error bars on the average reading indicate that there was very little variation along the length of the section.

Increases in the applied load (to 60 kN and then 80 kN) had very little effect on the rate of rut depth increase. Error bars on the average reading indicate that there was very little variation along the length of the section; however, rut depths were slightly deeper on the second half of the section compared to the first half.

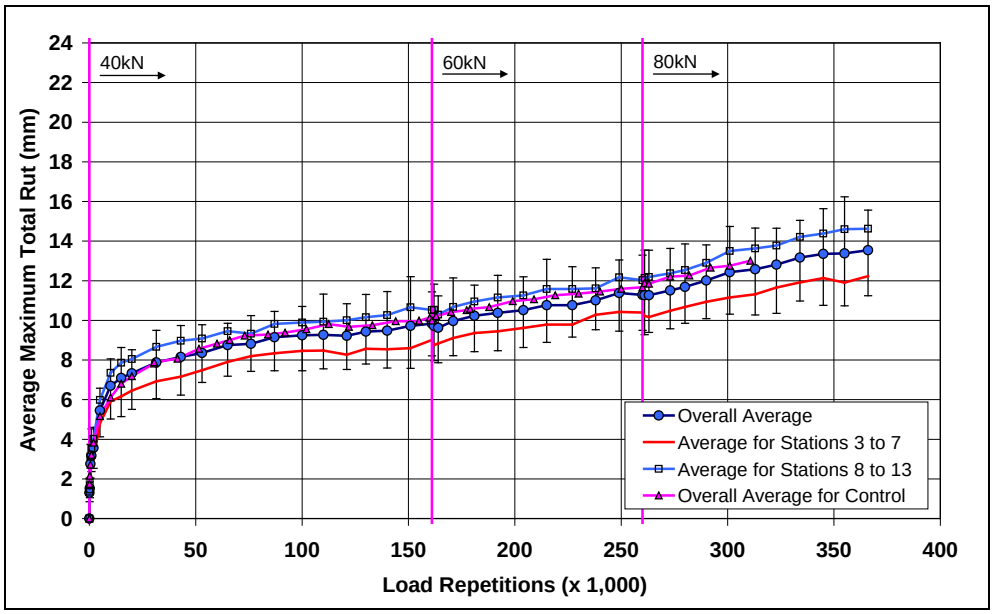

Figure 4.17: 625HA: Average maximum rut.

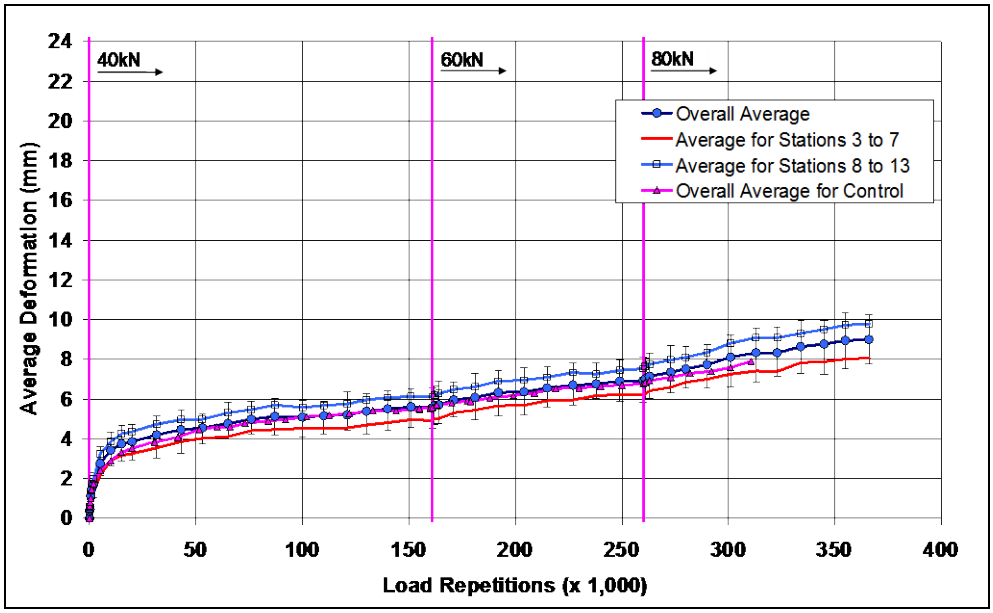

Figure 4.18: 625HA: Average deformation.

Figure 4.19 shows contour plots of the pavement surface at the start and end of the test (366,000 repetitions) that also indicate minimal variation along the section.

After completion of trafficking, the average maximum rut depth and the average deformation were 13.5 mm (0.53 in.) and 9.0 mm (0.35 in.), respectively. The maximum rut depth measured on the section was 15.6 mm (0.61 in.), recorded at Station 13.

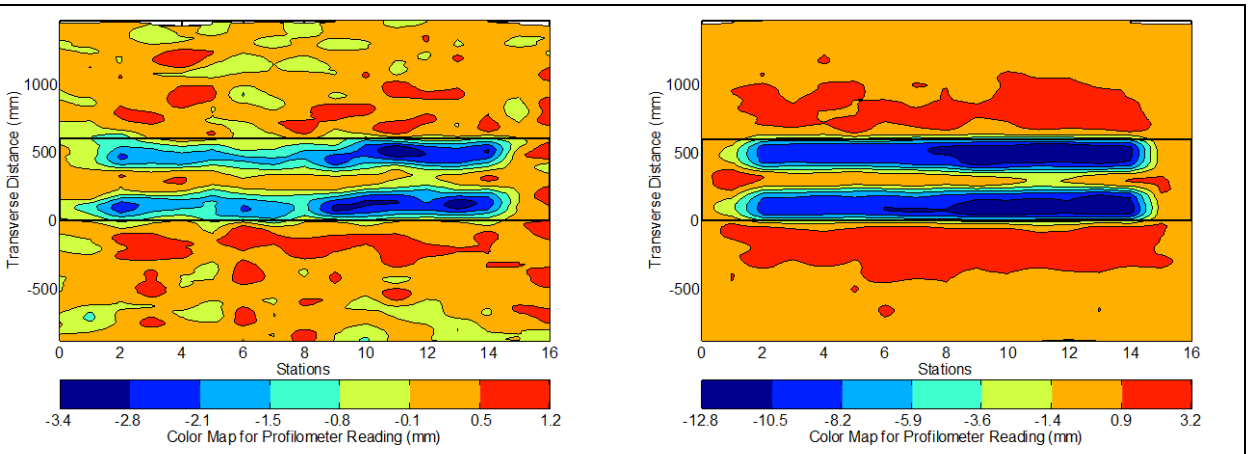

Start of test (1,000 load repetitions)

End of test (366,000 load repetitions)

Figure 4.19: 625HA: Contour plots of permanent surface deformation.
(Note that key scales are different.)

4.4.6 Visual Inspection

Apart from rutting, no other distress was recorded on the section, which was similar in appearance to the Control (Figure 4.11) at the end of testing. Figure 4.20 shows a photograph taken of the surface at the end of the test.

Figure 4.20: 625HA: Section photograph at test completion.

4.5 Section 626HA: Advera (Test #1)

4.5.1 Test Summary

Loading commenced on December 14, 2010, and ended on January 16, 2011. Testing was stopped for the holiday break. A total of just 50,000 load repetitions were applied to reach an average maximum rut depth of 12 mm, indicating significantly different performance to that recorded on the Control section. Testing was halted at this point to determine the cause of this difference in performance, and a second test to confirm these results was planned (see Section 4.8). The HVS loading history for Section 622HA is shown in Figure 4.21.

4.5.2 Outside Air Temperatures

Daily average outside air temperatures are summarized in Figure 4.22. Vertical error bars on each point on the graph show the daily temperature range. Temperatures ranged from 1°C to 11°C (34°F to 52°F) during the course of HVS testing, with a daily average of 9°C (48°F), an average minimum of 6°C (43°F), and an average maximum of 11°C (52°F). Outside air temperatures were considerably cooler during testing on Section 626HA compared to those during testing of the Control.

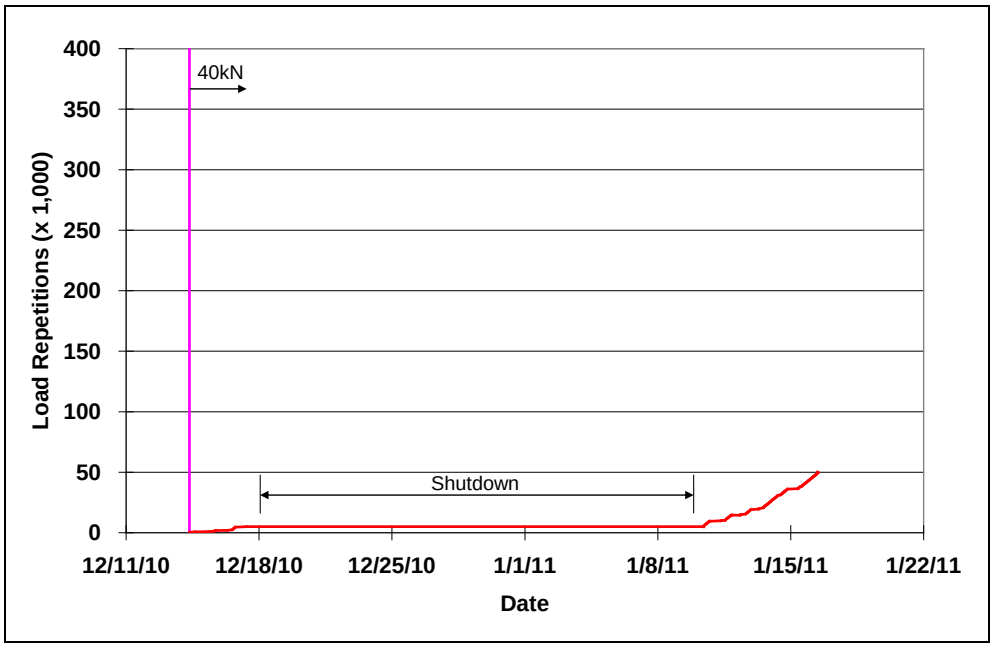

Figure 4.21: 626HA: Load history.

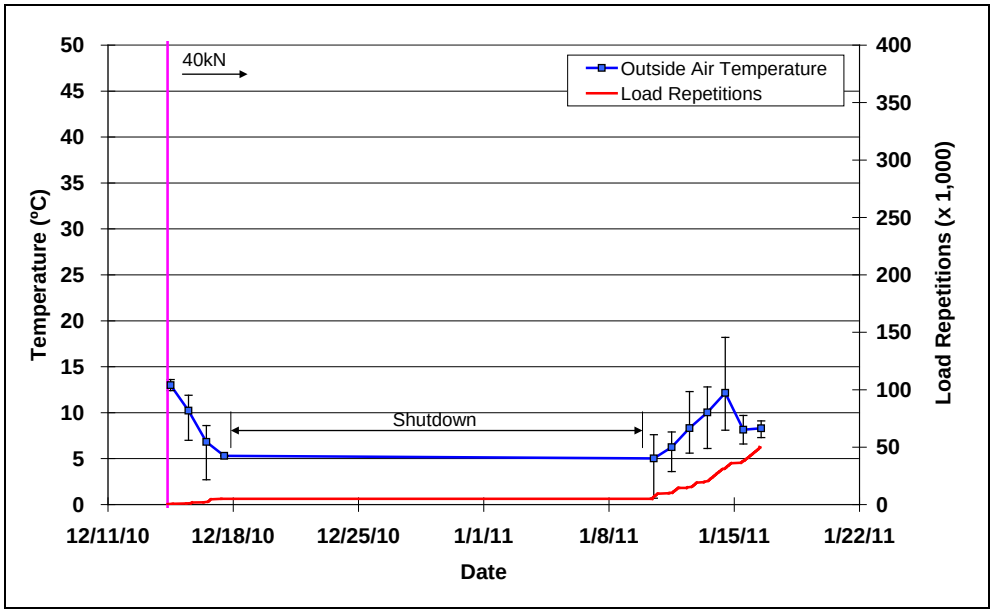

Figure 4.22: 626HA: Daily average outside air temperatures.

4.5.3 Air Temperatures in the Temperature Control Unit

During the test, air temperatures inside the temperature control chamber ranged from 25°C to 48°C (77°F to 118°F) with an average of 38°C (100°F) and a standard deviation of 4.3°C (7.7°F). The air temperature was adjusted to maintain a pavement temperature of 50°C±4°C (122°F±7°F). The daily average air temperatures recorded in the temperature control unit, calculated from the hourly temperatures recorded

during HVS operation, are shown in Figure 4.23. Vertical errors bars on each point on the graph show daily temperature range.

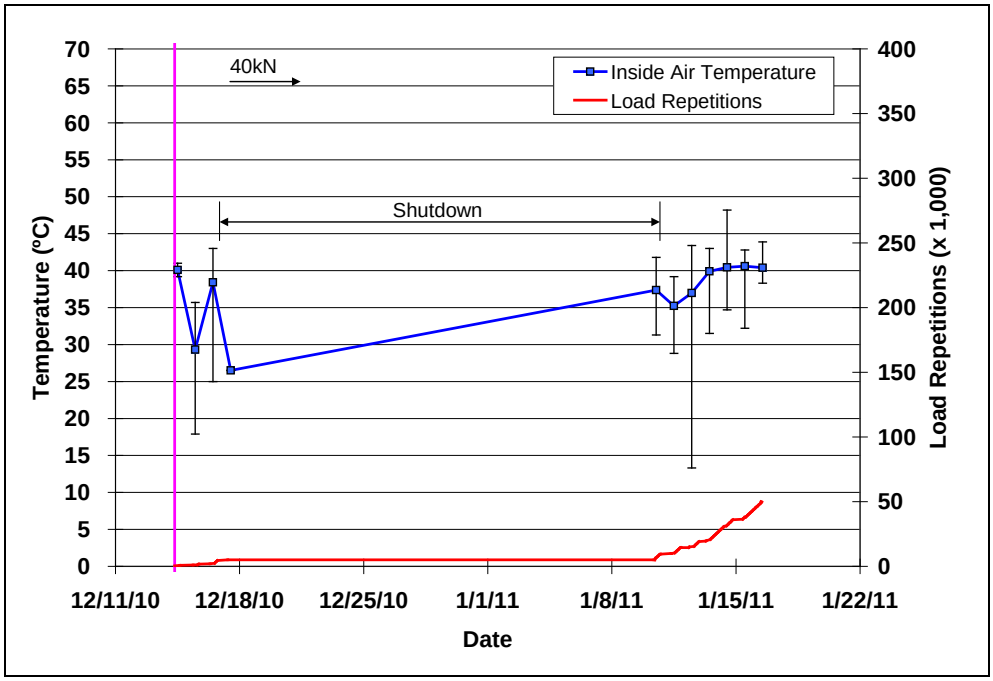

Figure 4.23: 626HA: Daily average inside air temperatures.

4.5.4 Temperatures in the Asphalt Concrete Layers

Daily averages of the surface and in-depth temperatures of the asphalt concrete layers are listed in Table 4.3 and shown in Figure 4.24. Pavement temperatures decreased slightly with increasing depth in the pavement, as expected. Average pavement temperatures at all depths of Section 626HA were similar to those recorded on the Control, despite significantly lower outside temperatures for this test.

Table 4.3: 626HA: Temperature Summary for Air and Pavement

Temperature	626HA				624HB
	Average (°C)	Std. Dev. (°C)	Average (°F)	Std. Dev. (°F)	Average (°C)
Outside air	9	-	48	-	24
Inside air	38	4.3	100	7.7	45
Pavement surface	49	1.9	120	3.4	51
- 25 mm below surface	51	1.7	124	3.1	51
- 50 mm below surface	50	1.3	122	2.3	50
- 90 mm below surface	48	1.6	118	2.9	49
- 120 mm below surface	47	1.2	117	2.2	49

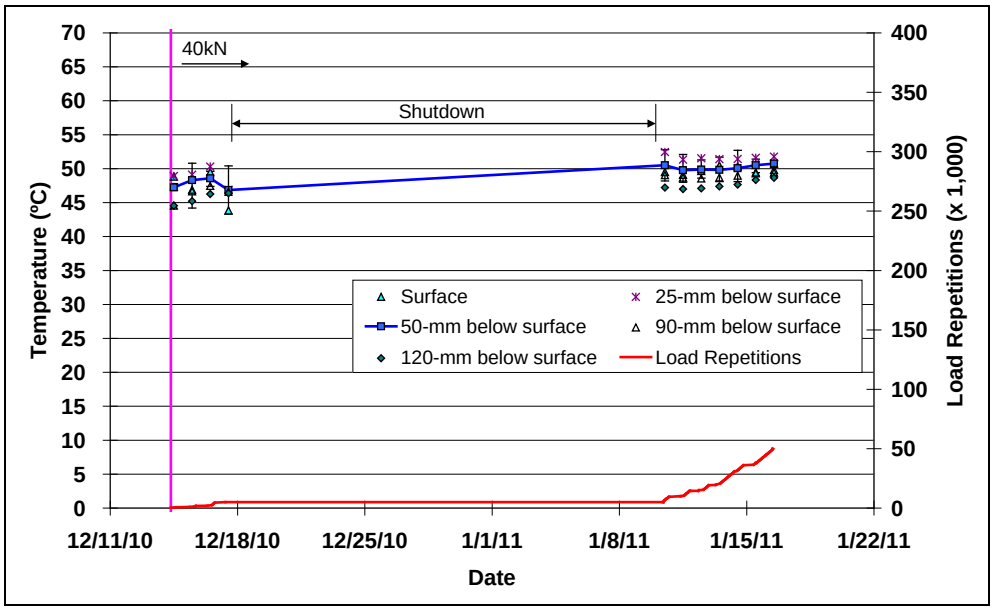

Figure 4.24: 626HA: Daily average temperatures at pavement surface and various depths.

4.5.5 Permanent Surface Deformation (Rutting)

Figure 4.25 shows the average transverse cross section measured with the laser profilometer at various stages of the test and shows the increase in rutting and deformation over time.

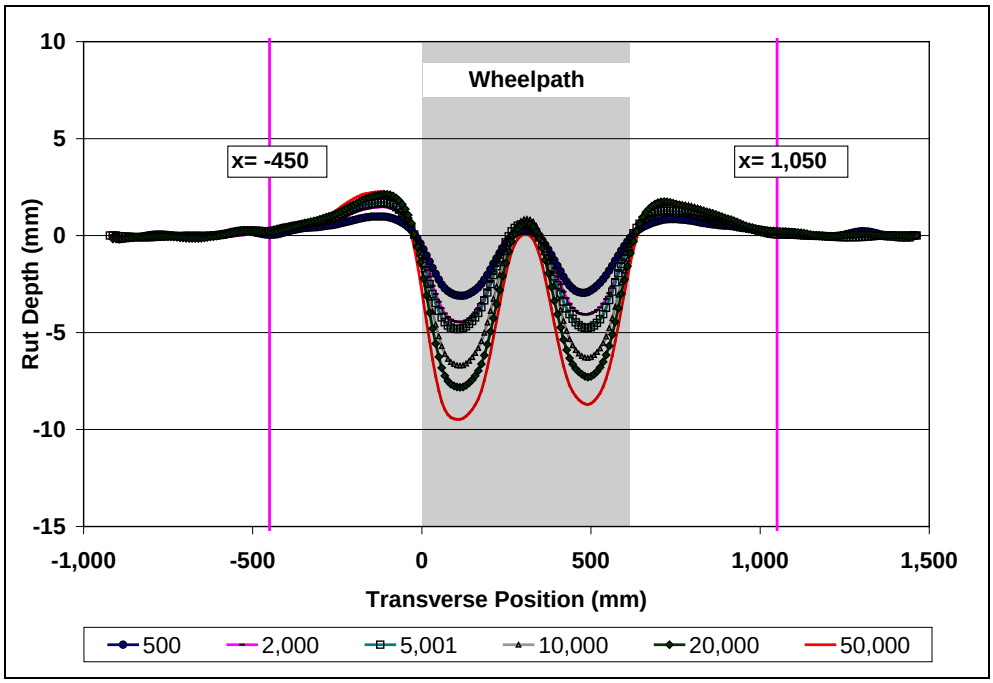

Figure 4.25: 626HA: Profilometer cross section at various load repetitions.

Figure 4.26 and Figure 4.27 show the development of permanent deformation (average maximum rut and average deformation, respectively) with load repetitions as measured with the laser profilometer for the test section. Results for the Control section (Section 624HB) are also shown for comparative purposes. Rutting behavior on this section was very different than that of the Control, despite having better compaction (lower air-void content) and was only explained after a forensic investigation on the section (see Section 5.7.3), which attributed this poor performance mostly to a high subgrade moisture content. Routine and additional load checks did not indicate any equipment problems that may have influenced the performance.

The test was essentially terminated before the rut rate had stabilized after the embedment phase. During this embedment phase the rate of rutting on the Advera section was significantly higher compared to the Control section, both in terms of duration and rut depth. Average deformation (down rut) on the Advera section was similar to that measured at the end of the Control test. Error bars on the average reading showed no variation along the length of the section.

Follow-up tests with the second HVS were scheduled to eliminate any equipment-related problems (see Sections 4.8 and 4.9).

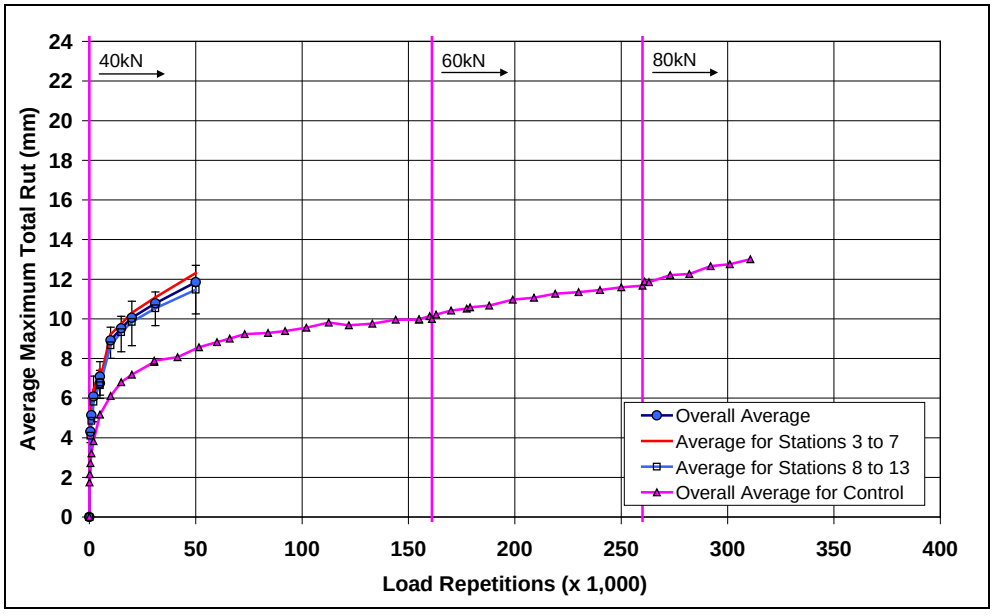

Figure 4.26: 626HA: Average maximum rut.

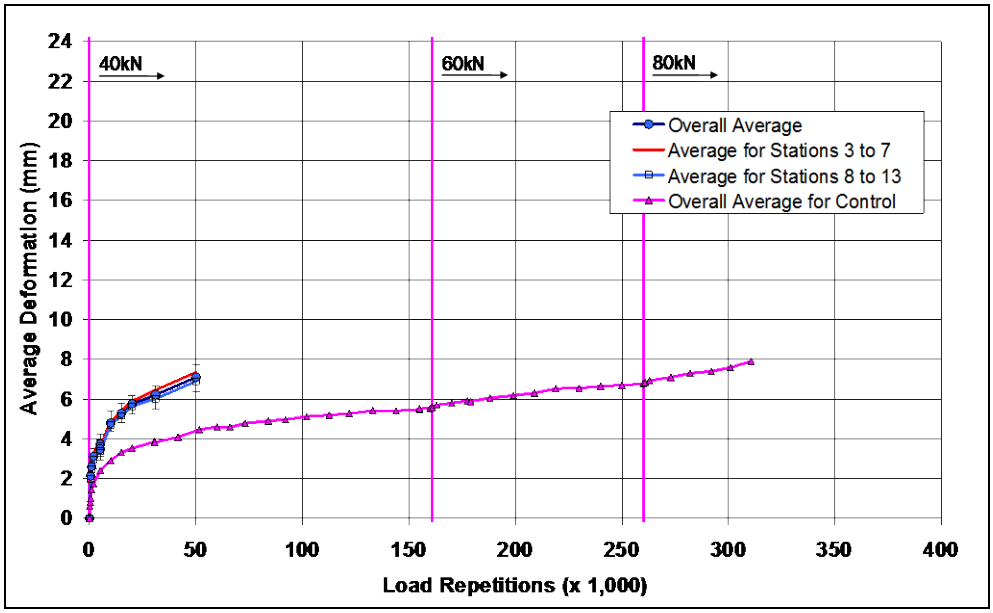

Figure 4.27: 626HA: Average deformation.

Figure 4.28 shows contour plots of the pavement surface at the start and end of the test (50,000 repetitions).

After completion of all trafficking, the average maximum rut depth and the average deformation were 11.9 mm (0.47 in.) and 7.1 mm (0.28 in.), respectively. The maximum rut depth measured on the section was 12.7 mm (0.50 in.), recorded at Station 3.

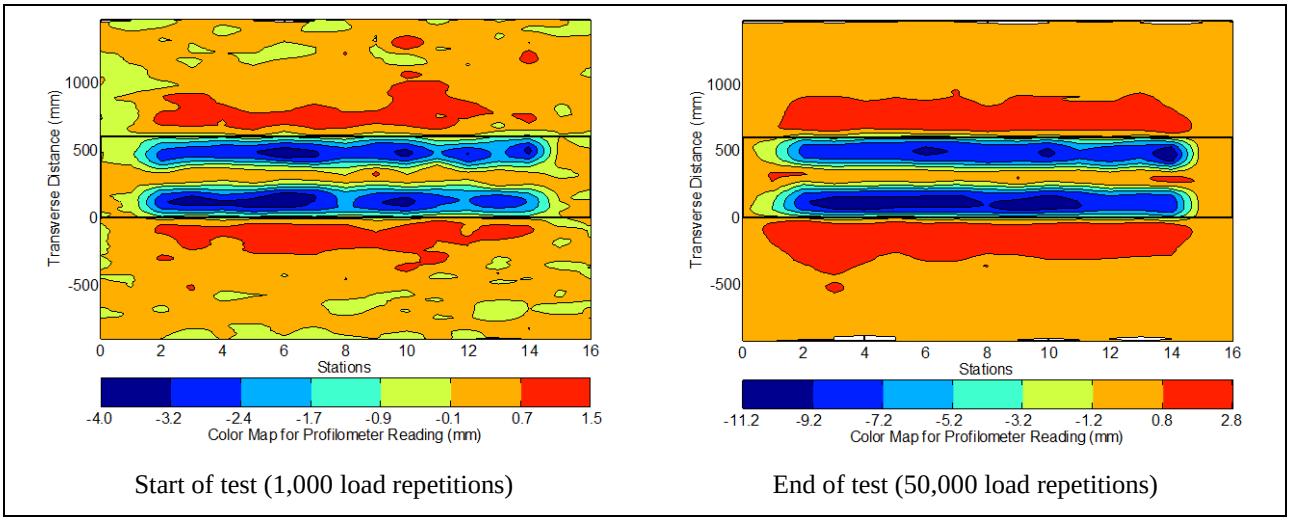

Start of test (1,000 load repetitions) End of test (50,000 load repetitions)

Figure 4.28: 626HA: Contour plots of permanent surface deformation.
(Note that key scales are different.)

4.5.6 Visual Inspection

Apart from rutting, no other distress was recorded on the section. Figure 4.29 shows a photograph taken of the surface at the end of the test.

Figure 4.29: 626HA: Section photograph at test completion.

4.6 Section 627HB: Astec

4.6.1 Test Summary

Loading commenced on November 11, 2010, and ended on December 16, 2010. A total of 242,000 load repetitions were applied and 33 datasets were collected. Load was increased to 60 kN (13,500 lb) after 160,000 load repetitions, in line with the test plan. The HVS loading history for Section 627HB is shown in Figure 4.30. One shutdown occurred in the middle of the test over the Thanksgiving holiday.

4.6.2 Outside Air Temperatures

Daily average outside air temperatures are summarized in Figure 4.31. Vertical error bars on each point on the graph show the daily temperature range. Temperatures ranged from 1°C to 26°C (34°F to 79°F) during the course of HVS testing, with a daily average of 12°C (54°F), an average minimum of 8°C (46°F), and an average maximum of 16°C (51°F). Average outside air temperatures were considerably cooler during testing on Section 627HB compared to those during testing on the Control (daily average of 12°C [22°F] cooler).

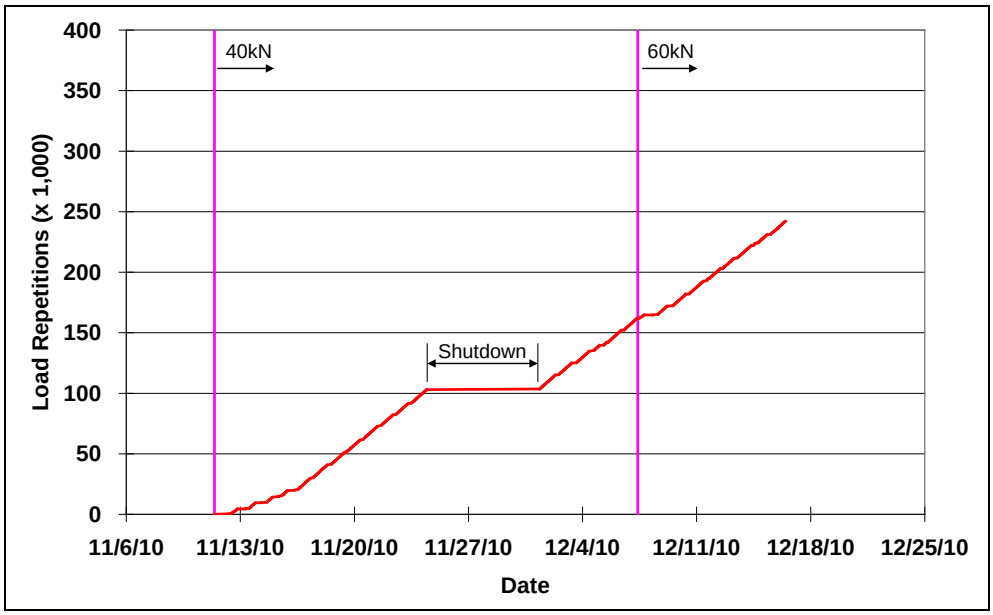

Figure 4.30: 627HB: Load history.

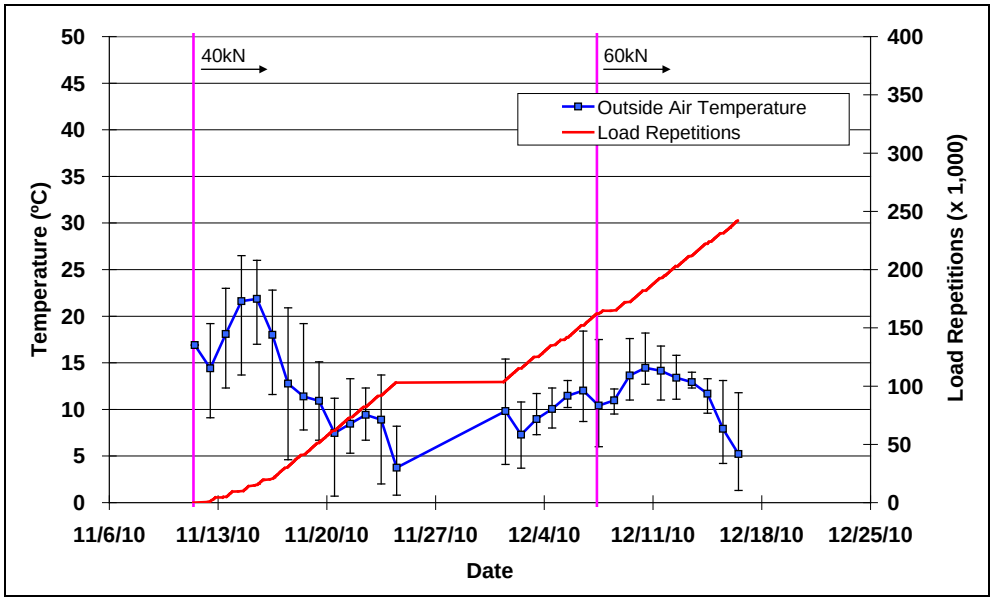

Figure 4.31: 627HB: Daily average outside air temperatures.

4.6.3 Air Temperatures in the Temperature Control Unit

During the test, air temperatures inside the temperature control chamber ranged from 23°C to 53°C (73°F to 127°F) with an average of 43°C (109°F) and a standard deviation of 2°C (4°F). The air temperature was adjusted to maintain a pavement temperature of 50°C±4°C (122°F±7°F). The daily average air temperatures recorded in the temperature control unit, calculated from the hourly temperatures recorded

during HVS operation, are shown in Figure 4.32. Vertical error bars on each point on the graph show daily temperature range.

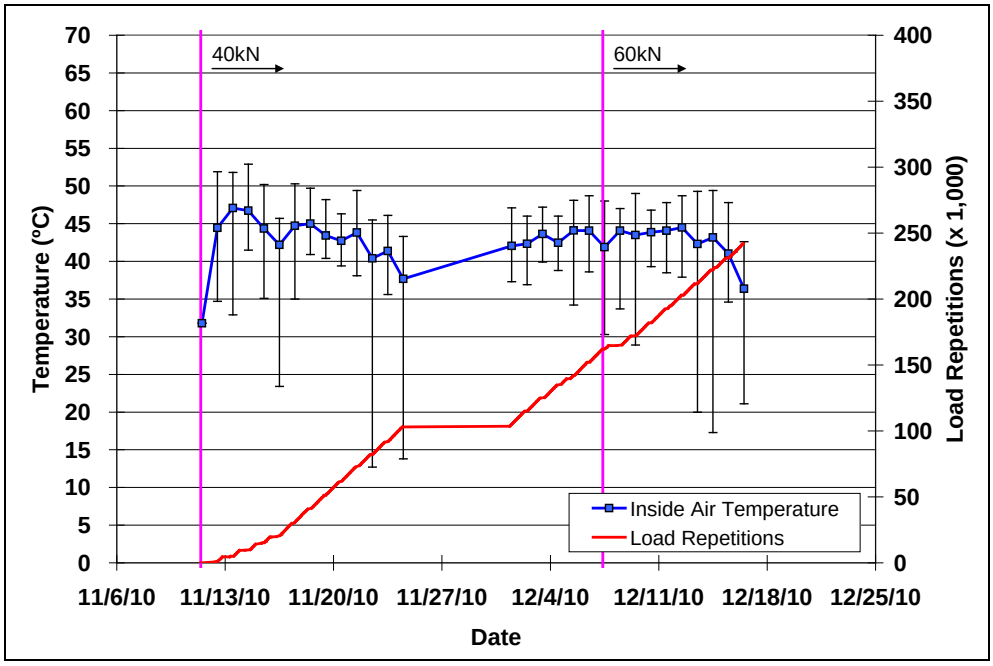

Figure 4.32: 627HB: Daily average inside air temperatures.

4.6.4 Temperatures in the Asphalt Concrete Layers

Daily averages of the surface and in-depth temperatures of the asphalt concrete layers are listed in Table 4.4 and shown in Figure 4.33. Pavement temperatures decreased slightly with increasing depth in the pavement, as expected. Average pavement temperatures at all depths on Section 627HB were similar to those recorded on the Control, despite lower outside temperatures.

Table 4.4: 627HB: Temperature Summary for Air and Pavement

Temperature	627HB				624HB
	Average (°C)	Std. Dev. (°C)	Average (°F)	Std. Dev. (°F)	Average (°C)
Outside air	12	-	54	-	24
Inside air	43	1.5	109	2.7	45
Pavement surface	49	1.8	120	2.2	51
- 25 mm below surface	50	0.8	122	1.4	51
- 50 mm below surface	50	0.6	122	1.1	50
- 90 mm below surface	48	0.6	118	1.1	49
- 120 mm below surface	48	0.7	118	1.3	49

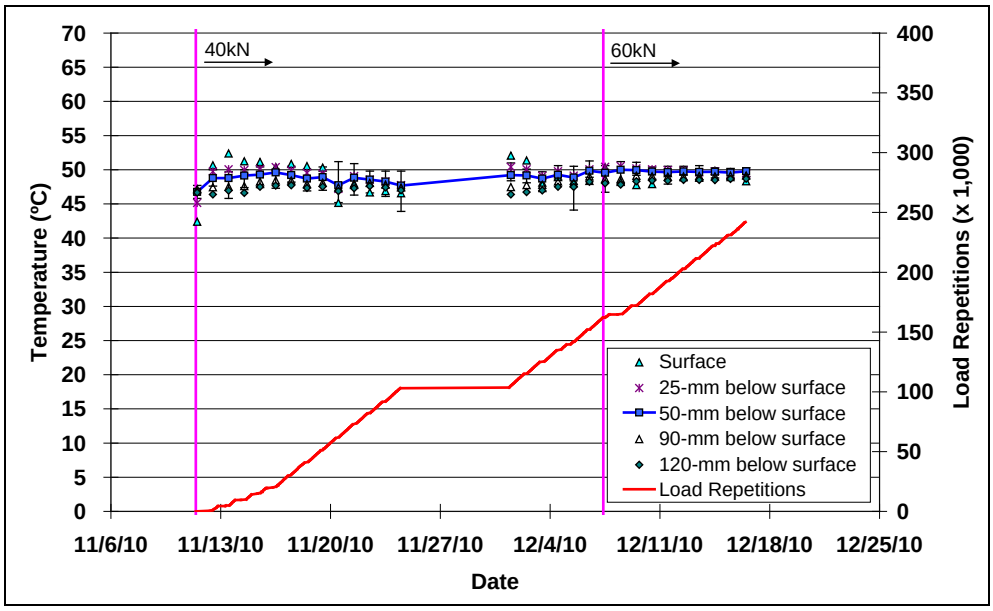

Figure 4.33: 627HB: Daily average temperatures at pavement surface and various depths.

4.6.5 Permanent Surface Deformation (Rutting)

Figure 4.34 shows the average transverse cross section measured with the laser profilometer at various stages of the test and shows the increase in rutting and deformation over time.

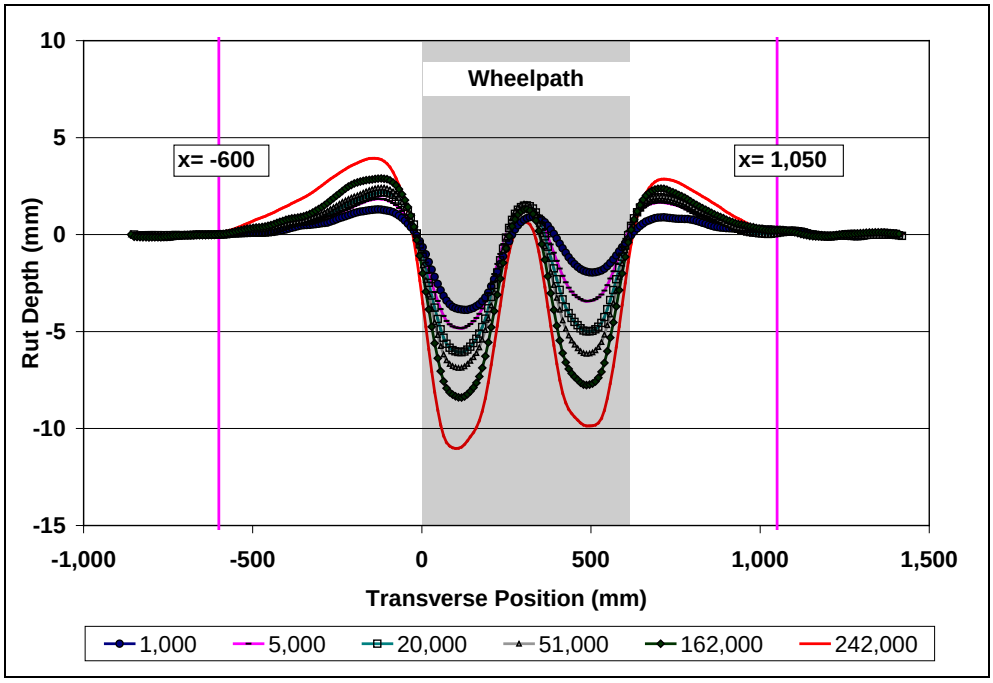

Figure 4.34: 627HB: Profilometer cross section at various load repetitions.

Figure 4.35 and Figure 4.36 show the development of permanent deformation (average maximum rut and average deformation, respectively) with load repetitions as measured with the laser profilometer for the test section. Results for the Control section (Section 624HB) are also shown for comparative purposes. Although the embedment phase was of similar duration for both sections, the Astec section had a slightly deeper average maximum rut compared to the Control after the same number of load repetitions (8.3 mm [0.33 in.]) compared to the Control (7.2 mm [0.28 in.]), despite this section having a lower air-void content than the Control section (9.1 percent compared to 11.6 percent). This behavior corresponds to results from earlier testing on dense-graded mixes with conventional binders, which typically showed warm-mixes to have deeper rutting than the control at the end of the embedment phase. After the embedment phase, the rate of deformation increase with increasing load repetitions was similar to the Control up to the load change to 60 kN. After the load change, the rate of deformation was higher than that on the Control. This was attributed in part to a second embedment phase (load sensitivity) as well as to an increase in subgrade moisture content after a relatively high rainfall event. Average deformation (down rut) on the Astec section was similar to that recorded on the Control up to the load change, but increased at a faster rate after the load change. At the end of the test, average deformation on the Astec section was 8.3 mm (0.33 in.) compared to 6.6 mm [0.26 in.) on the Control after the same number of load repetitions. Error bars on the average reading indicate some variation along the length of the section.

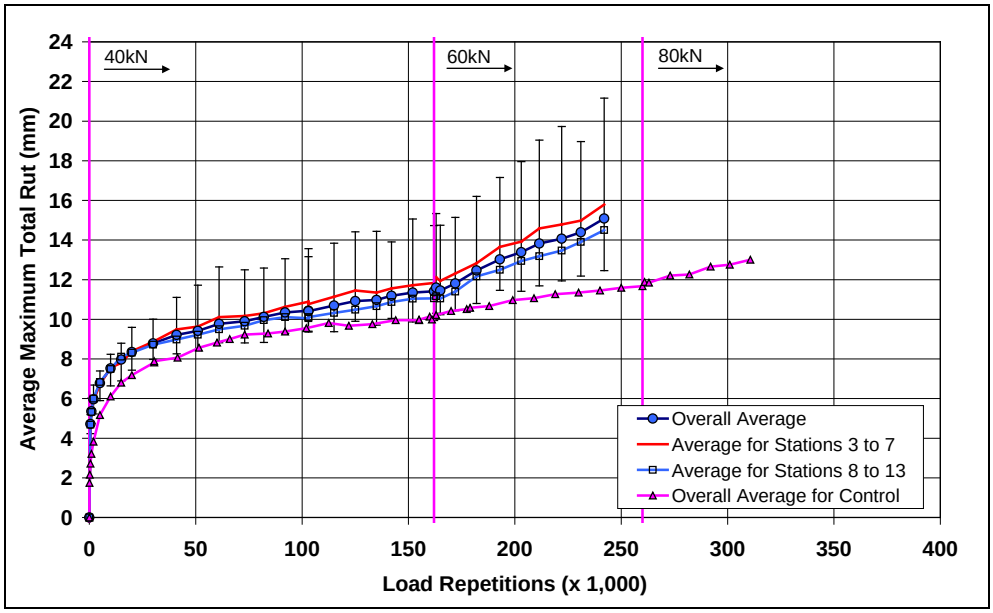

Figure 4.35: 627HB: Average maximum rut.

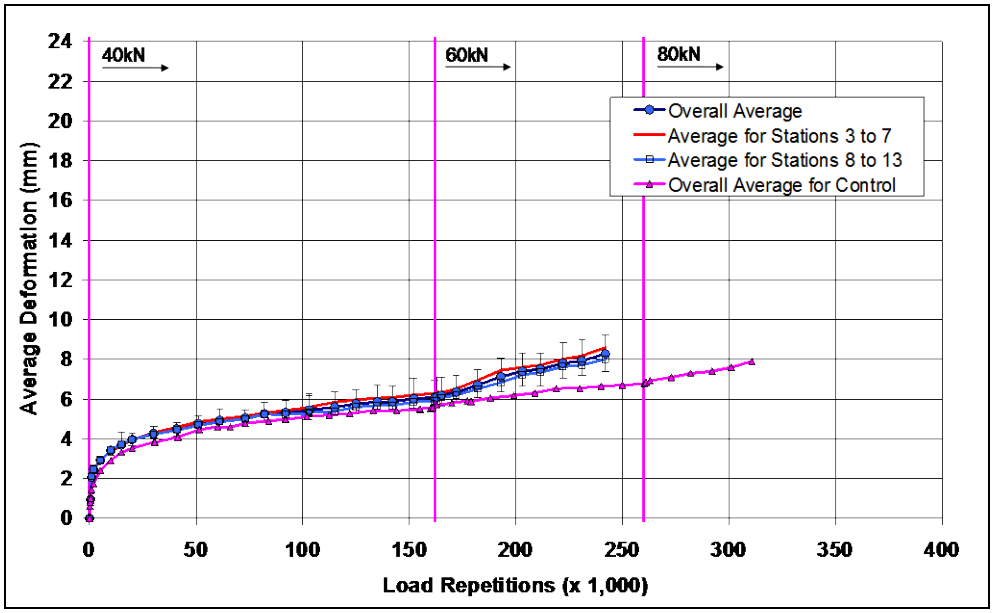

Figure 4.36: 627HB: Average deformation.

Figure 4.37 shows contour plots of the pavement surface at the start and end of the test (242,000 repetitions) that also indicate minimal variation along the section.

After completion of trafficking, the average maximum rut depth and the average deformation were 15.1 mm (0.59 in.) and 8.3 mm (0.33 in.), respectively. The maximum rut depth measured on the section was 21.2 mm (0.84 in.), recorded at Station 5.

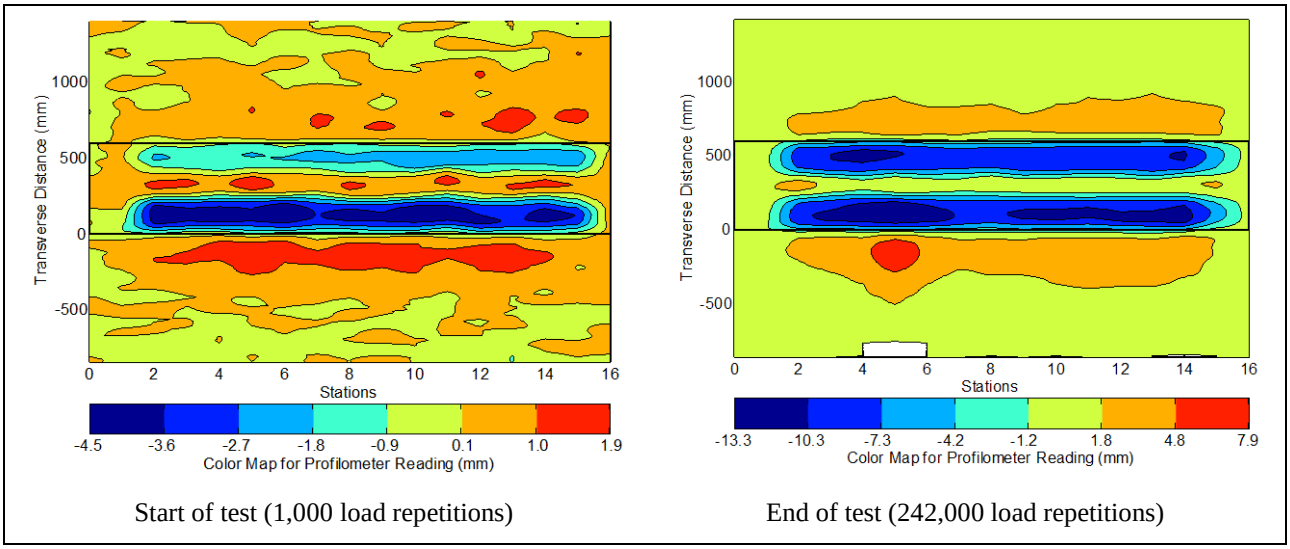

Start of test (1,000 load repetitions)

End of test (242,000 load repetitions)

Figure 4.37: 627HB: Contour plots of permanent surface deformation.
(Note that key scales are different.)

4.6.6 Visual Inspection

Apart from rutting, no other distress was recorded on the section. Its appearance was similar to that of the other sections. Figure 4.38 shows a photograph taken of the surface at the end of the test.

Figure 4.38: 627HB: Section photograph at test completion.

4.7 Section 628HB: Rediset

4.7.1 Test Summary

Loading commenced on October 1, 2010, and ended on November 8, 2010. A total of 309,000 load repetitions were applied and 41 datasets were collected. Load was increased to 60 kN (13,500 lb) after 160,000 load repetitions and to 80 kN (18,000 lb) after 260,000 load repetitions, in line with the test plan. The HVS loading history for Section 628HB is shown in Figure 4.39. No breakdowns or shutdowns occurred during the test.

4.7.2 Outside Air Temperatures

Daily average outside air temperatures are summarized in Figure 4.40. Vertical error bars on each point on the graph show the daily temperature range. Temperatures ranged from 5°C to 36°C (41°F to 97°F) during the course of HVS testing, with a daily average of 19°C (66°F), an average minimum of 13°C (55°F), and an average maximum of 26°C (79°F). Average outside air temperatures became progressively colder during testing on Section 628HB and on average were a little cooler compared to those during testing on the Control (daily average of 5°C [9°F] cooler).

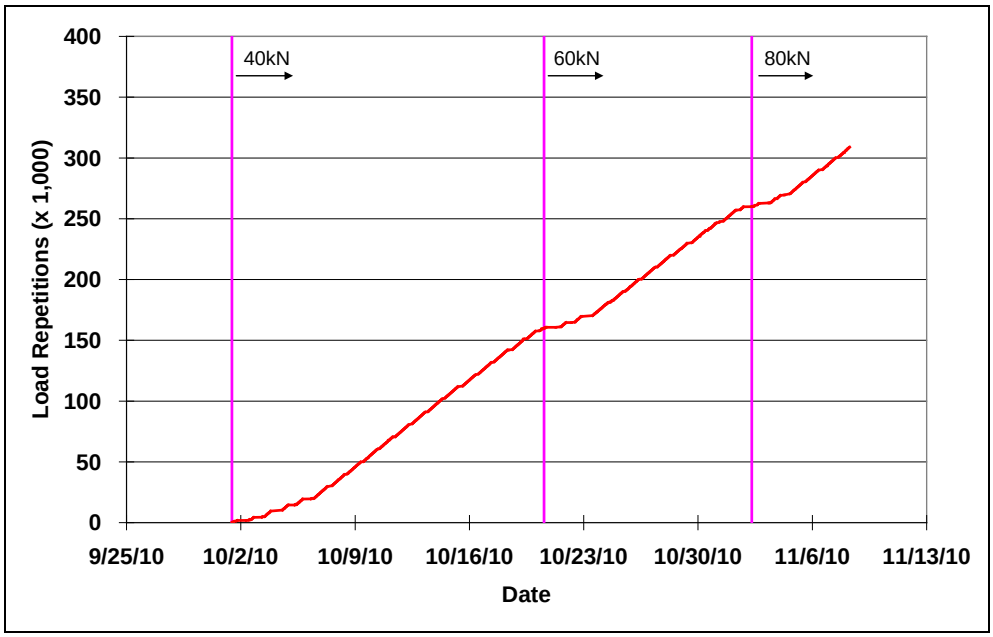

Figure 4.39: 628HB: Load history.

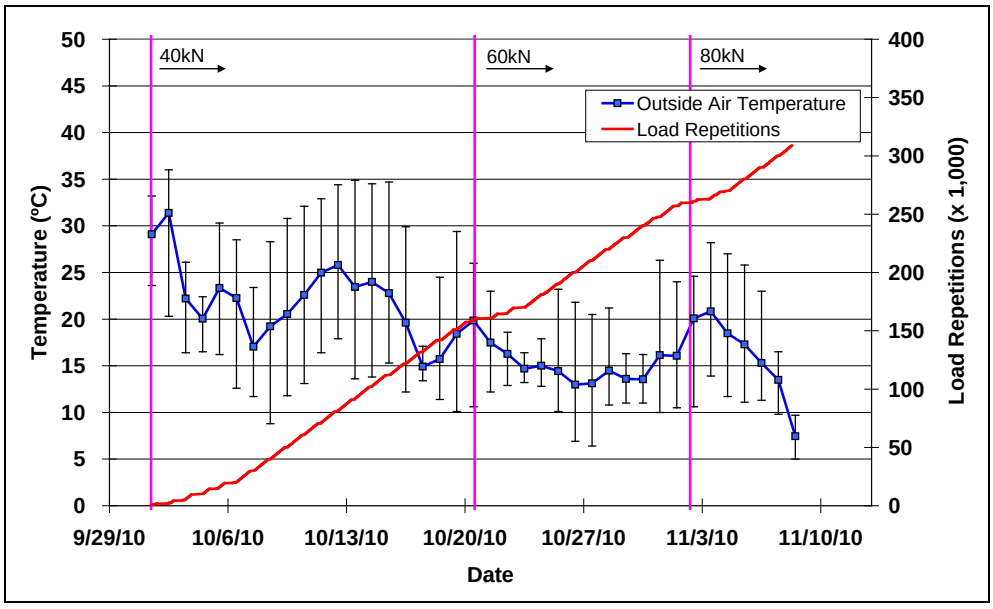

Figure 4.40: 628HB: Daily average outside air temperatures.

4.7.3 Air Temperatures in the Temperature Control Unit

During the test, air temperatures inside the temperature control chamber ranged from 26°C to 57°C (79°F to 135°F) with an average of 42°C (108°F) and a standard deviation of 3.2°C (5.8°F). The air temperature was adjusted to maintain a pavement temperature of 50°C±4°C (122°F±7°F). The daily average air temperatures recorded in the temperature control unit, calculated from the hourly temperatures recorded

during HVS operation, are shown in Figure 4.41. Vertical error bars on each point on the graph show daily temperature range.

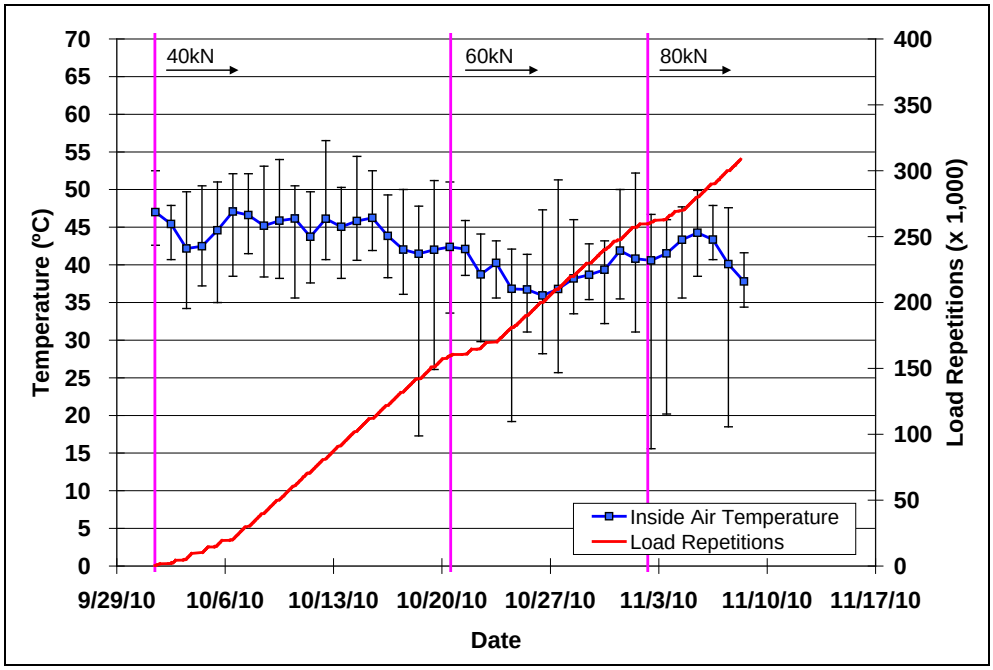

Figure 4.41: 628HB: Daily average inside air temperatures.

4.7.4 Temperatures in the Asphalt Concrete Layers

Daily averages of the surface and in-depth temperatures of the asphalt concrete layers are listed in Table 4.5 and shown in Figure 4.42. Pavement temperatures decreased slightly with increasing depth in the pavement, as expected. Average pavement temperatures at all depths on Section 628HB were similar to those recorded on the Control, despite lower outside temperatures.

Table 4.5: 628HB: Temperature Summary for Air and Pavement

Temperature	628HB				624HB
	Average (°C)	Std. Dev. (°C)	Average (°F)	Std. Dev. (°F)	Average (°C)
Outside air	19	-	66	-	24
Inside air	42	3.2	108	5.8	45
Pavement surface	51	1.3	123	2.3	51
- 25 mm below surface	51	0.5	123	0.9	51
- 50 mm below surface	50	0.3	123	0.5	50
- 90 mm below surface	50	0.5	121	0.9	49
- 120 mm below surface	49	0.6	120	1.1	49

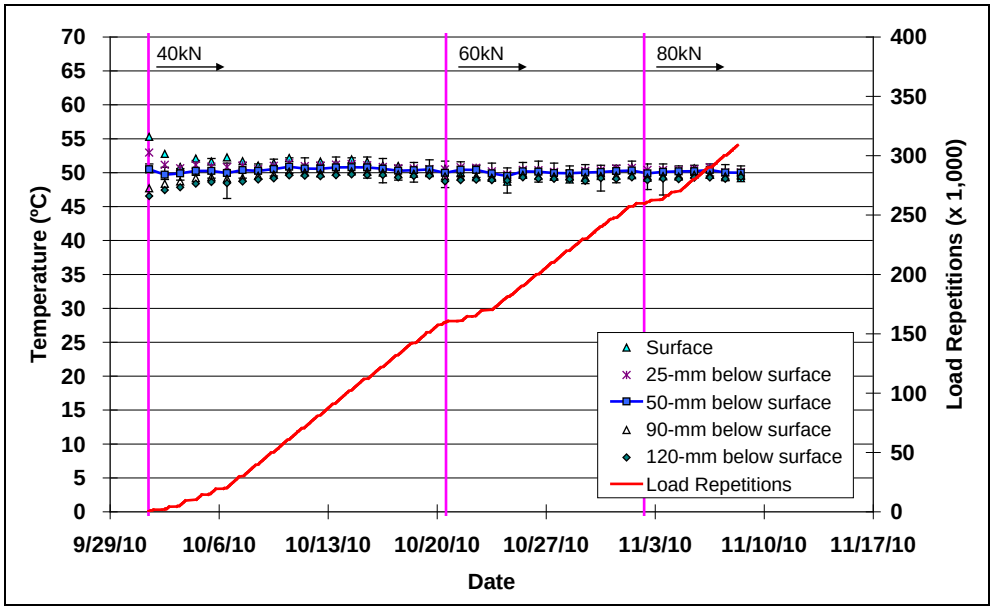

Figure 4.42: 628HB: Daily average temperatures at pavement surface and various depths.

4.7.5 Permanent Surface Deformation (Rutting)

Figure 4.43 shows the average transverse cross section measured with the laser profilometer at various stages of the test and shows the increase in rutting and deformation over time.

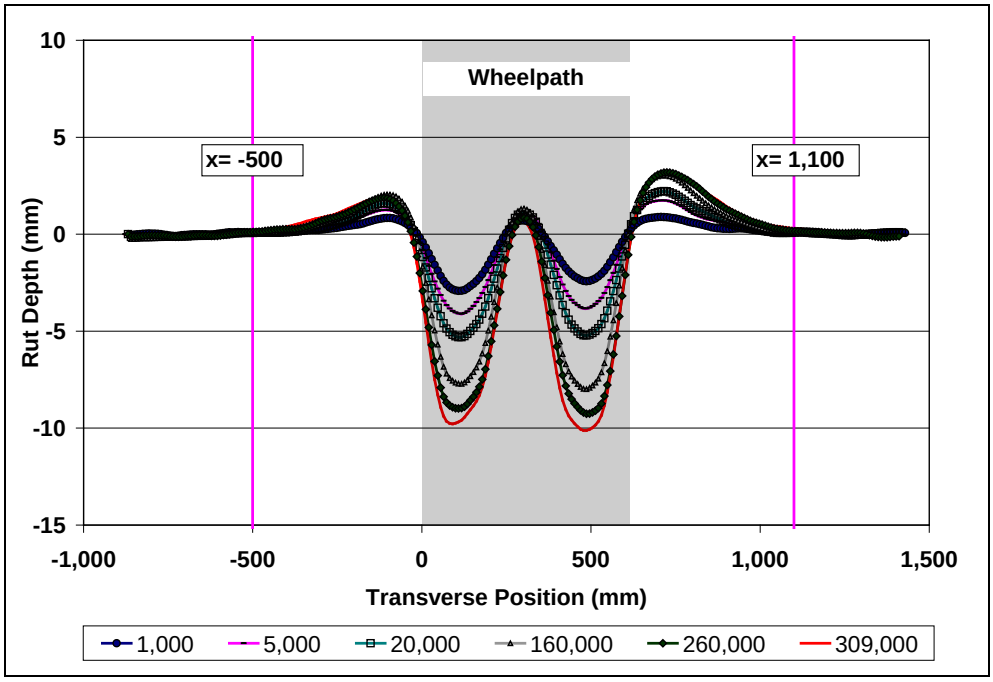

Figure 4.43: 628HB: Profilometer cross section at various load repetitions.

Figure 4.44 and Figure 4.45 show the development of permanent deformation (average maximum rut and average deformation, respectively) with load repetitions as measured with the laser profilometer for the test section. Results for the Control section (Section 624HB) are also shown for comparative purposes. There was very little difference in performance (both average maximum rut and average deformation) between the Rediset and Control mixes during both the embedment phase and remainder of the test, despite the significantly higher binder content of the Rediset mix (10.0 percent for the Rediset mix compared to 7.7 percent for the Control). Mixes with a higher than optimum binder content will often deform at a faster rate than those produced at or slightly below optimum binder content. However, the Rediset test section had a notably lower air-void content (8.4 percent) than the Control (11.6 percent), which may have compensated for the higher binder content in terms of the rutting performance. The Rediset mix did not appear to be sensitive to the load changes. Error bars on the average reading indicate minimal variation along the length of the section.

Figure 4.46 shows contour plots of the pavement surface at the start and end of the test (309,000 repetitions) that also indicate minimal variation along the section.

After completion of trafficking, the average maximum rut depth and the average deformation were 13.5 mm (0.53 in.) and 7.8 mm (0.31 in.), respectively. The maximum rut depth measured on the section was 17.8 mm (0.70 in.), recorded at Station 6.

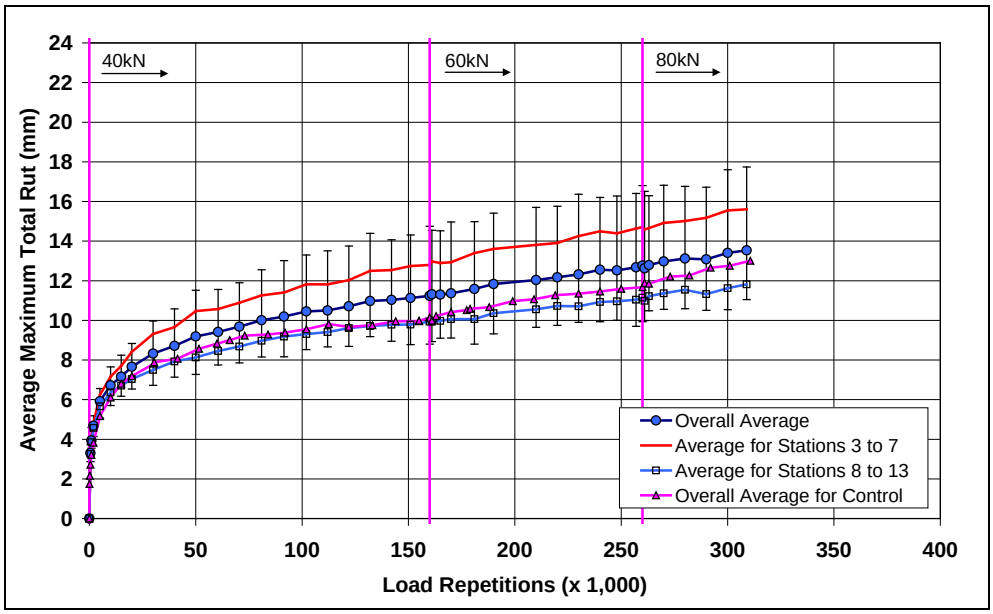

Figure 4.44: 628HB: Average maximum rut.

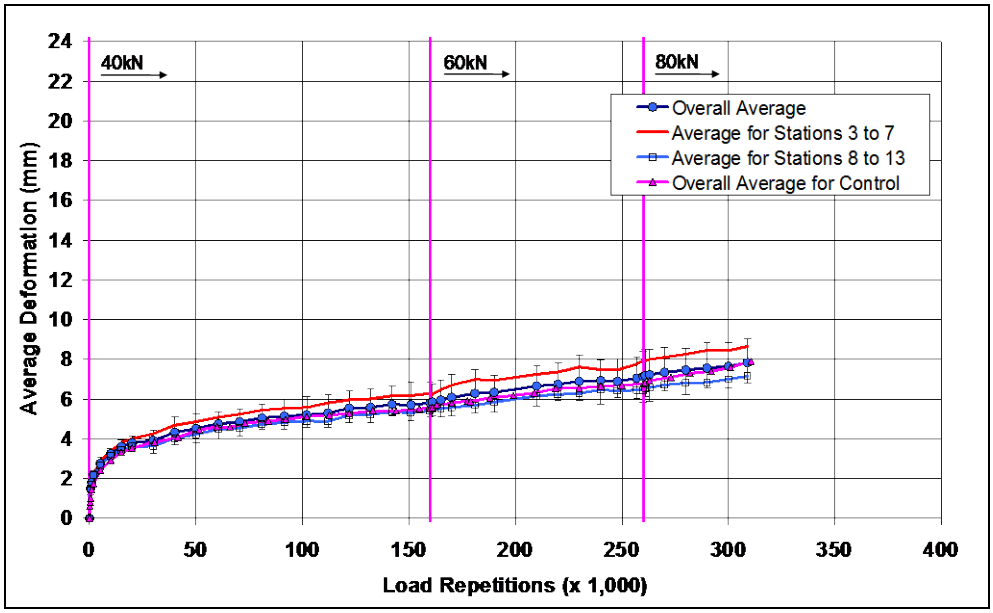

Figure 4.45: 628HB: Average deformation.

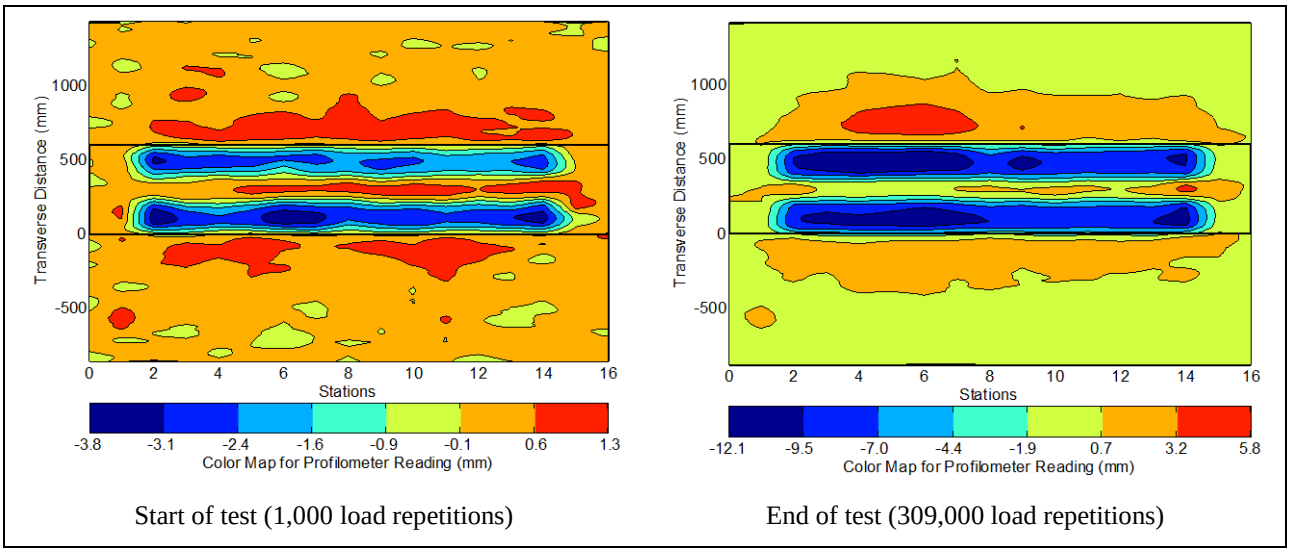

Start of test (1,000 load repetitions) End of test (309,000 load repetitions)

Figure 4.46: 628HB: Contour plots of permanent surface deformation.
(Note that key scales are different.)

4.7.6 Visual Inspection

Apart from rutting, no other distress was recorded on the section. Its appearance was similar to that of the other sections. Figure 4.47 shows a photograph taken of the surface at the end of the test.

Figure 4.47: 628HB: Section photograph at test completion.

4.8 Section 629HB: Advera (Test #2)

4.8.1 Test Summary

This test was carried out as a follow-up to the Section 626HA test to determine if the poor performance on that section was related to equipment, the long break in testing over the holiday period, or to the pavement structure. Loading commenced on January 24, 2011, and ended on February 7, 2011. A total of 73,500 load repetitions were applied and 14 datasets were collected. The HVS loading history for Section 629HB is shown in Figure 4.48. No improvement in performance was noted, indicating that the problem was probably related to the pavement structure or asphalt mix. No shutdowns or breakdowns occurred during the test.

4.8.2 Outside Air Temperatures

Daily average outside air temperatures are summarized in Figure 4.49. Vertical error bars on each point on the graph show the daily temperature range. Temperatures ranged from 0°C to 23°C (32°F to 73°F) during the course of HVS testing, with a daily average of 10°C (50°F), an average minimum of 6°C (43°F), and an average maximum of 15°C (59°F). Average outside air temperatures were very similar to those recorded on the first Advera test (Section 626HA), but considerably cooler compared to those during testing on the Control (daily average of 14°C [25°F] cooler).

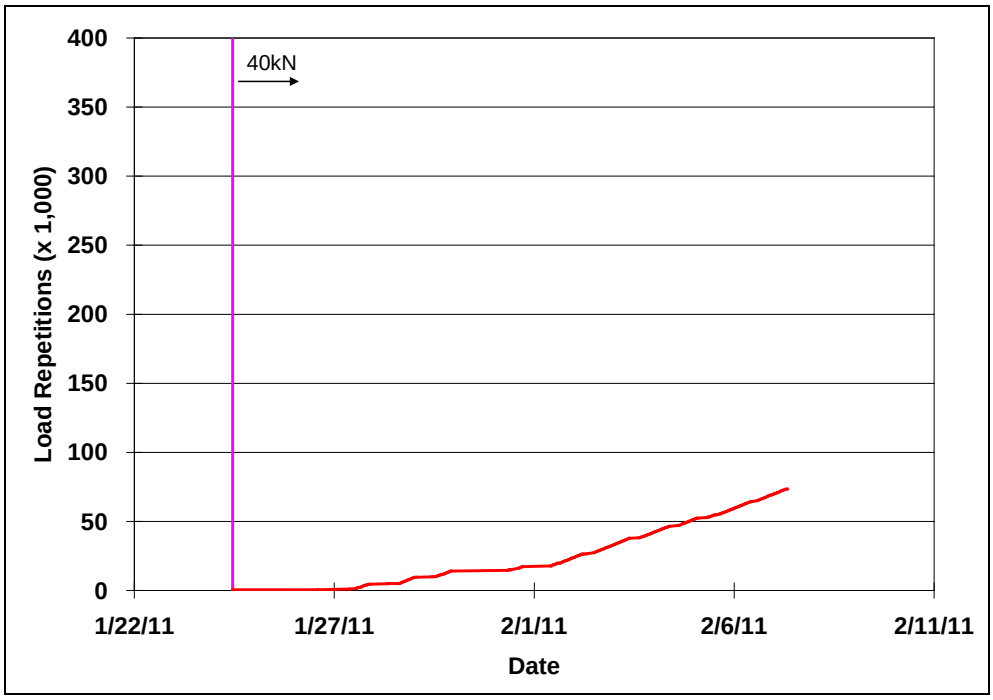

Figure 4.48: 629HB: Load history.

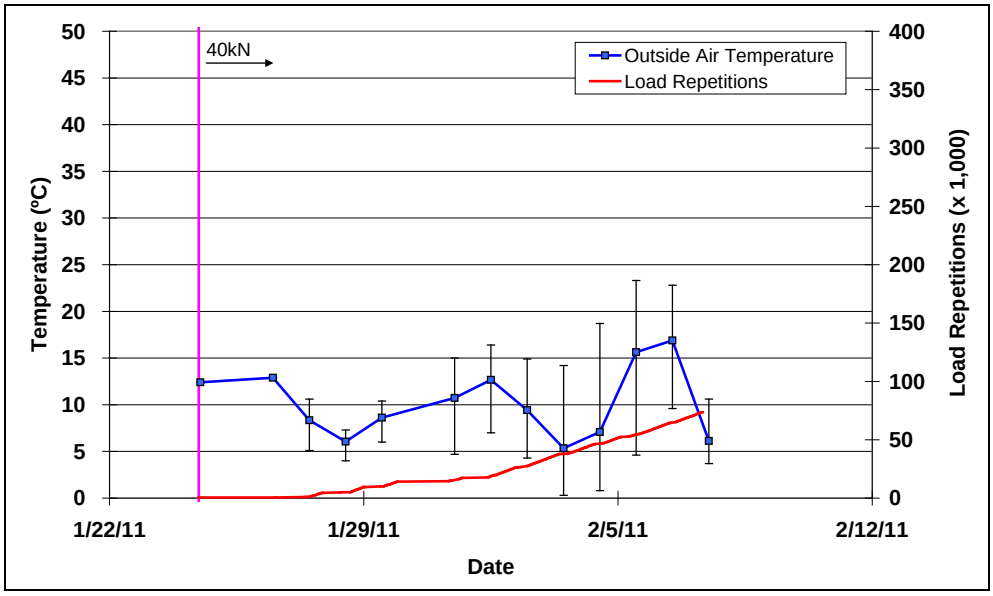

Figure 4.49: 629HB: Daily average outside air temperatures.

4.8.3 Air Temperatures in the Temperature Control Unit

During the test, air temperatures inside the temperature control chamber ranged from 17°C to 48°C (63°F to 118°F) with an average of 37°C (99°F) and a standard deviation of 2°C (4°F), very similar to those recorded on the first Advera test. The daily average air temperatures recorded in the temperature control

unit, calculated from the hourly temperatures recorded during HVS operation, are shown in Figure 4.50. Vertical error bars on each point on the graph show daily temperature range.

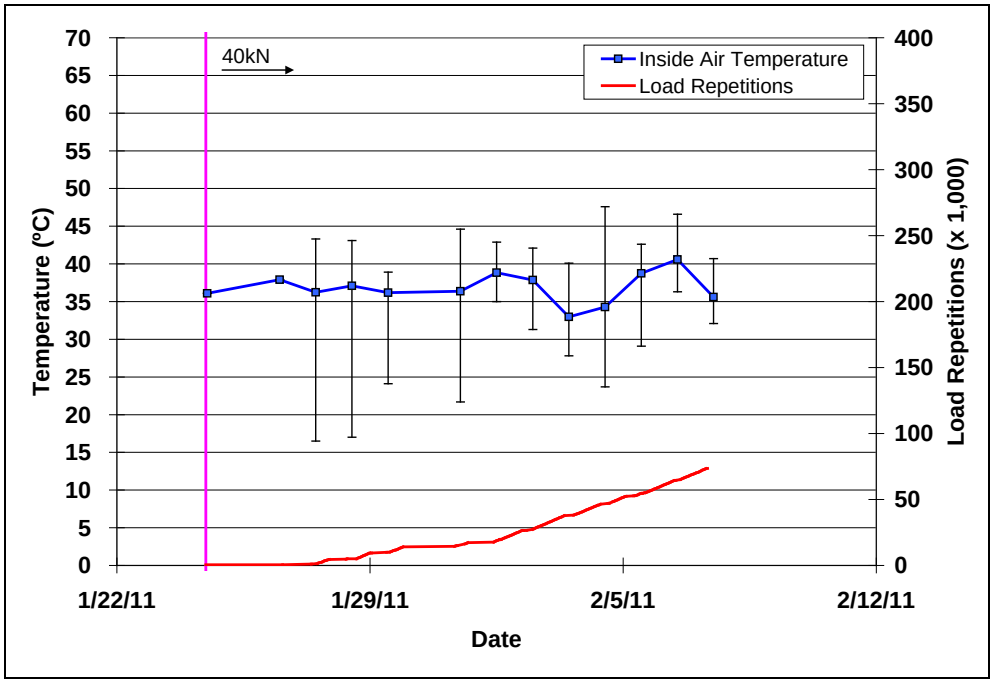

Figure 4.50: 629HB: Daily average inside air temperatures.

4.8.4 Temperatures in the Asphalt Concrete Layers

Daily averages of the surface and in-depth temperatures of the asphalt concrete layers are listed in Table 4.6 and shown in Figure 4.51. Average pavement temperatures at all depths on Section 629HB were similar to those recorded on both the first Advera test (626HA) and on the Control.

Table 4.6: 629HB: Temperature Summary for Air and Pavement

Temperature	629HB			626HA	624HB
	Average (°C)	Std. Dev. (°C)	Average (°F)	Average (°C)	Average (°C)
Outside air	10	-	50	9	24
Inside air	37	2.0	99	38	45
Pavement surface	47	2.3	117	49	51
- 25 mm below surface	50	0.4	122	51	51
- 50 mm below surface	49	0.8	120	50	50
- 90 mm below surface	48	1.0	118	48	49
- 120 mm below surface	47	1.4	117	47	49

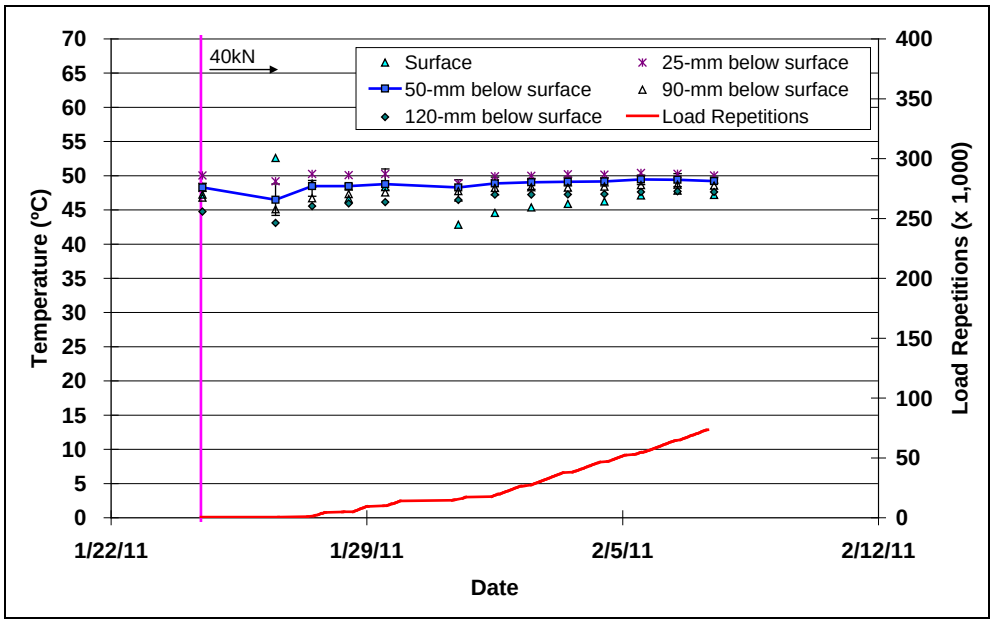

Figure 4.51: 629HB: Daily average temperatures at pavement surface and various depths.

4.8.5 Permanent Surface Deformation (Rutting)

Figure 4.52 shows the average transverse cross section measured with the laser profilometer at various stages of the test and shows the increase in rutting and deformation over time.

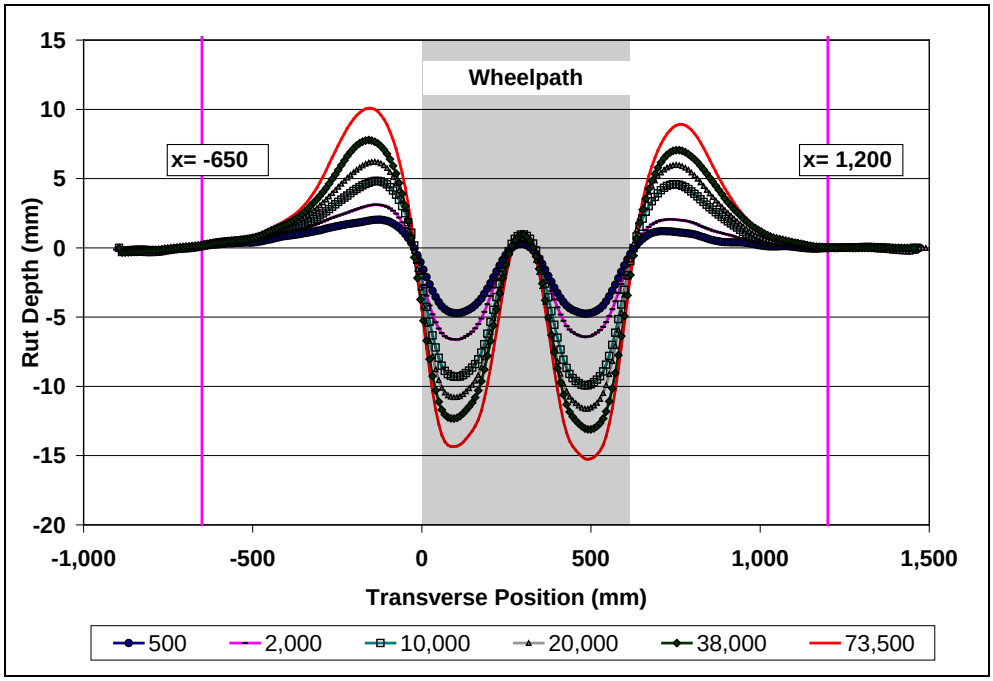

Figure 4.52: 629HB: Profilometer cross section at various load repetitions.

Figure 4.53 and Figure 4.54 show the development of permanent deformation (average maximum rut and average deformation, respectively) with load repetitions as measured with the laser profilometer for the test section. Results for the first Advera test (Section 626HA) and the Control section (Section 624HB) are also shown for comparative purposes.

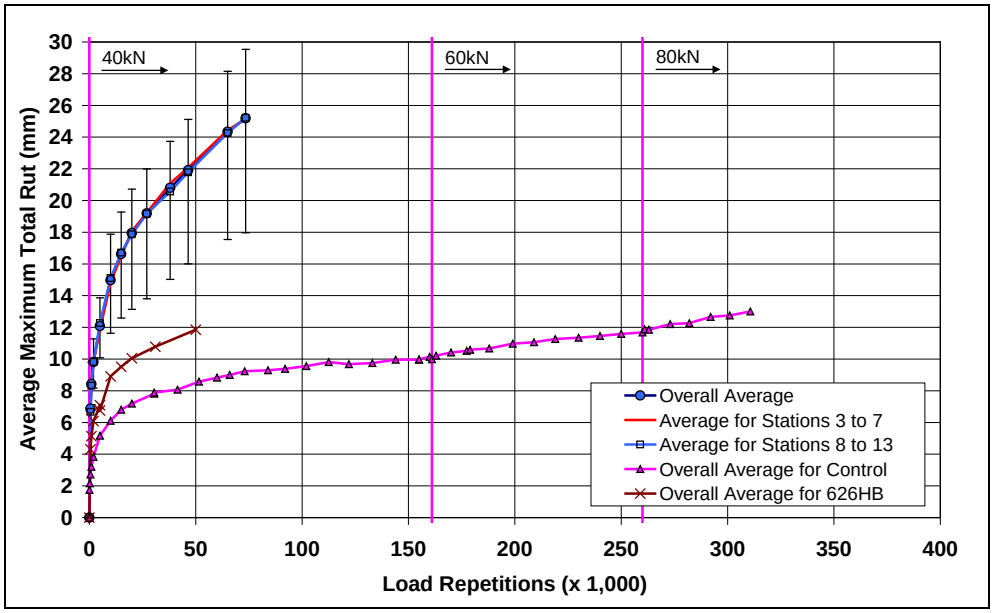

Figure 4.53: 629HB: Average maximum rut.

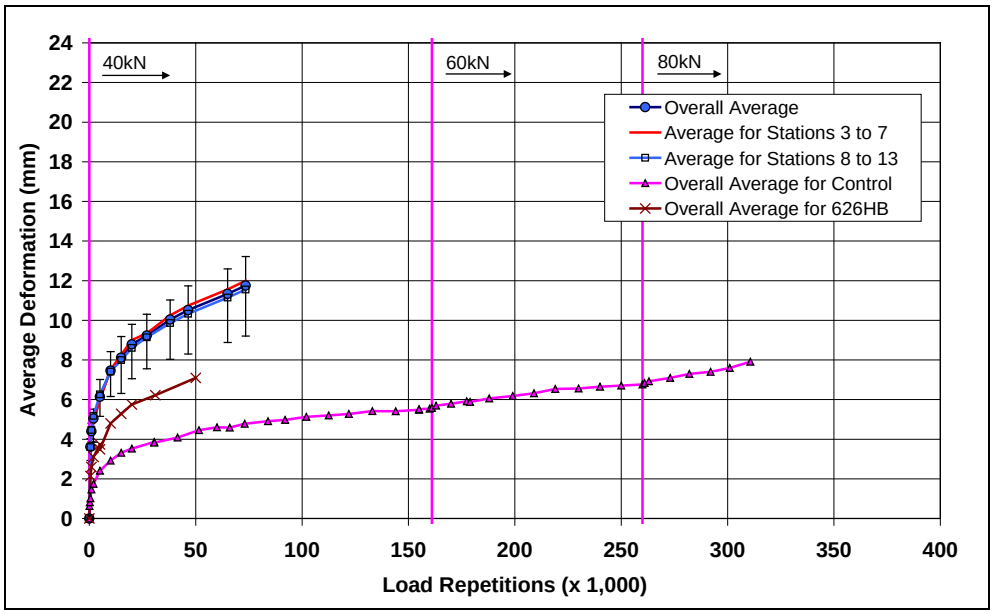

Figure 4.54: 629HB: Average deformation.

The plots clearly show that performance on this test was worse than that on the earlier test, indicating a pavement structure problem and not an equipment or testing protocol–related problem. The later forensic investigation (see Section 5.7.3) indicated that high subgrade moisture contents as well as thinner combined asphalt concrete layers on this section were probably the main contributory causes of the poor performance.

4.8.6 Visual Inspection

Apart from rutting, no other distress was recorded on the section. Its appearance was similar to that of the other sections. Figure 4.55 shows a photograph taken of the surface at the end of the test.

Figure 4.55: 629HB: Section photograph at test completion.

4.9 Section 630HB: Advera (Test #3)

4.9.1 Test Summary

This test was carried out as a follow-up to the Section 626HA and Section 629HB tests to determine if better performance could be achieved during testing in the summer after the subgrade had dried back. Loading commenced on July 26, 2011, and was terminated after just 5,000 repetitions as it was clear that there was no improvement in performance. Due to the short duration of the test, ambient temperatures are not discussed in the following sections.

4.9.2 Temperatures in the Asphalt Concrete Layers

Daily averages of the surface and in-depth temperatures of the asphalt concrete layers are listed in Table 4.7 and shown in Figure 4.56. Average pavement temperatures at all depths were similar to those

recorded on the first and second tests (Sections 626HA and 629HB) and on the Control despite considerable differences in ambient temperature.

Table 4.7: 630HB: Temperature Summary for Air and Pavement

Temperature	630HB		626HA	629HB	624HB
	Average (°C)	Std. Dev. (°C)	Average (°C)	Average (°C)	Average (°C)
Outside air	31	-	9	10	24
Inside air	42	2.4	38	37	45
Pavement surface	47	4.2	49	47	51
- 25 mm below surface	48	3.3	51	50	51
- 50 mm below surface	49	3.2	50	49	50
- 90 mm below surface	46	2.9	48	48	49
- 120 mm below surface	46	2.7	47	47	49

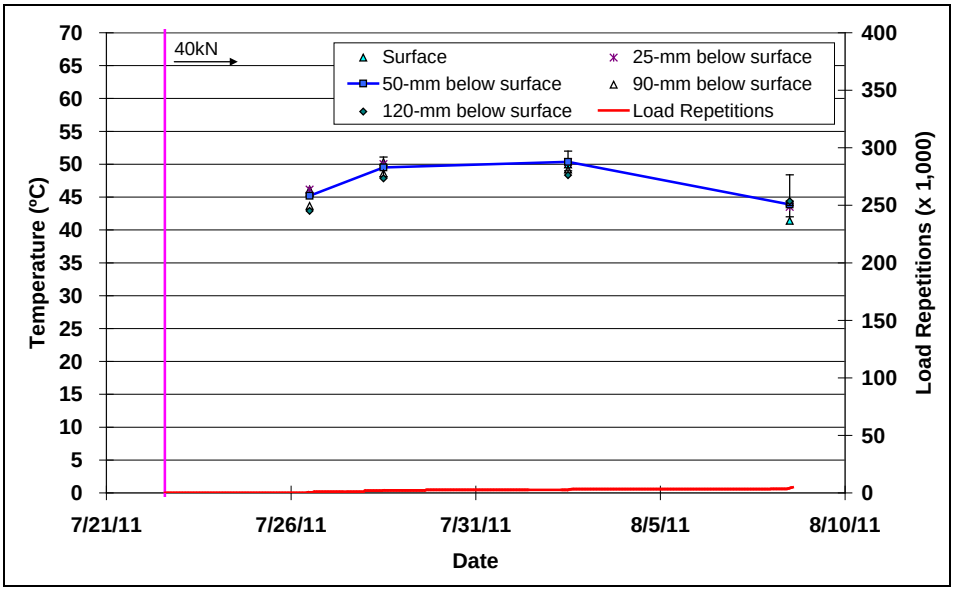

Figure 4.56: 630HB: Daily average temperatures at pavement surface and various depths.

4.9.3 Permanent Surface Deformation (Rutting)

Figure 4.57 shows the average transverse cross section measured with the laser profilometer at various stages of the test.

Figure 4.58 and Figure 4.59 show the development of permanent deformation (average maximum rut and average deformation, respectively) with load repetitions as measured with the laser profilometer for the test section. Results for the first and second tests as well as the Control section (Section 624HB) are also shown for comparative purposes. The rapid failure is clearly evident on the plots.

After completion of trafficking, the average maximum rut depth and the average deformation were 18 mm (0.71 in.) and 8.0 mm (0.32 in.), respectively. The maximum rut depth measured on the section was 22 mm (0.87 in.) recorded at Station 9.

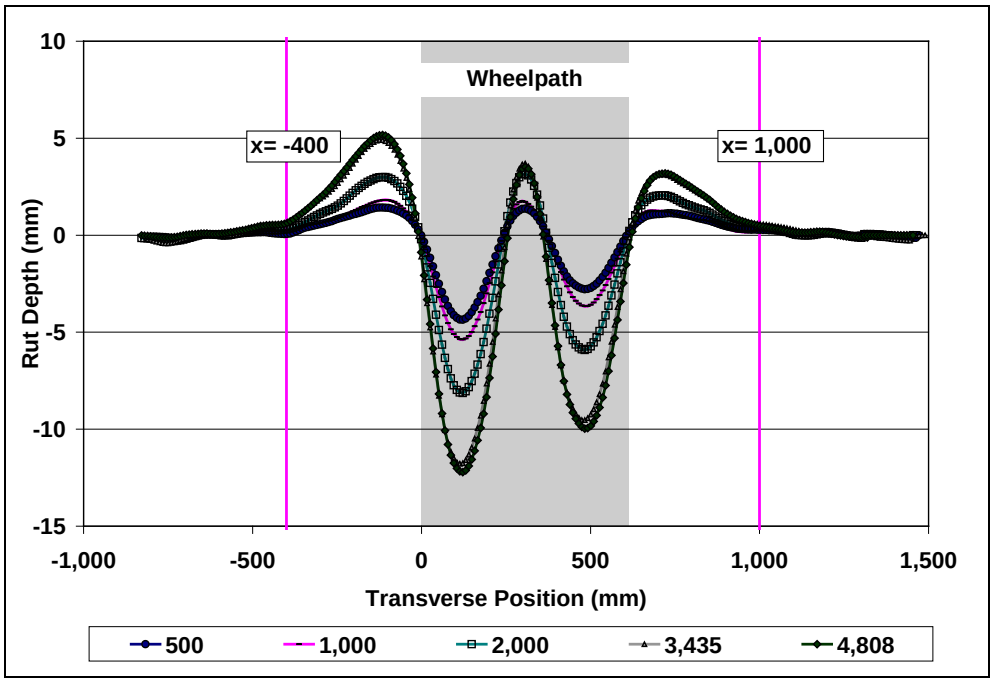

Figure 4.57: 630HB: Profilometer cross section at various load repetitions.

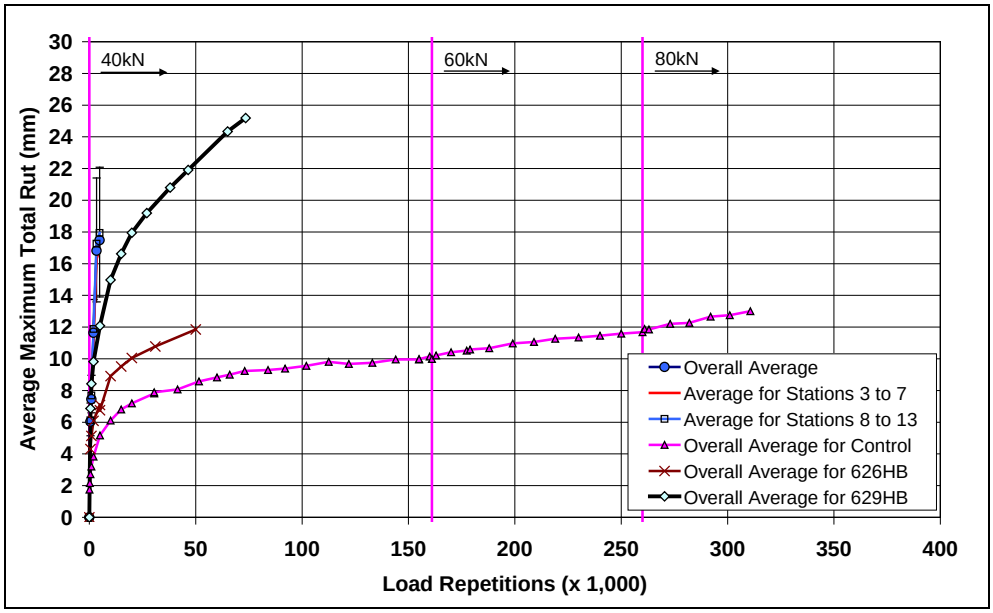

Figure 4.58: 630HB: Average maximum rut.

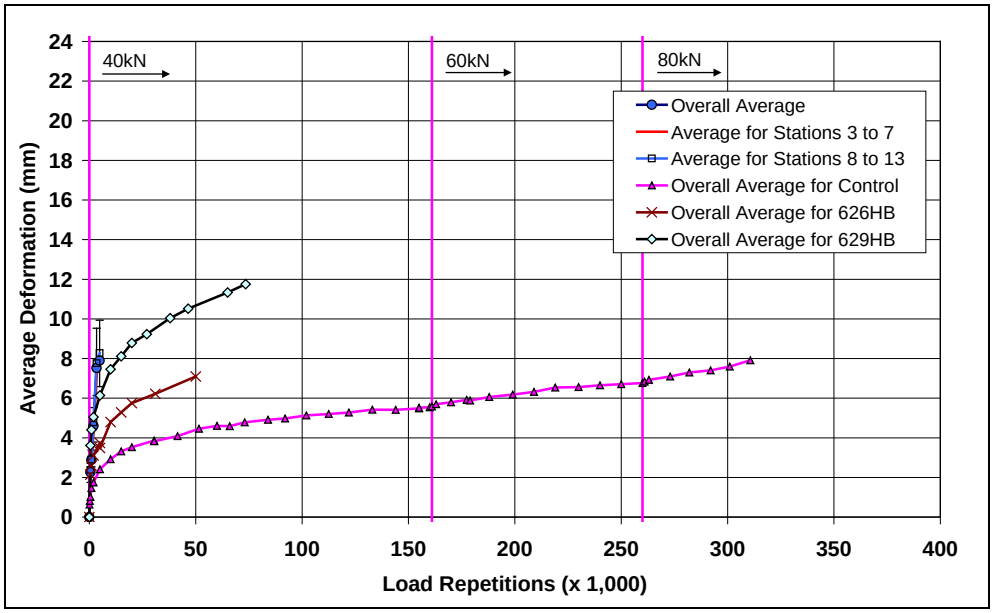

Figure 4.59: 630HB: Average deformation.

4.10 Section 631HB: Sasobit (Test #2)

4.10.1 Test Summary

This test was carried out as part of the follow-up to the Section 626HA and Section 629HB tests to determine if seasonal or any other factors (e.g., change in stiffness in the asphalt layers, different testing equipment, etc.) had also affected the other sections. Loading commenced on August 16, 2011, and ended on September 9, 2011. The test was terminated after 85,000 load repetitions had been applied when it was clear that similar rutting performance to that measured on the first test (Section 625HA, Sasobit Test #1) was evident. Load history is shown in Figure 4.60. No breakdowns or shutdowns occurred during the test.

4.10.2 Outside Air Temperatures

Daily average outside air temperatures are summarized in Figure 4.61. Vertical error bars on each point on the graph show the daily temperature range. Temperatures ranged between 15°C and 42°C (59°F to 108°F) during the course of HVS testing, with a daily average of 26°C (79°F), an average minimum of 20°C (68°F), and an average maximum of 32°C (90°F). Average outside air temperatures were warmer during testing on Section 631HB compared to those during testing on the first Sasobit test (daily average of 4°C [7°F] warmer) and on the Control.

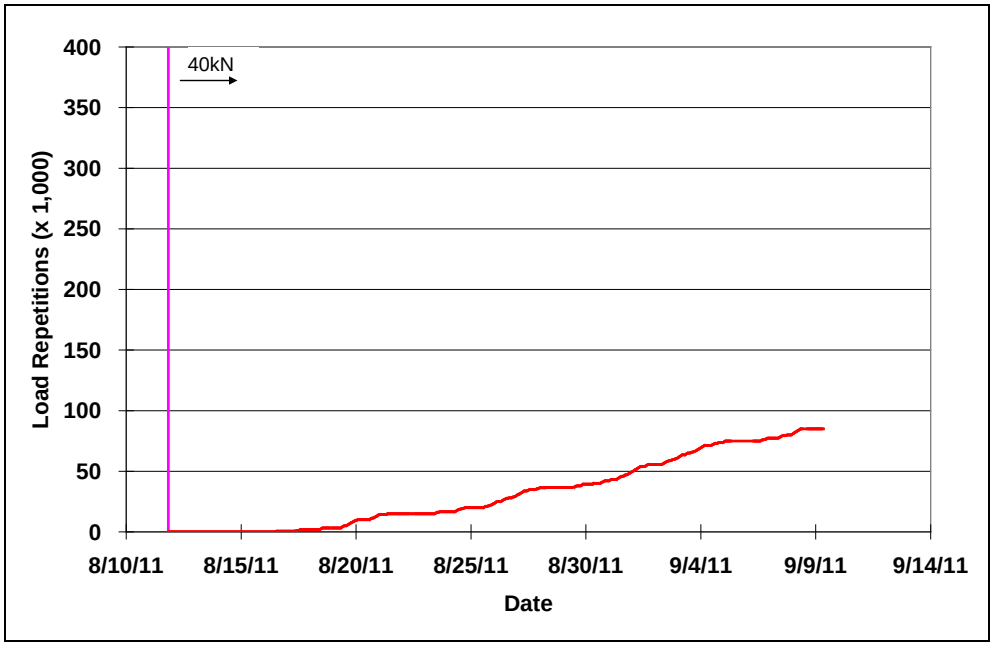

Figure 4.60: 631HB: Load history.

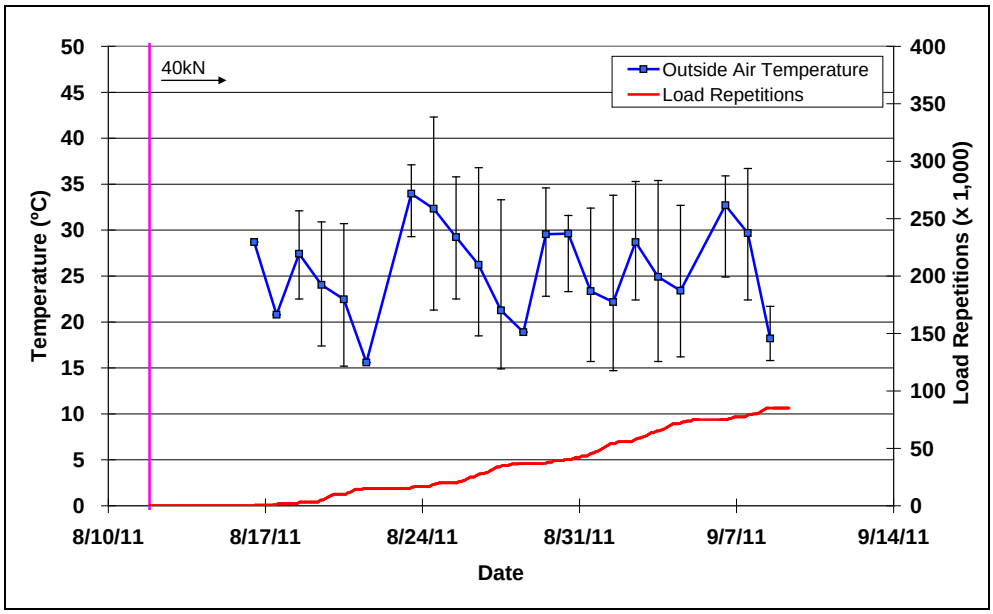

Figure 4.61: 631HB: Daily average outside air temperatures.

4.10.3 Air Temperatures in the Temperature Control Unit

During the test, air temperatures inside the temperature control chamber ranged from 40°C to 57°C (104°F to 135°F) with an average of 48°C (118°F) and a standard deviation of 3°C (5°F). The air temperature was adjusted to maintain a pavement temperature of 50°C±4°C (122°F±7°F). The daily average air temperatures recorded in the temperature control unit, calculated from the hourly temperatures recorded

during HVS operation, are shown in Figure 4.62. Vertical error bars on each point on the graph show daily temperature range.

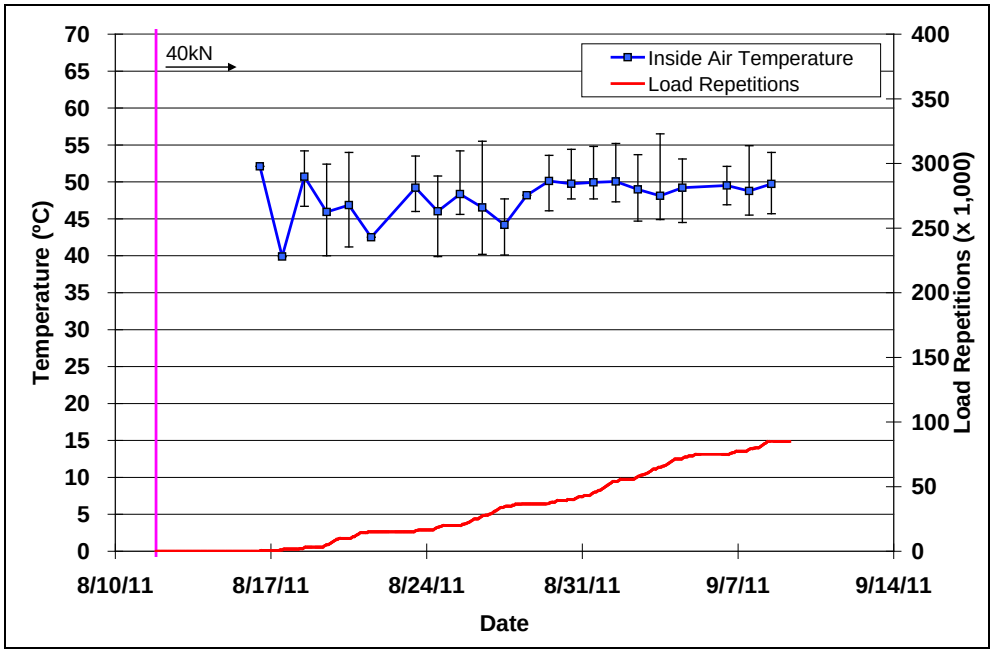

Figure 4.62: 631HB: Daily average inside air temperatures.

4.10.4 Temperatures in the Asphalt Concrete Layers

Daily averages of the surface and in-depth temperatures of the asphalt concrete layers are listed in Table 4.8 and shown in Figure 4.63. Pavement temperatures decreased slightly with increasing depth in the pavement, as expected. Average pavement temperatures at all depths on Section 631HB were similar to those recorded on the earlier Sasobit test and on the Control.

Table 4.8: 631HB: Temperature Summary for Air and Pavement

Temperature	631HB			625HB	624HB
	Average (°C)	Std. Dev. (°C)	Average (°F)	Average (°F)	Average (°C)
Outside air	26	-	79	22	24
Inside air	48	2.9	118	43	45
Pavement surface	49	1.9	120	50	51
- 25 mm below surface	50	1.7	122	51	51
- 50 mm below surface	50	1.6	122	50	50
- 90 mm below surface	49	1.6	120	50	49
- 120 mm below surface	48	1.8	118	50	49

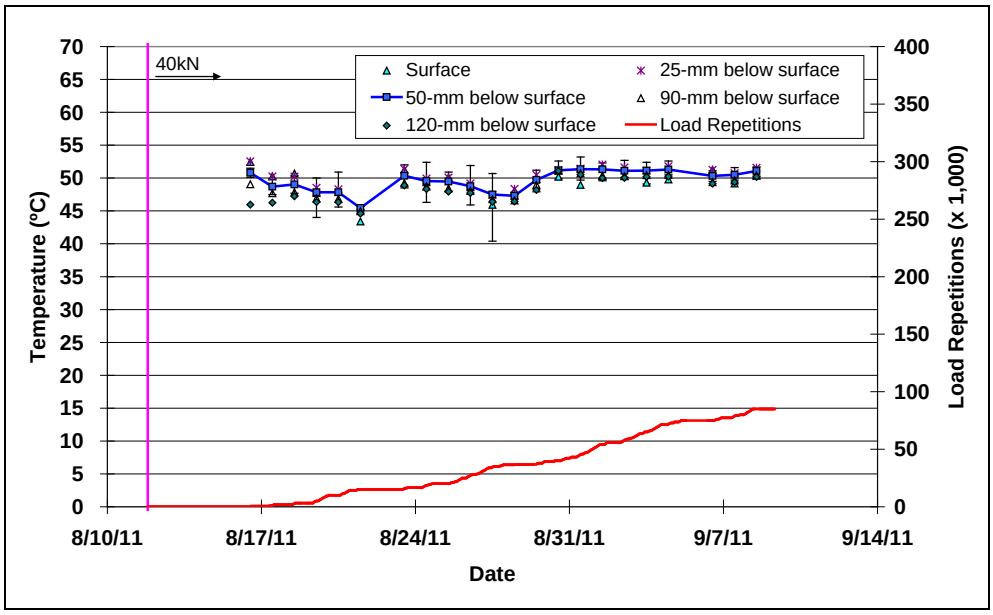

Figure 4.63: 631HB: Daily average temperatures at pavement surface and various depths.

4.10.5 Permanent Surface Deformation (Rutting)

Figure 4.64 shows the average transverse cross section measured with the laser profilometer at various stages of the test. This profile is similar to that measured on the first Sasobit (Section 625HA)test.

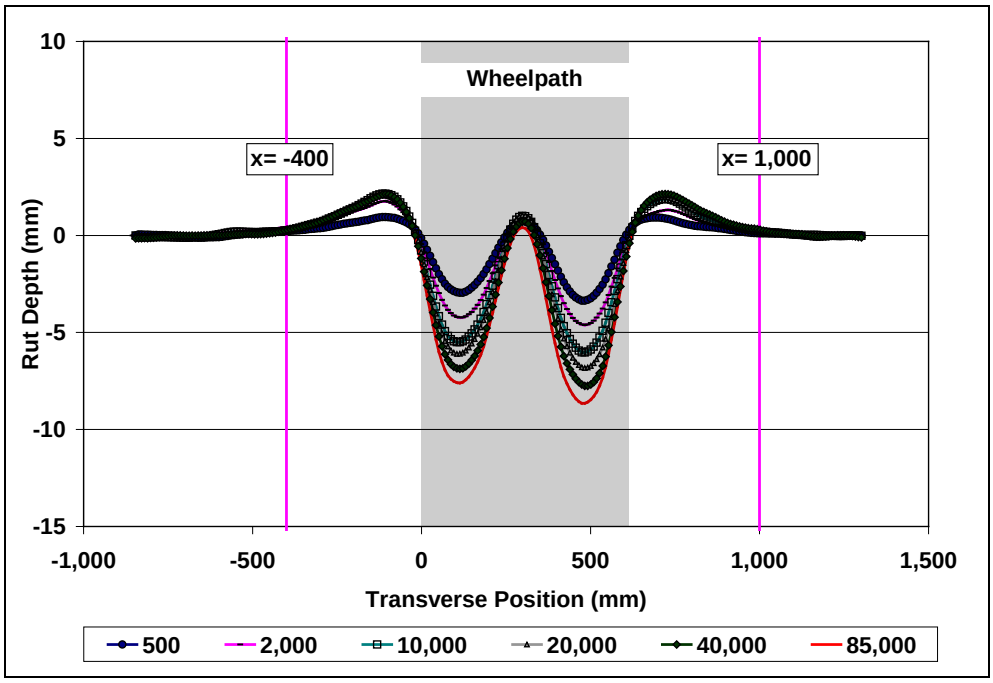

Figure 4.64: 631HB: Profilometer cross section at various load repetitions.

Figure 4.65 and Figure 4.66 show the development of permanent deformation (average maximum rut and average deformation, respectively) with load repetitions as measured with the laser profilometer for the test section. Results for the first Sasobit test (Section 625HA) and the Control section (Section 624HB) are also shown for comparative purposes. The average maximum rut measured at the end of the embedment phase was slightly deeper than that measured during the first Sasobit test. Apart from this, rutting trends (both total rut and average deformation) were the same as that measured on the first test and consequently the second test was halted after 85,000 repetitions, before the terminal rut depth was reached. This second test made clear that there was very little difference in performance between the two tests.

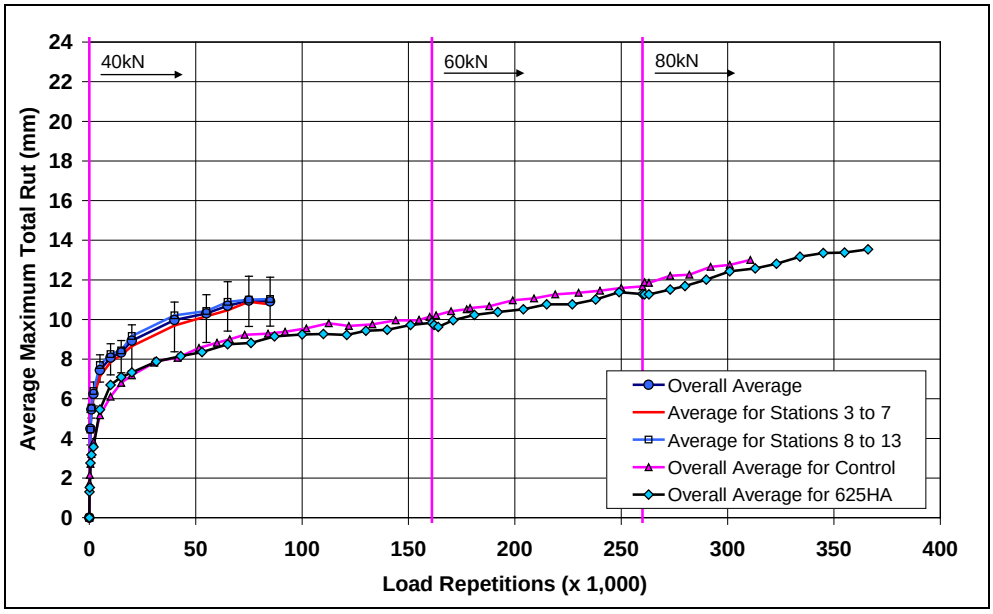

Figure 4.65: 631HB: Average maximum rut.

4.10.6 Visual Inspection

Apart from rutting, no other distress was recorded on the section and its appearance was similar to that of the other sections.

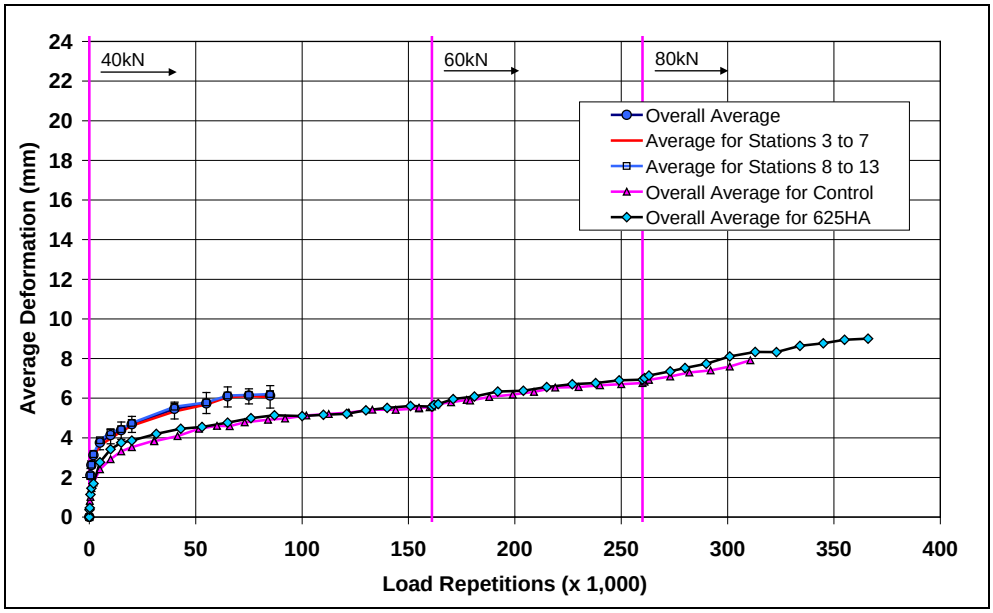

Figure 4.66: 631HB: Average deformation.

4.11 Section 632HA: Control (Test #2)

4.11.1 Test Summary

This test was also carried out as part of the follow-up to the Section 626HA and Section 629HB tests to determine if seasonal or any other factors had also affected the other sections. Loading commenced on September 15, 2011, and ended on September 28, 2011. The test was terminated after 80,000 load repetitions had been applied when it was clear that similar rutting performance to that measured on the first test (Section 624HA, Control #1) was evident. Load history is shown in Figure 4.67. No breakdowns or shutdowns occurred during the test.

4.11.2 Outside Air Temperatures

Daily average outside air temperatures are summarized in Figure 4.68. Vertical error bars on each point on the graph show the daily temperature range. Temperatures ranged from 26°C to 49°C (79°F to 120°F) during the course of HVS testing, with a daily average of 34°C (93°F), an average minimum of 30°C (86°F), and an average maximum of 37°C (99°F). Average outside air temperatures were considerably warmer during testing on Section 632HA compared to those during testing on the first Control test (daily average of 10°C [18°F] warmer).

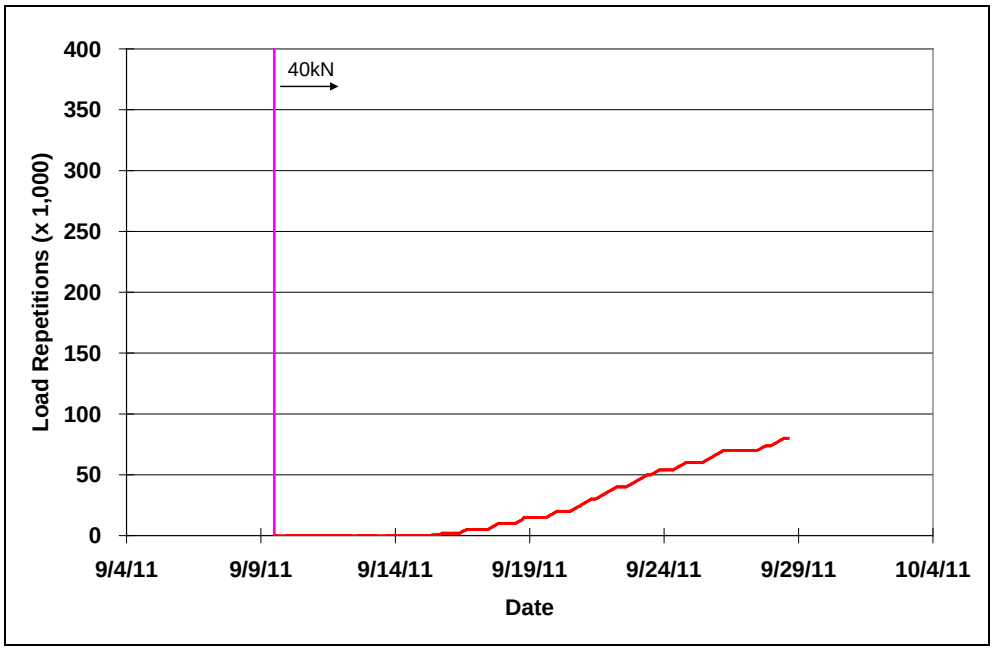

Figure 4.67: 632HA: Load history.

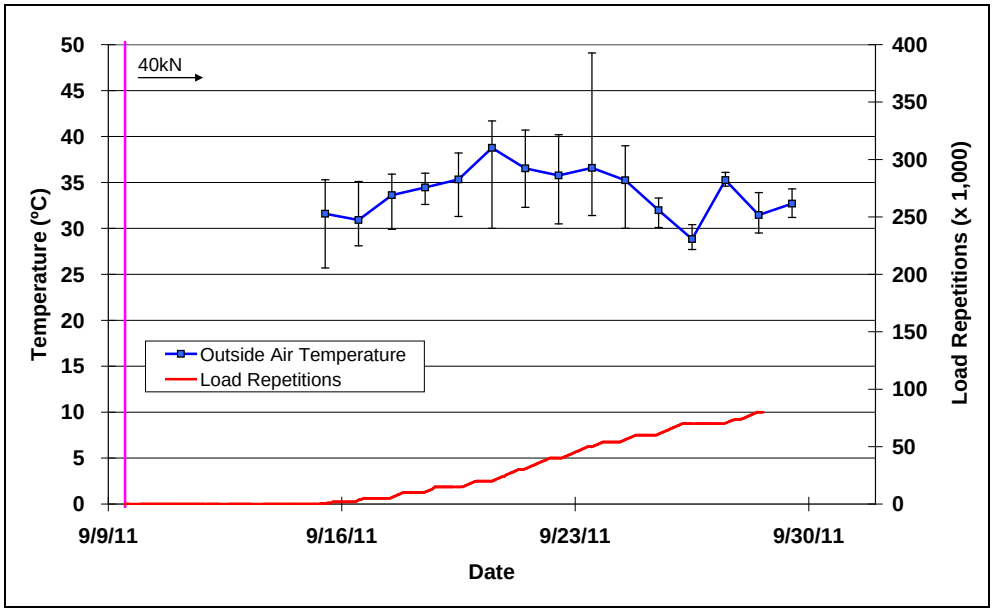

Figure 4.68: 632HA: Daily average outside air temperatures.

4.11.3 Air Temperatures in the Temperature Control Unit

During the test, air temperatures inside the temperature control chamber ranged from 37°C to 54°C (99°F to 129°F) with an average of 46°C (115°F) and a standard deviation of 3°C (5°F). The air temperature was adjusted to maintain a pavement temperature of 50°C±4°C (122°F±7°F). The daily average air temperatures recorded in the temperature control unit, calculated from the hourly temperatures recorded

during HVS operation, are shown in Figure 4.69. Vertical error bars on each point on the graph show daily temperature range.

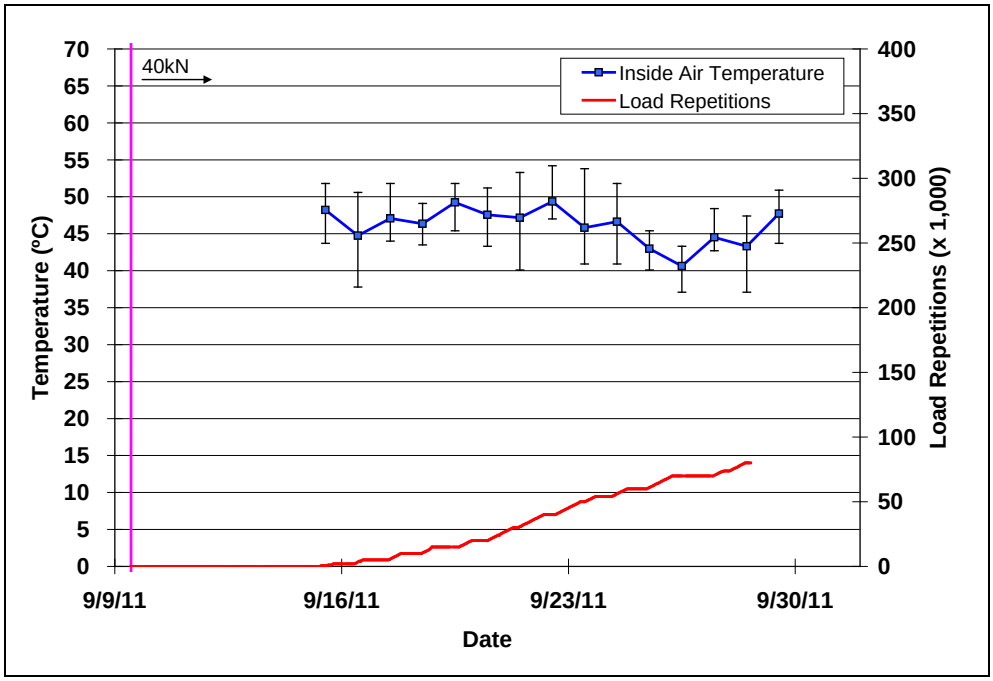

Figure 4.69: 632HA: Daily average inside air temperatures.

4.11.4 Temperatures in the Asphalt Concrete Layers

Daily averages of the surface and in-depth temperatures of the asphalt concrete layers are listed in Table 4.9 and shown in Figure 4.70. Pavement temperatures decreased slightly with increasing depth in the pavement, as expected. Average pavement temperatures at all depths on Section 632HA were similar to those recorded on the first Control test, despite higher outside temperatures.

Table 4.9: 632HA: Temperature Summary for Air and Pavement

Temperature	632HA				624HB
	Average (°C)	Std. Dev. (°C)	Average (°F)	Std. Dev. (°F)	Average (°C)
Outside air	34	-	93	-	24
Inside air	46	2.5	115	4.5	45
Pavement surface	50	1.5	122	2.7	51
- 25 mm below surface	50	0.5	122	0.9	51
- 50 mm below surface	50	0.5	122	0.9	50
- 90 mm below surface	49	0.7	120	1.3	49
- 120 mm below surface	48	0.6	118	1.1	49

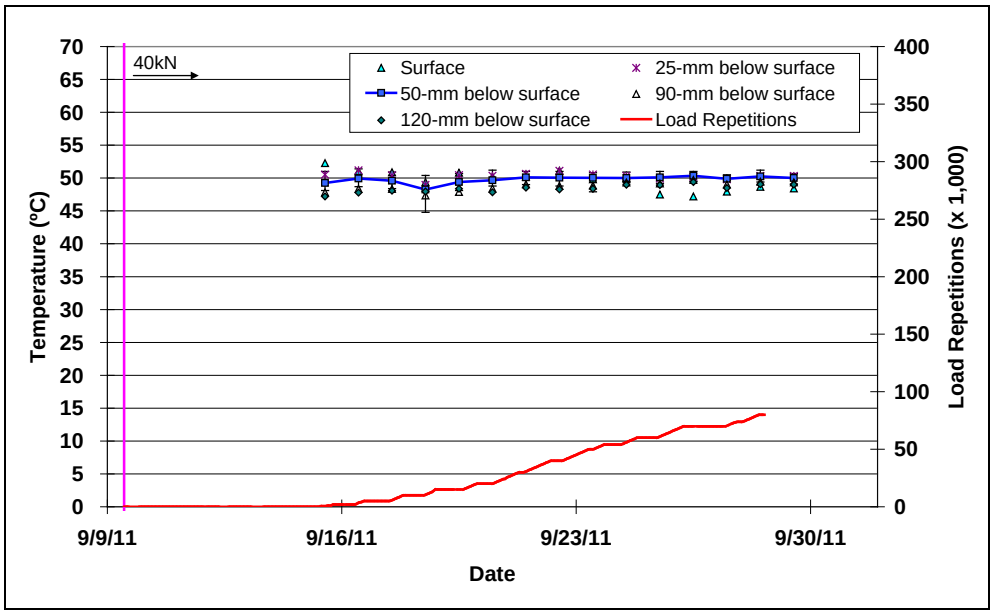

Figure 4.70: 632HA: Daily average temperatures at pavement surface and various depths.

4.11.5 Permanent Surface Deformation (Rutting)

Figure 4.71 shows the average transverse cross section measured with the laser profilometer at various stages of the test. This profile is similar to that measured on the first Control test.

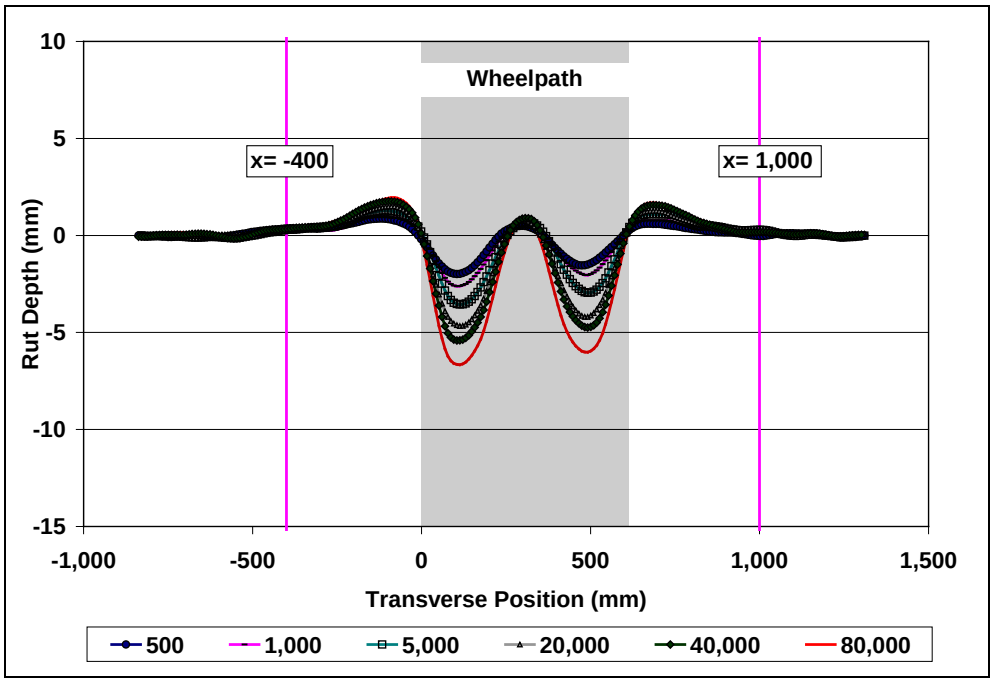

Figure 4.71: 632HA: Profilometer cross section at various load repetitions.

Figure 4.72 and Figure 4.73 show the development of permanent deformation (average maximum rut and average deformation, respectively) with load repetitions as measured with the laser profilometer for the test section. Results for the first Control section (Section 624HB) are also shown for comparative purposes. Average maximum rut, average deformation, and general change in rut rate trends measured during this test were the same as those measured during the first Control test and consequently the second test was halted after 80,000 repetitions, before the terminal rut depth was reached. This second test made clear that there was very little difference in performance between the two tests.

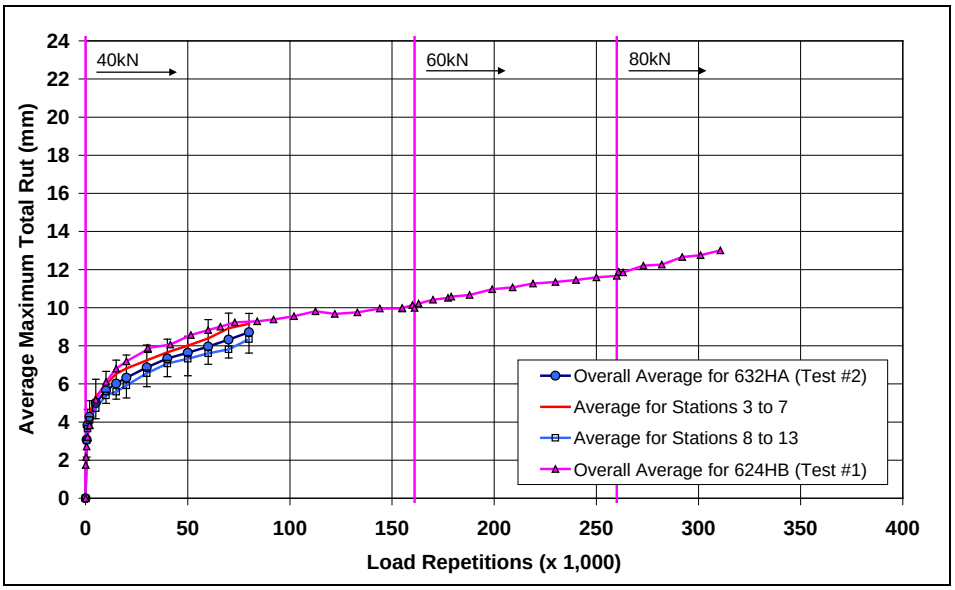

Figure 4.72: 632HA: Average maximum rut.

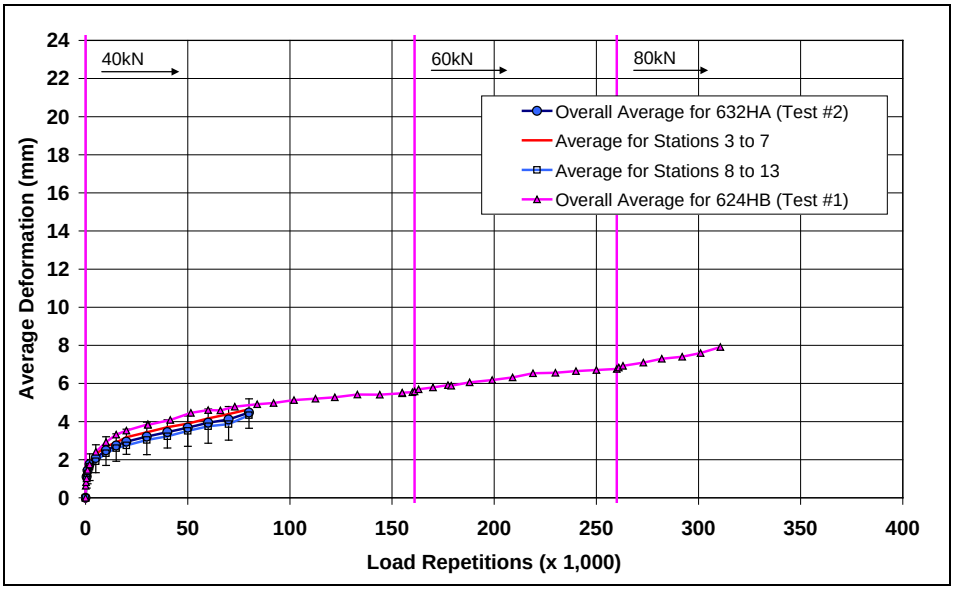

Figure 4.73: 632HA: Average deformation.

4.11.6 Visual Inspection

Apart from rutting, no other distress was recorded on the section and its appearance was similar to that of the other sections.

4.12 Test Summary

The first round of testing on the five sections was started in the late summer of 2010 and ended in the winter of the same year. A range of daily average temperatures was therefore experienced; however, pavement temperatures remained constant throughout HVS trafficking. Unexpected poor performance was measured on the Advera section (Section 626HA) and additional tests on this section as well as on the Control and Sasobit sections were undertaken to determine the cause and to eliminate possible seasonal and machine-related testing variables. The cause of this poor performance was attributed to a combination of high subgrade moisture content and thinner combined asphalt layers, which were both identified during the forensic investigation (discussed in Chapter 5). The duration of the tests to terminal rut (12.5 mm [0.5 in.]) on the five sections varied from 73,500 load repetitions (Section 629HB, Advera Test #2) to 365,000 load repetitions (Section 625HA, Sasobit Test #1) (Table 4.10).

Table 4.10: Summary of Embedment Phase and Test Duration.

Section		Embedment (mm/in.)	Repetitions to 12.5 mm Rut	Load Change to 60 kN	Load Change to 80 kN
Number	Technology				
624HB	Control (test #1)	6.5 (0.26)	290,000	Yes	Yes
625HA	Sasobit (test #1)	6.7 (0.26)	307,000	Yes	Yes
626HA	Advera (test #1)	8.9 (0.35)	Not applicable[1]	No	No
627HB	Astec	7.5 (0.30)	183,000	Yes	No
628HB	Rediset	6.5 (0.26)	240,000	Yes	Yes
629HB	Advera (test #2)	>24 (0.95)	7,500	No	No
630HB	Advera (test #3)	>18 (0.71)	Not applicable[1]	No	No
631HB	Sasobit (test #2)	8.0 (0.32)	Not applicable[1]	No	No
632HA	Control (test #2)	6.5 (0.26)	Not applicable[1]	No	No

[1] Test was terminated before terminal rut was reached.

Rutting behavior for the five sections is compared in Figure 4.74 (average maximum rut) and Figure 4.75 (average deformation). The duration of the embedment phases on all sections except the Advera section were similar. Apart from the Advera section, the depth of the ruts at the end of the embedment phases differed only slightly between sections, with the Astec (7.5 mm [0.3 in.]) having a slightly deeper embedment than the Control, Sasobit, and Rediset sections, which had similar embedment (6.5 to 6.7 mm [0.26 in.]). This is opposite to the early rutting performance in the Phase 1 study *(2)* and is being investigated in a separate study. Rut rate (rutting per load repetition) after the embedment phase on the Control and Sasobit sections was almost identical. The rut rate on the Astec and Rediset sections was slightly higher: on the Astec section, this was attributed to moisture in the asphalt layer and the subgrade (as determined during the forensic investigation); on the Rediset section it was attributed to the higher

binder content. On the Astec and Rediset sections, the rut rate was slightly higher and was attributed to some moisture in the asphalt layer and in the subgrade in the Astec section (determined during the forensic investigation) and to the higher binder content on the Rediset section. Although lower production and paving temperatures typically result in less oxidation of the binder, which can influence early rutting performance, differences in production and placement temperatures did not appear to influence performance in this set of tests.

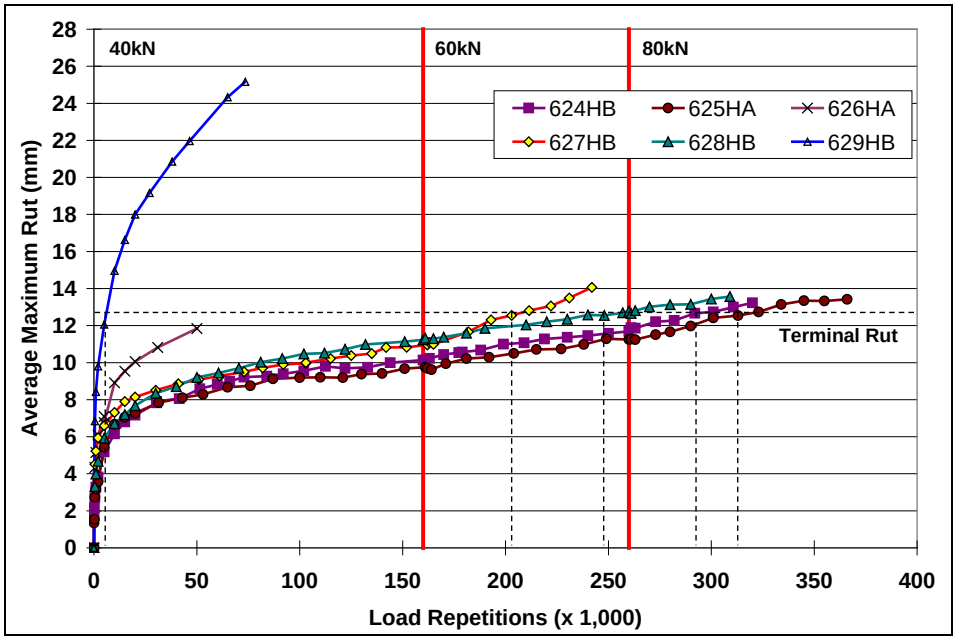

Figure 4.74: Comparison of average maximum rut.

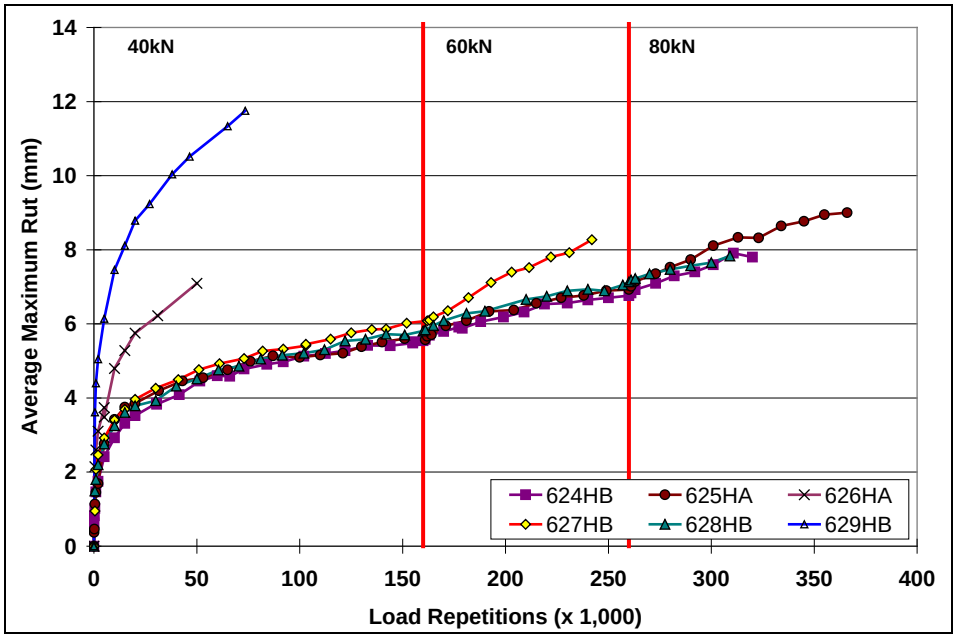

Figure 4.75: Comparison of average deformation.

Based on the results from this phase of accelerated pavement testing on gap-graded, rubberized mixes, it can be concluded that the use of any of the three warm-mix asphalt technologies assessed and subsequent compaction of the mixes at lower temperatures will not significantly influence rutting performance of the mix.

5. FORENSIC INVESTIGATION

5.1 Introduction

A forensic investigation was carried out after completion of all HVS testing to compare the condition of the asphalt concrete and underlying layers within and outside the HVS trafficked area, and to remove samples for laboratory testing.

5.2 Forensic Investigation Procedure

The forensic investigation included the following tasks:

1. Demarcate test pit locations;
2. Saw the asphalt concrete;
3. Remove the slab and inspect surfacing/base bond;
4. Determine the wet density of the base (nuclear density gauge);
5. Determine the in situ strength of the base and subgrade (dynamic cone penetrometer);
6. Remove the base and subgrade material;
7. Sample material from the base and subgrade for moisture content determination;
8. Measure layer thicknesses;
9. Describe the profile;
10. Photograph the profile;
11. Sample additional material from the profile if required; and
12. Reinstate the pit.

The following additional information is relevant to the investigation:

- The procedures for HVS test section forensic investigations, detailed in the document entitled *Quality Management System for Site Establishment, Daily Operations, Instrumentation, Data Collection and Data Storage for APT Experiments (8)* were followed.
- The saw cuts were made at least 50 mm into the base to ensure that the slab could be removed from the pit without breaking.
- Nuclear density measurements were taken between the test section centerline and the inside (caravan side) edge of the test section. Two readings were taken: the first with the gauge aligned with the direction of trafficking and the second at 90° to the first measurement (Figure 5.1).
- DCP measurements were taken between the test section centerline and the inside (caravan side) edge of the test section, and between the outside edge of the test section and the edge of the test pit on the traffic side (Figure 5.1). A third DCP measurement was taken between these two points if inconsistent readings were obtained.
- Layer thicknesses were measured from a leveled reference straightedge above the pit. This allowed the crossfall of the section to be included in the profile. Measurements were taken across the pit at 50-mm (2.0-in.) intervals.

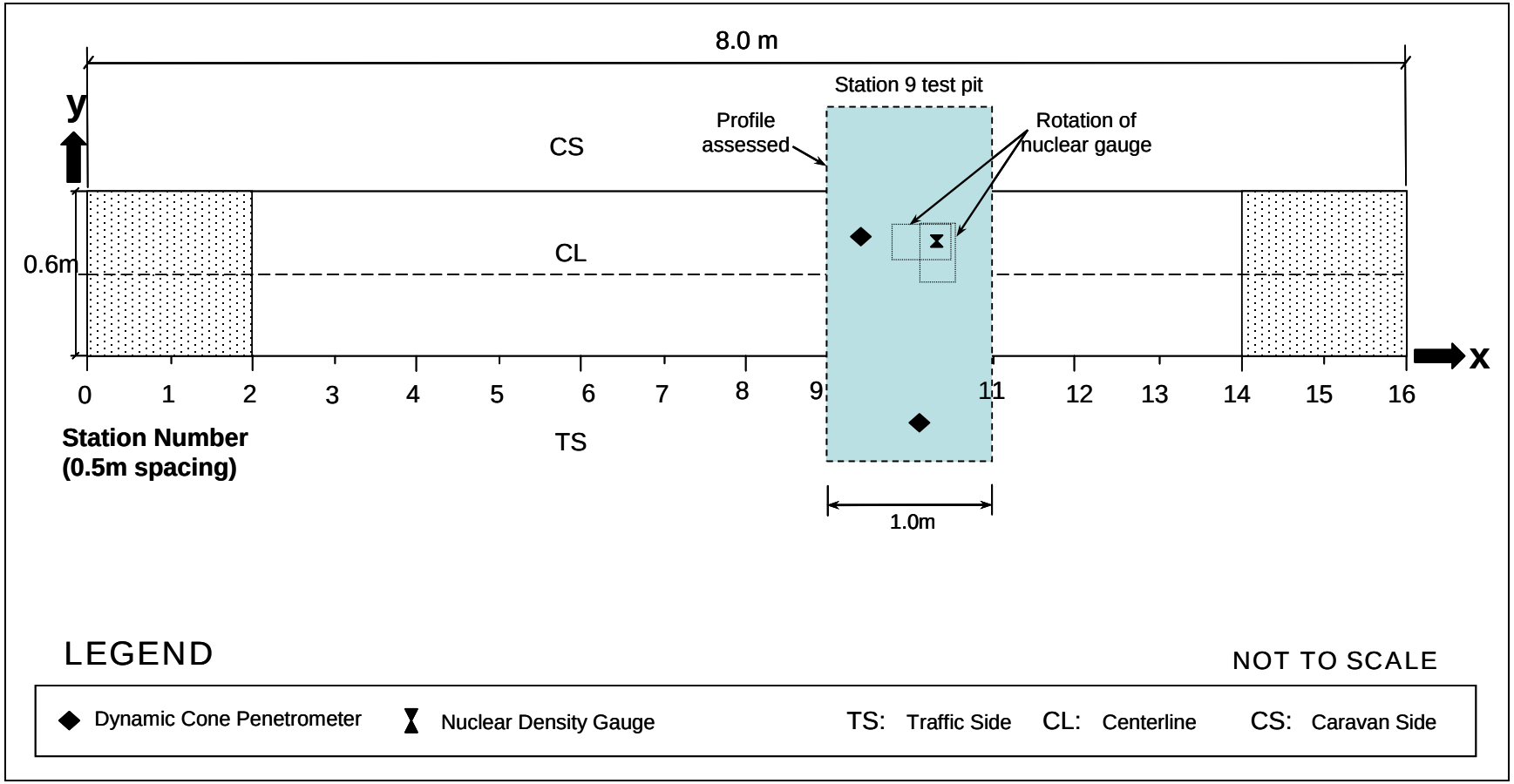

Figure 5.1: Test pit layout.

5.3 Test Pit Excavation

One test pit was excavated on seven of the nine HVS test sections (between Stations 9 and 11 [see Figure 5.1]). Test pits were not excavated on Section 631HB (Sasobit #2) and Section 632HA (Control #2) given that performance trends on the second tests were very similar to those on the first tests. The Station 9 test pit face was evaluated in each test pit. Test pits were excavated to a depth approximately 200 mm (8 in.) into the subgrade.

5.4 Base-Course Density and Moisture Content

Table 5.1 summarizes the base-course density and moisture content measurements on each section. The table includes the wet and dry density and moisture content of the base in the HVS wheelpath and in the adjacent untrafficked area (see Figure 5.1). Measurements were taken with a nuclear gauge. Laboratory-determined gravimetric moisture contents of the base material (average of two samples from the top and bottom of the excavated base) and subgrade material, as well as recalculated dry densities of the base (using the average gauge-determined wet density and laboratory-determined gravimetric moisture content), are also provided. Each gauge measurement is an average of two readings taken at each location in the pit (gauge perpendicular to wheelpath and parallel to wheelpath as shown in Figure 5.1). Subgrade densities were not measured. The following observations were made:

- Densities increased with increasing depth, following a similar pattern to the densities measured after construction of the test track.
- Some inconsistencies were noted in the densities from the different sections, with those sections with the highest number of applied load repetitions having higher densities in the upper regions of the base than the sections with lower numbers of repetitions (i.e., Advera sections). This implies that some densification under trafficking did occur. Average nuclear gauge–determined dry densities of the base-course for the six depths measured ranged between 2,085 kg/m^3 (130.2 lb/ft^3) in the trafficked area on Section 626HA (Advera) and 2,258 kg/m^3 (141.0 lb/ft^3) on the untrafficked area of Section 625HA (Sasobit) for the six test pits. The average dry density and standard deviation for the six test pits were 2,165 kg/m^3 (135.1 lb/ft^3) and 58 kg/m^3 (3.6 lb/ft^3), respectively, which corresponds with the average dry density of 2,200 kg/m^3 (137.3 lb/ft^3) recorded after construction, indicating that the base density over the test track did not change overall under trafficking. The laboratory-determined maximum dry density was 2,252 kg/m^3 (140.6 lb/ft^3). The average nuclear gauge–determined wet density was 2,347 kg/m^3 (146.1 lb/ft^3) with a standard deviation of 58 kg/m^3 (3.6 lb/ft^3).
- Nuclear gauge–determined moisture contents of the six test pits, measured at six intervals in the top 300 mm of the base, ranged between 7.0 percent and 9.7 percent with an average of 8.5 percent (standard deviation of 0.9 percent), slightly higher than the measurements recorded after construction (7.3 percent). Moisture contents at the top of the base were generally slightly higher compared to those in the lower regions of the base. The laboratory-determined optimum moisture content of the base material was 6.0 percent.

Table 5.1: Summary of Base-Course Density and Moisture Content Measurements

Section	Depth	Nuclear Gauge										Laboratory			
		Wheelpath					Untrafficked								
		Base Wet Density		MC[1]	Base Dry Density		Base Wet Density		MC	Base Dry Density		Base MC	Recalculated Dry Density*		SG[2] MC
		(kg/m^3)	(lb/ft^3)	(%)	(kg/m^3)	(lb/ft^3)	(kg/m^3)	(lb/ft^3)	(%)	(kg/m^3)	(lb/ft^3)	(%)	(kg/m^3)	(lb/ft^3)	(%)
624HB (Control)	50	2,306	114.0	8.1	2,133	131.1	2,251	140.5	9.6	2,056	128.4	5.4	2,162	135.0	17.3
	100	2,345	146.4	8.2	2,168	135.4	2,345	146.4	9.5	2,142	133.7		2,225	138.9	
	150	2,372	148.1	8.0	2,197	137.2	2,371	148.0	9.6	2,163	135.1		2,250	140.5	
	200	2,374	148.2	8.4	2,191	136.8	2,402	150.0	9.2	2,201	137.4		2,266	141.4	
	250	2,376	148.3	8.2	2,196	137.1	2,405	150.2	9.4	2,200	137.3		2,268	141.6	
	300	2,394	149.5	7.7	2,226	139.0	2,400	149.8	9.6	2,191	136.8		2,274	142.0	
	Avg[3]	2,361	147.4	8.1	2,185	136.4	2,362	147.5	9.5	2,159	134.8		2,241	139.9	
	SD[4]	31	2.0	0.2	32	2.0	59	3.7	0.2	55	3.5		43	2.7	
625HA (Sasobit #1)	50	2,108	131.6	7.9	1,954	122.0	2,305	143.9	10.4	2,088	130.3	5.0	2,030	126.7	16.7
	100	2,257	140.9	7.4	2,100	131.1	2,339	146.0	10.2	2,123	132.5		2,114	132.0	
	150	2,409	150.4	7.1	2,252	140.6	2,572	160.6	9.0	2,361	147.4		2,291	143.1	
	200	2,542	158.7	6.3	2,392	149.3	2,586	161.5	8.9	2,375	148.3		2,359	147.3	
	250	2,495	155.8	6.5	2,343	146.2	2,553	159.4	9.2	2,339	146.0		2,322	145.0	
	300	2,459	153.5	6.9	2,301	143.7	2,479	254.7	9.5	2,265	141.4		2,271	141.8	
	Avg	2,378	148.5	7.0	2,224	138.8	2,472	154.3	9.5	2,258	141.0		2,231	139.3	
	SD	165	10.3	0.6	166	10.3	123	7.7	0.7	125	7.8		130	8.1	
626HA (Advera #1)	50	2,164	135.1	9.2	1,982	123.7	2,279	142.3	9.6	2,080	129.8	8.7	2,116	132.1	19.2
	100	2,251	140.5	9.0	2,066	129.0	2,313	144.4	9.3	2,117	132.2		2,173	135.7	
	150	2,269	141.7	8.8	2,085	130.2	2,318	144.7	9.8	2,112	131.9		2,184	136.4	
	200	2,284	142.6	8.4	2,107	131.6	2,305	143.9	10.3	2,091	130.5		2,185	136.4	
	250	2,303	143.8	8.7	2,119	132.3	2,313	144.4	9.8	2,108	131.6		2,198	137.2	
	300	2,327	145.3	8.3	2,150	134.2	2,301	143.7	9.6	2,101	131.1		2,204	137.6	
	Avg	2,266	141.5	8.7	2,085	130.2	2,305	143.9	9.7	2,101	131.2		2,177	135.9	
	SD	57	3.5	0.4	58	3.6	14	0.9	0.3	14	0.9		32	2.0	
627HB (Astec)	50	2,292	143.1	8.6	2,111	131.8	2,371	148.0	7.6	2,204	137.6	5.7	2,206	137.7	18.2
	100	2,327	145.3	8.4	2,146	134.0	2,397	149.6	7.9	2,222	138.7		2,235	139.5	
	150	2,346	146.4	9.0	2,152	134.3	2,418	150.9	7.3	2,253	140.6		2,253	140.7	
	200	2,370	147.9	8.3	2,189	136.7	2,410	150.5	7.4	2,245	140.1		2,261	141.2	
	250	2,398	149.7	8.1	2,219	138.5	2,414	150.7	7.6	2,243	140.1		2,276	142.1	
	300	2,387	149.0	8.4	2,201	137.4	2,404	150.1	7.3	2,240	139.8		2,266	141.5	
	Avg	2,353	146.9	8.5	2,170	135.5	2,402	150.0	7.5	2,234	139.5		2,250	140.4	
	SD	40	2.5	0.3	40	2.5	17	1.1	0.2	18	1.1		26	1.6	

* Recalculated dry density using nuclear gauge wet density and laboratory gravimetric moisture content.
[1] MC = Moisture content [2] SG = Subgrade [3] Avg = Average [4] SD = Standard Deviation

Table 5.1: Summary of Base-Course Density and Moisture Content Measurements *(continued)*

Section	Depth	Nuclear Gauge										Laboratory			
		Wheelpath					Untrafficked								
		Base Wet Density		MC[1]	Base Dry Density		Base Wet Density		MC	Base Dry Density		Base MC	Recalculated Dry Density*		SG[2] MC
		(kg/m^3)	(lb/ft^3)	(%)	(kg/m^3)	(lb/ft^3)	(kg/m^3)	(lb/ft^3)	(%)	(kg/m^3)	(lb/ft^3)	(%)	(kg/m^3)	(lb/ft^3)	(%)
628HB (Rediset)	50	2,312	144.3	8.3	2,135	133.3	2,314	144.5	8.1	2,141	133.6	5.2	2,199	137.3	15.6
	100	2,364	147.6	7.7	2,194	137.0	2,334	145.7	7.9	2,163	135.0		2,233	139.4	
	150	2,358	147.2	7.5	2,194	137.0	2,330	145.5	8.2	2,154	134.5		2,228	139.1	
	200	2,364	147.6	7.6	2,198	137.2	2,333	145.6	7.8	2,164	135.1		2,233	139.4	
	250	2,366	147.7	7.5	2,201	137.4	2,354	146.9	7.5	2,189	136.6		2,243	140.0	
	300	2,392	149.3	7.3	2,228	139.1	2,349	146.7	7.6	2,183	136.3		2,253	140.7	
	Avg[3]	2,359	147.3	7.7	2,192	136.8	2,336	145.8	7.9	2,166	135.2		2,231	139.3	
	SD[4]	26	1.6	0.8	31	1.9	14	0.9	0.3	18	1.1		18	1.2	
629HB (Advera #2)		Not Recorded										8.6	-	-	19.1
630HB (Advera #3)	50	2,189	136.7	9.5	2,000	124.9	2,257	140.9	9.1	2,069	129.2	8.3	2,111	131.8	18.9
	100	2,246	140.2	9.4	2,053	128.2	2,285	142.7	9.1	2,096	130.8		2,152	134.3	
	150	2,282	142.5	9.0	2,093	130.7	2,296	143.4	8.5	2,117	132.1		2,174	135.7	
	200	2,293	143.2	8.7	2,109	131.7	2,309	144.2	8.6	2,127	132.8		2,185	136.4	
	250	2,305	143.9	9.2	2,111	131.8	2,313	144.4	8.8	2,126	132.7		2,193	136.9	
	300	2,318	144.7	8.2	2,158	134.8	2,335	145.8	4.0	2,143	133.8		2,209	137.9	
	Avg	2,272	141.8	9.0	2,088	130.3	2,299	143.5	8.8	2,113	131.9		2,171	135.5	
	SD	47	3.0	0.5	55	3.4	27	1.7	0.3	26	1.7		35	2.2	

* Recalculated dry density using nuclear gauge wet density and laboratory gravimetric moisture content.
[1] MC = Moisture content [2] SG = Subgrade [3] Avg = Average [4] SD = Standard Deviation

- Laboratory-determined gravimetric moisture contents varied between 5.0 percent (Section 625HA, Sasobit) and 8.7 percent (Section 626HA, Adera #1), with an average of 5.9 percent and standard deviation of 1.4 percent. These moisture contents were on average 2.6 percent lower than those recorded by the nuclear gauge and appeared more consistent with visual evaluations of the test pit face, and more representative of typical dryback conditions in base materials. The higher moisture contents determined with the nuclear gauge could be associated with the presence of some excess moisture from the saw-cutting operation during pit excavation. Recalculated dry densities, determined using the gauge wet density and gravimetric moisture content, were therefore slightly higher than the gauge-determined dry densities.

5.5 Subgrade Moisture Content

Laboratory-determined gravimetric moisture contents for the subgrade materials ranged between 15.6 percent (Section 628HB, Rediset) and 19.2 percent (Section 626HA, Advera #1) for the six test pits, indicating a significant difference in moisture contents between the base and subgrade materials. Visual observations in the test pits confirmed these differences. The sections with the highest subgrade moisture contents had the poorest rutting performance.

5.6 Dynamic Cone Penetrometer

Dynamic cone penetrometer (DCP) measurements were recorded in each test pit, both in the wheelpath and untrafficked areas. Measurements and plots are provided in Appendix A. A summary of the measurements is provided in Table 5.2. The results show some variation; however, this is attributed more to stones in the base material and not to any significant differences in strength/stiffness. Variation in the subgrade strengths was attributed to differences in moisture content and to remnants of lime treatments during construction of the UCPRC facility. The strength of the material was considered relatively low for base-course standard, but appropriate for accelerated pavement tests. Note that subgrade stiffnesses on the Advera sections (626HA, 629HB, and 630HB) were generally lower than those on the other sections; this was attributed to the higher moisture contents.

5.7 Test Pit Profiles and Observations

Test pit profile illustrations are provided in Appendix A. Average measurements for each profile at Station 9 are listed in Table 5.3. The average layer thicknesses include the wheelpath depression and adjacent material displacement (bulge). As expected, minimum thickness measurements were always recorded in one of the wheelpaths, while maximum thickness measurements were always recorded in one of the adjacent areas of displacement. Design thicknesses for the top and bottom lifts of asphalt and the base were 60 mm, 60 mm, and 450 mm, respectively (0.2 ft., 0.2 ft., and 1.5 ft.).

Table 5.2: Summary of Dynamic Cone Penetrometer Measurements

Section	Blows to 800 mm		Layer	mm/Blow		Estimated Modulus (MPa)	
	Wheelpath	Untrafficked		Wheelpath	Untrafficked	Wheelpath	Untrafficked
624HB	132	106	Base	5	6	223 (32)	179 (26)
625HA	93	88		6	7	478 (69)	140 (20)
626HA	133	132		4	10	256 (37)	223 (32)
627HB	121	117		5	5	209 (30)	194 (28)
628HB	150	110		4	6	256 (37)	173 (25)
629HB	134	109		4	6	266 (39)	197 (29)
630HB	133	111		4	5	256 (37)	191 (28)
624HB			Subgrade	14	17	70 (10)	56 (8)
625HA				22	26	41 (6)	35 (5)
626HA				30	14	30 (4)	70 (10)
627HB				13	12	71 (10)	77 (11)
628HB				11	15	85 (12)	65 (9)
629HB				18	33	52 (8)	28 (4)
630HB				30	20	30 (4)	48 (7)

Table 5.3: Average Layer Thicknesses from Test Pit Profiles (Station 9)

Section	Layer	Average		Std. Deviation		Minimum		Maximum	
		(mm)	(ft.)	(mm)	(ft.)	(mm)	(ft.)	(mm)	(ft.)
624HB	AC – top	66	0.22	4	0.01	55	0.18	75	0.25
	AC – bottom	77	0.25	5	0.02	66	0.22	85	0.28
	AC – total	143	0.47	3	0.01	136	0.45	146	0.48
	Base	481	1.58	5	0.02	470	1.54	492	1.61
625HA	AC – top	67	0.22	3	0.01	60	0.20	71	0.23
	AC – bottom	72	0.24	3	0.01	63	0.21	78	0.26
	AC – total	138	0.45	3	0.01	131	0.43	145	0.48
	Base	464	1.52	5	0.02	449	1.47	471	1.55
626HA	AC – top	63	0.21	3	0.01	59	0.19	75	0.25
	AC – bottom	71	0.23	3	0.01	63	0.21	76	0.21
	AC – total	134	0.44	4	0.01	122	0.40	139	0.46
	Base	462	1.52	9	0.03	447	1.47	476	1.56
627HB	AC – top	67	0.22	4	0.01	55	0.18	74	0.24
	AC – bottom	68	0.22	5	0.02	63	0.21	81	0.27
	AC – total	135	0.44	5	0.02	126	0.41	144	0.47
	Base	470	1.54	8	0.03	455	1.49	483	1.59
628HB	AC – top	66	0.22	4	0.01	56	0.18	75	0.25
	AC – bottom	77	0.25	5	0.02	65	0.21	84	0.28
	AC – total	143	0.47	3	0.01	136	0.45	146	0.48
	Base	442	1.45	10	0.03	426	1.40	456	1.50
629HB	AC – top	50	0.16	4	0.01	41	0.13	57	0.19
	AC – bottom	72	0.24	6	0.02	61	0.20	83	0.27
	AC – total	122	0.40	6	0.02	112	0.37	132	0.43
	Base	471	1.55	13	0.04	447	1.47	497	1.63
630HB	AC – top	59	0.19	3	0.01	51	0.17	68	0.22
	AC – bottom	75	0.25	7	0.02	62	0.20	94	0.31
	AC – total	134	0.44	6	0.02	123	0.40	130	0.43
	Base	475	1.56	8	0.03	459	1.51	490	1.61

The measurements from each test pit show that layer thickness consistency on each test section was fairly good based on the low standard deviations recorded. The average base thickness varied between 442 mm

(1.45 ft.) on the Rediset section (Section 628HB) and 481 mm (1.58 ft.) on the Control (Section 624HB) (somewhat thicker than the design), while the combined asphalt concrete thickness varied between 122 mm (0.4 ft.) on the Advera section (Section 626HA), slightly thinner than the design, and 143 mm (0.47 ft.) on the Control and Rediset sections (Sections 624HB and 628HB), about 23 mm (0.08 ft.) thicker than the design. Average asphalt concrete thicknesses measured in the test pits were consistent with the measurements from cores discussed in Section 2.7.10. A discussion of the observations from each test pit is provided in the following sections.

5.7.1 Section 624HB: Control (Test #1)

Observations from the Section 624HA test pit (Figure 5.2) include:

- The average thicknesses of the top and bottom lifts of asphalt concrete were marginally thicker than the design (66 mm [0.22 ft.] and 77 mm [0.25 ft.] respectively). The average combined thickness was considerably thicker (143 mm [0.47 ft.]) than the design (120 mm [0.4 ft.]).
- Rutting was visible in both asphalt layers, with some evidence of rutting was also noted at the top of the base (Figure 5.2b). No rutting was measured/observed in the subgrade. Some displacement was recorded on either side of the trafficked area in both lifts of asphalt and at the top of the base.
- The two asphalt concrete layers were well bonded to each other (Figure 5.2c) and well bonded to the aggregate base. The precise location of the bond between the two asphalt lifts was clear. The prime coat appeared to have penetrated between 10 mm and 15 mm (0.4 in. and 0.6 in.) into the base (Figure 5.2d).
- Apart from rutting, no other distresses were noted in the asphalt layers, apart from some signs of segregation and some visible voids in the top lift, attributed to the cool placement temperatures.
- Base thickness showed very little variation across the profile. The material was well graded and aggregates were mostly rounded (little evidence of crushing) with some flakiness. No oversize material was observed, and the properties appeared to be consistent (Figure 5.2e). Material consistency was rated as very hard throughout the layer. No organic matter was observed.
- Moisture content in the base was rated as moist, with moisture content appearing to increase near the subgrade. There was no indication of higher moisture content at the interface between the base and asphalt concrete layers.
- The layer definition between the base and subgrade was clear. Some punching of the base into the subgrade was noted.
- The subgrade was moist, silty-clay material. Consistency was rated as soft and some shrinkage and slickenslides were observed. Some evidence (hydrochloric acid reaction) of the lime treatment during the original site preparation for construction of the UCPRC facility in 2008 was noted (Figure 5.2f). No organic matter was observed.

(a) General view of test pit

(b) Rutting in top and bottom lifts

(c) Bond between lifts. Note voids in top lift.

(d) Penetration of prime into base layer

(e) Consistent base material and clear interface with subgrade

(f) Hydrochloric acid reaction on subgrade material. Note clay texture.

Figure 5.2: 624HB: Test pit photographs.

5.7.2 Section 625HA: Sasobit (Test #1)

Observations from the Section 625HA test pit (Figure 5.3) include:

- The average thicknesses of both lifts of asphalt concrete were thicker (67 mm and 72 mm [0.22 ft. and 0.23 ft.]) than the design thickness. The average combined thickness was also marginally thicker (138 mm [0.45 ft.]) than the design and on average 5.0 mm (0.02 ft.) thinner than the Control.

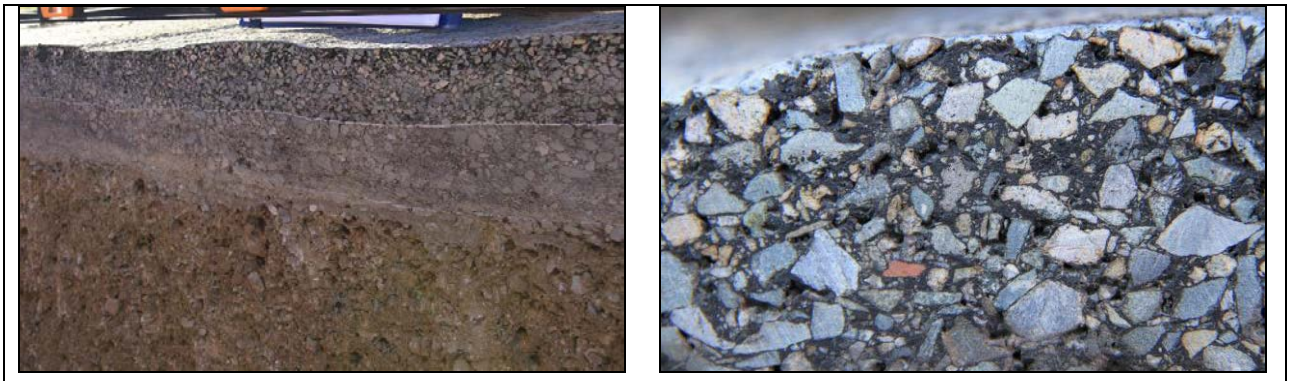

a) General view of test pit. **b) Areas of predominantly fine and coarse aggregates.**

Figure 5.3: 625HA: Test pit photographs.

- Rutting was mostly restricted to the upper region of the top lift of asphalt, although some evidence of slight rutting was noted in the bottom lift (about 3 mm to 5 mm [0.12 to 0.2 in.]) and top of the base. No deformation was noted in the subgrade. Some displacement was recorded on either side of the trafficked area in both lifts of asphalt and at the top of the base.
- The two asphalt concrete layers were well bonded to each other and well bonded to the aggregate base. The precise location of the bond between the two asphalt lifts was clear, but some upward penetration of the tack coat into the rubberized asphalt was visible. The prime coat appeared to have penetrated into the base in a similar way to that observed on the Control.
- Apart from rutting, no other distresses were noted in the asphalt layers other than some visible voids and some segregation (areas of predominantly fine material and others of predominantly coarse material) in the rubberized asphalt layer (Figure 5.3b).
- Base thickness showed very little variation across the profile. The material was consistent with the observations on the Control.
- Moisture content in the base was rated as moist, with moisture content appearing to increase near the subgrade. There was no indication of higher moisture content at the interface between the base and asphalt concrete layers.
- The layer definition between the base and subgrade was clear. Some punching of the base into the subgrade was noted.
- Observations of the subgrade were consistent with those of the Control except that no hydrochloric reaction was noted (i.e., no lime was present).

5.7.3 Sections 626HA, 629HB, and 630HB: Advera

Observations from the Advera sections test pits (Figure 5.4) include:

- The top lifts of asphalt in all three test pits were marginally thinner than the design (63 mm, 50 mm, and 59 mm [0.21 ft., 0.17 ft. and 0.19 ft.], respectively) and considerably thinner than the Control. Bottom lift thicknesses were similar to the Control. The average combined thickness was marginally thicker (135 mm, 122 mm, and 134 mm [0.44 ft., 0.4 ft. and 0.44 ft.], respectively) than

the design, but between 10 mm and 22 mm (0.03 ft. and 0.08 ft.) thinner than the Control. This probably had some influence on the poor performance of these sections.

- Rutting was clearly evident in all layers and in the subgrade (Figure 5.4b). Some displacement was recorded on either side of the trafficked area in both lifts of asphalt.
- The two asphalt concrete layers were well bonded to each other and well bonded to the aggregate base. The precise location of the bond between the two asphalt lifts was clear. The prime coat appeared to have penetrated into the base in a similar way to that observed on the Control.
- Apart from rutting and displacement of material adjacent to the ruts, no other distresses were noted in the asphalt layers.
- Base thickness showed very little variation across the profile. The material was consistent with the observations on the Control.
- Moisture content in the base was rated as moist, with moisture content appearing to increase near the subgrade. There was no indication of higher moisture content at the interface between the base and asphalt concrete layers.
- The layer definition between the base and subgrade was clear. Some punching of the base into the subgrade was noted (Figure 5.4c).
- Observations of the subgrade were consistent with those of the Control, although the material appeared visibly wetter (Figure 5.4d). No hydrochloric acid reaction was observed.

(a) General view of test pit face

(b) Rutting in both lifts of asphalt

(c) Stones punched into subgrade

(d) Wet lower base and subgrade

Figure 5.4: 626HA, 629HB, and 630HB: Test pit photographs.

5.7.4 Section 627HB: Astec

Observations from the Section 627HB test pit (Figure 5.5) include:

- The average thicknesses of both lifts of asphalt concrete were marginally thicker (67 mm [0.22 ft.] and 68 mm [0.23 ft.], respectively) than the design thickness. The average combined thickness was therefore also thicker (134 mm [0.44 ft.]) than the design but still less than the thickness of the asphalt layers on the Control (143 mm [0.47 ft.]).
- Rutting was clearly visible in both asphalt layers, and present, but less distinct at the top of the base and top of the subgrade. Some displacement was recorded on either side of the trafficked area in both lifts of asphalt and at the top of the base.
- The two asphalt concrete layers were well bonded to each other, and to the aggregate base. The precise location of the bond between the two asphalt lifts was clear, but some evidence of moisture in the bond was observed (Figure 5.5b). Bleeding was evident in the wheelpaths and some voids were visible in the rubberized asphalt layer. The prime coat appeared to have penetrated into the base in a similar way to that observed on the Control.
- Apart from rutting and some bleeding, no other distresses were noted in the asphalt layers.
- Base thickness showed very little variation across the profile. The material was consistent with the observations on the Control.
- Moisture content in the base was rated as moist, with moisture content appearing to increase near the subgrade. There was some indication of higher moisture content at the interface between the base and asphalt concrete layers (Figure 5.5a).
- The layer definition between the base and subgrade was clear. Some punching of the base into the subgrade was noted.
- Observations of the subgrade were consistent with those of the Control, but no hydrochloric acid reaction was observed.

(a) General view of test pit face

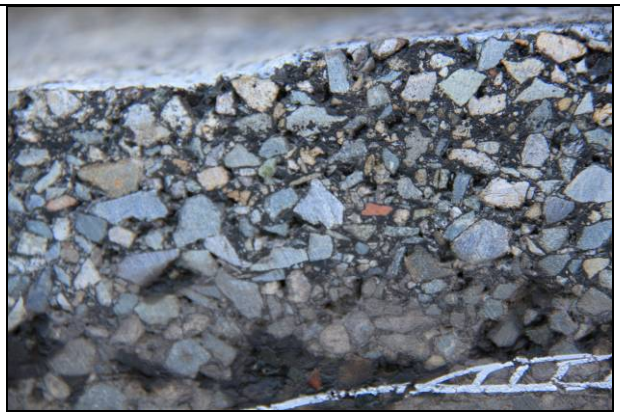

(b) Bleeding on surface and moisture in bond between asphalt layers

Figure 5.5: 627HB: Test pit photographs.

5.7.5 Section 628HB: Rediset

Observations from the Section 628HB test pit (Figure 5.6) include:

- The average thicknesses of both lifts of asphalt concrete were marginally thicker (66 mm [0.22 ft.] and 77 mm [0.25 ft.], respectively) than the design thickness and the same as the Control. The average combined thickness was 143 mm [0.47 ft.]).
- Rutting was mostly confined to the top lift of asphalt, with some evidence in the top of the underlying layer. Rutting was not visible at the top of the base or in the subgrade.
- The two asphalt concrete layers were well bonded to each other, and to the aggregate base. The precise location of the bond between the two asphalt lifts was clear (Figure 5.6b). Some voids were evident in the rubberized asphalt. The prime coat appeared to have penetrated into the base in a similar way to that observed on the Control.
- Apart from rutting, no other distresses were noted in the asphalt layers.
- Base thickness showed very little variation across the profile. The material was consistent with the observations on the Control.
- Moisture content in the base was rated as moist, with moisture content appearing to increase near the subgrade. There was some indication of higher moisture content at the interface between the base and asphalt concrete layers.
- The layer definition between the base and subgrade was clear. Some punching of the base into the subgrade was noted.
- Observations of the subgrade were consistent with those of the Control, but no hydrochloric acid reaction was observed.

(a) General view of test pit face

(b) Close-up of asphalt layers

Figure 5.6: 628HB: Test pit photographs.

5.8 Forensic Investigation Summary

A forensic investigation of all test sections indicated that rutting was mostly confined to the upper lift of the asphalt concrete, with limited rutting in the bottom lift, base, and top of the subgrade on most sections.

However, the test pits on the Advera sections revealed more significant rutting in all layers and in the subgrade, as well as notably higher moisture contents at the bottom of the base and in the subgrade when compared to the other sections. There was some variation in asphalt layer lift thicknesses among the five sections. Materials were consistent throughout and no evidence of moisture damage was noted. There was no visible difference in the appearance of the asphalt between the Control and warm-mix sections.

6. PHASE 3b LABORATORY TEST DATA SUMMARY

6.1 Experiment Design

Phase 3b laboratory testing included rutting performance (shear), fatigue cracking, and moisture sensitivity tests. Tests on these mix properties were carried out on beams and cores cut from the test track after construction (see Section 2.8). Typical experimental designs used in previous studies were adopted for this warm-mix asphalt study to facilitate comparison of results.

6.1.1 Shear Testing for Rutting Performance

Test Method

The AASHTO T 320 Permanent Shear Strain and Stiffness Test was used for shear testing in this study. In the standard test methodology, cylindrical test specimens 150 mm (6.0 in.) in diameter and 50 mm (2.0 in.) thick are subjected to repeated loading in shear using a 0.1-second haversine waveform followed by a 0.6-second rest period. Three different shear stresses are applied while the permanent (unrecoverable) and recoverable shear strains are measured. The permanent shear strain versus applied repetitions is normally recorded up to a value of five percent although 5,000 repetitions are called for in the AASHTO procedure. A constant temperature is maintained during the test (termed the *critical temperature)*, representative of the high temperature causing rutting in the local environment. In this study, specimens were cored from the test track and then trimmed to size.

Number of Tests

A total of 18 shear tests were carried out on each mix (total of 108 tests for the four mixes) as follows:

- Two temperatures (45°C and 55°C [113°F and 131°F])
- Three stresses (70 kPa, 100 kPa, and 130 kPa [10.2, 14.5, and 18.9 psi])
- Three replicates

6.1.2 Flexural Beam Testing for Fatigue Performance

Test Method

The AASHTO T-321 Flexural Controlled-Deformation Fatigue Test method was followed. In this test, three replicate beam test specimens, 50 mm (2.0 in.) thick by 63 mm (2.5 in.) wide by 380 mm (15 in.) long, which were sawn from the test track, were subjected to four-point bending using a haversine waveform at a loading frequency of 10 Hz. Testing was performed in both dry and wet condition at two different strain levels at one temperature. Flexural Controlled-Deformation Frequency Sweep Tests were used to establish the relationship between complex modulus and load frequency. The same sinusoidal waveform was used in a controlled deformation mode and at frequencies of 15, 10, 5, 2, 1, 0.5, 0.2, 0.1,

0.05, 0.02, and 0.01 Hz. The upper limit of 15 Hz is a constraint imposed by the capabilities of the test machine. To ensure that the specimen was tested in a nondestructive manner, the frequency sweep test was conducted at a small strain amplitude level, proceeding from the highest frequency to the lowest in the sequence noted above.

The wet specimens used in the fatigue and frequency sweep tests were conditioned following the beam-soaking procedure described in Appendix C. The beam was first vacuum-saturated to ensure a saturation level greater than 70 percent, and then placed in a water bath at 60°C (140°F) for 24 hours, followed by a second water bath at 20°C (68°F) for two hours. The beams were then wrapped with Parafilm™ and tested within 24 hours after soaking.

Number of Tests

A total of 12 beam fatigue tests and 12 flexural fatigue frequency sweep tests were carried out on each mix (total of 148 tests for the four mixes) as follows:

- Flexural fatigue test:
  + Two conditions (wet and dry)
  + One temperature (20°C [68°F])
  + Two strains (200 microstrain and 400 microstrain)
  + Three replicates
- Frequency sweep test:
  + Two conditions (wet and dry)
  + Three temperatures (10°C, 20°C, and 30°C [50°F, 68°F, and 86°F])
  + One strain (100 microstrain)
  + Two replicates

6.1.3 Moisture Sensitivity Testing

Test Methods

Two additional moisture sensitivity tests were conducted, namely the Hamburg Wheel-Track test and the Tensile Strength Retained (TSR) test.

- The AASHTO T 324 test method was followed for Hamburg Wheel-Track testing on 152 mm (6.0 in.) cores removed from the test track. All testing was carried out at 50°C (122°F).
- The Caltrans CT 371 test method was followed for the Tensile Strength Retained test on 100 mm cores removed from the test track and trimmed to a thickness of 63 mm (2.5 in.). This test method is similar to the AASHTO T 283 test, however, it has some modifications specific for California conditions.

Number of Tests

Four replicates of the Hamburg Wheel-Track test and four replicates of the Tensile Strength Retained test were carried out for each mix (24 tests per method).

6.2 Test Results

6.2.1 Rutting Performance Tests

Air-Void Content

Shear specimens were cored from the test track and trimmed to size. Air-void contents were measured using the CoreLok method and results are listed in Table C.1 through Table C.6 in Appendix C. Table 6.1 summarizes the air-void distribution categorized by mix type, test temperature, and test shear stress level. Figure 6.1 presents the summary boxplots of air-void content of all the specimens tested according to additive type. The differences in air-void content distributions between the mixes with various additives are clearly apparent. There is also a difference between the Day #1 and Day #2 Control mixes, with better compaction being achieved on Day #2. The mean difference for the highest mean air-void content (Day #1 Control) and the smallest mean air-void content (Sasobit and Rediset) could be as high as 4.0 percent. The two Control mix specimens had the largest range in air-void content. The Sasobit and Rediset specimens had lower mean air-void contents compared to the foaming technologies.

Table 6.1: Summary of Air-Void Contents of Shear Test Specimens

Temperature		Stress Level	Day #1 Air-Void Content (%)					
			Control #1		Sasobit		Advera	
°C	°F	(kPa)	Mean[1]	SD[2]	Mean	SD		
45	113	70	13.4	0.4	8.2	0.7	11.1	0.4
		100	13.5	1.3	8.4	0.1	10.3	0.6
		130	12.0	2.0	7.8	0.7	10.8	0.8
55	131	70	12.5	1.0	8.6	0.4	10.7	0.4
		100	12.3	1.1	9.2	0.6	10.4	0.6
		130	12.2	0.2	8.6	0.2	10.5	0.4
		Overall	12.7	1.0	8.5	0.4	10.7	0.5
Temp.		**Stress Level**	**Day #2 Air-Void Content (%)**					
			Control #2		**Astec**		**Rediset**	
°C	**°F**	**(kPa)**	**Mean**	**SD**	**Mean**	**SD**	**Mean**	**SD**
45	113	70	9.2	2.2	10.6	0.5	8.6	0.4
		100	8.3	0.4	9.5	1.0	8.6	0.8
		130	8.6	0.6	10.5	0.9	8.4	0.4
55	131	70	8.7	1.8	10.5	0.6	9.3	0.7
		100	9.8	3.1	9.9	0.7	7.8	0.3
		130	9.4	1.8	9.9	0.3	8.1	0.9
		Overall	9.0	1.6	10.2	0.6	8.5	0.6

[1] Mean of three replicates [2] SD: Standard deviation

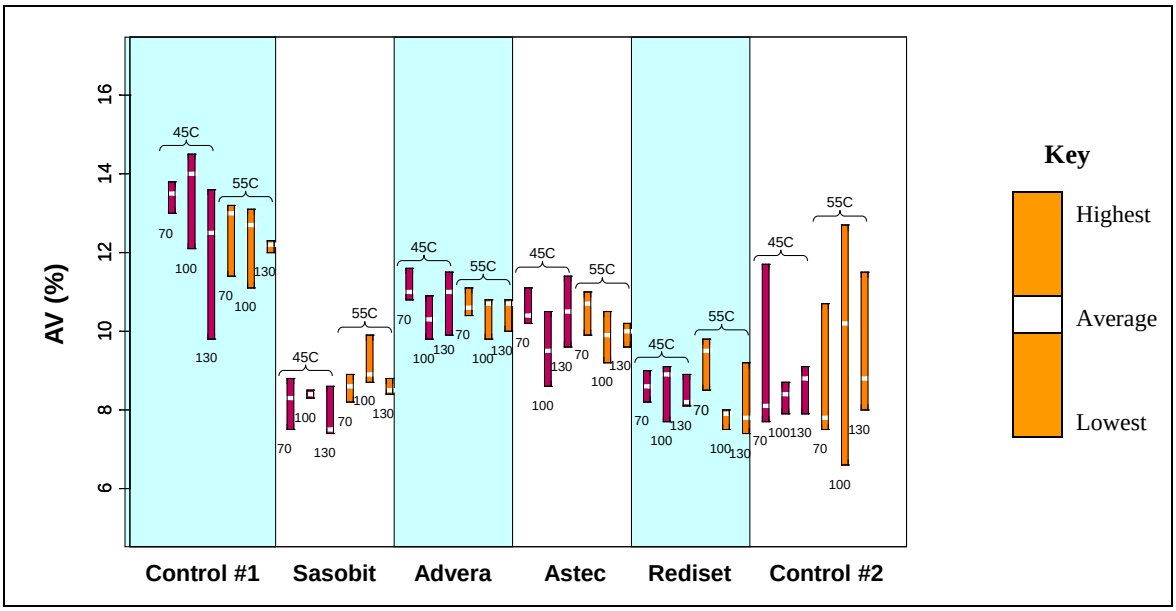

Figure 6.1: Air-void contents of shear specimens.

Resilient Shear Modulus (G*)

The resilient shear modulus results for the six mixes are summarized in Figure 6.2 and Figure 6.3. The following observations were made:

- The resilient shear modulus was influenced by temperature, with the modulus increasing with decreasing temperature. Resilient shear modulus was not influenced by stress.
- The variation of resilient shear moduli at 45°C was higher than at 55°C for all mixes and was generally attributed to higher sensitivity to air-void content variation at this testing temperature.

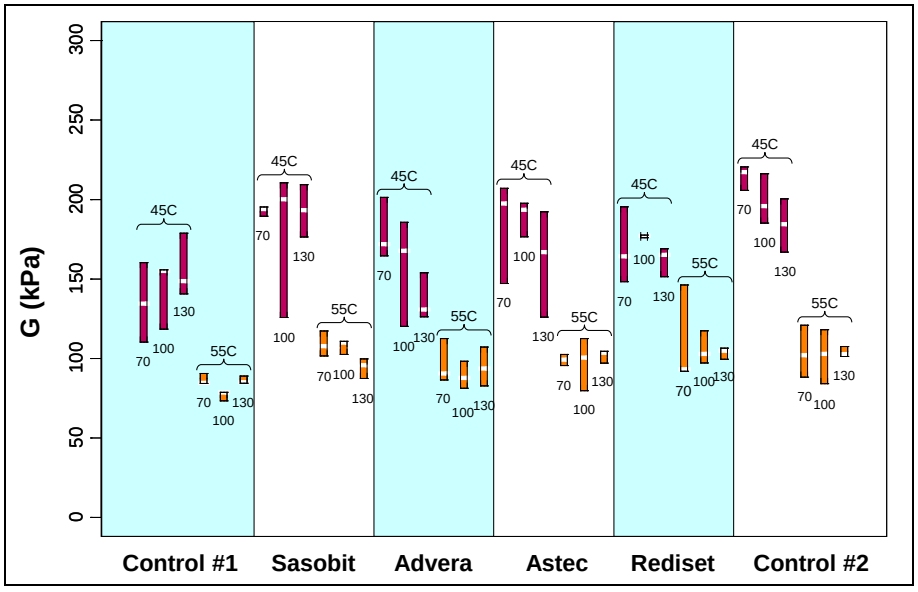

Figure 6.2: Summary boxplots of resilient shear modulus.

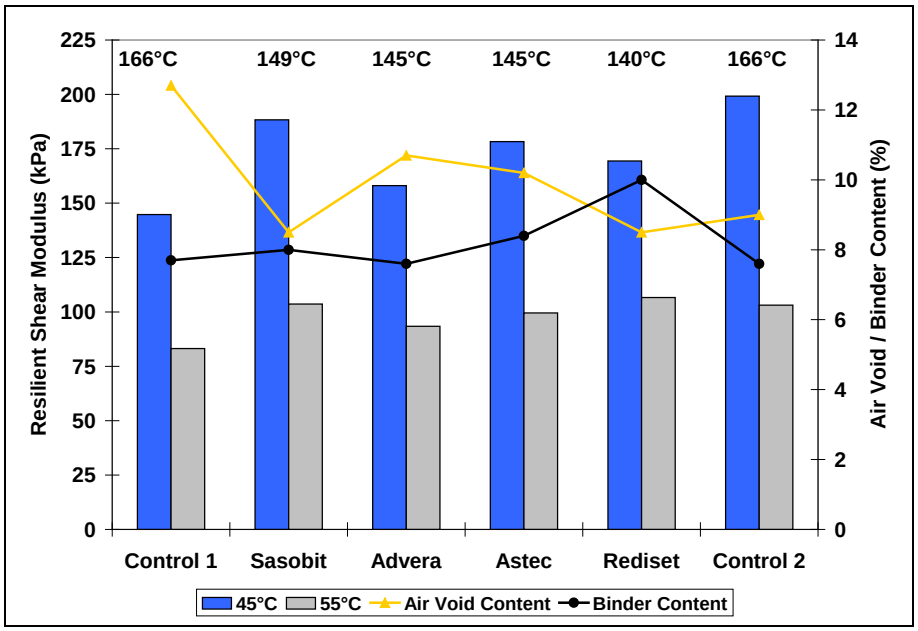

Figure 6.3: Average resilient shear modulus at 45°C and 55°C at 100 kPa stress level.
(Average mix production temperature, binder content, and air-void content shown.)

- Although the warm mixes appear to have slightly higher resilient shear moduli compared to the Day #1 Control, attributed in part to the lower air-void content, statistical analyses (t-test and Kolmogorov-Smirnov test) indicated that there was no statistically significant difference (confidence level of 0.1) in performance between the Controls and the four warm-mixes after variation in mix production temperature, binder content, specimen air-void content, actual test stress level, and actual test temperature were taken into consideration. This indicates that the use of the warm-mix technologies and lower production and compaction temperatures did not significantly influence the performance of the mixes in this test.

Cycles to Five Percent Permanent Shear Strain

The number of cycles to five percent permanent shear strain provides an indication of the rut-resistance of an asphalt mix, with higher numbers of cycles implying better rut-resistance. Figure 6.4 and Figure 6.5 summarize the shear test results in terms of the natural logarithm of this parameter. The following observations were made:

- Variation between results was in line with typical result ranges for this test.
- As expected, the rut-resistance capacity decreased with increasing temperature and stress level.
- The Day #1 Control and Advera mixes performed poorly in this test compared to the other mixes. This was attributed in part to the higher air-void contents of these specimens.
- Statistical analyses (t-test and Kolmogorov-Smirnov test) indicated that there was no statistically significant difference (confidence level of 0.1) in performance in this test between the Day #2 Control and the Sasobit, Astec, and Rediset mixes after variation in mix production temperature, binder content, specimen air-void content, actual test stress level, and actual test temperature were taken into consideration. This indicates that the use of these warm-mix technologies and lower

production and compaction temperatures did not significantly influence the performance of the mixes in this test.

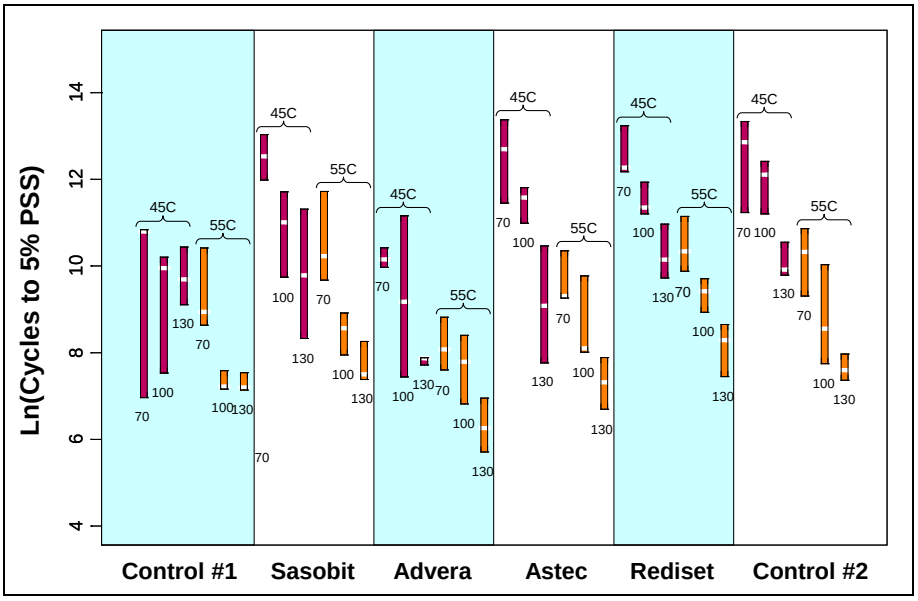

Figure 6.4: Summary boxplots of cycles to five percent permanent shear strain.

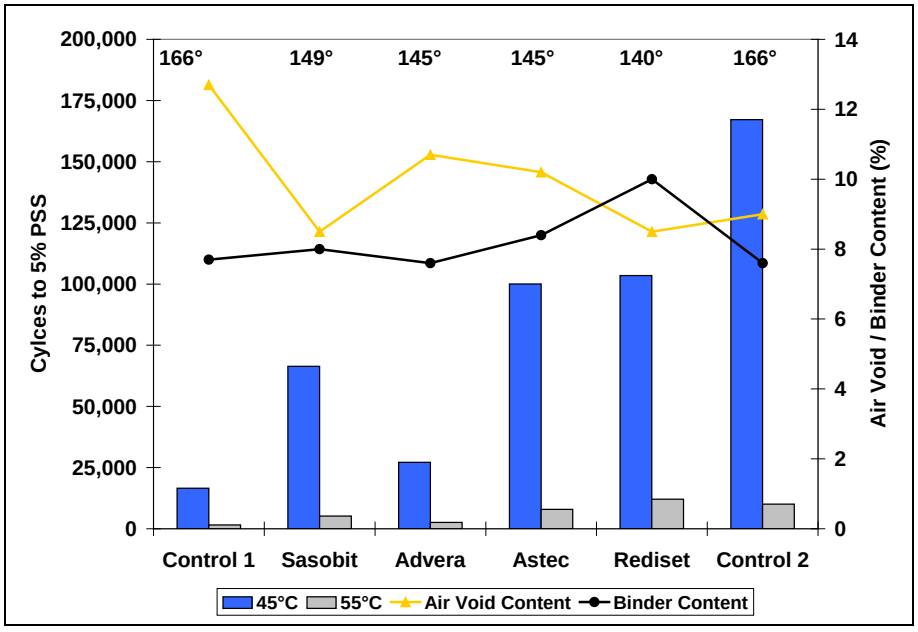

Figure 6.5: Average cycles to 5% permanent shear strain at 45°C and 55°C at 100 kPa stress level.
(Average mix production temperature, binder content, and air-void content shown.)

Permanent Shear Strain at 5,000 Cycles

The measurement of permanent shear strain (PSS) accumulated after 5,000 cycles provides an alternative indication of the rut-resistance capacity of an asphalt mix. The smaller the permanent shear strain the

better the mixture's rut-resistance capacity. Figure 6.6 and Figure 6.7 summarize the rutting performance of the six mixes in terms of the natural logarithm of this parameter (i.e., increasingly negative values represent smaller cumulative permanent shear strain). The following observations were made:

- Variation between results was in line with typical result ranges for this test.
- As expected, the effect of shear stress level was more significant at higher temperatures, and the higher the temperature and stress level the larger the cumulative permanent shear strain.

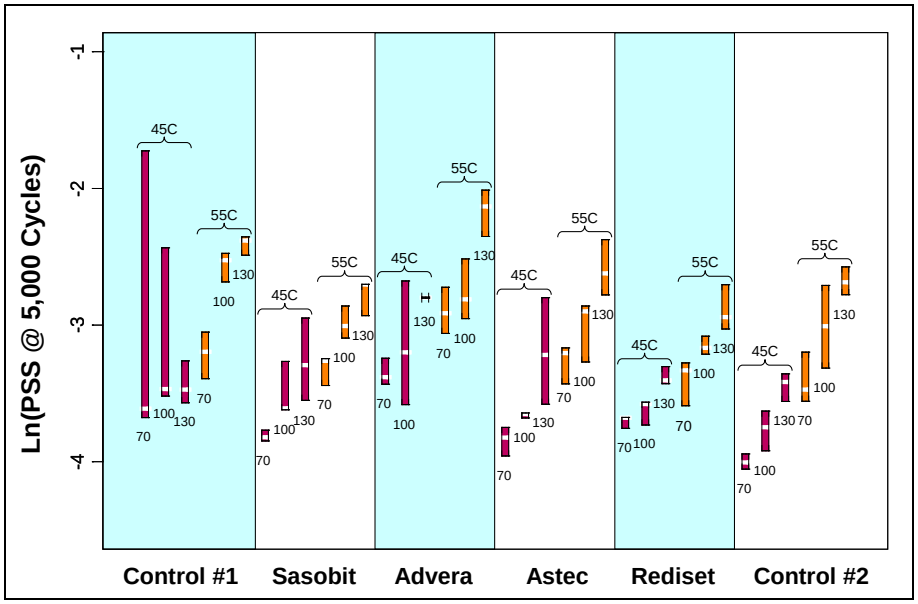

Figure 6.6: Summary boxplots of cumulative permanent shear strain at 5,000 cycles.

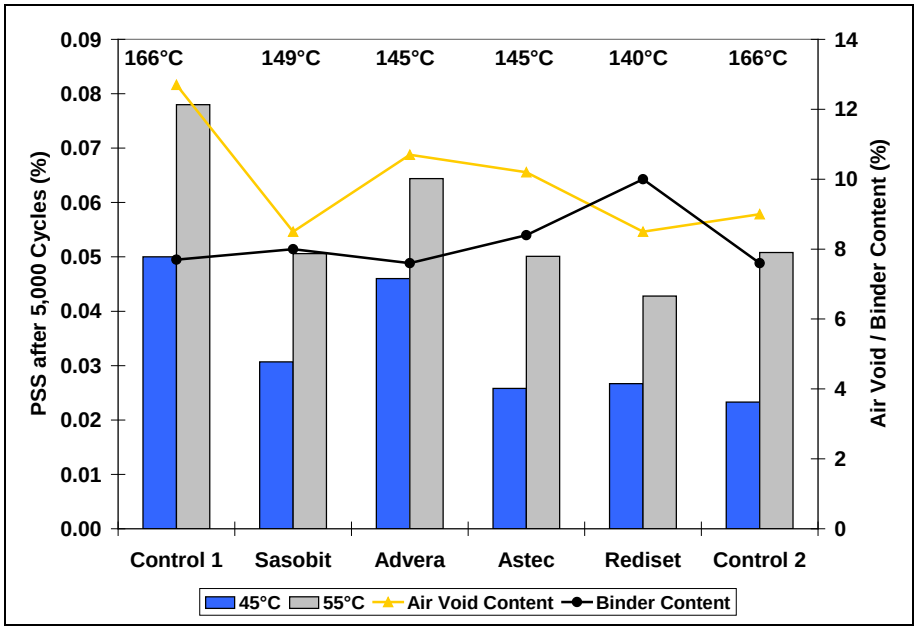

Figure 6.7: Average PSS after 5,000 cycles at 45°C and 55°C at 100 kPa stress level.
(Average mix production temperature, binder content, and air-void content shown.)

- The Day #1 Control and Advera mixes performed poorly in this test compared to the other mixes, in line with the results for the number of cycles to five percent permanent shear strain. This was again attributed in part to the higher air-void contents of these specimens.
- Statistical analyses (t-test and Kolmogorov-Smirnov test) indicated that there was no statistically significant difference (confidence level of 0.1) in performance in this test between the Day #2 Control and the Sasobit, Astec, and Rediset mixes after variation in mix production temperature, binder content, specimen air-void content, actual test stress level, and actual test temperature were taken into consideration. This indicates that the use of the warm-mix technologies and lower production and compaction temperatures did not significantly influence the performance of the mixes in this test.

6.2.2 Beam Fatigue Tests

Air-Void Content

Fatigue beams were saw-cut from the top lift of the slabs sampled from the test track. Air-void contents were measured using the CoreLok method and the results are listed in Table C.7 in Appendix C. Table 6.2 and Table 6.3 summarize the air-void distribution categorized by mix type and test tensile strain level for the beam fatigue and frequency sweep specimens, respectively.

Figure 6.8 shows summary boxplots of air-void content for the wet and dry beam fatigue specimens, which indicates some differences in air-void content between the specimens used for testing at the different strain levels and moisture condition within each mix, with the most variation in the Day #1 Control mix.

Table 6.2: Summary of Air-Void Contents of Beam Fatigue Specimens

Condition	Strain	Day #1 Air-Void Content (%)					
		Control #1		Sasobit		Advera	
	(µstrain)	Mean[1]	SD[2]	Mean	SD		
Dry	200	11.8	1.2	9.2	0.2	10.4	0.5
	400	12.3	1.4	9.0	0.3	10.5	0.4
Wet	200	11.0	0.9	8.8	0.3	10.6	0.3
	400	12.2	0.9	9.3	1.1	10.7	0.7
Overall		11.8	1.1	9.1	0.5	10.5	0.5
Condition	**Strain**	**Day #2 Air-Void Content (%)**					
		Control #2		**Astec**		**Rediset**	
	(µstrain)	**Mean**	**SD**	**Mean**	**SD**	**Mean**	**SD**
Dry	200	6.1	0.7	8.4	1.0	8.4	0.3
	400	6.4	0.4	8.1	1.0	8.5	0.1
Wet	200	6.5	0.4	8.2	0.7	9.0	0.9
	400	7.1	0.5	8.7	0.5	9.5	1.4
Overall		6.5	0.5	8.3	0.8	8.8	0.7

[1] Mean of three replicates [2] SD: Standard deviation

Table 6.3: Summary of Air-Void Contents of Flexural Frequency Sweep Specimens

Condition	Temperature		Day #1 Air-Void Content (%)					
			Control #1		Sasobit		Advera	
	°C	°F	Mean[1]	SD[2]	Mean	SD		
Dry	10	50	12.1	0.5	9.5	1.3	0.6	10.6
	20	68	12.0	1.1	9.2	0.4	0.1	10.7
	30	86	11.5	2.2	7.8	0.7	0.6	10.4
Wet	10	50	11.7	0.3	8.8	0.7	0.0	10.5
	20	68	10.8	2.2	9.1	0.7	1.4	11.0
	30	86	10.5	0.4	8.5	0.9	0.1	10.7
Overall			11.4	1.1	8.8	0.8	10.7	0.5
Condition	**Temperature**		**Day #2 Air-Void Content (%)**					
			Control #2		**Astec**		**Rediset**	
	°C	**°F**	**Mean**	**SD**	**Mean**	**SD**	**Mean**	**SD**
Dry	10	50	6.5	0.4	8.0	0.9	10.6	0.9
	20	68	7.3	0.1	8.0	0.9	9.0	0.8
	30	86	6.7	0.4	9.0	0.8	9.6	1.3
Wet	10	50	7.0	0.1	8.4	0.9	9.6	0.1
	20	68	6.	0.1	8.6	1.2	9.1	0.1
	30	86	7.1	0.1	9.0	0.9	8.4	0.4
Overall			6.8	0.2	8.5	0.9	9.4	0.6

[1] Mean of three replicates [2] SD: Standard deviation

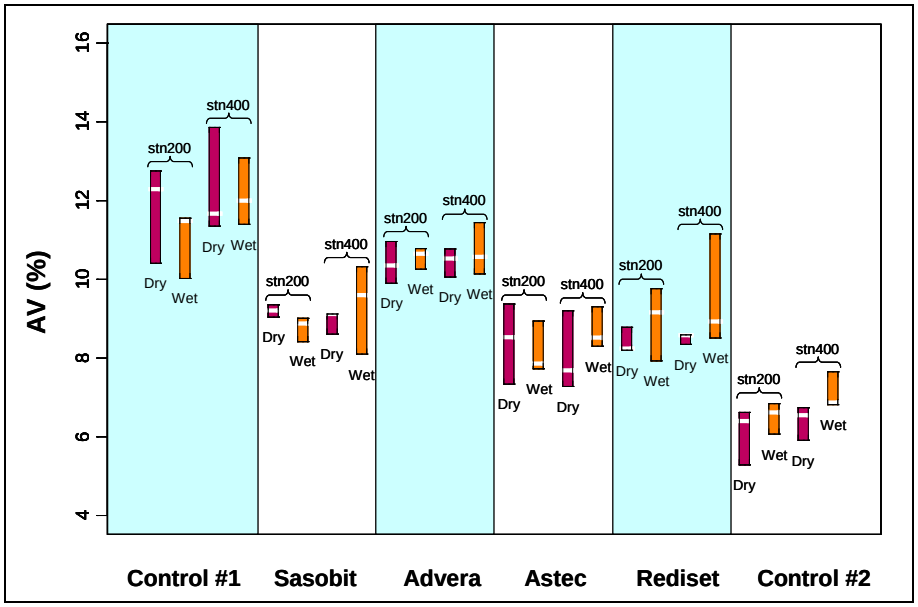

Figure 6.8: Air-void contents of beam fatigue specimens (dry and wet).

Average air-void contents in this Control mix and in the Advera mix were higher than the other mixes, similar to those measured in the shear testing specimens. For the Day #2 mixes, the Control mix specimens had lower air-void contents than the warm-mix specimens. For the frequency sweep specimens, where only two specimens for each variable were tested, the air-void contents show a little more variability, but show similar trends to the beam fatigue specimens. Suggested reasons for the difference in

air-void content are discussed in Section 2.7. The differences in air-void content were factored into the test result analysis discussed below.

Initial Stiffness

Figure 6.9 illustrates the initial stiffness comparison at various strain levels, temperatures, and conditioning for the different mix types. Figure 6.10 and Figure 6.11 show the average results for the dry and wet tests, respectively, in relation to production temperature, binder content, and average air-void content. The following observations were made:

- Variation between results was in line with typical result ranges for this test.
- Initial stiffness was generally strain-independent for both the dry and wet tests.
- In both the dry and wet tests, similar trends in results to those noted in the shear tests were observed. The mixes with the highest air-void contents (Day #1 Control and Advera) had the lowest initial stiffnesses. The high binder content on the Rediset mix also appeared to influence initial stiffness in this test, as expected. After these factors as well as variation in mix production temperature, actual test strain level, and actual test temperature were taken into consideration, there was no statistically significant difference (confidence level of 0.1) in performance in this test between the different mixes. This indicates that the use of the warm-mix technologies and lower production and compaction temperatures did not significantly influence the performance of the mixes in this test.
- A reduction of initial stiffness due to soaking was apparent for each mix type, indicating a potential loss of structural capacity due to moisture damage.

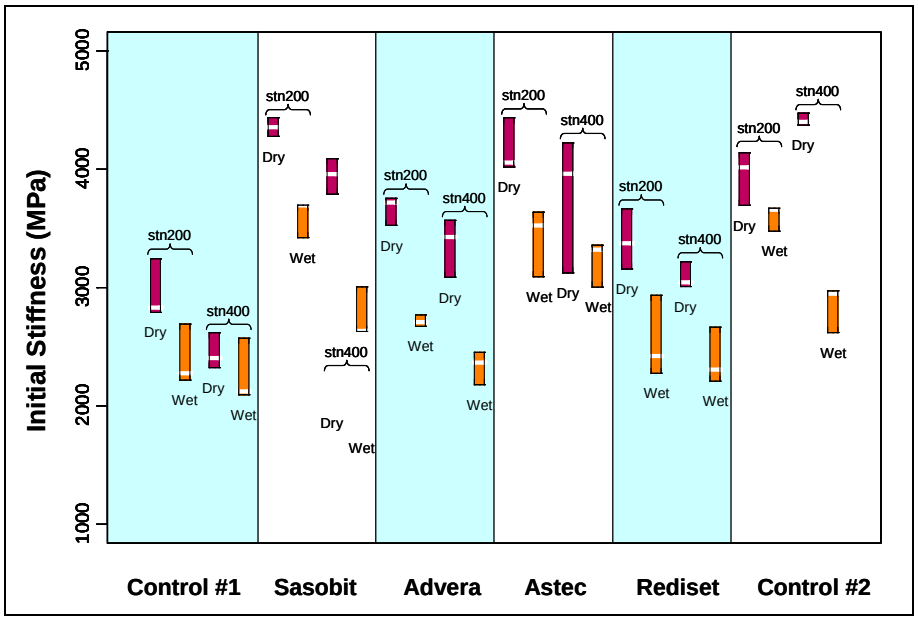

Figure 6.9: Summary boxplots of initial stiffness.

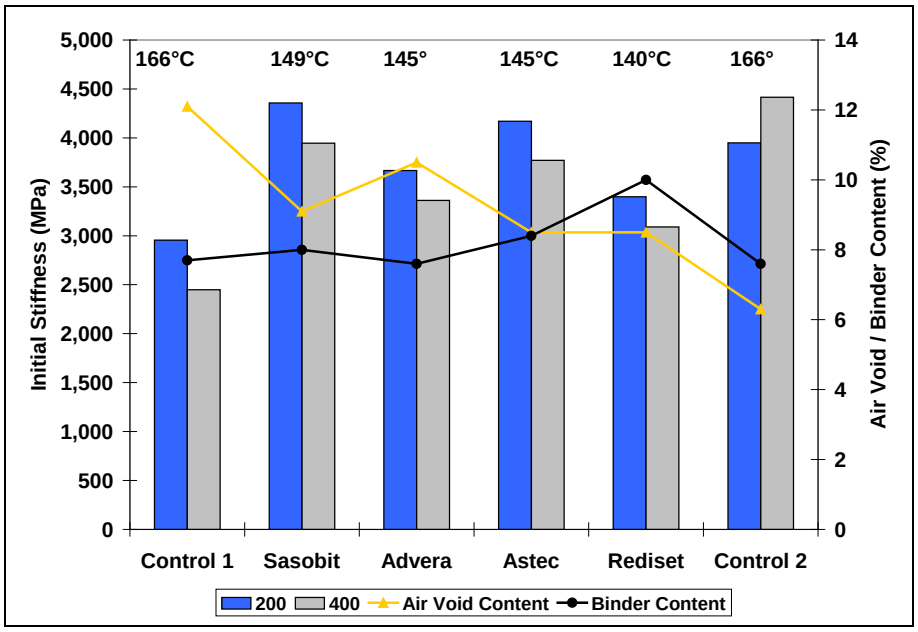

Figure 6.10: Plot of average initial stiffness for dry test.
(Average mix production temperature, binder content, and air-void content shown.)

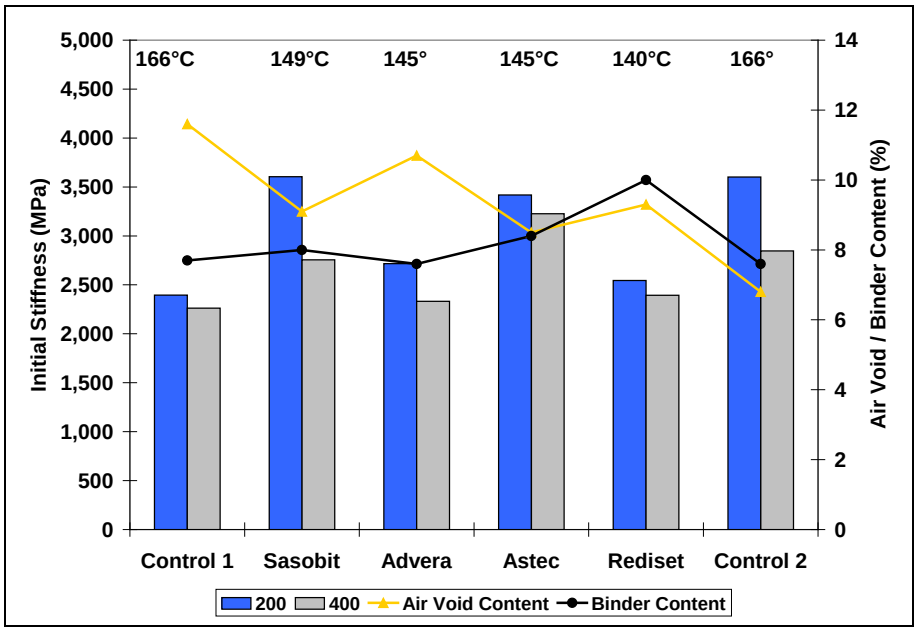

Figure 6.11: Plot of average initial stiffness for wet test.
(Average mix production temperature, binder content, and air-void content shown.)

Initial Phase Angle

The initial phase angle can be used as an index of mix viscosity properties, with higher phase angles corresponding to more viscous and less elastic properties. Figure 6.12 illustrates the side-by-side phase angle comparison of dry and wet tests for the six mixes. Figure 6.13 and Figure 6.14 show the average

results in relation to production temperature, binder content, and average air-void content for the dry and wet tests, respectively. The following observations were made:

- The initial phase angle appeared to be strain-independent.
- Soaking appeared to increase the phase angle slightly on all mixes except the Rediset. This was attributed to the higher binder content of this mix.
- The initial phase angle was highly negative-correlated with the initial stiffness.

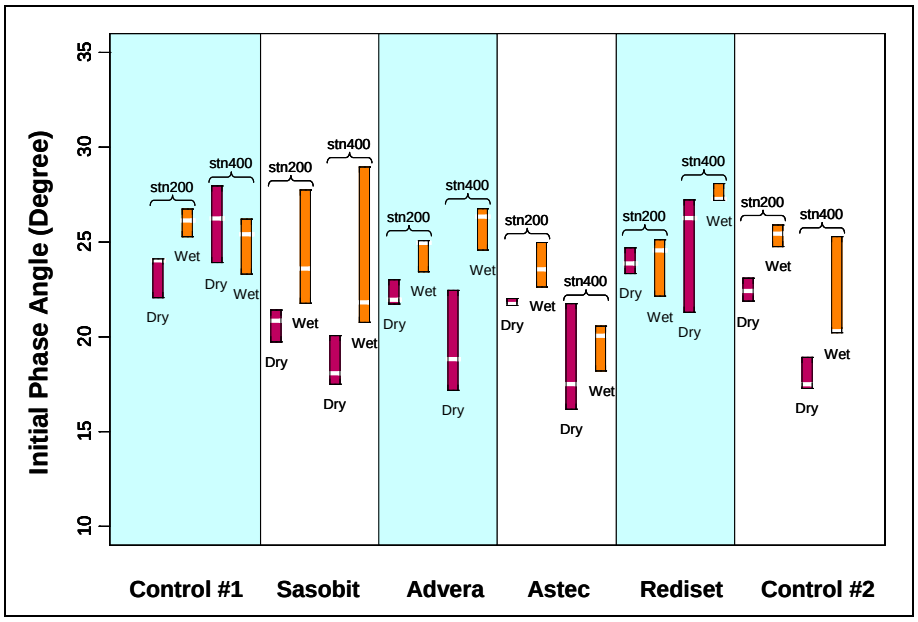

Figure 6.12: Summary boxplots of initial phase angle.

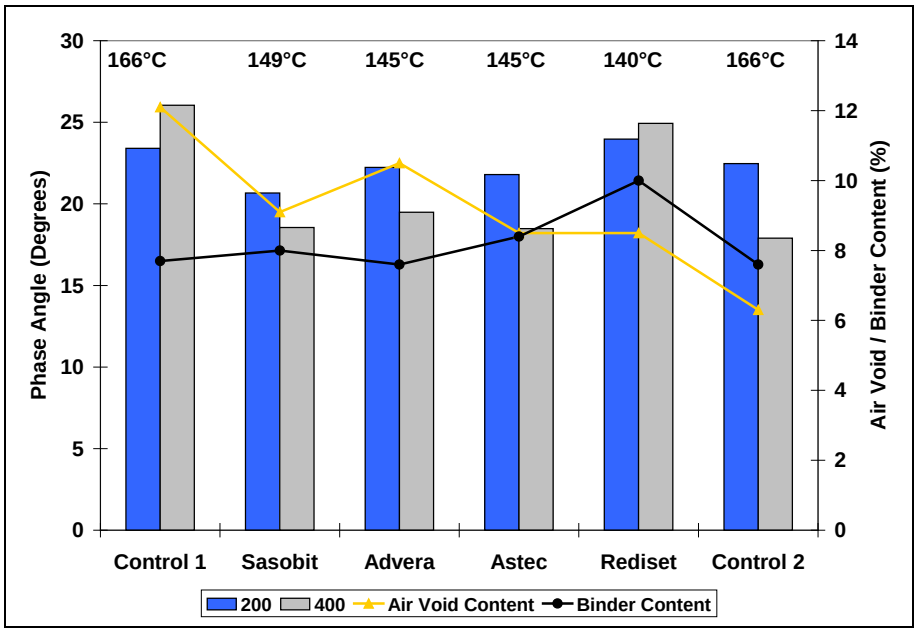

Figure 6.13: Plot of average initial phase angle for dry test.
(Average mix production temperature, binder content, and air-void content shown.)

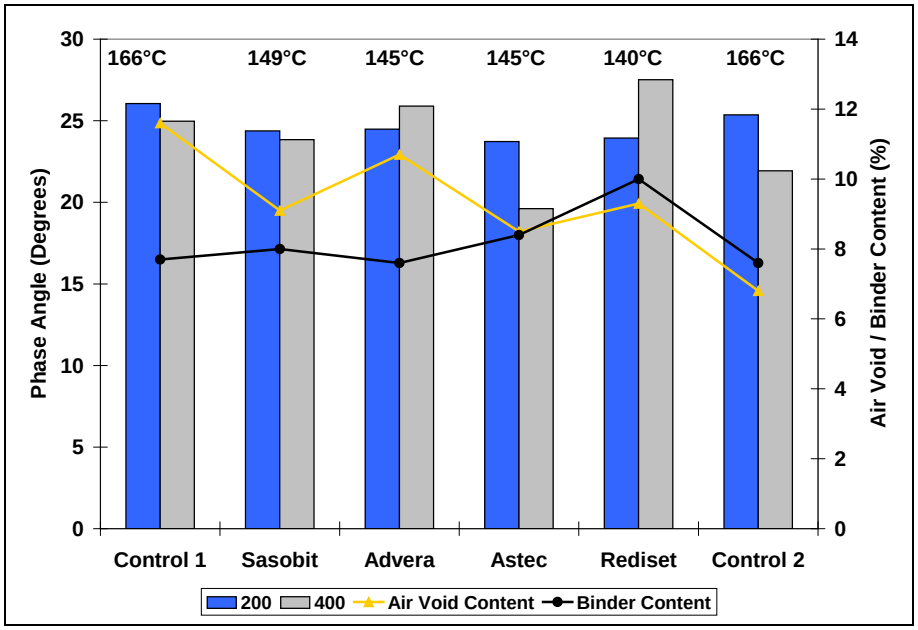

Figure 6.14: Plot of average initial phase angle for soaked test.
(Average mix production temperature, binder content, and air-void content shown.)

- Statistical analyses (t-test and Kolmogorov-Smirnov test) indicated that there was no statistically significant difference (confidence level of 0.1) in performance between the two Controls and the four warm-mixes after variation in mix production temperature, binder content, specimen air-void content, actual test strain level, and actual test temperature were taken into consideration. This indicates that the use of the warm-mix technologies and lower production and compaction temperatures did not significantly influence the performance of the mixes in this test.

Fatigue Life at 50 Percent Stiffness Reduction

Mix stiffness decreases with increasing test-load repetitions. Conventional fatigue life is defined as the number of load repetitions when 50 percent stiffness reduction has been reached. A high fatigue life implies a slow fatigue damage rate and consequently higher fatigue-resistance. The side-by-side fatigue life comparison of dry and wet tests is plotted in Figure 6.15. Figure 6.16 and Figure 6.17 show the average results in relation to production temperature, binder content, and average air-void content. The following observations were made:

- Fatigue life was strain-dependent as expected, with lower strains resulting in higher fatigue life.
- In both the dry and wet tests, no specimens failed in the 200 microstrain test.
- In the 400 microstrain test, results varied among the mixes, with air-void content and binder content appearing to have the biggest influence on performance. Soaking generally resulted in a lower fatigue life compared to that measured on the unsoaked specimens.
- Statistical analyses (t-test and Kolmogorov-Smirnov test) indicated that there was no statistically significant difference (confidence level of 0.1) in terms of fatigue life at 50 percent stiffness reduction performance between the Controls and the four warm-mixes after variation in mix production temperature, binder content, specimen air-void content, actual test strain level, and

actual test temperature were taken into consideration. This indicates that the use of the warm-mix technologies and lower production and compaction temperatures did not significantly influence the performance of the mixes in this test.

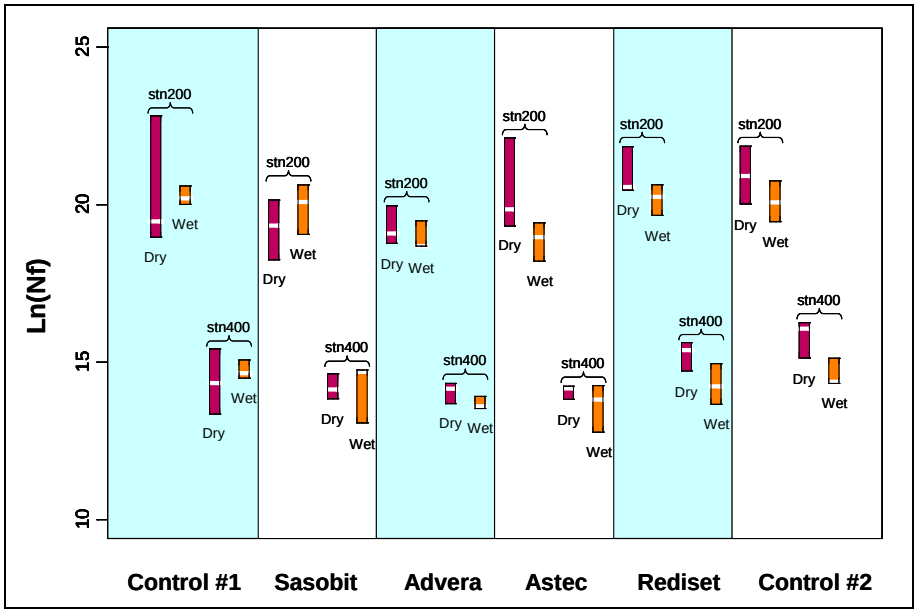

Figure 6.15: Summary boxplots of fatigue life.

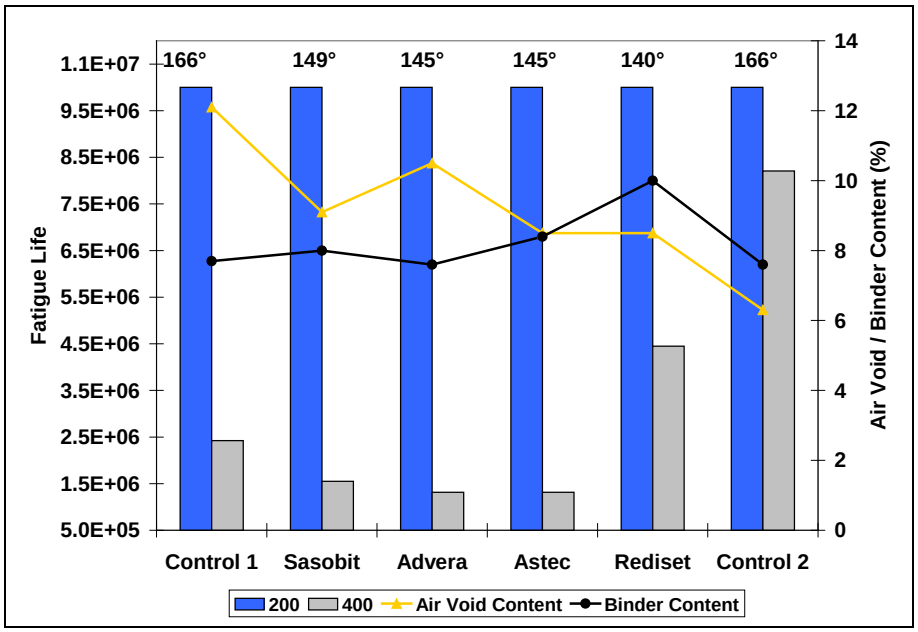

Figure 6.16: Plot of average fatigue life for dry test.
(Average mix production temperature, binder content, and air-void content shown.)

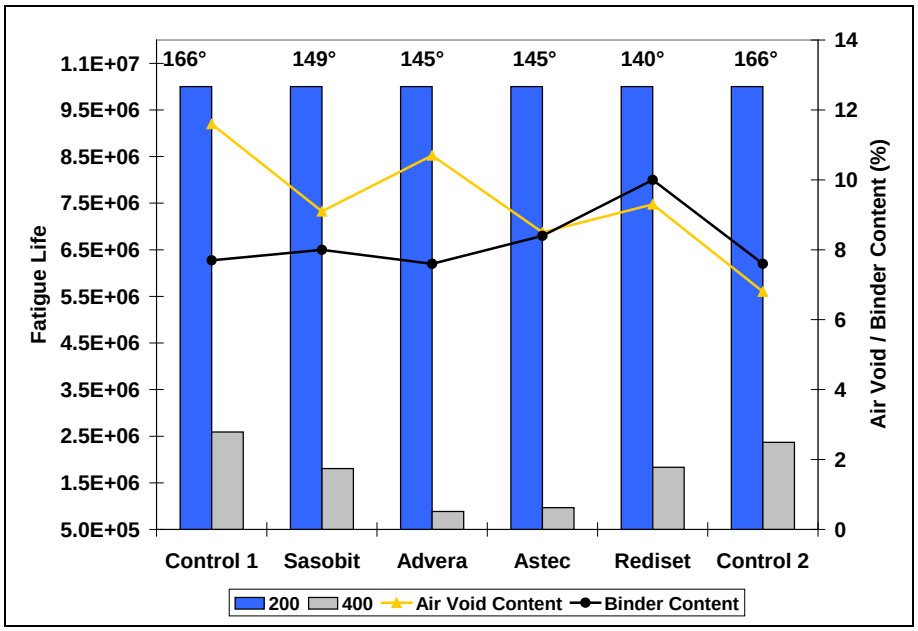

Figure 6.17: Plot of average fatigue life for wet test.
(Average mix production temperature, binder content, and air-void content shown)

Flexural Frequency Sweep

The average stiffness values of the two replicates tested at the three temperatures were used to develop the flexural complex modulus (E^*) master curve. This is considered a useful tool for characterizing the effects of loading frequency (or vehicle speed) and temperature on the initial stiffness of an asphalt mix (i.e., before any fatigue damage has occurred). The shifted master curve with minimized residual-sum-of-squares derived using a generic algorithm approach can be appropriately fitted with the following modified Gamma function (Equation 6.1):

$$E^* = D + A \cdot \left(1 - \exp\left(-\frac{(x-C)}{B}\right) \cdot \sum_{m}^{n-1} \frac{(x-C)^m}{B^m m!}\right) \quad \textbf{(6.1)}$$

where: E^* = flexural complex modulus (MPa);
$x = \ln freq + \ln aT$ = is the loading frequency in Hz and $\ln aT$ can be obtained from the temperature-shifting relationship (Equation 6.2);
A, *B*, *C*, *D*, and *n* are the experimentally determined parameters.

$$\ln aT = A \cdot \left(1 - \exp\left(-\frac{T - Tref}{B}\right)\right) \quad \textbf{(6.2)}$$

where: $lnaT$ = is a horizontal shift to correct the temperature effect with the same unit as ln *freq*,
T = is the temperature in °C,
$Tref$ = is the reference temperature, in this case, $Tref$ = 20°C
A and *B* are the experimentally determined parameters.

The experimentally determined parameters of the modified Gamma function for each mix type are listed in Table 6.4, together with the parameters in the temperature-shifting relationship.

Table 6.4: Summary of Master Curves and Time-Temperature Relationships

Mix	Conditioning	Master Curve					Time-Temperature Relationship	
		Number	A	B	C	D	A	B
Control #1	Dry	3	65185.38	16.68907	-10.33457	166.0683	-12.8706	42.2242
Sasobit		3	41636.90	11.67888	-10.41706	233.9687	-23.9813	72.6576
Advera		3	40030.55	13.01153	-10.60661	195.6566	-24.2057	62.2001
Astec		3	38307.72	10.79889	-9.57990	270.4176	-17.6635	49.1620
Rediset		3	76405.67	18.79974	-10.93444	137.4891	-38.4196	104.5640
Control #2		3	90900.69	18.14866	-10.46183	195.7631	-10.2721	26.6838
Control #1	Wet	3	26959.08	10.66411	-8.921682	233.7634	-7.0014	28.1143
Sasobit		3	27923.74	9.82421	-9.452820	281.4075	-21.5381	67.9045
Advera		3	42750.11	13.69030	-9.358028	148.9378	-22.3126	60.3803
Astec		3	21390.42	7.97569	-8.707633	244.0572	-245.7500	812.8880
Rediset		3	22047.36	9.32112	-8.973161	163.5170	6.3879	-20.6931
Control #2		3	42809.53	11.92817	-9.478977	203.9396	52.9295	-145.2040

Notes:

1. The reference temperature is 20°C.
2. The wet test specimens were soaked at 60°C.
3. Master curve Gamma-fitted equations:

   If $n = 3$, $E^* = D + A\left(1 - \exp\left(-\frac{(x-C)}{B}\right)\cdot\left(1 + \frac{x-C}{B} + \frac{(x-C)^2}{2B^2}\right)\right)$,

   where $x = \ln freq + \ln aT$

4. Time-temperature relationship:

   $\ln aT = A\left(1 - \exp\left(-\frac{T - Tref}{B}\right)\right)$

Figure 6.18 and Figure 6.19 show the shifted master curves with Gamma-fitted lines and the temperature-shifting relationships, respectively, for the dry frequency sweep tests. The temperature-shifting relationships were obtained during the construction of the complex modulus master curve and can be used to correct the temperature effect on initial stiffness. Note that a positive temperature shift (lnaT) value needs to be applied when the temperature is lower than the reference temperature, while a negative temperature-shift value needs to be used when the temperature is higher than the reference temperature.

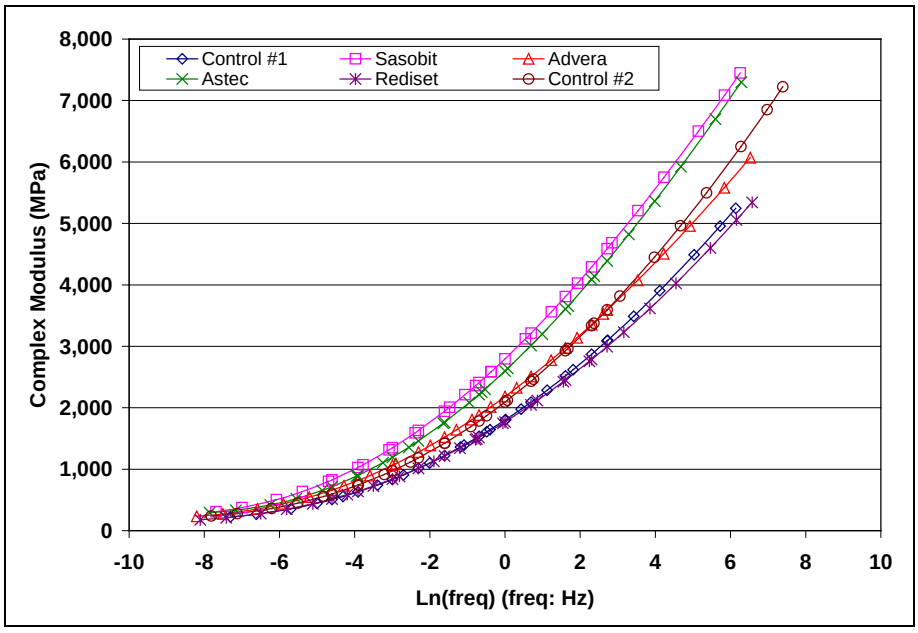

Figure 6.18: Complex modulus (*E) master curves (dry) at 20°C reference temperature.**

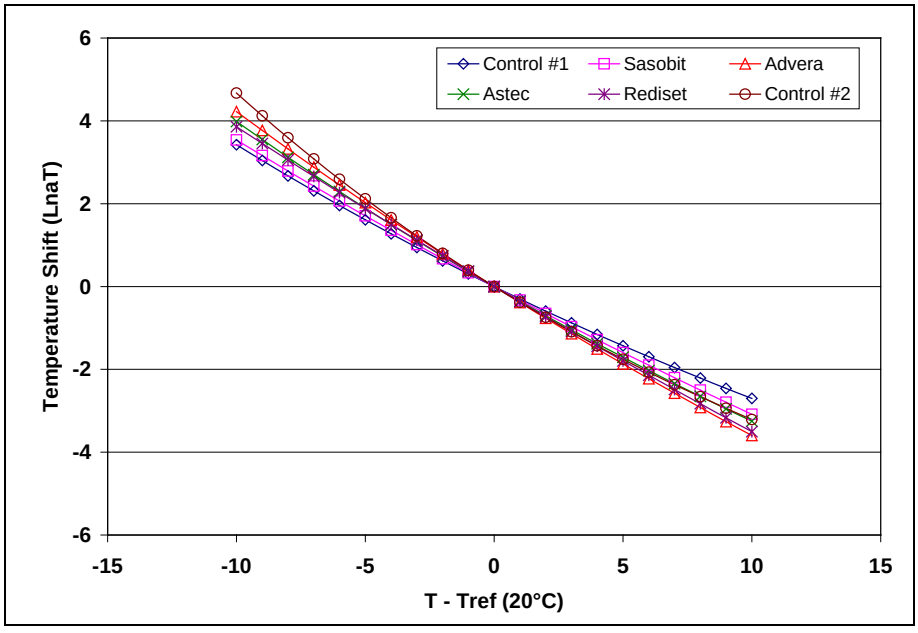

Figure 6.19: Temperature-shifting relationship (dry) at 20°C reference temperature.

The following observations were made from the dry frequency sweep test results:

- The complex modulus master curves appeared to be influenced primarily by specimen air-void content and binder content.
- The temperature-shifting relationships indicate that there was very little difference in temperature sensitivity between the six mixes. Higher temperature-sensitivity implies that a per unit change of temperature will cause a larger change of stiffness (i.e., larger change of lnaT).

Figure 6.20 and Figure 6.21 respectively show the shifted master curves with Gamma-fitted lines and the temperature-shifting relationships for the wet frequency sweep tests. The comparison of dry and wet complex modulus master curves is shown in Figure 6.22 and Figure 6.23 for each mix type. The following observations were made with regard to the wet frequency sweep test results:

- The complex modulus master curves appeared to be influenced primarily by specimen air-void content and binder content and showed similar trends to the dry tests.
- There was a small difference in temperature-sensitivity among the six mixes at lower temperatures (i.e., lower than 20°C). At higher temperatures (i.e., higher than 20°C), the Day #1 Control appeared to be less temperature sensitive than the other mixes.
- Some loss of stiffness attributed to moisture damage was apparent in all six mixes, with air-void content having the biggest influence.

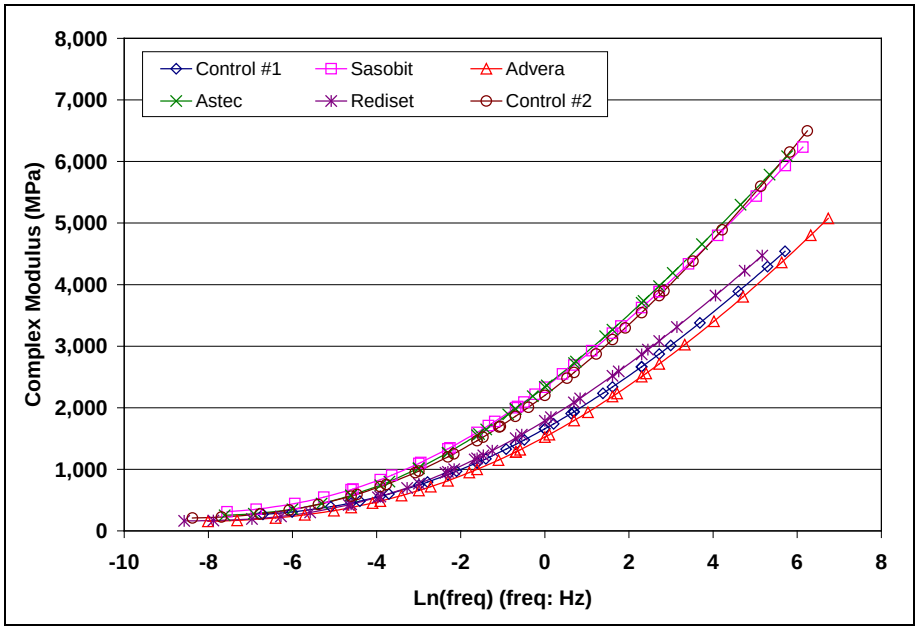

Figure 6.20: Complex modulus (*E) master curves (wet) at 20°C reference temperature.**

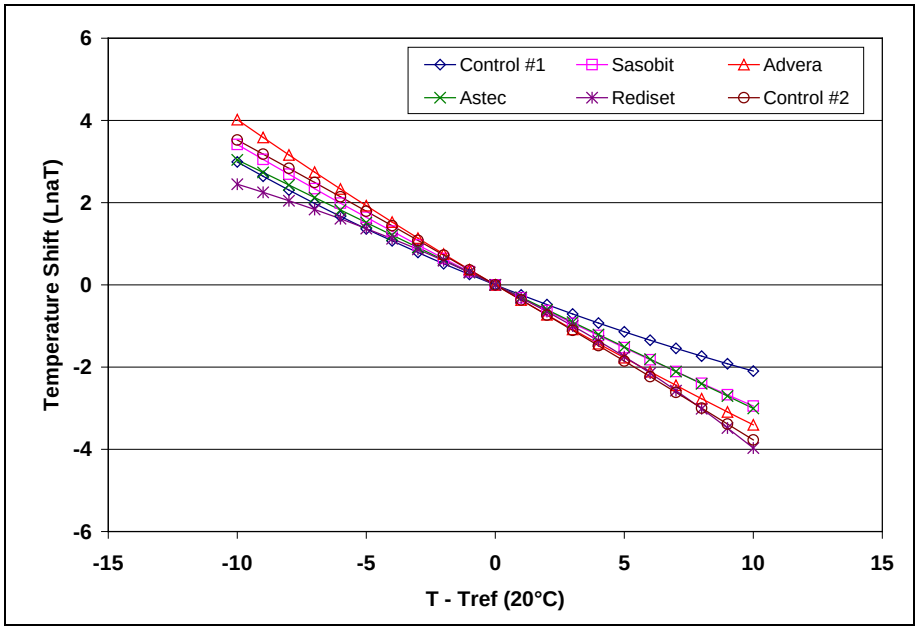

Figure 6.21: Temperature-shifting relationship (wet) at 20°C reference temperature.

6.2.3 Moisture Sensitivity: Hamburg Wheel-Track Test

Air-Void Content

The air-void content of each core was determined using the CoreLok method. Results are summarized in Table 6.5. The air-void contents ranged between 11.1 and 14.0 percent and showed similar trends to those observed for the specimens used in the other tests.

Table 6.5: Summary of Air-Void Contents of Hamburg Test Specimens

Day #1 Air-Void Content (%)					
Control #1		Sasobit		Advera	
Mean[1]	SD[2]	Mean	SD	Mean	SD
13.7	1.7	11.2	1.0	11.5	0.6
Day #2 Air-Void Content (%)					
Control #2		Astec		Rediset	
13.5	0.7	14.0	0.4	11.1	0.7

[1] Mean of four replicates [2] SD: Standard deviation

Testing

The testing sequence of the specimens was randomized to avoid any potential block effect. Rut depth was recorded at 11 equally spaced points along the wheelpath on each specimen. The average of the middle seven points was then used in the analysis. This method ensures that localized distresses are smoothed and variance in the data is minimized. It should be noted that some state departments of transportation only measure the point of maximum final rut depth, which usually results in a larger variance in the test results. Average maximum rut depths after 10,000 and 20,000 passes and the creep and stripping slopes are summarized in Table 6.6. There was no apparent stripping inflection point.

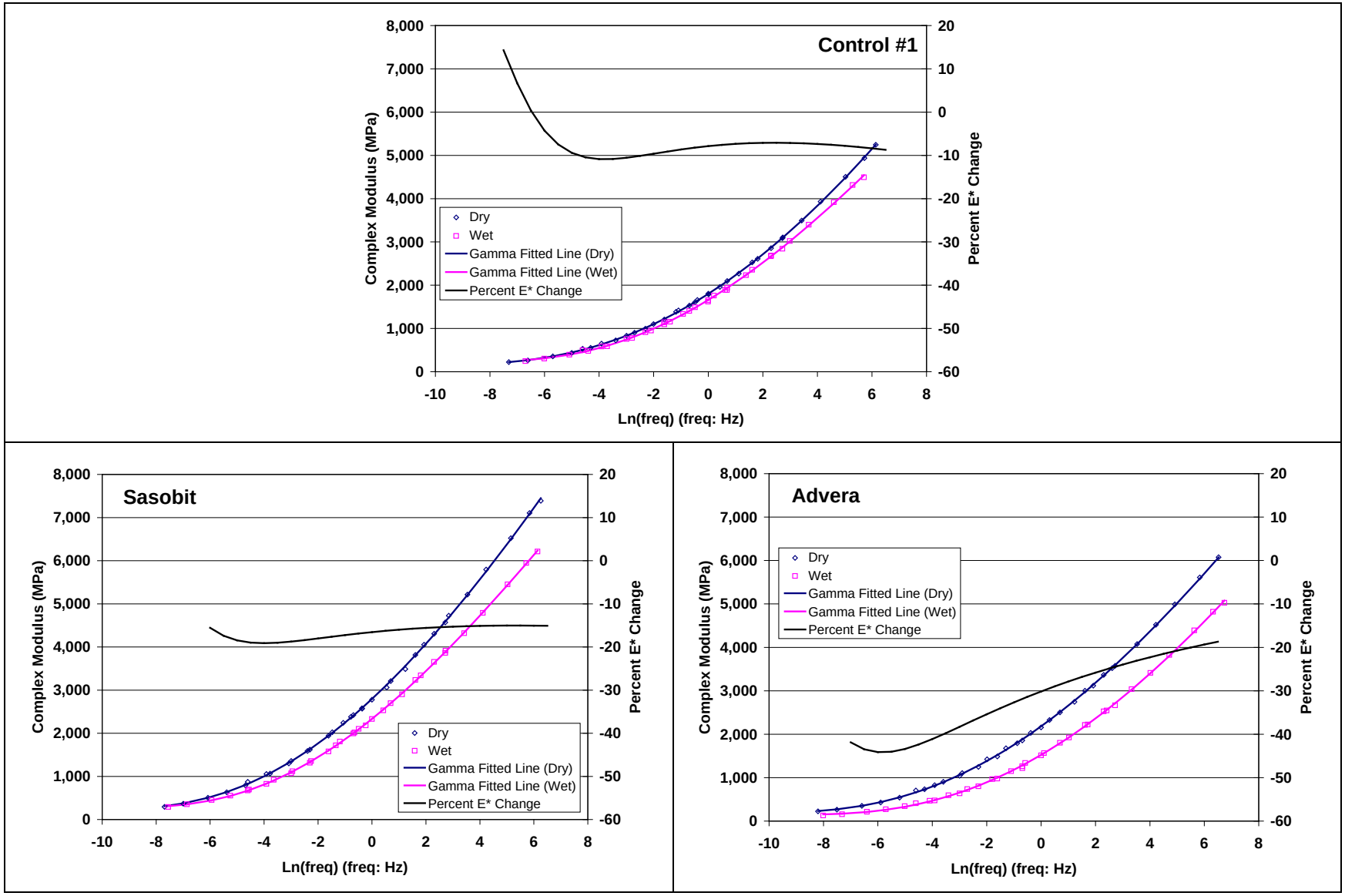

Figure 6.22: Comparison of dry and wet complex modulus master curves (Day #1).

(Includes percent reduction in stiffness at each frequency from dry to wet master curve.)

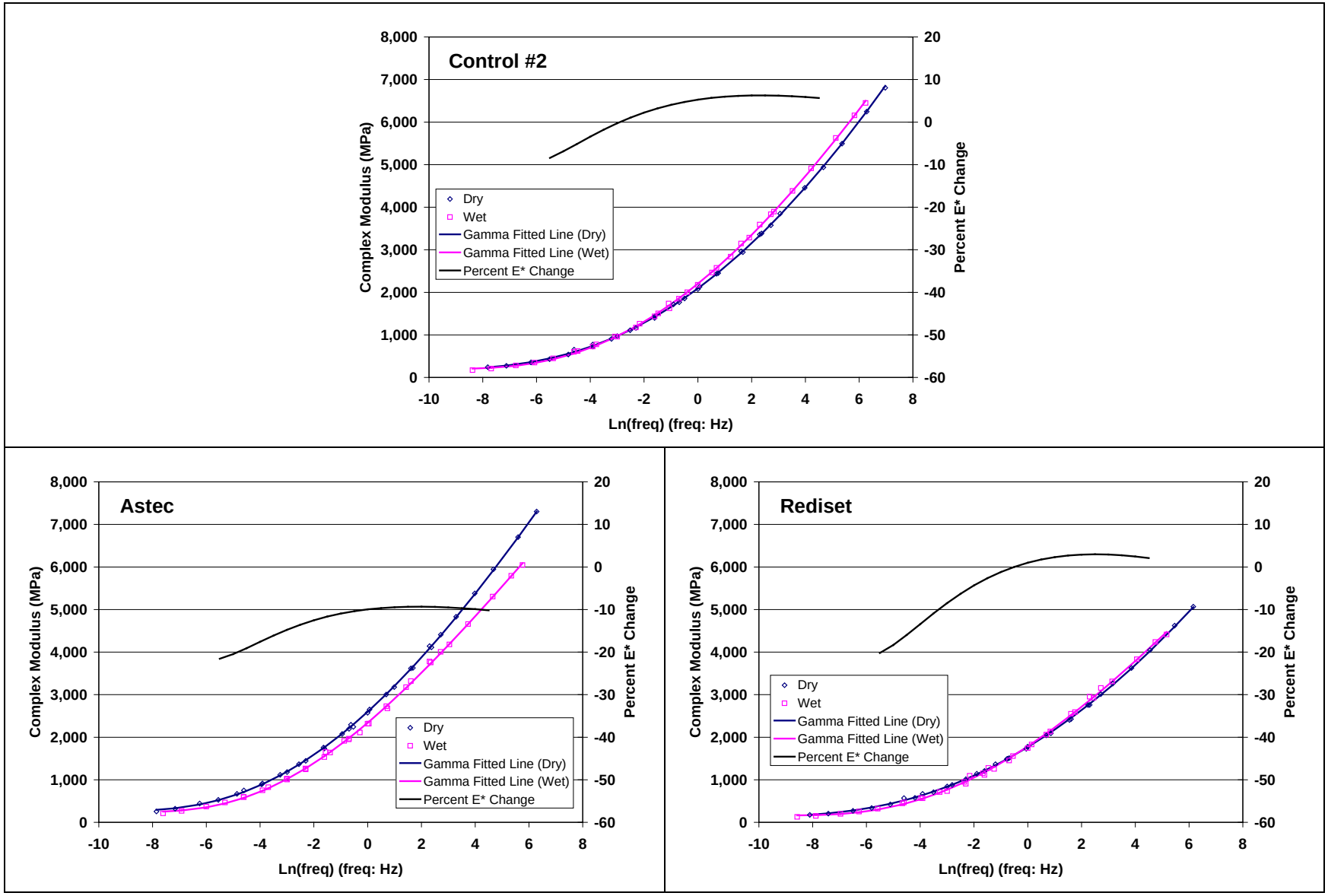

Figure 6.23: Comparison of dry and wet complex modulus master curves (Day #2).

(Includes percent reduction in stiffness at each frequency from dry to wet master curve.)

Table 6.6: Summary of Results of Hamburg Wheel-Track Tests

Test Set	Rut Depth (mm) for Day #1 Mixes					
	Control #1		Sasobit		Advera	
	Mean	SD	Mean	SD	Mean	SD
	10,000 passes					
1	5.7	0.9	4.5	0.7	5.2	0.0
2	6.4	0.6	4.4	0.5	5.3	0.3
Overall	6.0	0.7	4.4	0.5	5.2	0.2
	20,000 passes					
1	7.4	0.4	5.3	0.7	7.4	0.2
2	7.9	0.9	5.7	0.4	6.5	0.4
Overall	7.6	0.6	5.5	0.5	6.9	0.6
	Creep Slope (mm/pass)					
1	-0.0003		-0.0003		-0.0003	
2	-0.0003		-0.0003		-0.0003	
Overall	-0.0003		-0.0003		-0.0003	
	Stripping Slope (mm/pass)					
1	-0.0003		-0.0003		-0.0003	
2	-0.0003		-0.0003		-0.0003	
Overall	-0.0003		-0.0003		-0.0003	
Test Set	**Rut Depth (mm) for Day #2 Mixes**					
	Control #2		Astec		Rediset	
	Mean	SD	Mean	SD	Mean	SD
	10,000 passes					
1	6.5	0.7	6.6	0.1	2.2	0.3
2	6.6	0.7	7.7	1.6	5.7	0.1
Overall	6.6	0.6	7.1	1.1	4.0	2.0
	20,000 passes					
1	8.6	1.4	9.1	0.8	3.7	0.7
2	8.5	0.8	10.4	2.6	7.1	0.2
Overall	8.5	0.9	9.7	1.8	5.4	2.0
	Creep Slope (mm/pass)					
1	-0.0003		-0.0003		-0.0003	
2	-0.0003		-0.0003		-0.0003	
Overall	-0.0003		-0.0003		-0.0003	
	Stripping Slope (mm/pass)					
1	-0.0003		-0.0003		-0.0003	
2	-0.0003		-0.0003		-0.0003	
Overall	-0.0003		-0.0003		-0.0003	

[1] Mean of four replicates [2] SD: Standard deviation

Figure 6.24 shows the average rut progression curves of all tests, and Figure 6.25 and Figure 6.26 show the average rut progression curves and average maximum rut for each mix, respectively. No clear stripping inflection points were noted in any tests (even when the tests were continued to 50,000 repetitions [Figure 6.26]), indicating that no stripping occurred in any of the mixes.

The mixes all show similar trends. The Sasobit and Rediset mixes had the smallest rut depths and performed better than the Control mixes. The Advera mix performed similarly to the Control mix. Rut depths on the Astec mix were marginally higher than those on the Control mixes.

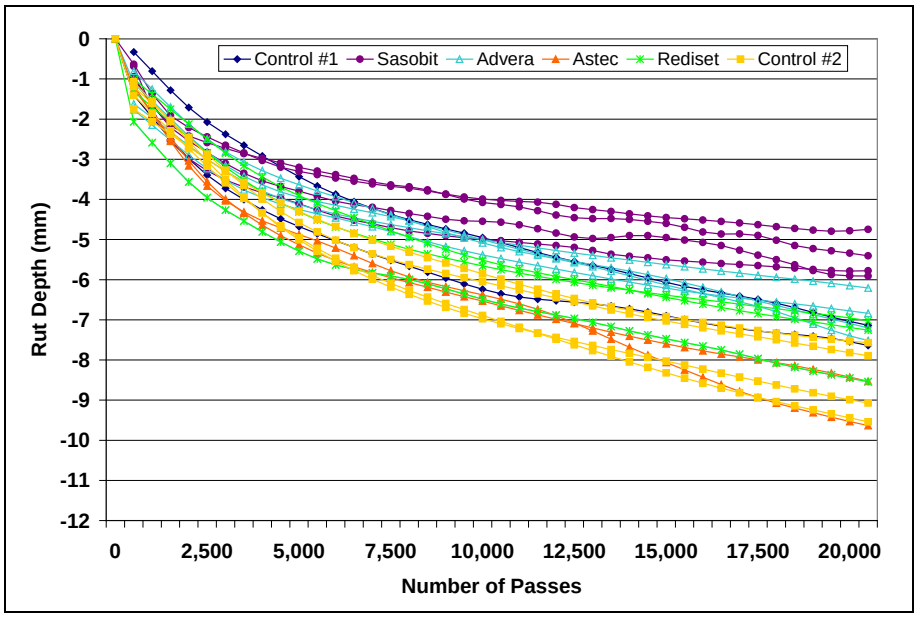

Figure 6.24: Hamburg Wheel-Track rut progression curves for all tests.

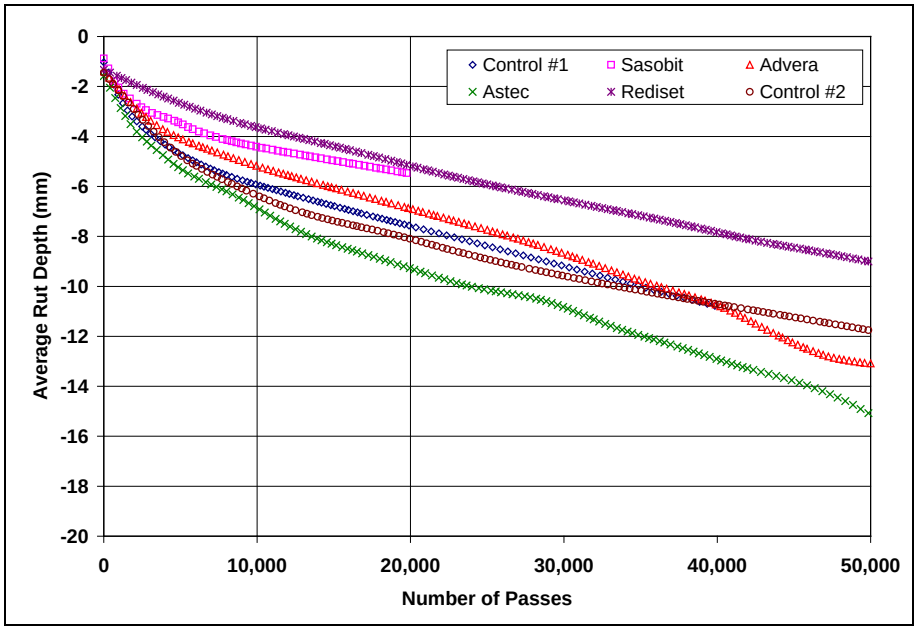

Figure 6.25: Average Hamburg Wheel-Track rut progression curve for each mix.

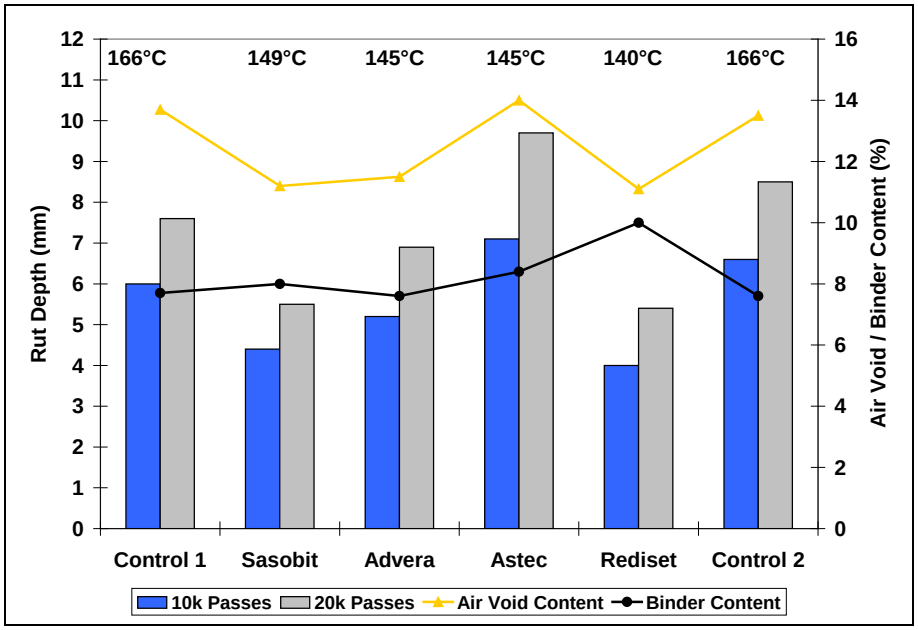

Figure 6.26: Average Hamburg Wheel-Track rut depth for each mix.
(Average mix production temperature, binder content, and air-void content shown.)

6.2.4 Moisture Sensitivity: Tensile Strength Retained (TSR)

Air-Void Content

The air-void content of each core was determined using the CoreLok method. The air-void contents ranged between 6.7 and 11.1 percent and were consistent with those measured for the other tests (Table 6.7). It should be noted that laboratory TSR tests that are carried out as part of a mix design require a specimen air-void content of seven percent. Most specimens had air-void contents above this value.

Table 6.7: Summary of Air-Void Contents of Tensile Strength Retained Test Specimens

Condition	Day #1 Air-Void Content (%)					
	Control #1		Sasobit		Advera	
	Mean[1]	SD[2]	Mean	SD	Mean	SD
Dry test	9.7	0.9	7.8	0.6	11.0	0.4
Wet test	10.0	0.6	7.7	0.9	11.1	0.6
Condition	**Day #2 Air-Void Content (%)**					
	Control #2		Astec		Rediset	
	Mean	SD	Mean	SD	Mean	SD
Dry test	7.2	0.4	9.1	0.7	7.1	0.4
Wet test	6.9	0.5	8.4	0.5	6.7	0.4

[1] Mean of six replicates [2] SD: Standard deviation

Testing

Results of Tensile Strength Retained (TSR) tests are listed in Table C.7 in Appendix C and summarized for each mix in Table 6.8. A plot of the average results is shown in Figure 6.27. The results indicate that:

- On the Day #1 mixes, the Sasobit mix performed better than the Control and Advera in terms of both dry and wet strengths.

Table 6.8: Summary of Tensile Strength Retained Test Results

Parameter	Indirect Tensile Strength (kPa) for Day #1 Mixes					
	Control #1		Sasobit		Advera	
	Mean[1]	SD[2]	Mean	SD	Mean	SD
Dry	720	78	878	22	636	23
Wet	522	65	696	33	429	26
TSR	73		79		67	
Damage	-	Yes	-	Yes	-	Yes
Parameter	**Indirect Tensile Strength (kPa) for Day #2 Mixes**					
	Control #2		Astec		Rediset	
	Mean	SD	Mean	SD	Mean	SD
Dry	689	52	802	60	766	35
Wet	606	55	519	46	594	11
TSR	88		65		78	
Damage	-	Yes	-	Yes	-	Yes

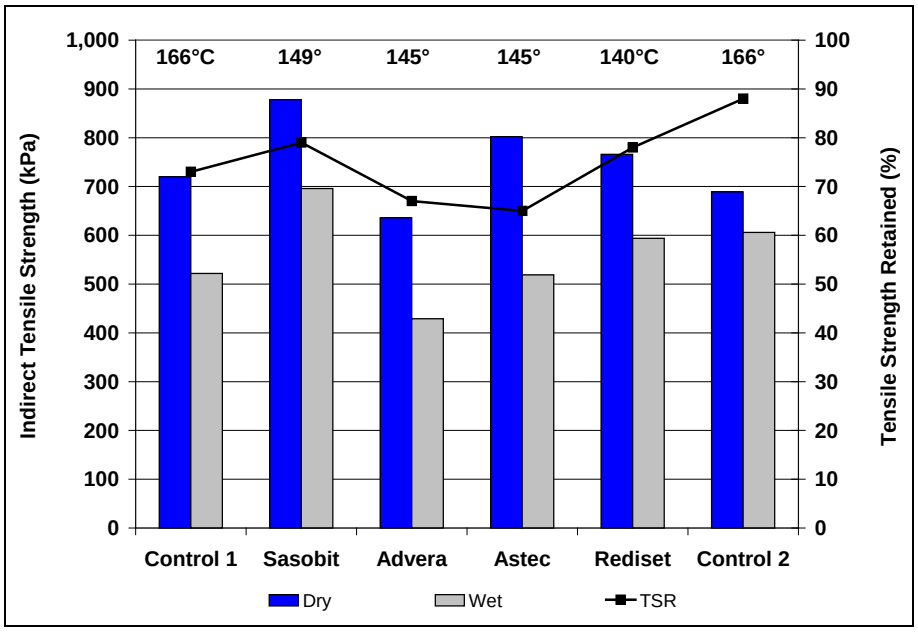

Figure 6.27: Average tensile strength retained for each mix.

- On the Day #2 mixes, the Astec and Rediset mixes had higher dry strengths than the Control, but in terms of wet strength, the Astec mix was lower than the Control and Rediset mixes, which had similar strengths.
- The recorded TSR values varied considerably between the mixes and appeared to be influenced by air-void content.
- The Astec and Advera mixes, both of which had high air-void contents, did not meet the minimum tentative criteria of 70 percent for low environmental risk or the minimum 75 percent for medium and high environmental risk regions in the Caltrans Testing and Treatment Matrix to ensure moisture resistance. The Day #1 Control did not meet the 75 percent requirement. The Day #2 Control, Sasobit, and Rediset mixes exceeded both requirements. Treatment would typically be required for mixes that do not meet these minimum requirements at seven percent air-void content in order to reduce the risk of moisture damage in the pavement in these regions.

The results generally did not show similar trends to the Hamburg Wheel-Track test results; however, the warm-mixes had the same ranking in terms of performance (i.e., Rediset followed by Sasobit, Advera, and then Astec).

Observation of the split faces of the cores revealed very little internal stripping (loss of adhesion between asphalt and aggregate evidenced by clean aggregate on the broken face) after moisture conditioning.

6.3 Summary of Laboratory Testing Results

The laboratory test results indicate that use of the warm-mix technologies assessed in this study, which were produced and compacted at lower temperatures, did not significantly influence the performance of the asphalt concrete when compared to control mixes produced and compacted at conventional hot-mix asphalt temperatures. Specific observations include:

- Laboratory performance in all tests appeared to be mostly dependent on air-void content and binder content, as expected, and less dependent on mix production temperature.
- The water-based warm-mix technology mixes (Advera and Astec) appeared to have lower moisture resistance compared to the other three mixes in all the moisture sensitivity tests.
- Test results were influenced by mix production temperatures, actual binder content, specimen air-void content, actual stress and strain levels, and actual test temperature. Variation in these parameters needs to be taken into consideration when comparing performance between the different mixes.

7. CONCLUSIONS AND RECOMMENDATIONS

7.1 Conclusions

This first-level report describes part of the third phase of a warm-mix asphalt study comparing the performance of two gap-graded rubberized asphalt control mixes, produced and constructed at conventional hot-mix asphalt temperatures (335°F [166°C]), with four warm-mixes produced at between 35°F (17°C) and 50°F (26°C) lower than the controls. The technologies tested included an organic wax-based additive (*Sasobit*®, produced at 300°F [149°C]), a chemical foaming agent (*Advera WMA*®, produced at 295°F [145°C), water injection (*Astec Double Barrel Green*®, produced at 295°F [145°C]), and a chemical surfactant (*Rediset*™, produced at 285°F [140°F]). The test track layout and design, mix design and production, and test track construction are discussed, as well as results of Heavy Vehicle Simulator (HVS) and laboratory testing.

Key findings from the study include the following:

- A consistent subgrade was prepared and consistent base-course and underlying dense-graded hot-mix asphalt concrete layers were constructed on the test track using materials sourced from a nearby quarry and asphalt plant. Thickness and compaction of the base and bottom layer of asphalt were consistent across the test track.
- Asphalt plant modifications were required to accommodate the three powder/pellet based warm-mix technologies. The delivery systems were approved under the Caltrans Material Plant Quality Program. The water injection equipment was integral to the asphalt plant.
- A number of problems related to blocked nozzles occurred during the production of the water-injection–technology mix (Astec); these problems resulted in a seven-day delay in construction of the Astec and the Rediset mix sections so equipment could be replaced and additional binder sourced. This also resulted in the need to construct a second Control section. Target mix production temperatures (335°F, 300°F, 295°F, 295°F, and 280°F [166°C, 149°C, 145°C, 145°C, and 140°C] for the Control, Sasobit, Advera, Astec, and Rediset mixes respectively), set by the warm-mix technology providers, were all achieved. There was some variation in binder content among the six mixes, with the Rediset mix having a significantly higher binder content compared to the other mixes and to the design.
- Compaction temperatures varied between 279°F (137°C) and 259°F (126°C) for the Control and Rediset mixes, respectively, and were consistent with production temperatures. As expected, the mixes produced at lower temperatures lost heat during transport and placement at a slower rate than the mixes produced at the higher temperatures. Compaction was generally poor on all sections, especially on the Day #1 Control and Advera sections.
- Smoke and odors were significantly more severe on the Control section compared to the warm-mix sections.
- Workability of the mix, determined through observation of and interviews with the paving crew, was considerably better on the warm-mix sections compared to the Control.

- Average thicknesses of the top (rubberized) and bottom asphalt layers across the four sections were 0.22 ft. (66 mm) and 0.24 ft. (74 mm), respectively. The average thickness of the combined two layers was 0.45 ft. (137 mm), 0.5 ft. (17 mm) thicker than the design thickness of 0.4 ft. (120 mm). General consistency of thickness across the track was considered satisfactory and representative of typical construction projects.
- Nuclear gauge–determined density measurements were inconsistent with core-determined air-void contents. The core-determined air-void contents indicated that slightly higher density was achieved on the warm-mix sections compared to the Control sections (88 percent of the RICE specific gravity) compared to the warm-mix sections (92, 89, 91, and 92 percent for the Sasobit, Advera, Astec, and Rediset sections, respectively). Compaction across the test track appeared to be consistent and demonstrated that adequate compaction can be achieved on rubberized warm-mixes at lower temperatures. Based on observations from the test track construction and interviews with roller operators, optimal compaction temperatures will differ among the different warm-mix technologies. Roller operators will also need to consider that there might be differences in roller response between warm-mix and conventional hot-mixes, and that rolling operations and patterns may need to be adjusted to ensure that optimal compaction is always achieved.
- HVS trafficking on four of the five sections indicated generally consistent performance among the mixes. Unexpected poor performance was measured on the Advera section (Section 626HA) and additional tests on this section as well as on the Control and Sasobit sections were undertaken to determine the cause and to eliminate possible seasonal and machine-related testing variables. The cause of this poor performance was attributed to a combination of high subgrade moisture content and thinner combined asphalt layers, identified during the forensic investigation. The duration of the tests to terminal rut (12.5 mm [0.5 in.]) on the five sections varied from 73,500 load repetitions (Section 629HB, Advera Test #2) to 365,000 load repetitions (Section 625HA, Sasobit Test #1).
- The duration of the embedment phases on all sections except the Advera section were similar. Apart from the Advera section, the depth of the ruts at the end of the embedment phases differed only slightly among sections, with the Astec (7.5 mm [0.3 in.]) having a slightly deeper embedment than the Control, Sasobit, and Rediset sections, which had similar embedment (6.5 to 6.7 mm [0.26 in.]). This is opposite to the early rutting performance in the Phase 1 study and is being investigated in a separate study.
- Rut rate (increase in rut depth per load repetition) after the embedment phase on the Control and Sasobit sections was almost identical. On the Astec and Rediset sections, the rut rate was slightly higher and was attributed to some moisture in the asphalt layer and in the subgrade in the Astec section (determined during the forensic investigation), and to the higher binder content on the Rediset section. Although lower production and paving temperatures typically result in less oxidation of the binder, which can influence early rutting performance, differences in production and placement temperatures did not appear to influence performance in this set of tests.
- The laboratory test results indicate that use of the warm-mix technologies assessed in this study, which were produced and compacted at lower temperatures, did not significantly influence the performance of the asphalt concrete when compared to control specimens produced and compacted at conventional hot-mix asphalt temperatures. Specific observations include:
  + Laboratory performance in all tests appeared to be mostly dependent on air-void content and binder content, as expected, and less dependent on mix production temperature.

+ The water-based warm-mix technology mixes (Advera and Astec) appeared to have lower moisture resistance compared to the other three mixes in all the moisture sensitivity tests.
+ Test results were influenced by mix production temperatures, actual binder content, specimen air-void content, actual stress and strain levels, and actual test temperature. Variation in these parameters needs to be taken into consideration when comparing performance between the different mixes.

The findings of the study are also summarized below in the form of answers to the questions identified in Section 1.3.

7.1.1 Comparative Energy Usage

Comparative energy usage could not be assessed in this study due to the very small quantities produced. These studies will need to be carried out during larger full-scale pilot studies on in-service pavements when large quantities of mix are produced (i.e., more than 5,000 tonnes).

7.1.2 Achieving Compaction Density at Lower Temperatures

Compaction measurements during construction indicated that average air-void contents on the warm-mix sections were marginally higher than on the Control sections, but were typical of full-scale construction projects. Based on these observations it is concluded that adequate compaction can be achieved on warm-mixes at lower temperatures. Optimal compaction temperatures will differ among the different warm-mix technologies. Roller operators will need to consider that there might be differences in roller response between warm-mix and conventional hot mixes, and that rolling operations and patterns may need to be adjusted to ensure that optimal compaction is always achieved. Contractors will need to determine mix production temperatures based on required compaction temperatures, and take loss of temperature during silo storage and transportation into consideration.

7.1.3 Optimal Temperature Ranges for Warm-Mixes

Optimal compaction temperatures will differ between the different warm-mix technologies. This study has shown that temperatures of at least 35°C (60°F) lower than conventional temperatures are appropriate for producing and compacting the modified mixes.

7.1.4 Cost Implications

The cost benefits of using the warm-mix technologies could not be assessed in this study due to the very small quantities produced.

7.1.5 Rutting Performance

Based on the results of HVS testing, it is concluded that the use of any of the three warm-mix asphalt technologies used in this experiment will not significantly influence the rutting performance of the mix, provided that standard specified construction limits for hot-mix asphalt are met.

7.1.6 Moisture Sensitivity

Laboratory moisture sensitivity testing indicated that the water-based technologies (Astec and Advera) showed lower moisture resistance compared to the other mixes, and did not meet Caltrans-specified performance requirements. This was attributed in part to the high air-void content of the tested specimens. No moisture sensitivity was noted during accelerated pavement testing.

7.1.7 Fatigue Performance

Laboratory fatigue testing indicated that the warm-mix technologies used in this study will not influence the fatigue performance of a mix.

7.1.8 Other Effects

Smoke and odors were significantly reduced during construction of the warm-mix sections compared to the Control. The workability of the warm-mixes in terms of raking and shoveling was also considerably better than the Control mix.

7.2 Recommendations

The HVS and laboratory testing completed in this phase have provided no results to suggest that warm-mix technologies should not be used in gap-graded rubberized mixes in California, provided that standard specified construction and performance limits for hot-mix asphalt are met. Significant reductions in smoke and odors and improved workability of the warm-mixes also support wider use of these technologies. Consideration should be given to further study into the effects of warm-mix asphalt technologies, and production and placement of warm-mixes at lower temperatures, on binder oxidation/aging rates and the effects that these may have on performance over the life of the asphalt surfacing. Research in this study has shown differences in early rutting performance between conventional and rubber mixes, between mixes tested after different curing periods, and between pavements subjected to mostly shade and mostly sun, respectively.

8. REFERENCES

1. JONES, D. and Harvey, J. 2007. **Warm-Mix Asphalt Study: Workplan for Comparison of Conventional and Warm-Mix Asphalt Performance Using HVS and Laboratory Testing.** Davis and Berkeley, CA: University of California Pavement Research Center. (UCPRC-WP-2007-01).
2. JONES, D., Wu, R., Tsai, B., Lu, Q. and Harvey, J. 2008. **Warm-Mix Asphalt Study: Test Track Construction and First-level Analysis of Phase 1 HVS and Laboratory Testing.** Davis and Berkeley, CA: University of California Pavement Research Center. (UCPRC-RR-2008-11).
3. JONES, D., Wu, R., Tsai, B., Lu, Q. and Harvey, J. 2008. **Warm-Mix Asphalt Study: First-Level Analysis of Phase 2 HVS and Laboratory Testing, and Phase 1 and Phase 2 Forensic Assessments.** Davis and Berkeley, CA: University of California Pavement Research Center. (UCPRC-RR-2009-02).
4. JONES, D. and Tsai, B. 2012. **Warm-Mix Asphalt Study: First-Level Analysis of Phase 2b Laboratory Testing on Laboratory Prepared Specimens.** Davis and Berkeley, CA: University of California Pavement Research Center. (UCPRC-RR-2012-07).
5. JONES, D., Wu, R., Tsai, B. and Harvey, J. 2011. **Warm-Mix Asphalt Study: Test Track Construction and First-Level Analysis of Phase 3a HVS and Laboratory Testing (Rubberized Asphalt, Mix Design #1).** Davis and Berkeley, CA: University of California Pavement Research Center. (UCPRC-RR-2011-02).
6. JONES, D. 2012. **Warm-Mix Asphalt Study: Field Test Performance Evaluation.** Davis and Berkeley, CA: University of California Pavement Research Center. (UCPRC-RR-2012-08).
7. **Standard Specifications.** 2006. Sacramento, CA: State of California Department of Transportation.
8. JONES, D. 2005. **Quality Management System for Site Establishment, Daily Operations, Instrumentation, Data Collection and Data Storage for APT Experiments.** Pretoria, South Africa: CSIR Transportek. (Contract Report CR-2004/67-v2).

APPENDIX A: TEST PIT PROFILES

A.1 Dynamic Cone Penetrometer

Dynamic cone penetrometer (DCP) profiles taken outside and within the wheelpath are shown in Figure A.1 through Figure A.7. Profiles were taken after removal of the asphalt concrete during excavation of the test pits. DCP profile details are as follows:

- Figure A.1: 624HB: Phase 3b Control (Test #1)
- Figure A.2: 625HA: Phase 3b Sasobit (Test #1)
- Figure A.3: 626HA: Phase 3b Advera (Test #1)
- Figure A.4: 627HB: Phase 3b Astec
- Figure A.5: 628HB: Phase 3b Rediset
- Figure A.6: 629HB: Phase 3b Advera (Test #2)
- Figure A.7: 630HB: Phase 3b Advera (Test #3)

DCP tests were not undertaken on Section 631HB (Sasobit #2) and Section 632HA (Control #2).

A.2 Layer Thickness and Rutting

Test pit profiles for each test section are shown in Figure A.8 through Figure A.15. All test pits were excavated between Station 9 and Station 11. All profiles show the test pit face at Station 9. Test pit details are as follows:

- Figure A.8: 624HB: Phase 3b Control (Test #1) after 320,000 repetitions
- Figure A.9: 625HA: Phase 3b Sasobit (Test #1) after 365,000 repetitions
- Figure A.10: 626HA: Phase 3b Advera (Test #1) after 50,000 repetitions
- Figure A.11: 627HB: Phase 3b Astec after 242,000 repetitions
- Figure A.12: 628HB: Phase 3b Rediset after 309,000 repetitions
- Figure A.13: 629HB: Phase 3b Advera (Test #2) after 73,500 repetitions
- Figure A.14: 630HB: Phase 3b Advera (Test #3) after 5,000 repetitions

Test pits were not excavated on Section 631HB (Sasobit #2) and Section 632HA (Control #2).

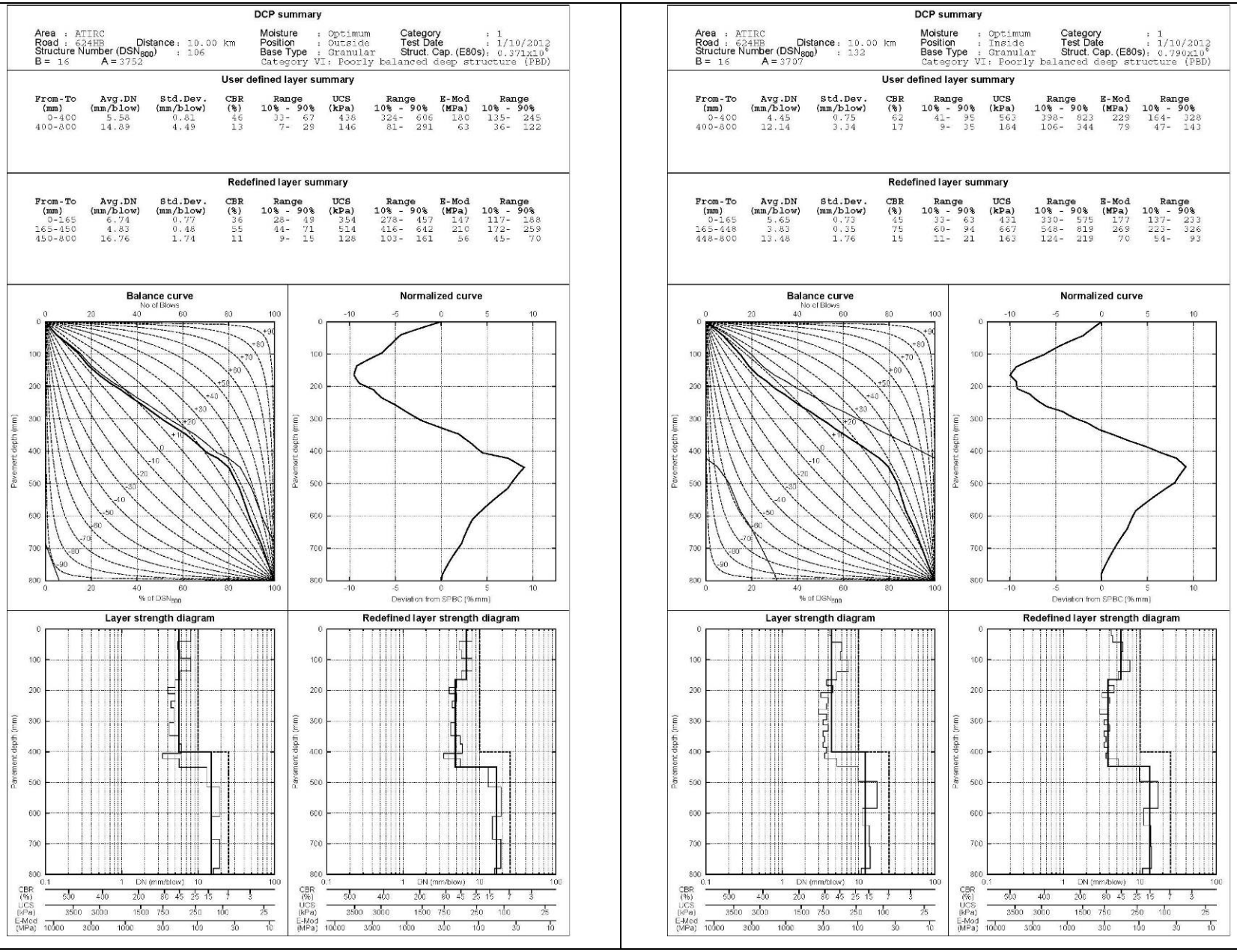

Figure A.1: 624HB: Control DCP profile (untrafficked [left] and wheelpath [right]).

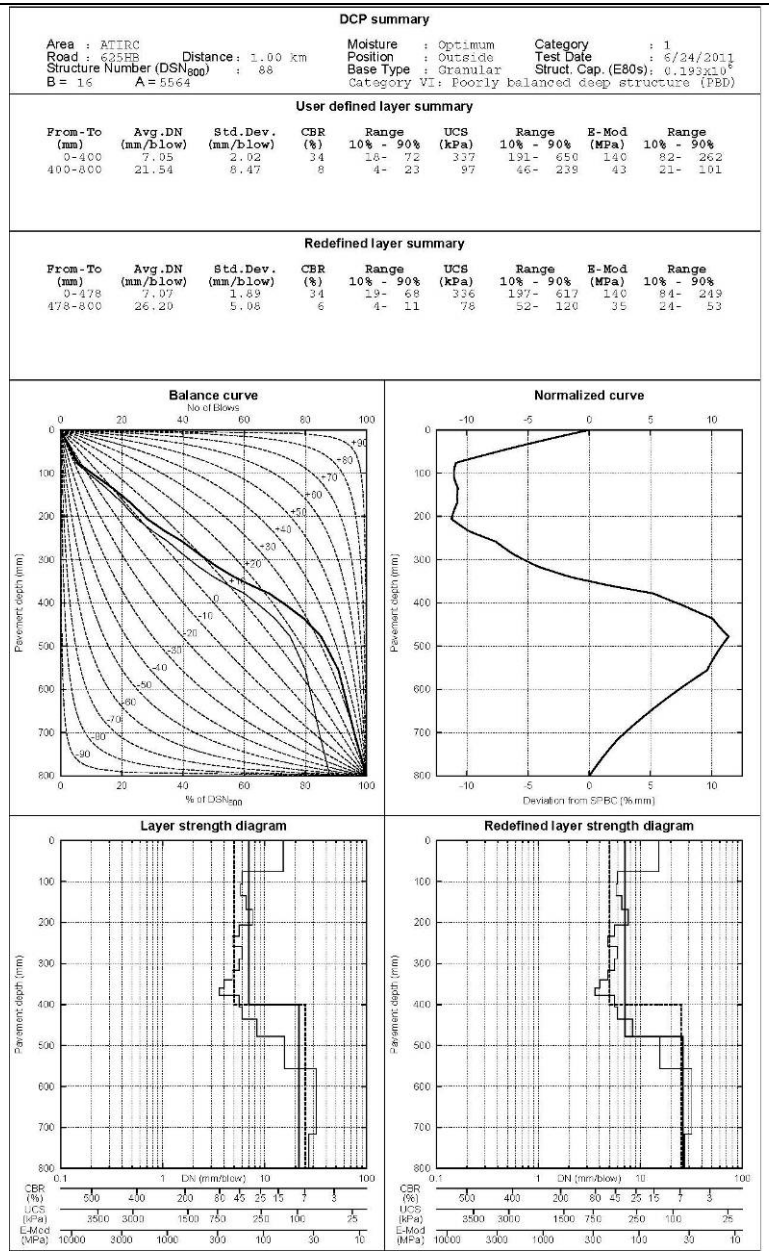

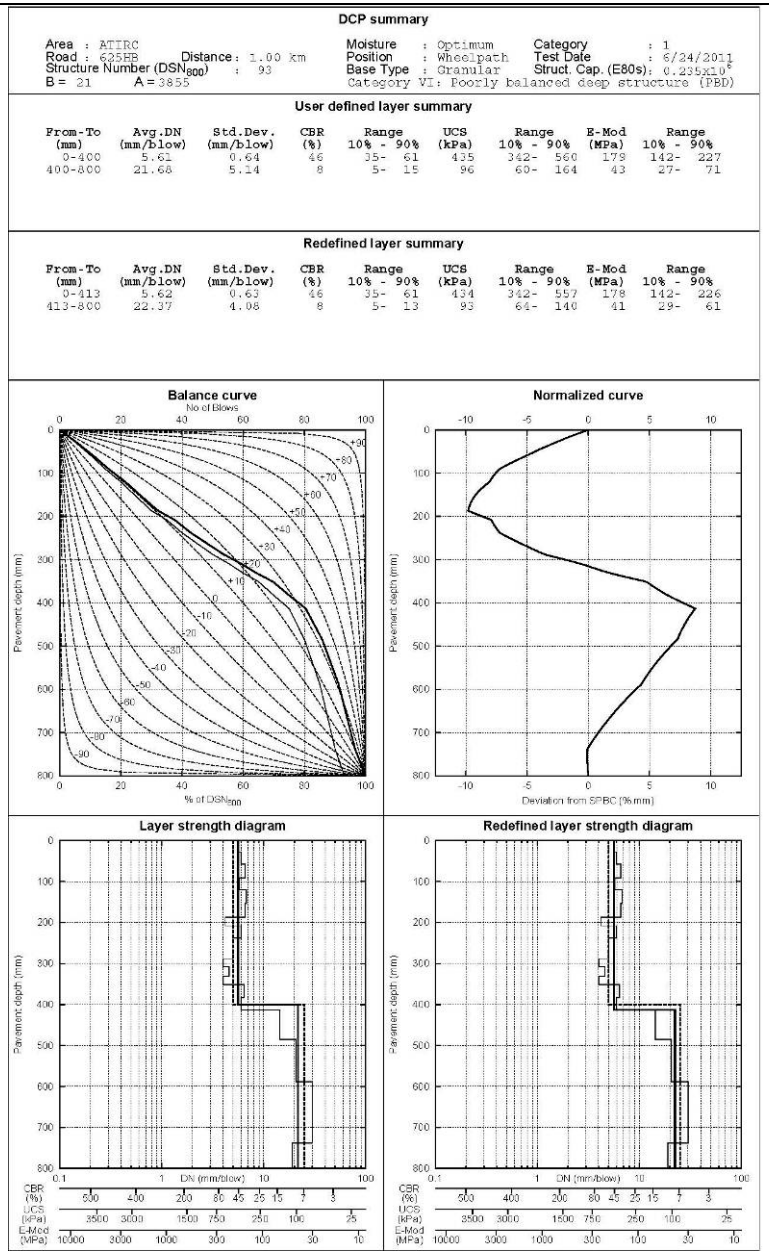

Figure A.2: 625HA: Sasobit #1 DCP profile (untrafficked [left] and wheelpath [right]).

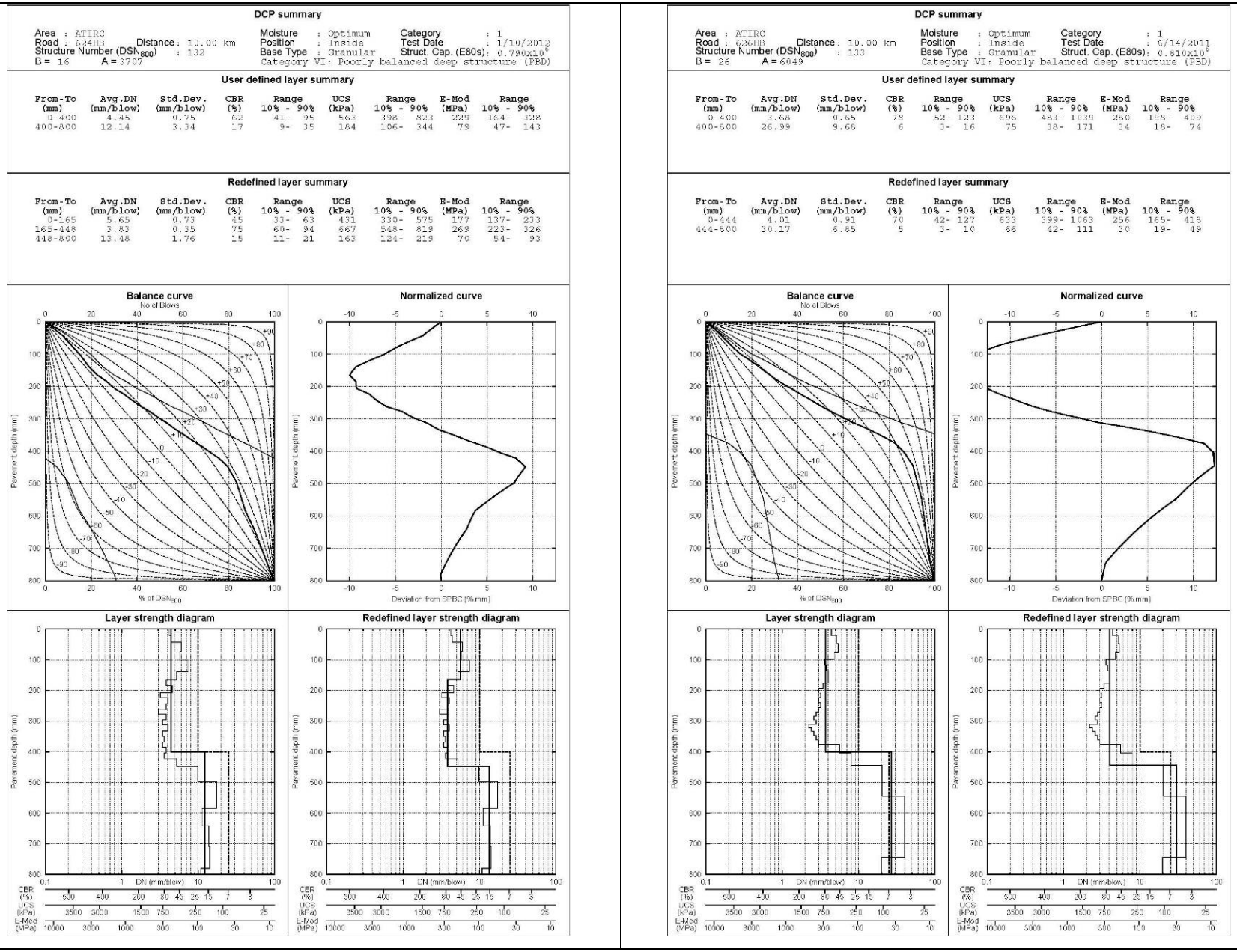

Figure A.3: 626HA: Advera #1 DCP profile (untrafficked [left] and wheelpath [right]).

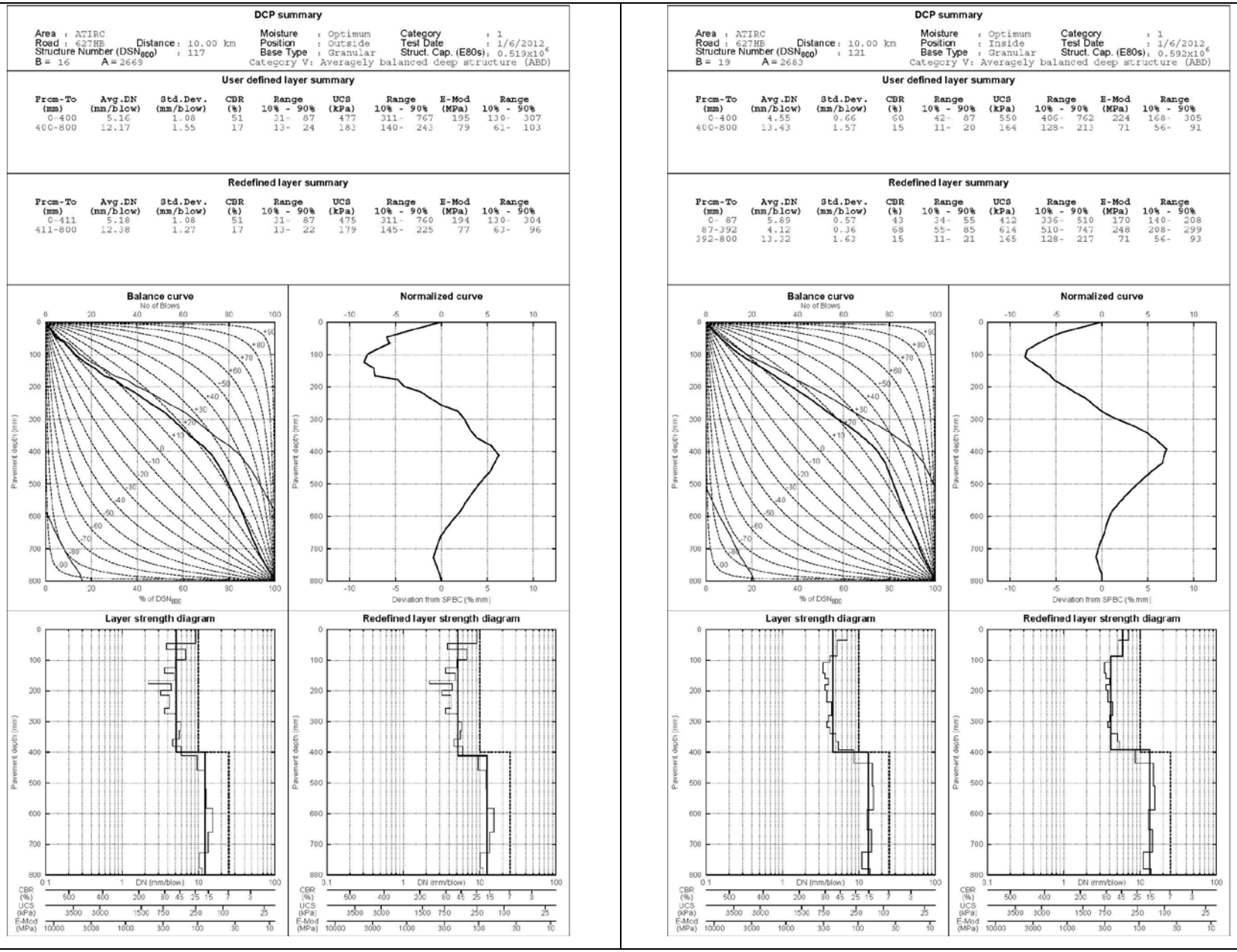

Figure A.4: 627HB: Astec DCP profile (untrafficked [left] and wheelpath [right]).

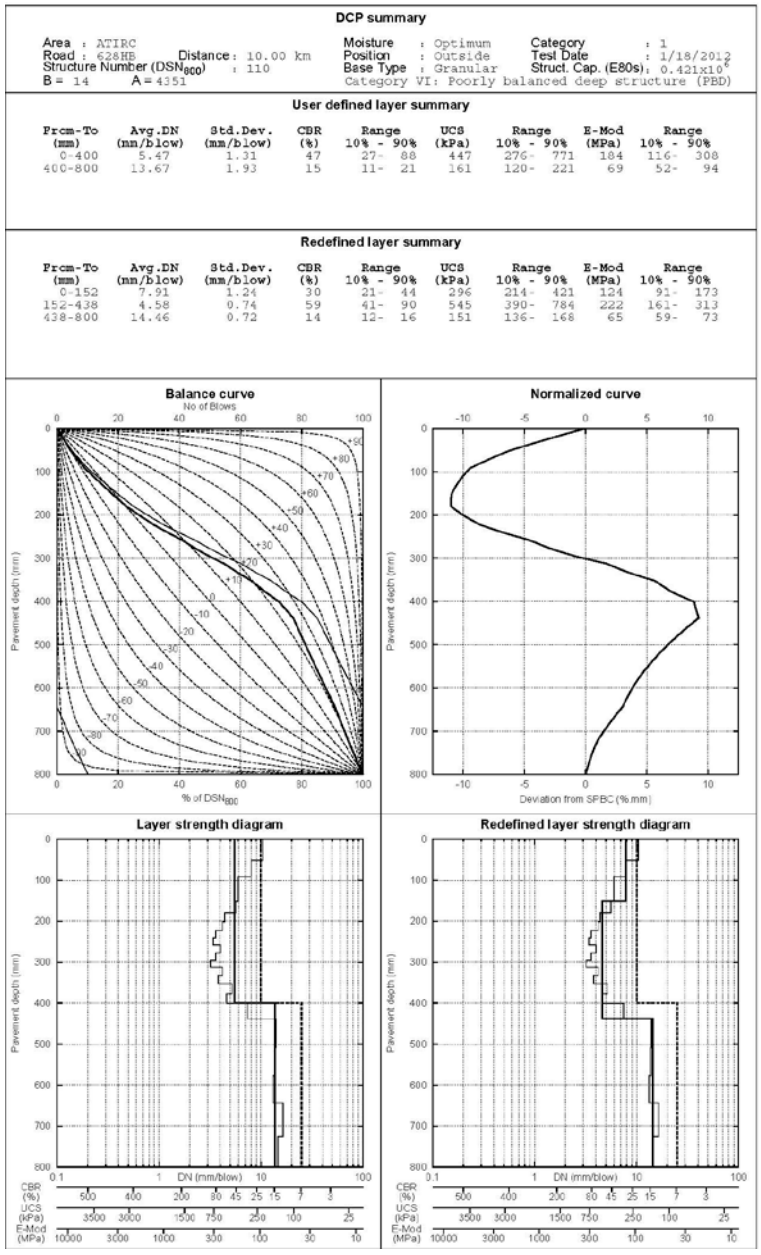

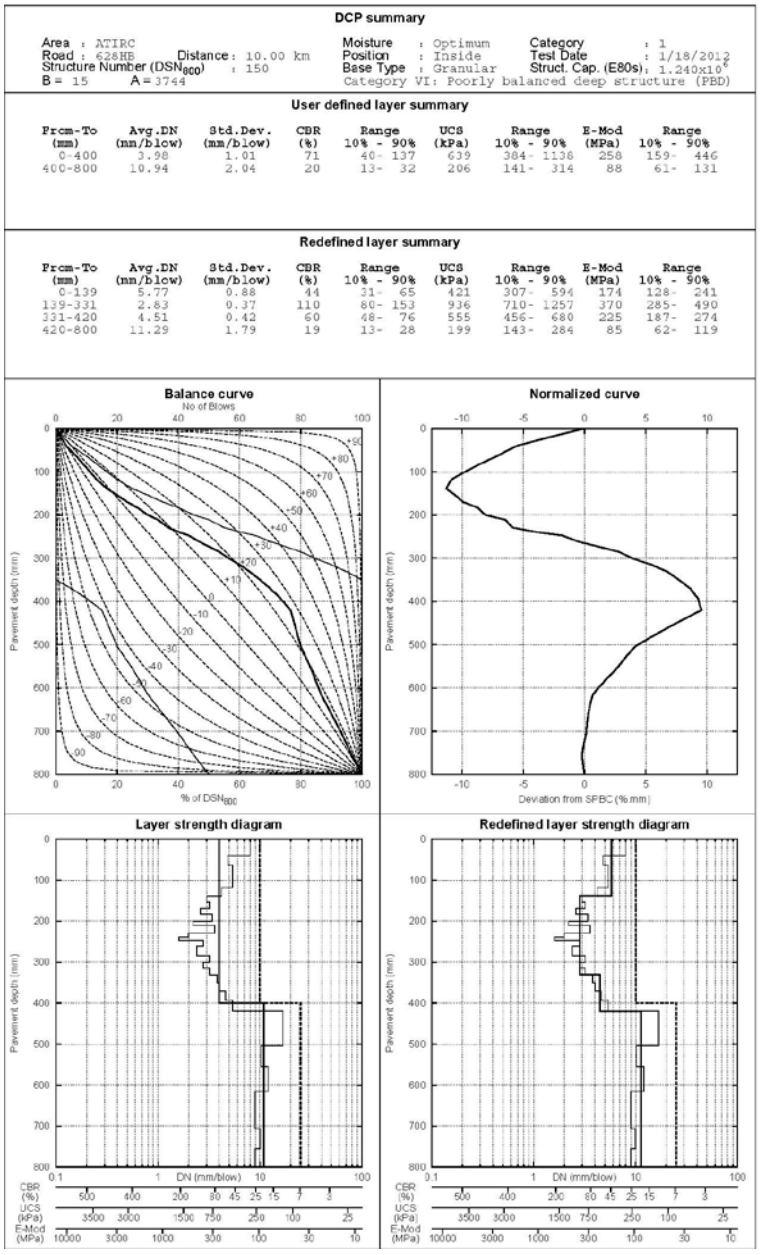

Figure A.5: 628HB: Rediset DCP profile (untrafficked [left] and wheelpath [right]).

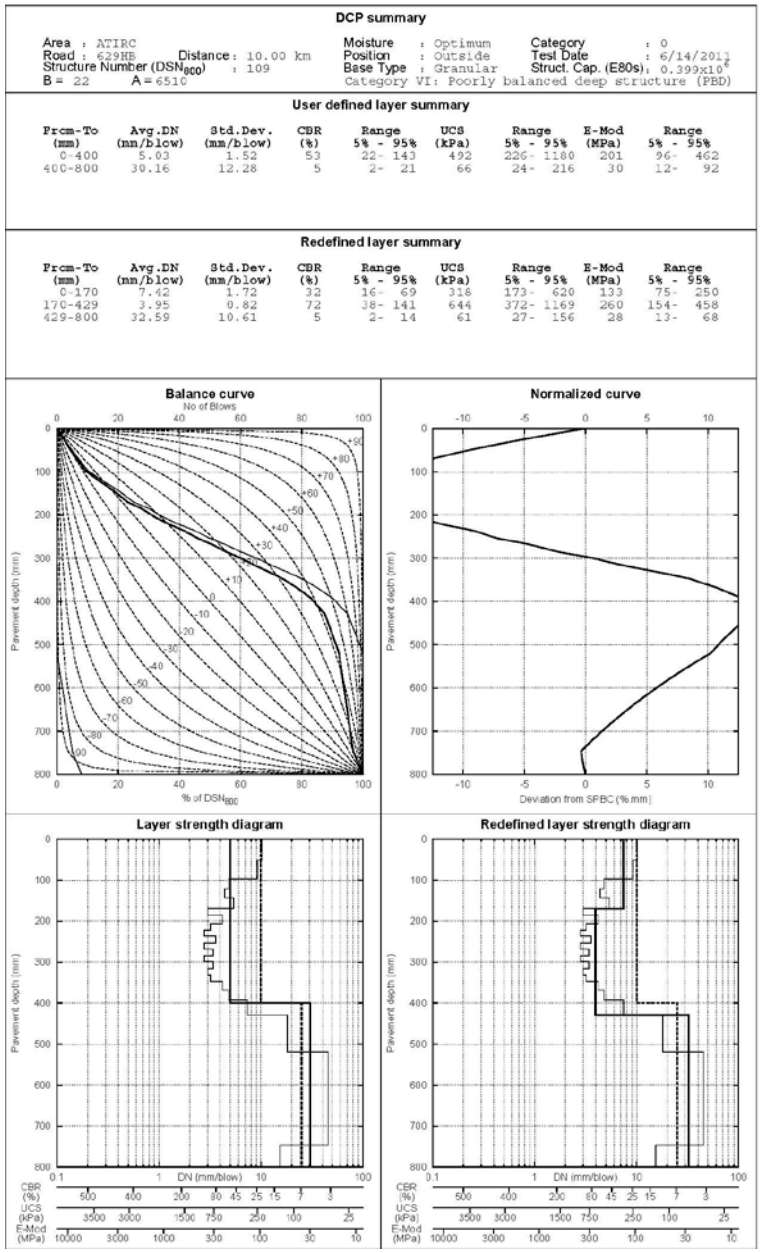

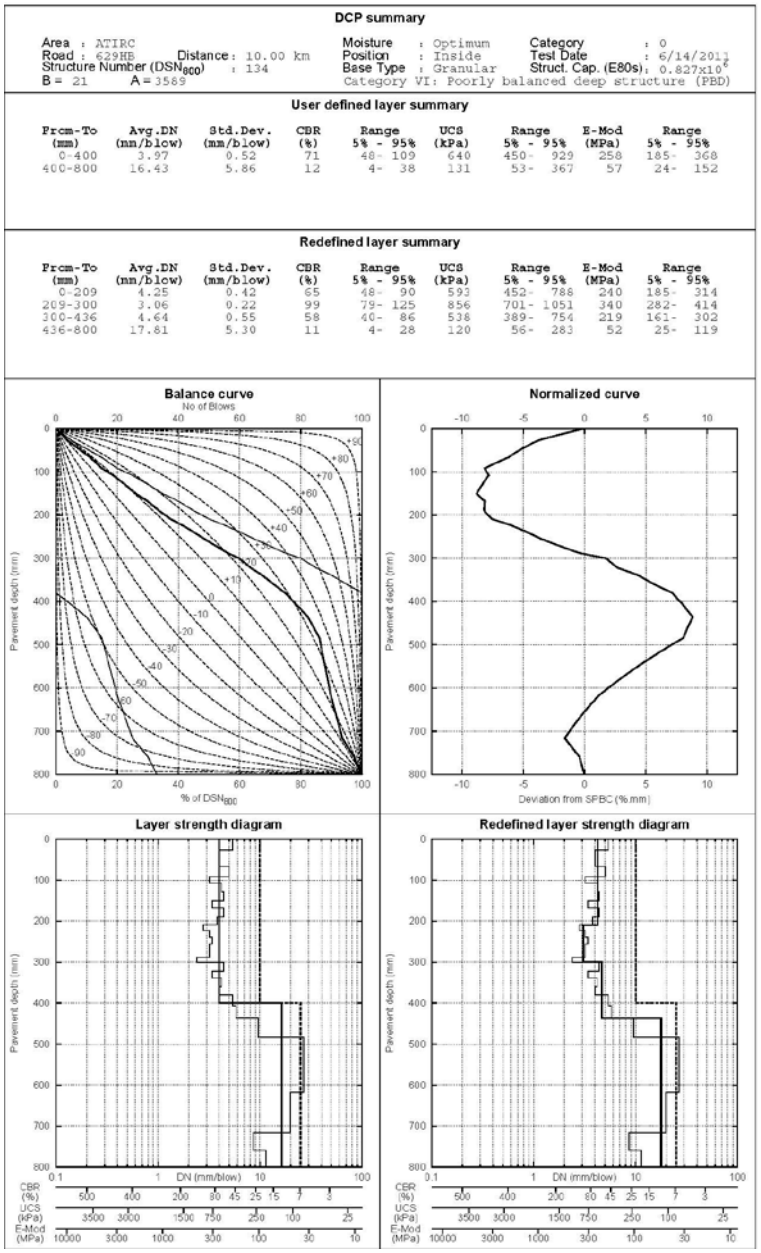

Figure A.6: 629HB: Advera #2 DCP profile (untrafficked [left] and wheelpath [right]).

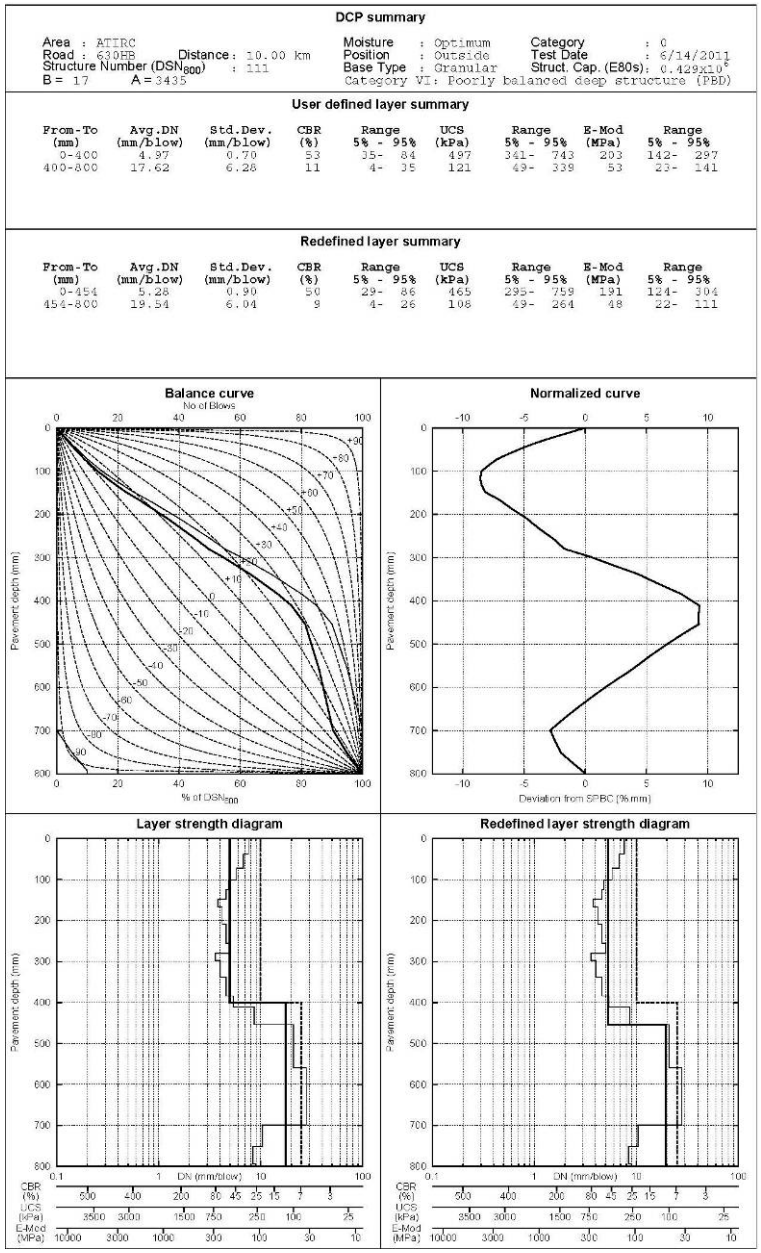

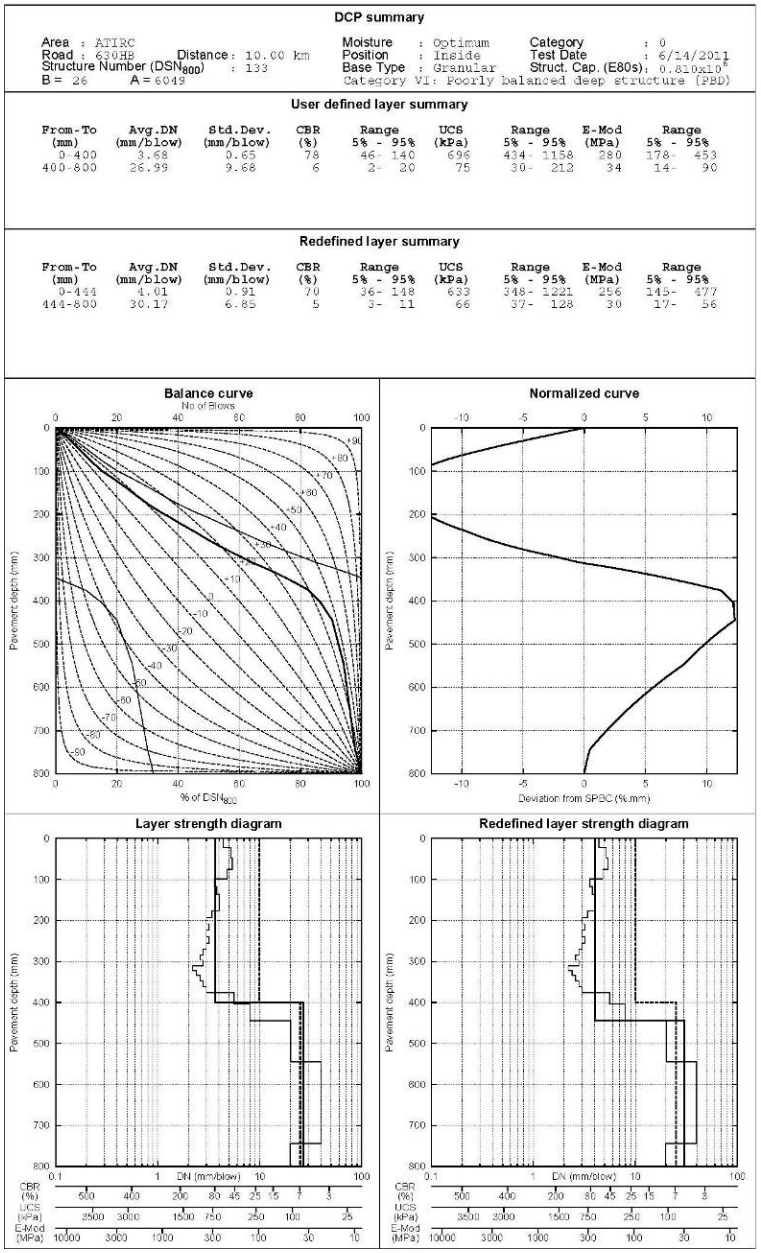

Figure A.7: 630HB: Advera #3 DCP profile (untrafficked [left] and wheelpath [right]).

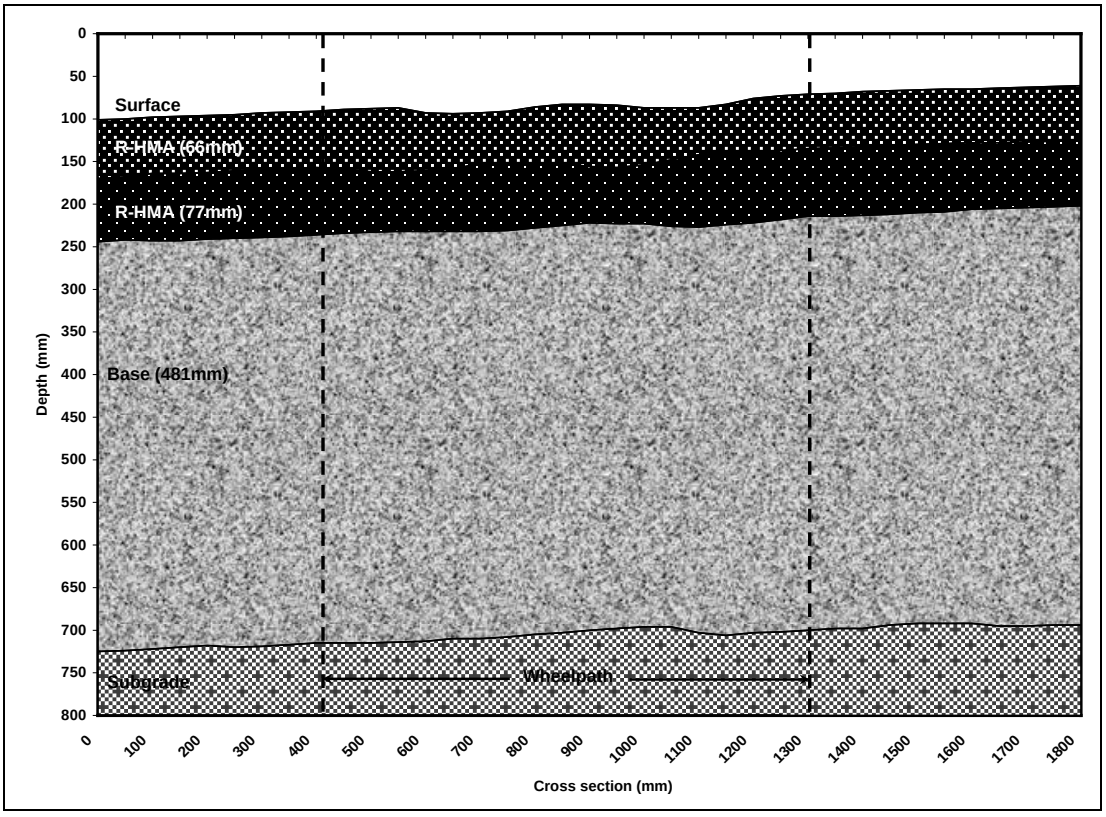

Figure A.8: 624HB: Control #1 test pit profile (after 320,000 load repetitions).

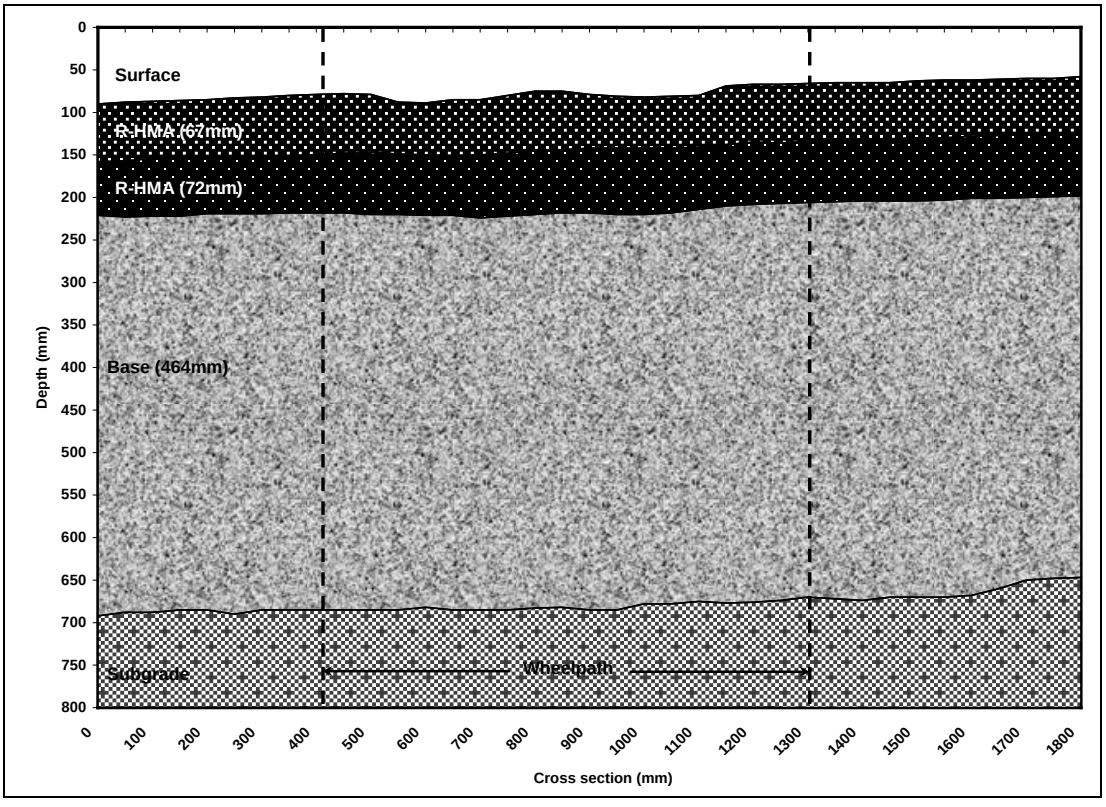

Figure A.9: 625HA: Sasobit #1 test pit profile (after 365,000 load repetitions).

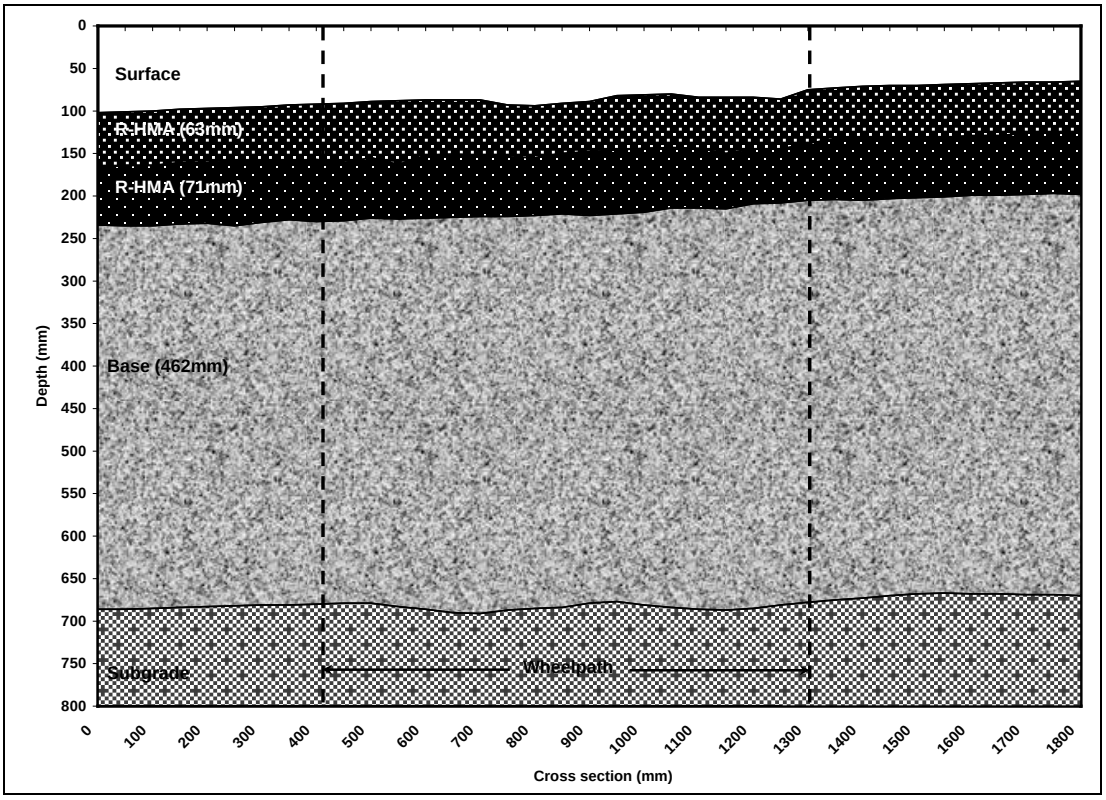

Figure A.10: 626HA: Advera #1 test pit profile (after 50,000 load repetitions).

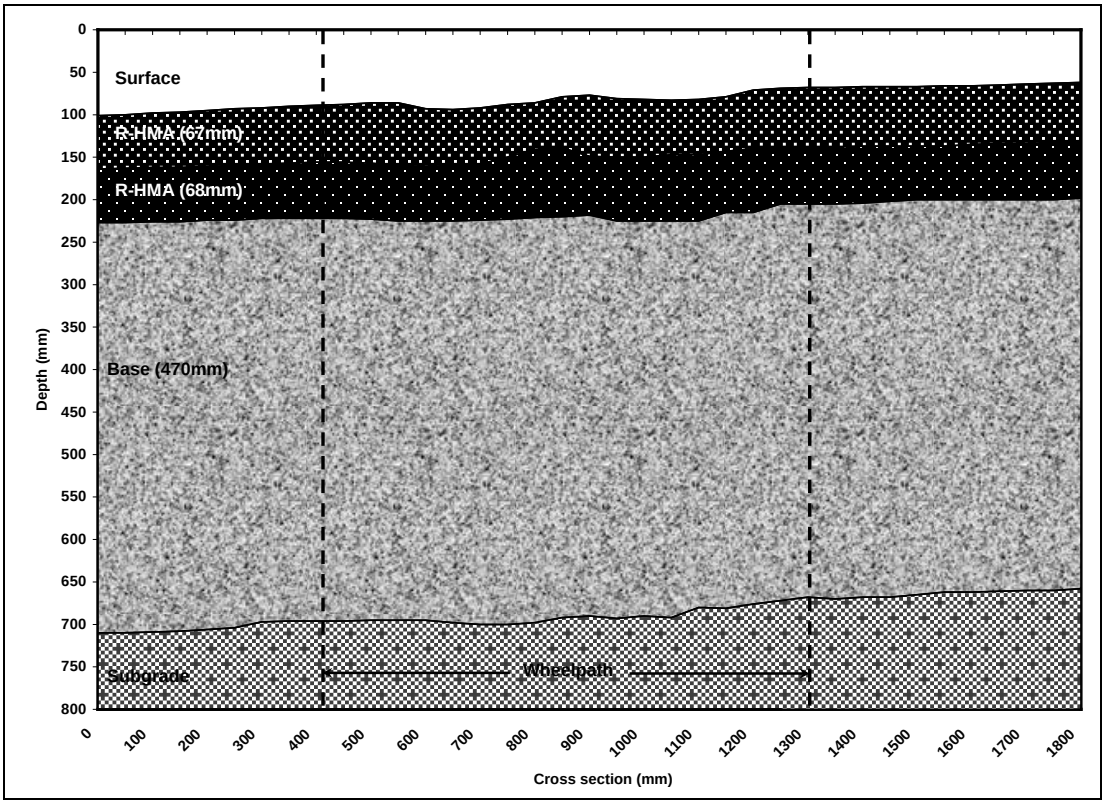

Figure A.11: 627HB: Astec test pit profile (after 242,000 load repetitions).

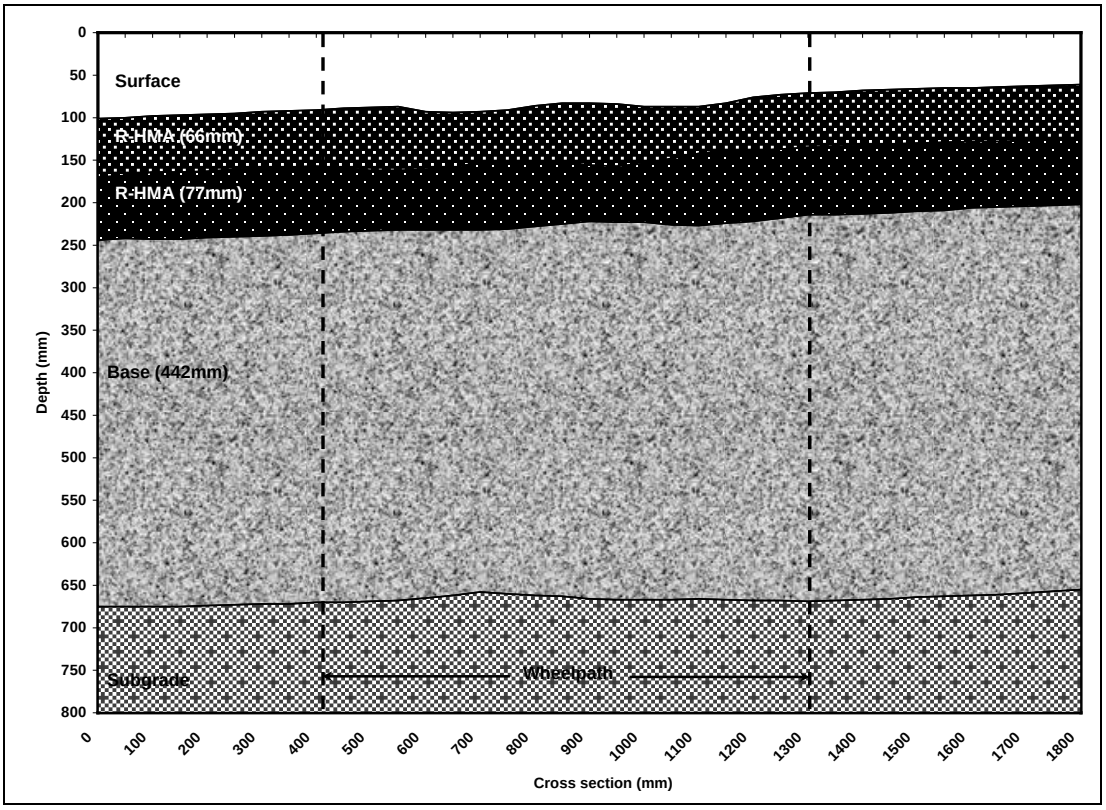

Figure A.12: 628HB: Rediset test pit profile (after 309,000 load repetitions).

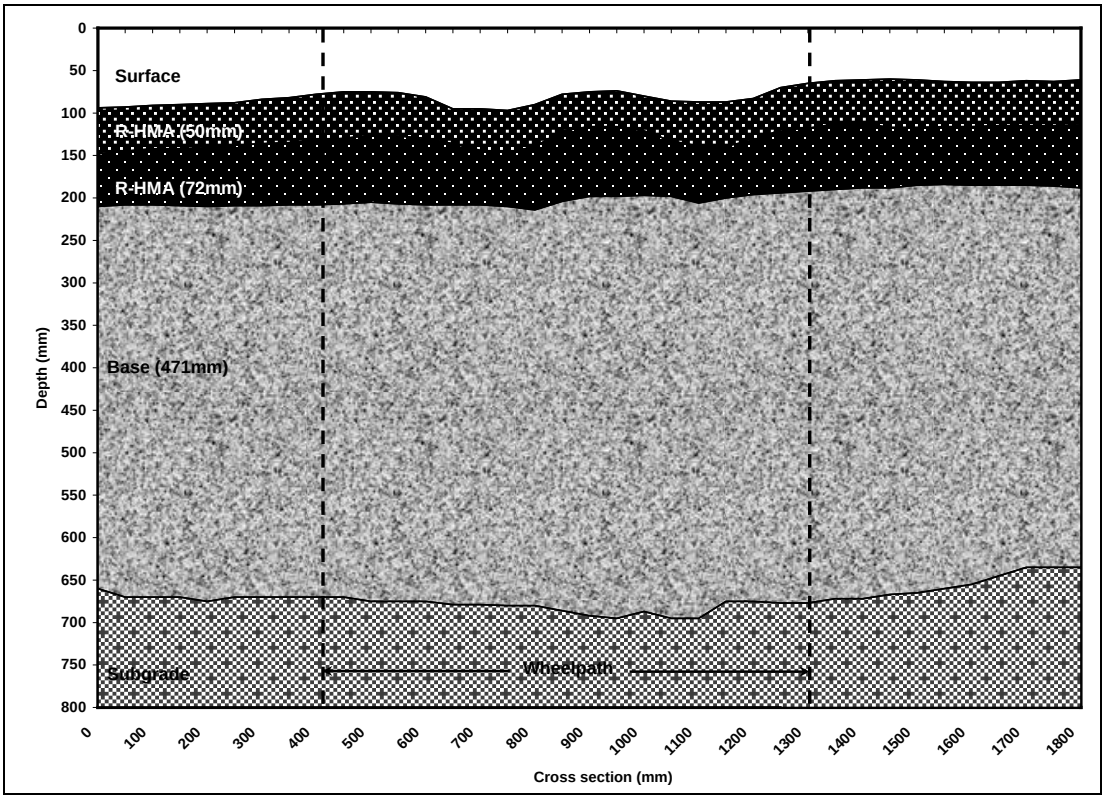

Figure A.13: 629HB: Advera #2 test pit profile (after 73,500 load repetitions).

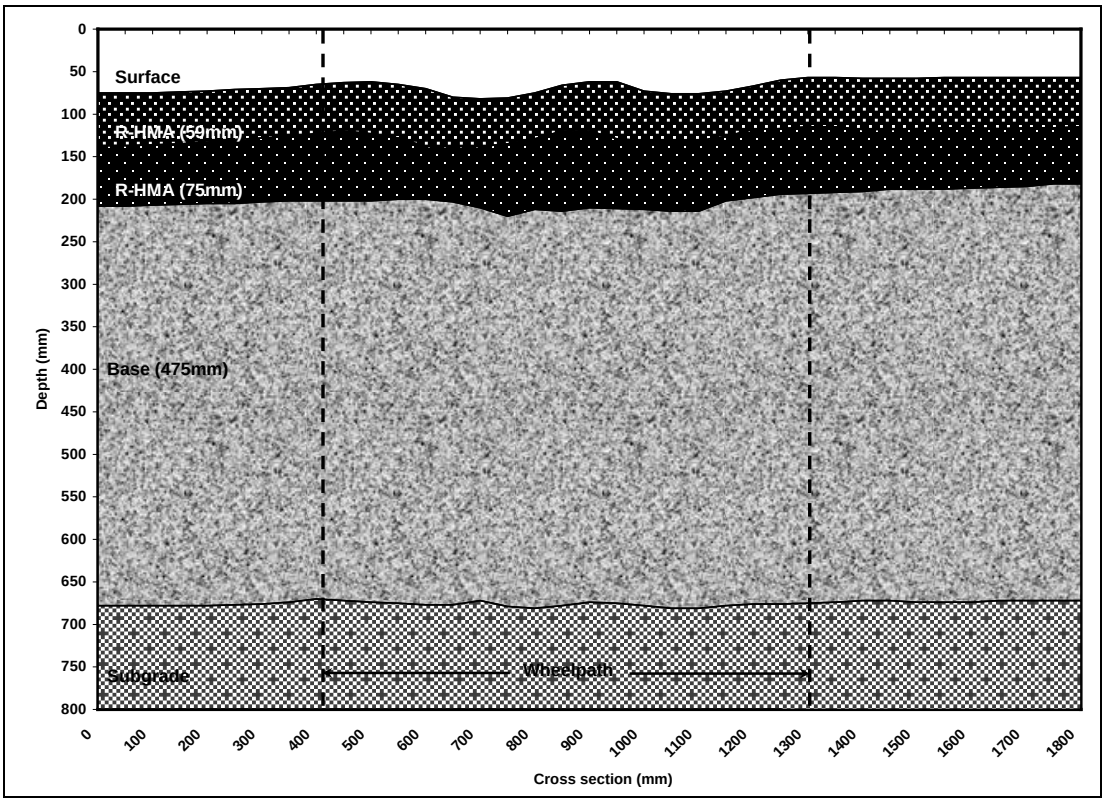

Figure A.14: 630HB: Advera #3 test pit profile (after 5,000 load repetitions).

APPENDIX B: BEAM FATIGUE SOAKING PROCEDURE

B.1 Preparation of Specimens

Prepare the specimens as follows:

1. Measure and record the bulk specific gravity, width, and height of each beam.
2. Dry each beam is dried at room temperature (around 30°C) in a forced draft oven or in a concrete conditioning room to constant mass (defined as the mass at which further drying does not alter the mass by more than 0.05 percent at two-hour drying intervals). Record the final dry mass. Note: Place beams on a rigid and flat surface during drying.
3. Using epoxy resin, bond a nut to be used for supporting the LVDT to the beam. Record the mass of the beam with the nut.

B.2 Conditioning of Specimens

1. Place the beam in the vacuum container supported above the container bottom by a spacer. Fill the container with water so that the beam is totally submerged. Apply a vacuum of 635 mm (25 in.) of mercury for 30 minutes. Remove the vacuum and determine the saturated surface dry mass according to AASHTO T-166. Calculate the volume of absorbed water and determine the degree of saturation. If the saturation level is less than 70 percent, vacuum saturate the beam for a longer time and determine the saturated surface dry mass again.
2. Place the vacuum-saturated beam in a water bath with the water temperature pre-set at 60°C. The beam should be supported on a rigid, flat (steel or wood) plate to prevent deformation of the beam during conditioning. The top surface of the beam should be about 25 mm below the water surface.
3. After 24 hours, drain the water bath and refill it with cold tap water. Set the water bath temperature to 20°C. Wait for two hours for temperature equilibrium.
4. Remove the beam from the water bath, and determine its saturated surface dry mass.
5. Wrap the beam with Parafilm to ensure no water leakage.
6. Check the bonded nut. If it becomes loose, remove it and rebond it with epoxy resin.
7. Apply a layer of scotch tape to the areas where the beam contacts the clamps of the fatigue machine. This will prevent adhesion between the Parafilm and the clamps.
8. Start the fatigue test of the conditioned beam within 24 hours.

APPENDIX C: LABORATORY TEST RESULTS

C.1 Shear Test Results

Shear test results are summarized in Table C.1 through Table C.6.

C.2 Beam Fatigue Test Results

Beam fatigue test results are summarized in Table C.7.

C.3 Tensile Strength Retained Test Results

Tensile Strength Retained test results are summarized in Table C.8.

Table C.1: Summary of Shear Test Results for Day #1 Control Mix

Specimen Designation	Air-Void Content (%)	Test Temp. (°C)	Test Shear Stress Level (kPa)	Initial Resilient Shear Modulus (kPa)	Percent Permanent Shear Strain at 5,000 Cycles	Cycles to 5% Permanent Shear Strain
R1-31-ST-7045	13.5	44.91	75.68	134.45	0.027014	48,724*
R1-32-ST-7045	13.0	45.15	73.85	160.36	0.025312	50,859*
R1-36-ST-7045	13.8	44.76	71.76	110.30	0.178203*	1,058
R1-20-ST-10045	12.1	44.93	101.32	155.11	0.031164	26,960
R1-29-ST-10045	14.0	44.74	102.97	155.82	0.029631	20,932
R1-35-ST-10045	14.5	45.01	98.84	118.47	0.087648*	1,864
R1-12-ST-13045	9.8	44.86	135.92	178.80	0.028223	34,131*
R1-22-ST-13045	12.5	44.91	136.71	148.64	0.031044	16,137
R1-28-ST-13045	13.6	44.88	132.97	140.71	0.038342	9,032
R1-19-ST-7055	11.4	54.96	70.80	90.59	0.033646	33,321*
R1-25-ST-7055	13.0	55.07	72.19	84.58	0.047268	5,623
R1-30-ST-7055	13.2	54.90	72.41	84.30	0.040965	7,636
R1-21-ST-10055	12.7	54.93	97.46	78.66	0.084152	1,284
R1-26-ST-10055	11.1	54.75	98.23	73.35	0.080088	1,365
R1-33-ST-10055	13.1	55.07	98.11	78.59	0.068328	1,968
R1-16-ST-13055	12.3	55.42	127.82	88.90	0.094993*	1,338
R1-17-ST-13055	12.2	55.03	125.77	84.45	0.092445*	1,258
R1-23-ST-13055	12.0	55.42	127.48	85.12	0.082965	1,876

*: Extrapolated results

Table C.2: Summary of Shear Test Results for Sasobit Mix

Specimen Designation	Air-Void Content (%)	Test Temp. (°C)	Test Shear Stress Level (kPa)	Initial Resilient Shear Modulus (kPa)	Percent Permanent Shear Strain at 5,000 Cycles	Cycles to 5% Permanent Shear Strain
R2-16-ST-7045	8.3	44.50	72.77	195.26	0.023079	160,205*
R2-29-ST-7045	7.5	44.48	78.60	189.53	0.021908	456,084*
R2-30-ST-7045	8.8	44.68	72.99	194.07	0.021346	276,430*
R2-14-ST-10045	8.4	44.34	103.46	125.79	0.038150	17,043
R2-21-ST-10045	8.5	44.74	103.20	200.18	0.026781	60,334*
R2-28-ST-10045	8.3	44.52	100.09	210.53	0.027088	121,710*
R2-12-ST-13045	7.4	44.39	139.44	193.33	0.052433	4,128
R2-13-ST-13045	7.5	44.30	137.64	209.39	0.028695	81,630*
R2-36-ST-13045	8.6	44.29	137.46	176.47	0.037159	17,769
R2-17-ST-7055	8.2	55.20	75.56	107.74	0.032001	123,092*
R2-25-ST-7055	8.6	54.89	73.52	117.27	0.038319	15,895
R2-35-ST-7055	8.9	54.83	73.08	101.62	0.038975	27,682
R2-20-ST-10055	8.7	55.32	102.49	102.54	0.057227	2,831
R2-23-ST-10055	8.9	55.09	100.68	109.96	0.045258	7,436
R2-32-ST-10055	9.9	54.93	100.54	110.74	0.049428	5,240
R2-22-ST-13055	8.8	54.54	133.58	87.41	0.066995	1,811
R2-26-ST-13055	8.5	55.01	132.20	99.76	0.053350	3,856
R2-37-ST-13055	8.4	54.97	132.71	95.85	0.067065	1,601

*: Extrapolated results

Table C.3: Summary of Shear Test Results for Advera Mix

Specimen Designation	Air-Void Content (%)	Test Temp. (°C)	Test Shear Stress Level (kPa)	Initial Resilient Shear Modulus (kPa)	Percent Permanent Shear Strain at 5,000 Cycles	Cycles to 5% Permanent Shear Strain
R3-31-ST-7045	11.0	45.05	75.36	201.40	0.032298	25,614
R3-32-ST-7045	10.8	44.95	74.27	164.61	0.039039	21,343
R3-36-ST-7045	11.6	45.11	75.56	171.98	0.034009	33,527*
R3-20-ST-10045	9.8	44.76	98.32	120.26	0.068785	1,705
R3-29-ST-10045	10.3	44.55	98.77	185.63	0.040804	9,642
R3-35-ST-10045	10.9	44.82	102.45	167.72	0.027837	70,054*
R3-13-ST-13045	11.5	44.55	131.26	130.77	0.061142	2,616
R3-22-ST-13045	9.9	44.53	130.12	153.97	0.060857	2,650
R3-28-ST-13045	11.0	44.69	131.78	126.29	0.060570	2,251
R3-12-ST-7055	10.4	55.10	71.37	86.44	0.065630	1,998
R3-25-ST-7055	10.6	55.21	73.80	90.59	0.046866	6,732
R3-30-ST-7055	11.1	54.93	72.33	112.56	0.054301	3,212
R3-17-ST-10055	10.7	55.04	98.30	81.26	0.052208	4,442
R3-21-ST-10055	9.8	55.05	98.56	87.78	0.080845	912
R3-27-ST-10055	10.8	55.21	100.64	98.19	0.060136	2,415
R3-18-ST-13055	10.7	54.96	131.68	82.76	0.133551*	302
R3-23-ST-13055	10.0	54.96	131.60	93.70	0.118659*	523
R3-26-ST-13055	10.8	54.95	134.81	107.20	0.095263*	1,042

*: Extrapolated results

Table C.4: Summary of Shear Test Results for Astec Mix

Specimen Designation	Air-Void Content (%)	Test Temp. (°C)	Test Shear Stress Level (kPa)	Initial Resilient Shear Modulus (kPa)	Percent Permanent Shear Strain at 5,000 Cycles	Cycles to 5% Permanent Shear Strain
R4-25-ST-7045	10.2	44.65	75.28	207.04	0.019115	643,073*
R4-34-ST-7045	10.4	44.88	76.06	197.56	0.021865	326,655*
R4-36-ST-7045	11.1	44.85	72.03	147.22	0.023562	93,997*
R4-15-ST-10045	8.6	44.84	101.20	197.67	0.025980	134,218*
R4-16-ST-10045	9.5	44.63	100.85	193.50	0.025247	106,765*
R4-17-ST-10045	10.5	44.78	100.39	176.56	0.026183	59,103*
R4-13-ST-13045	9.6	45.09	133.19	126.02	0.060883	2,358
R4-33-ST-13045	10.5	45.45	131.58	192.22	0.027905	34,921*
R4-35-ST-13045	11.4	45.00	133.02	166.94	0.040040	8,783
R4-14-ST-7055	9.9	54.83	72.75	102.57	0.042144	10,487
R4-26-ST-7055	10.7	55.44	70.71	95.60	0.040546	10,996
R4-27-ST-7055	11.0	54.80	71.88	99.31	0.032384	31,239*
R4-12-ST-10055	9.2	55.02	100.11	79.79	0.057220	3,015
R4-29-ST-10055	10.5	54.86	98.76	112.51	0.037991	17,560
R4-32-ST-10055	9.9	54.82	101.21	100.56	0.055054	3,294
R4-22-ST-13055	10.2	54.89	130.44	97.09	0.092999*	809
R4-28-ST-13055	9.6	54.88	132.24	103.55	0.062089	2,663
R4-30-ST-13055	10.0	55.43	129.85	104.55	0.072688	1,504

*: Extrapolated results

Table C.5: Summary of Shear Test Results for Rediset Mix

Specimen Designation	Air-Void Content (%)	Test Temp. (°C)	Test Shear Stress Level (kPa)	Initial Resilient Shear Modulus (kPa)	Percent Permanent Shear Strain at 5,000 Cycles	Cycles to 5% Permanent Shear Strain
R5-20-ST-7045	8.2	44.76	71.93	164.29	0.025277	559,897*
R5-27-ST-7045	8.6	45.44	75.16	195.39	0.023406	212,741*
R5-30-ST-7045	9.0	45.48	77.44	148.37	0.025348	193,639*
R5-16-ST-10045	7.7	45.45	101.95	177.13	0.028307	73,270*
R5-29-ST-10045	8.9	44.60	104.14	177.65	0.023962	152,183*
R5-34-ST-10045	9.1	44.64	106.35	176.02	0.027925	84,933*
R5-17-ST-13045	8.2	44.65	133.31	169.06	0.032424	25,491
R5-23-ST-13045	8.1	45.42	128.97	165.14	0.033216	57,707*
R5-33-ST-13045	8.9	44.56	136.54	151.48	0.036737	16,738
R5-25-ST-7055	8.5	55.21	72.40	146.27	0.027586	69,258*
R5-31-ST-7055	9.5	55.13	74.06	93.29	0.037766	19,522
R5-35-ST-7055	9.8	55.06	71.90	91.91	0.035769	30,837*
R5-14-ST-10055	7.9	55.14	100.93	102.85	0.042148	12,308
R5-18-ST-10055	7.5	55.22	99.55	117.46	0.040252	16,443
R5-21-ST-10055	8.0	54.98	99.65	97.14	0.045899	7,561
R5-13-ST-13055	7.8	55.16	131.80	104.87	0.048412	5,721
R5-19-ST-13055	7.4	55.12	132.53	106.50	0.052786	3,977
R5-32-ST-13055	9.2	54.90	131.08	99.47	0.066947	1,715

*: Extrapolated results

Table C.6: Summary of Shear Test Results for Day #2 Control Mix

Specimen Designation	Air-Void Content (%)	Test Temp. (°C)	Test Shear Stress Level (kPa)	Initial Resilient Shear Modulus (kPa)	Percent Permanent Shear Strain at 5,000 Cycles	Cycles to 5% Permanent Shear Strain
R6-21-ST-7045	8.1	45.35	76.62	205.73	0.019402	382,855*
R6-28-ST-7045	7.7	45.31	75.49	220.56	0.017354	618,069*
R6-37-ST-7045	11.7	45.45	74.36	217.22	0.018232	75,685*
R6-14-ST-10045	7.9	45.39	103.42	216.21	0.023595	246,707*
R6-20-ST-10045	8.7	45.49	103.84	195.89	0.019845	181,498*
R6-31-ST-10045	8.4	45.39	100.95	185.23	0.026529	73,364*
R6-23-ST-13045	7.9	45.40	133.91	184.48	0.028475	38,118*
R6-25-ST-13045	8.8	45.38	138.24	200.44	0.032840	20,255
R6-32-ST-13045	9.1	45.45	136.72	166.88	0.034835	17,809
R6-13-ST-7055	7.5	54.91	73.29	120.96	0.031077	52,138*
R6-19-ST-7055	7.8	55.13	77.28	88.21	0.028503	30,474*
R6-34-ST-7055	10.7	55.02	71.91	102.07	0.040829	11,006
R6-15-ST-10055	6.6	54.77	103.90	118.16	0.036335	22,754
R6-33-ST-10055	10.2	54.86	99.62	102.84	0.049357	5,189
R6-36-ST-10055	12.7	54.93	98.92	84.20	0.066558	2,319
R6-18-ST-13055	8.8	55.06	133.18	102.74	0.062227	2,886
R6-27-ST-13055	8.0	54.56	135.57	101.26	0.068083	1,575
R6-35-ST-13055	11.5	55.02	134.23	107.49	0.076238	1,990

*: Extrapolated results

Table C.7: Summary of Beam Fatigue Test Results

Mix	Cond.	Specimen	Air-Void Content[1] (%)	Test Temp. (°C)	Test Strain Level (μstrain)	Initial Phase Angle (Deg.)	Initial Stiffness (MPa)	Fatigue Life (Nf)
Control #1	Dry	R1-5-B1	12.29	20.91	0.000208	24.11	2,831	8,110,882,139*
		R1-6-B3	10.41	19.95	0.000206	24.04	3,243	173,356,206*
		R1-7-B2	12.75	20.12	0.000209	22.07	2,791	285,818,397*
		R1-4-B1	11.67	20.16	0.000414	23.92	2,618	1,678,854
		R1-6-B1	11.35	20.74	0.000423	27.96	2,405	4,957,819*
		R1-7-B1	13.86	21.09	0.000409	26.25	2,323	630,417
	Wet	R1-6-B2	11.48	20.40	0.000213	26.14	2,219	874,229,361*
		R1-7-B4	10.02	20.37	0.000210	26.74	2,275	593,232,143*
		R1-10-B2	11.55	19.99	0.000206	25.29	2,691	490,506,070*
		R1-4-B2	13.08	19.74	0.000414	23.31	2,094	1,967,977
		R1-7-B3	12.00	20.21	0.000414	26.21	2,122	3,505,168
		R1-8-B4	11.40	19.87	0.000406	25.41	2,571	2,298,217
Sasobit	Dry	R2-2-B2	9.04	20.36	0.000211	21.41	4,355	84,594,738*
		R2-3-B3	9.35	19.98	0.000201	20.85	4,278	559,960,138*
		R2-4-B2	9.21	19.78	0.000207	19.74	4,436	249,202,486*
		R2-3-B1	8.61	19.71	0.000410	20.07	3,959	1,376,406
		R2-4-B4	9.12	19.78	0.000410	17.50	4,089	2,245,868
		R2-6-B2	9.12	19.73	0.000408	18.08	3,790	1,029,086
	Wet	R2-3-B3	8.42	20.46	0.000211	23.60	3,697	906,950,935*
		R2-4-B1	9.01	20.04	0.000204	27.75	3,696	189,025,577*
		R2-6-B3	8.88	20.15	0.000206	21.77	3,422	526,658,625*
		R2-1-B2	10.32	19.72	0.000417	20.76	3,006	476,567
		R2-5-B4	8.10	19.72	0.000413	21.82	2,629	2,540,975
		R2-10-B1	9.60	20.43	0.000419	28.96	2,634	2,402,629
Advera	Dry	R3-1-B2	10.35	20.33	0.000209	23.01	3,718	468,624,752*
		R3-8-B2	10.96	19.93	0.000203	21.95	3,526	142,256,890*
		R3-10-B1	9.90	20.14	0.000207	21.73	3,755	194,527,402*
		R3-3-B3	10.77	19.74	0.000413	18.83	3,088	1,660,123
		R3-5-B2	10.06	19.96	0.000406	22.45	3,569	878,898
		R3-5-B3	10.53	19.75	0.000411	17.18	3,428	1,407,957
	Wet	R3-2-B1	10.65	19.90	0.000207	24.96	2,768	130,337,988*
		R3-2-B3	10.26	20.25	0.000204	23.44	2,672	130,472,271*
		R3-8-B1	10.78	20.47	0.000210	25.07	2,708	289,428,299*
		R3-3-B2	11.44	19.72	0.000416	24.58	2,180	750,056
		R3-4-B3	10.57	20.02	0.000411	26.76	2,452	1,103,501
		R3-6-B3	10.14	19.96	0.000411	26.34	2,365	802,595
Astec	Dry	R4-2-B2	9.37	20.35	0.000209	22.02	4,019	247,111,697*
		R4-7-B2	8.53	20.15	0.000206	21.73	4,057	419,207,740*
		R4-8-B4	7.34	20.00	0.000203	21.65	4,434	4,021,157,645*
		R4-1-B4	9.20	19.91	0.000409	21.75	3,125	1,425,860
		R4-4-B2	7.69	19.68	0.000408	17.51	3,962	1,001,722
		R4-9-B1	7.28	19.95	0.000408	16.18	4,223	1,515,270
	Wet	R4-2-B4	8.94	20.52	0.000208	24.98	3,092	80,566,677*
		R4-4-B1	7.73	20.36	0.000209	23.56	3,525	272,620,714*
		R4-4-B3	7.86	19.90	0.000202	22.63	3,636	172,727,226*
		R4-2-B3	9.30	19.72	0.000412	20.56	3,004	354,704
		R4-9-B3	8.52	19.69	0.000414	18.21	3,358	1,550,170
		R4-10-B3	8.30	19.73	0.000413	20.06	3,320	998,652
Rediset	Dry	R5-7-B2	8.78	20.18	0.000208	23.87	3,158	3,046,527,044*
		R5-7-B3	8.24	19.95	0.000203	23.34	3,664	767,058,429*
		R5-8-B1	8.20	20.34	0.000212	24.70	3,374	850,588,788*
		R5-4-B2	8.59	20.14	0.000407	27.22	3,009	4,789,879
		R5-5-B2	8.58	20.46	0.000415	26.27	3,044	2,488,669
		R5-6-B3	8.35	19.75	0.000412	21.30	3,217	6,071,302*
	Wet	R5-3-B1	9.16	20.11	0.000207	24.56	2,422	346,251,170*
		R5-3-B2	9.76	19.79	0.000208	22.15	2,275	909,512,175*
		R5-8-B3	7.93	20.25	0.000205	25.12	2,935	621,041,766*
		R5-1-B2	11.15	19.88	0.000409	27.20	2,306	859,240
		R5-4-B1	8.93	19.96	0.000410	28.09	2,209	3,118,440
		R5-6-B2	8.51	20.40	0.000417	27.27	2,664	1,520,703

Table C.7: Summary of Beam Fatigue Test Results *(continued)*

Mix	Cond.	Specimen	Air-Void Content[1] (%)	Test Temp. (°C)	Test Strain Level (µstrain)	Initial Phase Angle (Deg.)	Initial Stiffness (MPa)	Fatigue Life (Nf)
Control #2	Dry	R6-4-B2	6.62	20.03	0.000202	22.42	4,016	498,038,192*
		R6-5-B4	6.40	20.39	0.000208	23.09	4,138	3,090,912,600*
		R6-9-B2	5.29	20.13	0.000206	21.89	3,695	1,202,309,566*
		R6-6-B1	6.74	19.72	0.000408	17.28	4,474	3,747,132
		R6-10-B1	5.91	19.74	0.000408	17.50	4,373	11,432,335*
		R6-10-B3	6.55	19.69	0.000406	18.91	4,400	9,442,018*
	Wet	R6-6-B2	6.84	19.91	0.000202	25.90	3,670	520,856,476*
		R6-6-B4	6.07	20.48	0.000209	25.44	3,658	283,832,508*
		R6-8-B4	6.62	20.52	0.000209	24.76	3,477	1,028,364,717*
		R6-2-B3	7.65	19.75	0.000414	20.30	2,620	1,667,126
		R6-3-B3	6.87	20.16	0.000410	25.29	2,948	3,686,245
		R6-4-B3	6.82	19.76	0.000411	20.22	2,972	1,757,852

* Extrapolated results

[1] Air-void content was measured with the CoreLok method.

Table C.8: Summary of Tensile Strength Retained Test Results

Mix	Condition	Specimen	Air-Voids (%)	Strength (kPa)	Average (kPa)	Std. Dev.	TSR (%)
Control #1	Dry	R1-56-T	8.63	772.14	720.16	77.66	72.5
		R1-53-T	9.17	712.77			
		R1-55-T	9.33	818.56			
		R1-57-T	9.61	746.21			
		R1-54-T	9.94	672.72			
		R1-63-T	11.22	598.57			
	Wet	R1-65-T	11.29	403.21	522.21	64.57	
		R1-60-T	9.66	515.95			
		R1-59-T	10.00	585.87			
		R1-61-T	9.62	516.68			
		R1-62-T	9.63	568.20			
		R1-58-T	9.92	543.34			
Sasobit	Dry	R2-62-T	7.48	879.15	877.51	21.84	79.4
		R2-55-T	7.98	845.01			
		R2-64-T	8.23	895.93			
		R2-61-T	6.77	906.34			
		R2-66-T	8.34	866.05			
		R2-54-T	8.14	872.57			
	Wet	R2-65-T	6.89	702.16	696.49	32.74	
		R2-58-T	6.73	714.16			
		R2-56-T	7.68	708.69			
		R2-68-T	9.30	633.07			
		R2-60-T	7.72	725.54			
		R2-63-T	7.98	695.30			
Advera	Dry	R3-61-T	11.04	610.94	635.73	23.25	67.4
		R3-67-T	10.10	648.82			
		R3-53-T	11.03	669.14			
		R3-58-T	11.43	648.66			
		R3-56-T	10.96	614.27			
		R3-60-T	11.14	622.57			
	Wet	R3-63-T	11.55	422.64	428.61	25.80	
		R3-64-T	11.42	412.61			
		R3-65-T	11.24	450.89			
		R3-68-T	10.07	427.81			
		R3-59-T	11.61	393.21			
		R3-66-T	10.60	464.47			
Astec	Dry	R4-62-T	9.99	745.50	802.00	60.39	64.7
		R4-67-T	8.96	804.19			
		R4-68-T	9.48	787.56			
		R4-54-T	8.88	910.47			
		R4-66-T	8.04	748.40			
		R4-63-T	9.13	815.90			
	Wet	R4-61-T	9.44	464.50	518.53	45.92	
		R4-64-T	8.39	481.70			
		R4-58-T	8.27	504.00			
		R4-65-T	7.96	520.50			
		R4-55-T	8.37	551.50			
		R4-57-T	8.25	589.00			
Rediset	Dry	R5-63-T	6.51	790.05	765.86	35.33	77.5
		R5-61-T	7.59	712.12			
		R5-65-T	7.50	785.56			
		R5-59-T	6.83	798.92			
		R5-53-T	7.49	776.80			
		R5-62-T	6.90	731.70			
	Wet	R5-64-T	6.11	598.20	593.85	10.96	
		R5-56-T	6.48	601.40			
		R5-58-T	6.64	594.30			
		R5-66-T	7.19	607.00			
		R5-57-T	6.99	577.50			
		R5-60-T	6.80	584.70			

Table C.8: Summary of Tensile Strength Retained Test Results *(continued)*

Mix	Condition	Specimen	Air-Voids (%)	Strength (kPa)	Average (kPa)	Std. Dev.	TSR (%)
Control #2	Dry	R6-57-T	6.75	704.50	688.93	51.88	88.0
		R6-56-T	7.24	733.80			
		R6-66-T	7.31	697.25			
		R6-60-T	6.69	745.61			
		R6-65-T	7.57	631.20			
		R6-64-T	7.60	621.20			
	Wet	R6-59-T	6.80	626.65	606.02	54.92	
		R6-62-T	6.98	644.21			
		R6-61-T	6.61	633.12			
		R6-8-T	6.69	635.37			
		R6-67-T	7.93	498.61			
		R6-63-T	6.51	598.15			